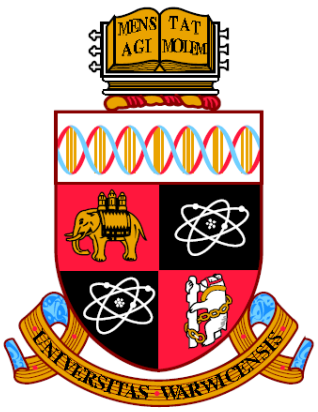

Synthesis and application of new polymers for agriculture: pesticide formulation

by

Nuttapol Risangud

Thesis

Submitted to the University of Warwick
for the degree of

Doctor of Philosophy in Chemistry

Department of Chemistry

April 2017

Contents

List of Tables

List of Figures

Acknowledgments

First, I would like to thank my supervisor, Professor Haddleton, for giving me the great opportunity to work in the Haddleton group and also for all his help and advice during the whole of my studies. The freedom that he gives me to design and work out the experiment is the valuable experience in which I believe is the best way to be trained and learn. Secondly, I would like to thank my sponsor, The Royal Thai Government (DPST), for the financial support throughout my studies in the UK.

My next thanks go to the senior researcher in the group, Dr Paul Wilson, who has taught and helped me a lot since the first day I was here. It was a real pleasure to have you as a fume hood neighbour. I also would like to thank Dr Kristian Kempe for his advice from the beginning of my PhD. More importantly, it was a great opportunity to play football with Paul and was coached by Kristian, I am looking forward to the next Warwick polymer conference.

I also would like to thank Raj, Kay and Dan for the great service and advice for SEC characterisation since the early stage of my polymer research. It has been a great experience for becoming a member of Haddleton group. I would like to thank you the member of the C210 office, Jenny, Danielle, Patrick, Rachel and Both Sams, for a big help and smile during past three years. I would also like to thank ex-group members: Zhang, Alex, Athina, Jamie, Waldron, and Vasiliki for their advice in the group meeting. In addition, my thanks go to the current group members: Chongyu, Richard, Nik, Atty, Glen, George, Pawel, Evelina and Alan for the nice working environment in the group.

I also want thank to my friends outside the group including, people in Manchester/Warwick Thai Society and Warwick staff football team for letting me join the team during my studies. There are also other people who I have known during the time I have spent in the UK.

Finally, I want to thank my whole family, particularly my dad and mum who have supported my study from the beginning. I also thank my brother and all my lovely friends in Thailand, especially Siriporn and Ratchapan, without your love and motivation during the time here this would not be done.

Declarations

Experimental results contained in this thesis are original research carried out by the author, unless otherwise stated, in the Department of Chemistry at the University of Warwick, between January 2014 and April 2017. No materials contained herein has been submitted for any other degree, or at any other institution. Results from other authors are cited in the usual manner throughout the text.

Signature:

Nuttapol Risangud

Date:

Abstract

The objective of this work was to synthesise potential polymeric materials to use in agricultural applications, particularly as pesticide carriers. Synthesis of solid microcapsules, which contain hydrophobic pesticides, from functional polymers, was the primary goal. In addition, promising materials such as poly(dimethylsiloxane) (PDMS) and acid-labile containing polymers were also explored. The extraordinary reactivity of isocyanates towards nucleophiles offers an interesting synthetic tool as a catalyst-free reaction. Unfortunately, the high reactivity of isocyanate during the polymerisation process is a major concern, thus a facile approach in order to synthesise stable functional polymer was first investigated.

Chapter 2 details the synthesis of two types of isocyanate side chain containing copolymers, poly(methyl methacrylate-*co*-isocyanatoethyl methacrylate) (P(MMA_m-*co*-IEM_n)) and poly(benzyl methacrylate-*co*-isocyanatoethyl methacrylate) P($BnMA_m$-*co*-IEM_n), via Cu(0)-mediated controlled radical polymerisation. Both copolymers were functionalised with dibutylamine, octylamine, and (R)-(+)-α-methylbenzylamine, which further proved the successful incorporation of the isocyanate groups. Subsequently, P($BnMA_m$-*co*-IEM_n) was used for the fabrication of liquid core microcapsules via an oil-in-water interfacial polymerisation with diethylenetriamine as a crosslinker.

Furthermore, chapter 3 illustrates the synthetic route of solid microcapsules containing hydrophobic pesticides; this illustrates the incorporation of biodegradable materials, modern controlled radical polymerisation techniques and isocyanate chemistry. An α, ω-poly (ε-caprolactone) SET-LRP initiator is first prepared by esterification to obtain a degradable halide initiator. Subsequently, biodegradable P($BnMA_n$-*co*-IEM_n) was polymerised via the conditions from chapter 2. An isocyanate-containing copolymer was used to fabricate a microcapsule which consists of imidacloprid (IMI), followed by water removal via spray dryer.

Chapter 4 details an efficient tool to synthesise an amphiphilic copolymer containing PDMS. The versatility of hydrosilylation has been exploited for the preparation of an ABA block copolymer of PDMS and poly(ethylene glycol) methacrylate (PEGMA), which can be potentially used to prepare polymeric micelles. Also, to

demonstrate the adaptability of this method, different methacrylates and vinyl terminated methacrylic macromonomers were applied to modified hydride terminated PDMS.

Finally, the α, ω-hydroxyl terminated poly(acetal) SET-LRP initiator was synthesised from the condensation and esterification reaction. A favourable Cu(0)-mediated controlled radical polymerisation and degradation under an acidic conditions of acetal initiator was affirmed. Thus, this offers a great opportunity of using this initiator to synthesise isocyanate-containing copolymers, certainly, an acid-labile microcapsule to use as an agrochemical carrier is potentially achievable.

Abbreviations

AIBN – 2,2 -azobis(2-methylpropionitrile)

AI – active ingredients

ATRP – atom transfer radical polymerisation

Aza – azadirachtin

BiBB – α-bromoisobutyryl bromide

BnMA – benzyl methacrylate

BOP – benzoyl peroxide

CL – caprolactone

CMC –critical micelle concentration

CRFs – controlled release formulations

CTA – chain transfer agent

DCM – dichloromethane

DCTB – trans-2-[3-(4-tert-Butylphenyl)-2-methyl-2-propenylidene] malononitrile

DETA –diethylenetriamine

DMS – dimethyl siloxane

DMSO –dimethyl sulfoxide

DP – degree of polymerisation

EBiB – ethyl-α-bromoisobutyrate

FRP – free radical polymerisation

GA – gum arabic

GTP – group transfer polymerisation

H_2PDMS – hydride terminated polydimethyl siloxane

IEM – 2-isocyanatoethyl methacrylate

IMI – imidacloprid

IPA – isopropyl alcohol

IR – infrared spectroscopy

LRP – living radical polymerisation

MA – methyl acrylate

MALDI-ToF MS – matrix-assisted laser desorption/ionization mass spectrometry

Me_6Tren – tris[2-(dimethylamino)ethyl]amine

MMA – methyl methacrylate

M_n – number average molecular weight

NIPAAm – *N*-isopropylacrylamide

NMP – nitroxide mediated polymerization

NMR – nuclear magnetic resonance

PAA – polyacrylic acid

PBnMA – poly(benzyl methacrylate)

PCL – poly(caprolactone)

PDA – polydopamine

PDMAEMA – poly(2-(dimethylamino)ethyl methacrylate)

PDMS – poly(dimethylsiloxane)

PEG – poly(ethylene glycol)

PEGMA – poly(ethylene glycol) methacrylate

PIEM – poly(isocyanatoethyl methacrylate)

PLA – polylactide

PLGA – poly(lactic-co-glycolic acid)

PMAA – polymethacrylic acid

PMDETA – *N, N, N, N, N* -pentamethyldiethylenetriamine

PMMA – poly(methyl methacrylate)

PVA – poly(vinyl alcohol)

RAFT – addition-fragmentation chain transfer polymerisation

RDRP – reversible deactivation radical polymerisation

ROP – ring-opening polymerisation

SDS – sodium dodecyl sulfate

SEC – size-exclusion chromatography

SEM – scaning electron microscopy

SET-LRP – single electron transfer living radical polymerisation

$Sn(Oct)_2$ – tin(II) ethyl hexanoate

TEA – triethylamine

TEMPO – 2,2,6,6-tetramethylpiperidynyl-*N*-oxy

TFA – trifluoroacetic acid

T_g – glass transition temperature

TGA – thermogravimetric analysis

THF –tetrahydrofuran

TREN – tris(2-aminoethyl) amine

UV-Vis – ultraviolet-visible

Chapter 1: Introduction

1.1 Research motivation

I was born in a farming family from an undeveloped area called Kalasin in Thailand. Agriculture is noted as the economic backbone of Thailand, and most other South East Asian countries, unfortunately, agronomics in those countries provides a deficient return resulting from several causes including; poor farmer education, land management, irrigation systems, and more importantly, expensive labour and agrochemical costs. As a polymer chemist, the improvement of my beloved motherland has been set as the major objective during my academic career. Different agrochemicals have been used to increase crop productivity because of high global demand, however, conventional agrochemical solutions may cause too many problems to both humans and the environment. Hence, all of my research interests are based on the development of new materials to use in agricultural applications.

1.2 Macromolecules and preparation techniques

The word *polymer* has been used to represent a macromolecule which is synthesised from small molecules, called monomers. Both natural and synthetic polymers have been used in many applications including pharmaceutical, sport, agriculture, industry, electronic and astronomy [1-7]. Tunable physical and chemical characteristics make polymeric materials interesting and gain a huge interest from the industrial point of view as well as in academic research. There are different methods to classify polymers, however, polymer structure is used herein. Homopolymers and copolymers indicate a macromolecule that consists of only one type of monomer and

more than one monomer respectively. Furthermore, a copolymer can further be classified into different classes such as statistical, alternating, block and graft copolymers.

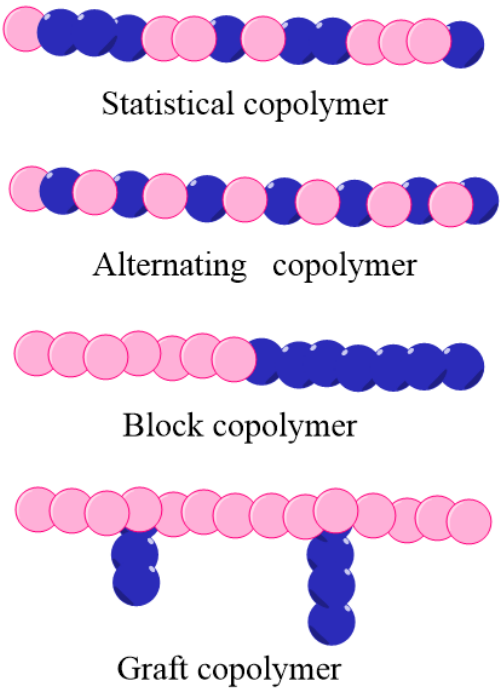

Figure 1.1: Schematic illustration of different types of copolymers.

Macromolecular preparations from monomers normally fall into two main polymerisation techniques: step-growth and chain-growth polymerisation. Step-growth polymerisation (also called condensation polymerisation) occurs from the reaction of A and B monomers, where A and B proceed to form covalent bonds via chemical reaction, for example, polyester (diol and dicarboxylic acid) and polyamide (diamine and dicarboxylic acid). The formation of the polymers via condensation occurs as a single-step reaction and generates by-products such as water. Thus, high efficiency of water

removal is required to achieve the polymer at a desired molecular weight for this method of synthesis.

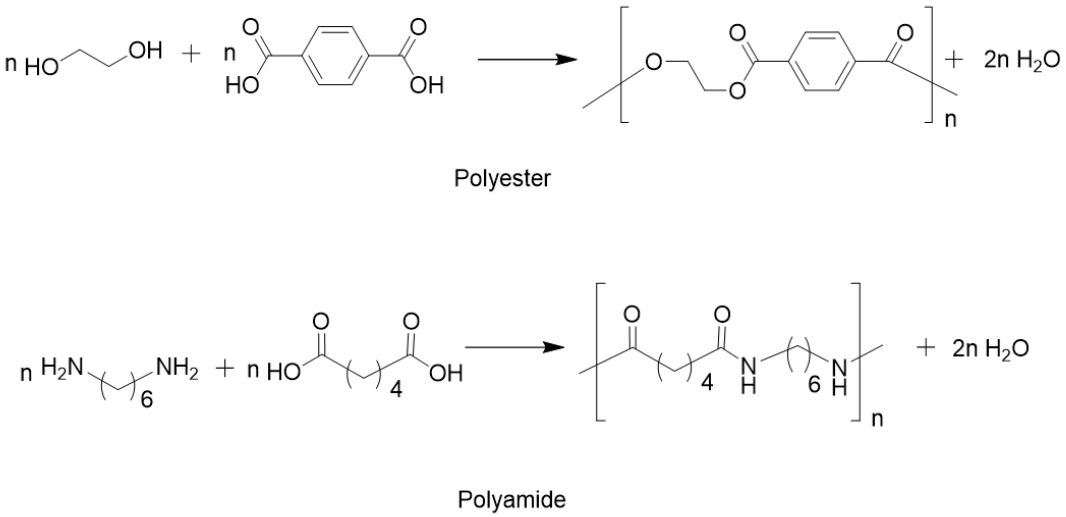

Figure 1.2: Examples of polymer synthesis (polyester and polyamide) via condensation reaction.

Conversely, chain-growth polymerisation (also known as addition polymerisation) occurs via an addition reaction, often via an active radical centre reacting with vinyl monomers, for example, ethylene (polyethylene), styrene (polystyrene) and methyl methacrylate (polymethyl methacrylate). Notably, ring-opening polymerisation of cyclic monomers (and active centre reacts with monomers via opening cyclic ring) is also classified as an addition polymerisation. The degree of polymerisation depends on the number of used monomers. The active radical centre forms via an initiation reaction. Subsequently, the active chains are generated by the reaction of initiator radical to monomers. Thus, high molecular weight polymers can be immediately obtained unless termination reactions happen. The details of chain-growth

polymerisation will be presented in the following section with an example of a free radical polymerisation.

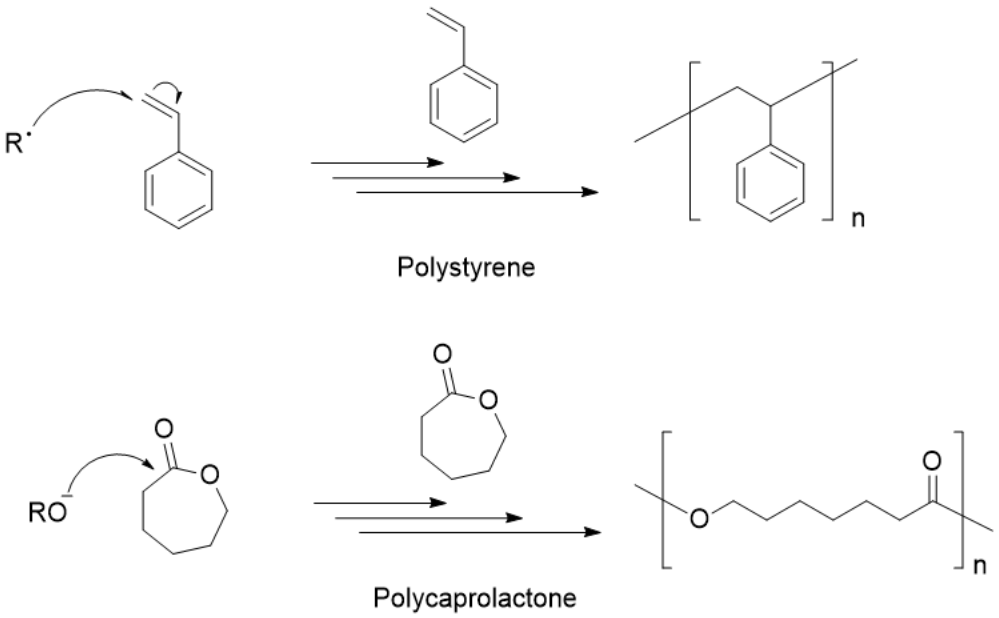

Figure 1.3: Examples of polymer synthesis via chain-growth polymerisation.

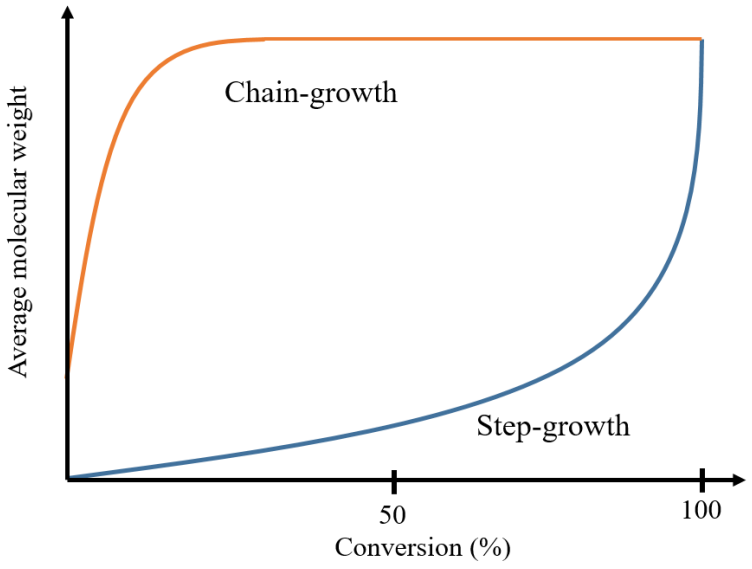

Figure 1.4: Plots of average molecular weight against monomer conversion for step-growth and chain-growth polymerisation.

1.2.1 Step-growth polymerisation

Step-growth polymerisation happens through a series of steps. The size of the macromolecule is typically represented via the degree of polymerisation (DP) in which step-growth polymerisation is usually displayed regarding the extent of reaction (p): the mole fraction of reacted functional group. Thus, the unreacted functional group fraction is represented by the term 1-p. For example, considering the polymerisation of A and B monomer in which A reacts with B to form AB i-mer, the number average degree of polymerization (DP_n) is considered from the ratio of the total number of initial functional groups A ($[N]^0$) to the number of functional groups A at any extent of reaction ($[N]^t$).

$$\text{Degree of polymerisation} = \frac{[\mathrm{N}]^0}{[\mathrm{N}]^\mathrm{t}}$$

Considering the kinetics of the reaction of A and B monomers, to simplify the kinetic scheme the reactivity of functional A and B is equal.

$$\mathrm{A} + \mathrm{B} \longrightarrow \mathrm{AB}$$

The overall polymerisation rate is k[A][B] (catalyst step growth polymerisation), which the same reactivity and monomer A and B is represented as M.

$$\text{Rate of Polymerisation} = k[M]^2$$

$$\frac{d[M]}{d[t]} = k[M]^2$$

$$\int_{M_0}^{M_t} \frac{d[M]}{[M]^2} = \int_0^t k dt$$

$$\frac{1}{[M]_t} = kt + \frac{1}{[M]_0}$$

$$\frac{[M]_0}{[M]_t} = kt[M]_0 + 1$$

Therefore, the degree of polymerisation can be derived as follows:

$$\text{Degree of polymerisation} = \frac{1}{(1-p)} = \ kt[M]_0 + 1$$

1.2.2 Chain-growth polymerisation

Chain-growth polymerisation occurs with the initiation of active growth centres which subsequently react with a reservoir of vinyl monomers. At least three reactions occur in chain-growth polymerisation: initiation, propagation and termination. Free radical polymerisation (FRP) is used herein to illustrate the characteristics of this type of polymerisation. The first step of a free radical polymerisation is initiation in which a radical is generated from initiator decomposition. Consequently, an initiating primary radical is formed resulting from the addition reaction of radical initiator and monomer. There are different types of initiators such as organic peroxides, hydroperoxides, redox systems, electromagnetic radiation, and azo compounds. A commonly used type initiator is an organic peroxide such BPO (benzoyl peroxide), because of the low dissociation energy of the O-O bond that breaks to generate primary oxygen centered radicals. Furthermore, azo compounds are also favoured due to the stability of N_2 which drives the decomposition of initiator to form cyano isopropyl radicals. The efficiency (*f*) of the initiator, the ratio of radicals incorporated into the polymer and the total primary radicals generated form the initiators should be considered.

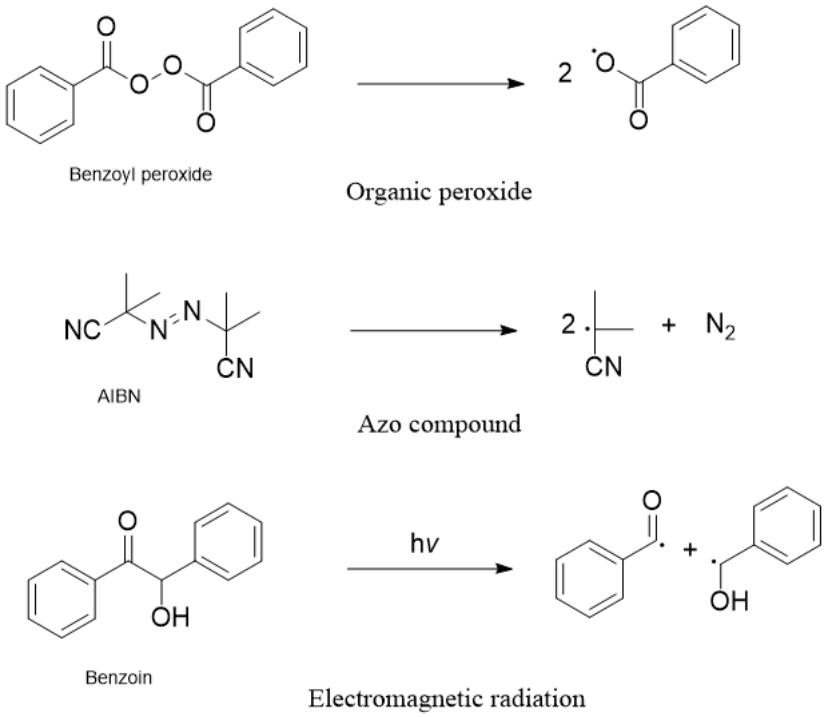

Figure 1.5: Examples of free radical initiation reactions.

Considering the decomposition of azo or peroxide initiator, one molecule generates two active radicals:

$$\text{I-I} \longrightarrow 2\text{I}^{\bullet}$$

The concentration of active radicals at a particular reaction time (t) is represented as:

$$R_i = \frac{d[I^{\bullet}]}{dt} = 2fk_d[I]$$

Where *f* is the initiator efficiency. The next step is propagation in which primary radicals react with monomers (M) to generate active chains.

$$I^{\bullet} \longrightarrow IM^{\bullet} \longrightarrow P^{\bullet}$$

The rate of propagation is described as:

$$R_p = \frac{-d[M]}{dt} = k_p[M][P^\bullet]$$

Finally, the termination processes take place, however, this process also occurs during the polymerisation resulting in the removal of active radicals. There are two principal modes of termination: combination and disproportionation, as shown in figure 1.6.

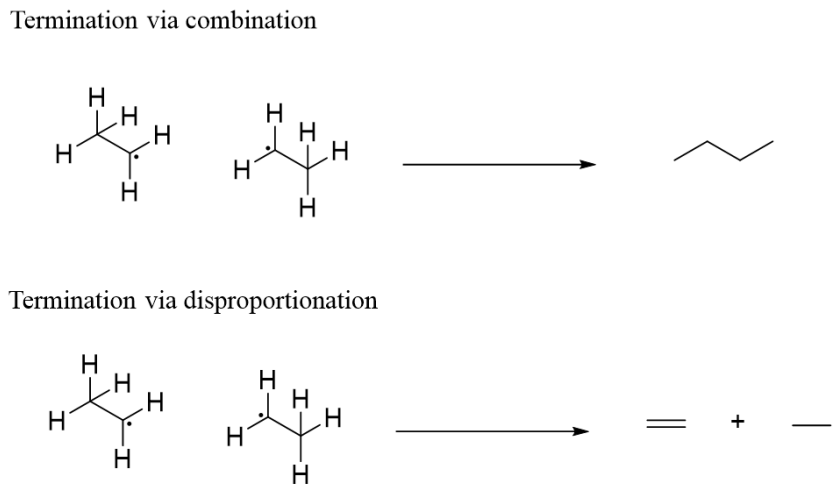

Figure 1.6: Examples of combination and disproportionation termination reactions.

One termination reaction requires two polymer radicals. Thus the rate of termination is represented as:

$$R_t = \frac{-d[P^\bullet]}{dt} = 2k_t[P^\bullet]^2$$

In order to determine the rate of propagation, a steady state of the total radical concentration is assumed. Thus, a constant total concentration of free radical is calculated from the equal rate of initiation and termination, this is named stationary-state radical concentration.

$$2fk_d[I] = 2k_t[P^\bullet]^2$$

Or

$$[P^\bullet] = \sqrt{f\left(\frac{k_d}{k_t}\right)[I]}$$

Finally, the propagation rate of free radical polymerisation can be derived as:

$$R_p = k_p[M]\sqrt{f\left(\frac{k_d}{k_t}\right)[I]} = k_{app}[M][I]^{1/2}$$

1.2.3 From free radical polymerisation to controlled radical polymerisation

Free radical polymerisation (FRP) has great industrial interest due to its robustness and ease of scale up. Nevertheless, FRP usually provides relatively broad molecular weight distributions due to a lack of selectivity, which leads to bimolecular termination and disproportionation in the polymerisation as well as a lack of end-group fidelity which results in limitations for certain applications. Living radical polymerisation (LRP) offers an advantage over several limitations of FRP, particularly the variety of polymer architectures and functionalities. An ideal living radical polymerisation is described as a chain-growth reaction with no transfer reaction. The kinetic scheme for LRP can be compared to the FRP reaction as follows:

Initiation step:

$$M + I \longrightarrow P_1^\bullet$$

Propagation step:

$$P_1^{\bullet} + M \longrightarrow P_2^{\bullet}$$

$$P_i^{\bullet} + M \longrightarrow P_{i+1}^{\bullet}$$

The rate of propagation step:

$$R_p = \frac{-d[M]}{dt} = k_p[M][P^{\bullet}]$$

To follow the distribution of polymer chains after the propagation reaction (i-mers), the change of concentration of active radical needs to be considered. In addition, the term of kinetic chain length (v) (the ratio of the number of propagation steps to initiation step) is also introduced.

Considering when i = 1

$$-\frac{d[P^{\bullet}]}{dt} = k_p[M][P^{\bullet}]$$

Chain rule is applied:

$$\frac{d[P^{\bullet}]}{dt} = \frac{d[P^{\bullet}]}{dv}\frac{dv}{dt}$$

The change of kinetic chain length over time is detailed as follows:

$$\frac{dv}{dt} = -\frac{1}{[I]_0}\frac{d[M]}{dt} = k_p[M]$$

$$\frac{d[P^{\bullet}]}{dt} = \frac{d[P^{\bullet}]}{dv}k_p[M]$$

Therefore,

$$-\frac{d[P_1^{\bullet}]}{dv} = [P^{\bullet}]$$

$$\int \frac{1}{[P^{\bullet}]}\, d[P^{\bullet}] = -\int dv$$

$$[P_1^{\bullet}] = [P_1^{\bullet}]_0 e^{-v} = [I]_0 e^{-v}$$

The concentration of i-mers radical (i = 1) as the function of kinetic chain length is represented by the above equation, however, the chain length distribution of the polymers is complicated due to the active radical chain reacting with the monomer to generate i-mer.

$$P_1^{\bullet} + M \longrightarrow P_2^{\bullet}$$

$$P_2^{\bullet} + M \longrightarrow P_3^{\bullet}$$

$$\frac{d[P_2^{\bullet}]}{dt} = k_p[M][P_1^{\bullet}] - k_p[M][P_2^{\bullet}]$$

$$\frac{d[P_2^{\bullet}]}{dt} = k_p[M]([P_1^{\bullet}] - [P_2^{\bullet}])$$

$$\frac{d[P_2^{\bullet}]}{dv} + [P_2^{\bullet}] = [P_1^{\bullet}] = [I]_0 e^{-v}$$

$$\frac{d[P_2^{\bullet}]}{dv} + [P_2^{\bullet}] = [I]_0 e^{-v}$$

$$[P_2^{\bullet}] = v[I]_0 e^{-v}$$

When i = 3

$$\frac{d[P_3^{\bullet}]}{dt} = k_p[M][P_2^{\bullet}] - k_p[M][P_3^{\bullet}]$$

$$\frac{d[P_3^{\bullet}]}{dt} = k_p[M]([P_2^{\bullet}] - [P_3^{\bullet}])$$

$$\frac{d[P_3^{\bullet}]}{dv} + [P_3^{\bullet}] = [P_2^{\bullet}] = v[I]_0 e^{-v}$$

$$\frac{d[P_3^{\bullet}]}{dv} + [P_3^{\bullet}] = v[I]_0 e^{-v}$$

$$[P_3^{\bullet}] = \frac{1}{2} v^2 [I]_0 e^{-v}$$

The population of i-mer during polymerisation is described by the kinetic chain length as follows:

$$[P_i^{\bullet}] = \frac{1}{(i-1)!}\, v^{i-1}[I]_0 e^{-v}$$

This leads to the population of activated radicals (X_i) in polymerisation (i-mer), the ratio of mole of i-mer to the initial concentration of initiator. Thus, the mole fraction distribution of i-mer in function of kinetic chain length is represented as follows:

$$[x_i] = \frac{v^{i-1}e^{-v}}{(i-1)!}$$

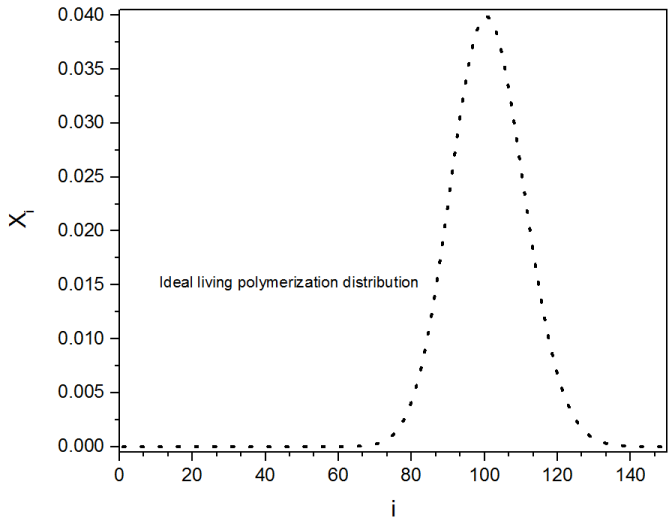

Figure 1.7: The distribution of chains in an ideal living radical polymerization when v = 100.

The concept of living radical polymerisation offers a powerful tool to synthesise macromolecules with a well-defined material architecture as well as chemical and physical properties, however, termination reactions cannot be disregarded in LRP. Thus, the term of "reversible deactivation radical polymerisation" (RDRP) is often more

favoured than LRP. RDRP benefits from the advantages of free radical such as fast polymerisation, easy to scale up, and a wide range of suitable monomers, furthermore, living radical polymerisation characteristics, including narrow molecular weight distribution, complex polymer architecture, and end-group fidelity, also contribute in RDRP. The key process of the RDRP technique is a reversible step between dormant species and active radicals, with a very high concentration of dormant species compared to active species. Notably, the significant low concentration of active radical species is also necessary. A reversible and dynamic equilibrium process is typically accommodated by a catalyst or physical stimulus.

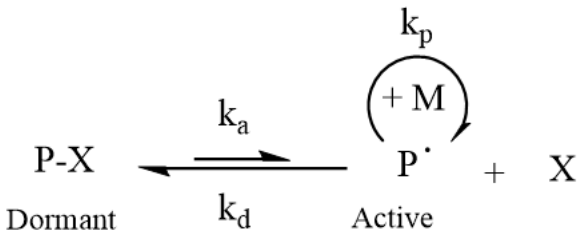

Figure 1.8: Reversible and dynamic equilibrium between active radical growing species and dormant species.

The kinetic scheme of reversible deactivation radical polymerisation (RDRP) is illustrated below:

Propagation step:

$$-\frac{d[M]}{dt} = k_p[M][P_i^{\bullet}]$$

$$-\frac{d[M]}{[M]} = k_p[P_i^{\bullet}]dt$$

When $[P_i^{\bullet}]$ is constant:

$$\frac{d[M]}{[M]} = -k_{app}dt$$

$$\int_{M_0}^{M_t} \frac{d[M]}{[M]} = \int_{0}^{t} -k_{app}dt$$

$$ln\frac{[M]_0}{[M]_t} = k_{app}t$$

1.2.4 Copper-mediated polymerisation

Transition metals have been commonly used in many organic addition reactions to form chemical bonds, for example, carbon-carbon, carbon-halogen, and carbon-hydrogen [8, 9]. The concept of using transition metals in radical polymerisations applies from the radical addition reaction, for example, the reaction between an olefin and carbon tetrachloride by using a ruthenium (II) complex as the catalyst [10]. However, the discovery and the development of transition metals including ruthenium, cobalt and copper as efficient catalysts for controlled radical polymerisation began in early 1990 with the polymerisation of vinyl monomers [11-18]. Thousands of publications describing transition metal-catalysed controlled polymerisation have been published [19-21]. Active radicals are generated by the homolytic bond cleavage of a carbon-halogen bond in an initiator [22].

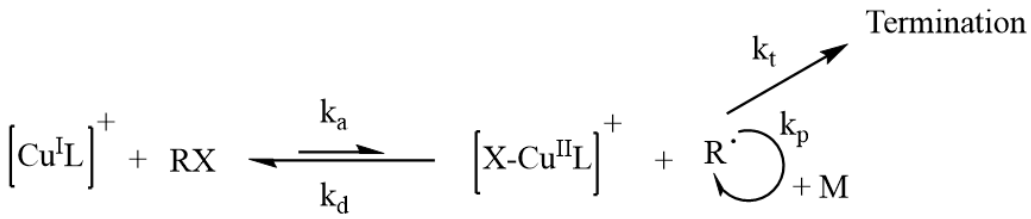

Figure 1.9: Model of copper mediated polymerisation technique.

Many transition metals, especially from groups 8-11 including ruthenium, iron, nickel and copper, have been used in controlled radical polymerisation. However, copper complexes are most commonly used and are often highly effective. The most widely used copper(I) catalysed polymerisation is known as atom transfer radical polymerisation (ATRP) [23,24]. There are several factors to consider when looking at ATRP efficiency, including the monomer concentration and ligand/copper complex, monomer solubility, monomer and ligand compatibility. Conversely, Cu(0) is introduced for use in controlled radical polymerisation via a nascent copper(0) particle, which is usually produced *in situ* by a rapid disproportion from Cu(I) in the presence of nitrogen donor ligands, usually in a polar solvent such as dimethylsulfoxide (DMSO), methanol (MeOH), 2-isopropanol (IPA) or ethanol (EtOH). During the activation process of the carbon-halide initiator, two metal mediated reactions occur: production of active radical from the reaction of Cu (0) and formation of a deactivated radical and a Cu(II) halide. Both processes occur via a one electron transfer mechanism with significant low activation energy thus, polymerisation can occur at low temperature. Controlled radical polymerisation from Cu (0) is often named as single electron transfer living radical polymerisation (SET-LRP).

1.2.5 Single electron transfer living radical polymerisation (SET-LRP)

SET-LRP offers well-defined polymer architectures, molecular mass, narrow molar mass dispersity and high-end group fidelity polymers [25]. Since SET-LRP was introduced two decades ago, many publications have described this polymerisation

technique for a variety of monomers including acrylates, methacrylates, and acrylamides [26-31]. In addition, the capacity of *in situ* chain extension and block copolymerisation to often be carried out within an hour at ambient temperature results in SET-LRP being used over other reversible deactivation radical polymerisation techniques. Notwithstanding, monomer and solvent are considered as the major limitations of SET-LRP. Highly reactive radicals of some monomers, such as vinyl chloride, show difficulty in obtaining well-defined polymers. On the other hand, less reactive monomers such as *N*-vinylpyrrolidone and vinyl acetate (VP) are challenging to be polymerised. The copper (0) catalyst can be employed in different forms including copper powder and copper wire, interestingly, copper wire provides some advantages such as polymerisation rate, catalyst preparation, and purification processes [32, 33]. In general, the copper wire surface does not contain 100% of Cu (0). The copper oxide complex (Cu_xO) is usually detected due to the reaction of copper wire with oxygen in the atmosphere. The slow polymerisation rate during an induction period is the initial evidence of this assumption [34-37], thus, removal of Cu_xO is a crucial procedure. A simple method can be exploited via different chemicals including hydrazine, nitric acid, glacial acetic acid, and hydrochloric acid [38]. Notably, acid is more favoured to use due to lower toxicity as compared to hydrazine.

Most SET-LRP initiators contain a halide leaving group and an electron-withdrawing substituent. The polymerisation efficiency directly depends upon both the physical and chemical properties of the initiator, including a solubility match with monomers, activation energy to generate radical, and stability/reversibility of the

radical. Notably, solvent selectivity is a crucial part for SET-LRP polymerisation. Dimethyl sulfoxide (DMSO) [39-41], dimethyl formamide (DMF) [42-44], and aqueous media [30, 45-48] have all been intensively studied because well-defined polymers with narrow molar mass distribution and high end-group functionality can be obtained. In addition, alcohols, including EtOH, IPA, MeOH, and t-BuOH [49-53] are also reported as good solvents for Cu(0)-mediated polymerisation. Interestingly, polymerisation in poor disproportionation solvents, including toluene, acetone, acetonitrile (MeCN) and dichloromethane (DCM), shows that the disproportionation process is important for Cu(0)-mediated controlled radical polymerisation. The lack of end group fidelity and broad molar mass distribution indicates that solvent plays a vital role in polymerisation [54, 55].

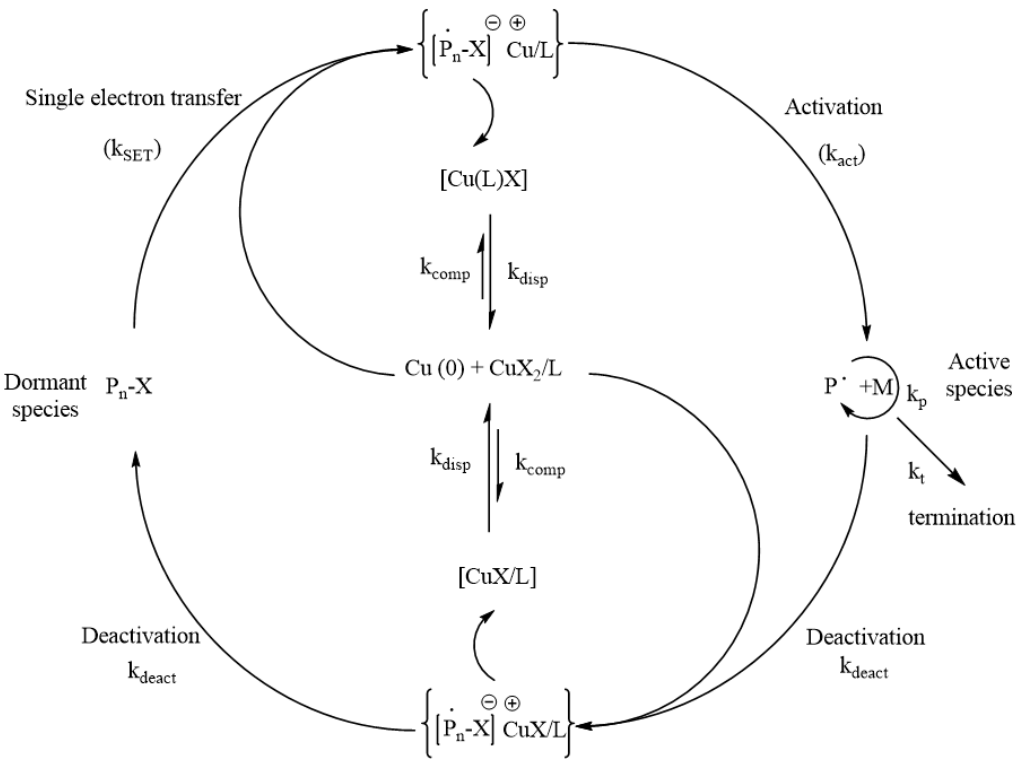

Figure 1.10: The proposed mechanism of SET-LRP.

Noteworthy, polymer synthesis without further complicated purification offers an advantage, thus binary phase polymerisation has been investigated to minimise the cost of polymerisation. Cu(0)-mediated polymerisation of butyl acrylate (BA) in DMSO was reported; a polymer layer separated from the solution mixture after reaching a certain molecular weight [56]. In the proposed SET-LRP mechanism (Figure 1.10), the ligand plays an important role during the disproportionation and comproportionation process. Interestingly, the optimisation of the [initiator]: [ligand]: Cu(II)Br_2 ratio is required to avoid bimolecular termination to obtain a well-defined polymers [57, 58]. The key feature of deactivated reversible radical polymerisation is to maintain the dormant species at high concentration compared to the active species. *N*-Containing ligands such as tris[2-(dimethylamino)ethyl]amine (Me_6Tren) are the most widely exploited to use as a catalytic system for SET-LRP [26, 27, 40, 46, 52, 59], in addition, other commercial ligands including tris(2-aminoethyl)amine (TREN) [48,60] and *N, N, N′ , N′′ , N′′* -pentamethyldiethylenetriamine (PMDETA) [61-64] also have been reported as good ligands for Cu(0)-mediated polymerisation with respect to end-group fidelity and molecular mass distribution.

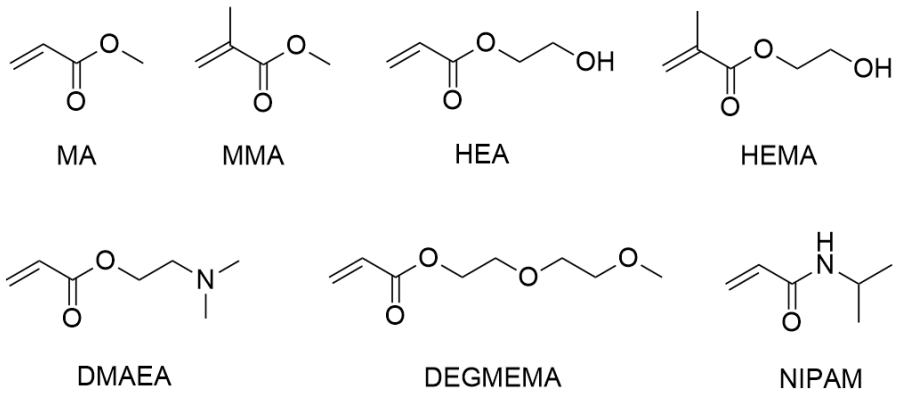

Figure 1.11: Common monomers in SET-LRP.

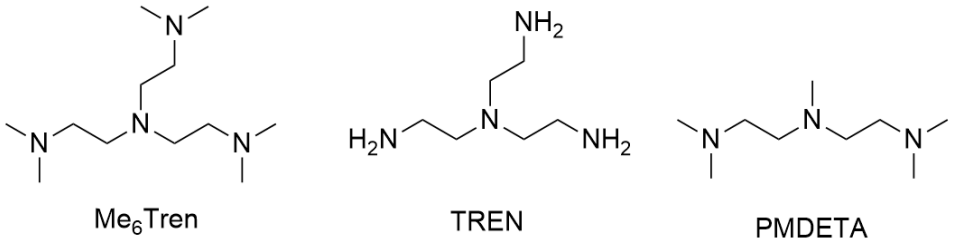

Figure 1.12: Common ligands in SET-LRP.

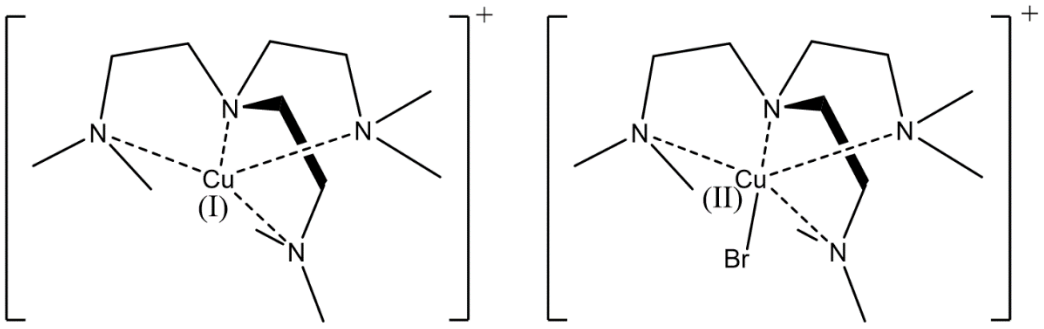

Figure 1.13: Schematic diagram of Me_6Tren with CuBr (left) and $CuBr_2$ (right).

1.2.6 Other RDRP polymerisation techniques

There are also other RDRP techniques apart from copper-mediated polymerisation that have been introduced and exploited to give well-defined polymers in the last few decades including, reversible addition-fragmentation chain transfer polymerisation (RAFT), nitroxide mediated polymerisation (NMP) and ring opening polymerisation (ROP).

NMP, was first introduced in the early 1980s [65] and expanded by Georges *et. al.* in 1993 describing the polymerisation of styrene by using benzoyl peroxide (BOP)/2,2,6,6-tetramethylpiperidynyl-N-oxy (TEMPO) as initiator [66]; it is classified as RDRP due to the reversibility of the process. An NMP initiator is known as an alkoxyamine; homolytic cleavage of the alkoxyamine starts the polymerisation via the radical addition reaction of a radical carbon centre to a vinyl monomer. Subsequently, alkoxyamines are reformed to maintain the dormant species at high concentration (Figure 1.14). Different NMP initiators have been introduced, for example TEMPO and 2,2,5-trimethyl-3- (1-phenylethoxy)-4-phenyl-3-azahexane. A wide range of monomers can be polymerised via this technique, mostly vinyl monomers such as styrene, acrylates and methacrylate derivatives [67].

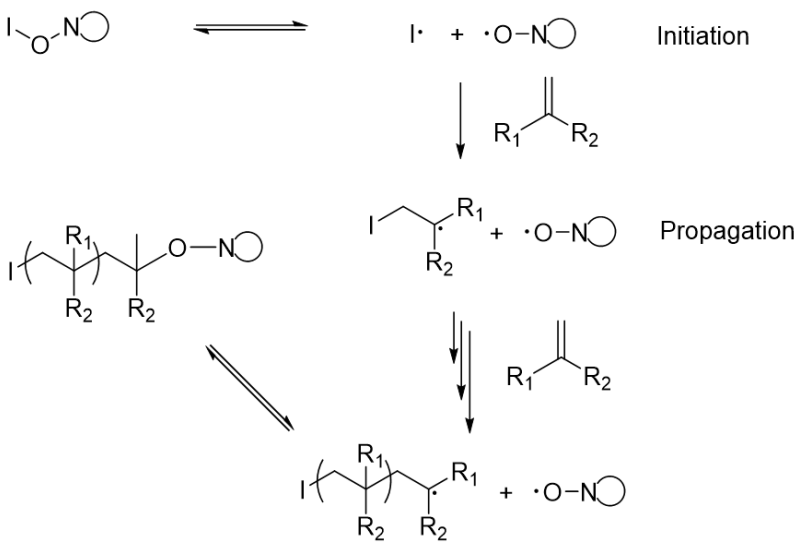

Figure 1.14: The proposed mechanism of NMP.

RAFT was discovered at Commonwealth Scientific and Industrial Research Organization (CSIRO), Australia, in 1998 [68]. The concept of RAFT is the combination of conventional free radical polymerisation and the reversible chain transfer process by chain transfer agent (CTA). Trithioester compounds such as dithiobenzoate, trithiocarbonate and dithiocarbamate are generally used to assist the chain transfer process. The polymerisation is initiated via radical generation from a conventional FRP initiation process. The main advantage of RAFT is a variety of accessible monomers such as styrene, acrylates, methacrylate, and vinyl acetate [69, 70]. Of note is that specific CTA and monomers are required to obtain a controlled polymerisation.

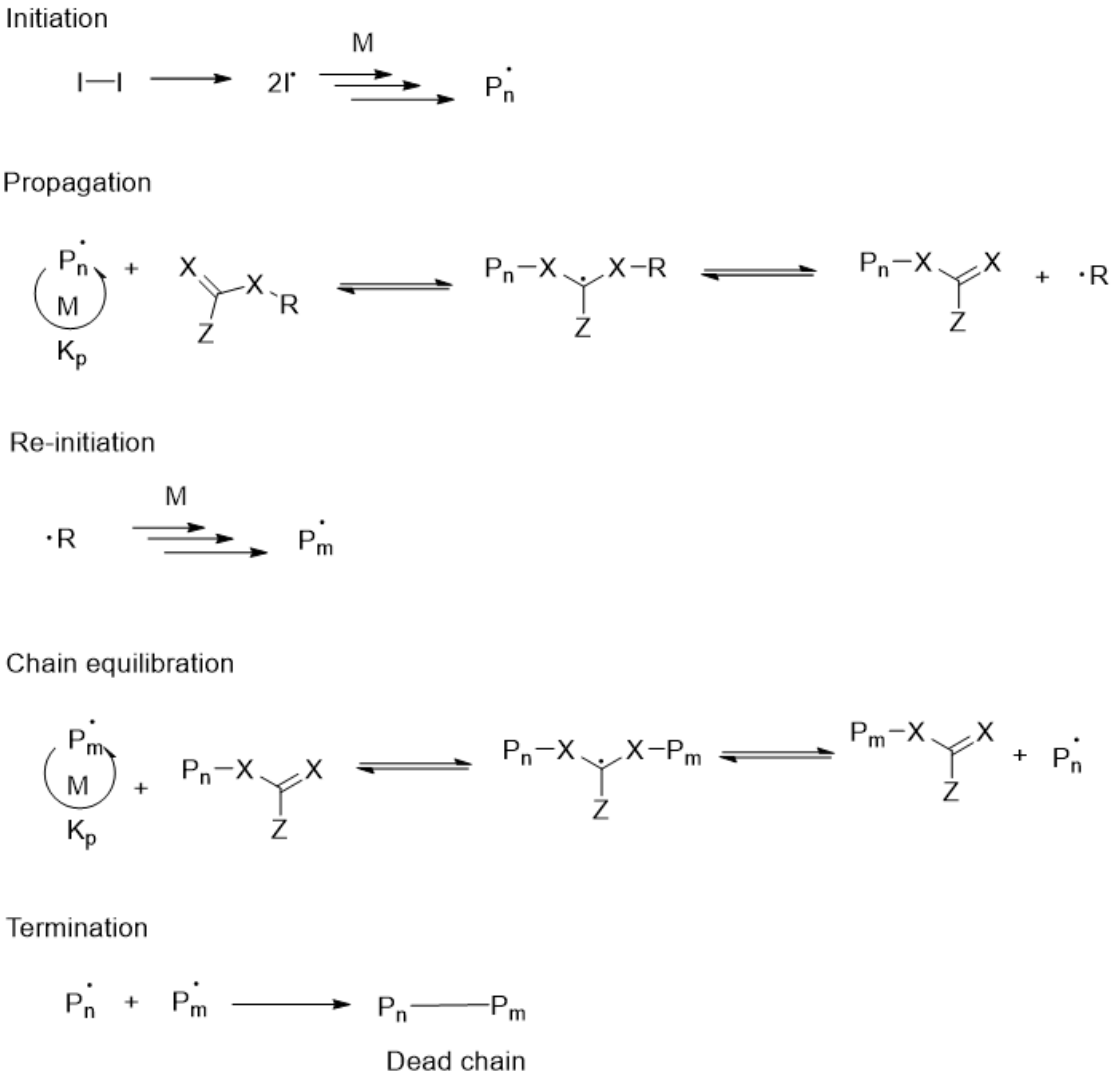

Figure 1.15: The proposed mechanism of RAFT.

1.2.7 Copolymers

Chain-growth polymerisation, particularly reversible deactivation radical polymerisation (RDRP), provides a broad range of accessible polymer architectures compared to step-growth polymerisation. Conventional free radical polymerisation is an effective technique to synthesise simple copolymers such as random copolymers, however, this technique struggles to provide more complex polymer architectures.

Conversely, RDRP has been known as a powerful tool to exploit complicated polymer structure such as block, graft and star copolymers [71-73]. In general, block copolymers are prepared via different approaches such as macroinitiators and chain extension. Notably, polymerisation via RDRP techniques offers an excellent possibility for chain extension because of high end-group fidelity [27, 74-77]. Copolymer synthesis via macroinitiator techniques will be represented in a later chapter of this thesis; homopolymers are usually functionalised by using organic reactions to obtain a macroinitiator [78-80], however, the difficulty of synthesis of complex copolymers by FRP is represented via the different reactivity of monomers.

$$M_1^{\bullet} + M_1 \longrightarrow M_1M_1^{\bullet}$$

$$M_1^{\bullet} + M_2 \longrightarrow M_2M_1^{\bullet}$$

$$M_2^{\bullet} + M_1 \longrightarrow M_1M_2^{\bullet}$$

$$M_2^{\bullet} + M_2 \longrightarrow M_2M_2^{\bullet}$$

The rate of reaction:

$$R_{11} = k_{11}[M_1^{\bullet}][M_1]$$

$$R_{12} = k_{12}[M_1^{\bullet}][M_2]$$

$$R_{21} = k_{11}[M_2^{\bullet}][M_1]$$

$$R_{22} = k_{11}[M_2^{\bullet}][M_2]$$

The change of concentration of monomer M_1 and M_2:

$$-\frac{d[M_1]}{dt} = k_{11}[M_1^{\bullet}][M_1] + k_{21}[M_2^{\bullet}][M_1]$$

$$-\frac{d[M_2]}{dt} = k_{12}[M_1^{\bullet}][M_1] + k_{22}[M_2^{\bullet}][M_2]$$

To simplify the copolymerisation reaction, the stationary-state of radical concentration is employed:

$$k_{12}[M_1^{\bullet}][M_2] = k_{21}[M_2^{\bullet}][M_1]$$

This leads to the copolymer composition equation as shown below:

$$\frac{d[M_1]/dt}{d[M_2]/dt} = \frac{[M_1]}{[M_2]} \frac{\left(\frac{k_{11}}{k_{12}}\right)[M_1] + [M_2]}{\left(\frac{k_{22}}{k_{12}}\right)[M_2] + [M_1]}$$

$$r_1 = \frac{k_{11}}{k_{12}}, r_2 = \frac{k_{22}}{k_{21}}$$

The monomer reactivity ratio is described as r; the possibility of monomer to either self-propagate or cross propagate. This term is usually used to predict copolymer structure, for example, the alternating copolymer is synthesised when r value is close to zero. In addition, block copolymer from free radical polymerisation can be obtained when $r_1 * r_2$ is ≥ 1 (each radical trends to self-propagate and eventually cross-propagate). Interestingly, the reactivity of the monomer depends upon the temperature. To conclude this section, reversible deactivation radical polymerisation offers an extensive copolymer design with a facile polymerisation process.

1.3 Current pesticide encapsulations

The world's population has dramatically increased over the past few decades which has led to a remarkable increase in food demand [81]. Consequently, different state-of the-art technologies, for example, fertilisers, herbicides, pesticides, and growth

hormones have been introduced in the agricultural field to enhance and maximise crop production [82-87]. More than one million tonnes of agrochemicals are applied during farming each year. However, only small amounts of chemicals reach their targets because of several factors, including degradation by photolysis, leaching, hydrolysis, evaporation, washing away by rain, and microbial activity. Thus, more chemicals are applied to maintain the effective level than should be required, which increases an ecosystem toxicity. Hence, the term controlled release formulations (CRFs) has been introduced to offer a sustainable release as well as reduce an environmental concern [88-90]. Pesticides are commonly prepared from different formulations such as emulsion, suspension, and solution [91]. Unfortunately some formulations, such as wettable powders, have recently been banned from agricultural registration authorities due to safety concerns, thus, polymeric pesticide encapsulation has been introduced to provide a safer and more stabilised formulation [92-94].

1.3.1 Polymer based materials

Polymeric encapsulation, to apply as a guard material for agrochemical protection, is widely used and intensively researched. There are many active ingredients (AI) which are encapsulated by polymer based techniques including polymeric micro- and nanocapsule, micro- and nanogel, and micelles. These smart delivery systems offer an advantage over conventional agrochemicals, particularly in improving chemicals lost during an application before reaching the target.

Formation of micelles arises from the different solubility properties of an amphiphilic copolymer in binary phase solutions. Characteristics of the micelle and their

encapsulation properties depend upon how they are prepared; a micelle is an ideal vehicle for the encapsulation of hydrophobic agrochemicals, however, to encapsulate hydrophilic chemicals inverse-micelles have been used. Several factors could tune micelle characteristics, including, appropriate solvents, copolymer concentration, amphiphilic blocks, the degree of polymerisation, and polymer architectures. Interestingly, the radius of gyration is directly proportional to the hydrophilic part of the copolymer, in other words, an amphiphilic copolymer with higher degree of hydrophilic segment provides a larger micelle. Materials that have been widely used to prepare the hydrophilic segment of micelles are often based on polyethylene glycol (PEG) due to several advantages, including, their high-water solubility, cost effectiveness, and low toxicity to both humans and the environment [95-97].

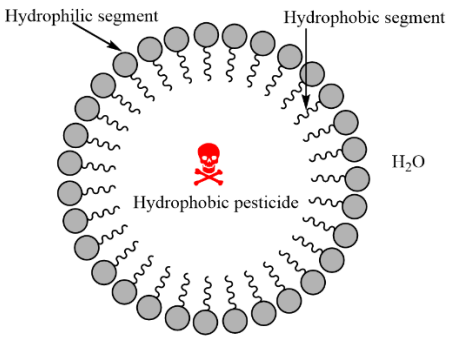

Figure 1.16: Schematic representation of micelle formation to encapsulate a hydrophobic pesticide.

Different insecticides have been entrapped via micelle formation to protect them from environmental degradation and to increase the solubility and stability of water insoluble pesticides. The concept of using a surfactant to enhance the stability of

pesticides began a long time ago; Lukas Schreiber investigated the influence of cuticular wax of barley leaves (tetracosanoic acid) on stabilisation of pentachlorophenol (PCP) [98]. An amphiphilic copolymer containing a PEG hydrophilic segment offered outstanding properties, including tremendous micelle stability resulting from its water solubility. The PEG derivative copolymers have been widely used to capture several pesticides. A. C. Watterson and coworkers introduced amphiphilic copolymers for controlled release formulation of carbofuran [99]. They illustrated the carbofuran encapsulation via micelle formation; pesticide micelle formulation showed the improvement of insect control due to slow release. In addition, other insecticides, including imidacloprid, *β*-cyfluthrin, thiamethoxam, and triazophos, are also encapsulated via micelle formulation [100-104]. Similar micelle preparation methods were applied; a significant improvement on pesticide release was obtained after applying a polymeric micelle formulation compared to the commercial pesticide. In addition, amphiphilic chitosan carriers to deliver imidacloprid (IMI) was recommended by Min Li and colleagues. The result indicated a reasonable preservation of IMI in a PLA-chitosan formulation with a controlled release profiles [105]. Interestingly, many synthetic amphiphilic copolymers and surfactants have also been used to provide a controlled release micelle formulation. For example, an amphiphilic block copolymer of benzyl methacrylate (BnMA) and methoxyhexa (ethylene glycol) methacrylate (HEGMA) was synthesised via group transfer polymerization (GTP). Consequently, a micelle was formed to assemble diazinon [106]. In addition, other materials such as sodium dodecyl sulphate (SDS), Tween 20, modified clay and poly (succinimide) star copolymers, also

have been used to encapsulate different pesticides including chlorpyriphos and imidacloprid [107-109].

Micro- and nanogels are defined as the particles dispersion in an aqueous solution; a hydrogel is linked with either physical or chemical interactions. Micro- and nanogels with an encapsulation of hydrophobic active ingredients are formed as follows; amphiphilic copolymers are dispersed and form a controlled aggregation. Subsequently, several interactions between the hydrophobic active ingredient and polymer matrix, including electrostatic and Van der Waals forces, lead to high efficiency of hydrophobic active ingredient encapsulation. Some applications of using micro- and nanogel have been reported, particularly for application in medical, industrial, and agricultural fields [110-118]. Paula *et. al.* described the use of chitosan to synthesise nano-gels to entrap Lippia sidoides essential oil (commonly used as antimicrobial). The comparison of encapsulated oil and pure oil was studied with a slow release profile with the acceptable efficiency of larvae treatment reported [119].

Polymeric micro- and nanocapsules are also widely used to increase the agrochemical efficiency. Notably, the factor that makes polymeric capsules look promising to utilize in modern crop protection technology is that the material wall can be easily varied. A natural material, such as carbohydrate derivatives, offers a non-toxic by-product after degradation and can also be relatively low cost compared to synthetic polymers. Conversely, synthetic materials often degrade to release non-toxic fragments after a certain time, including poly (ethylene glycol) (PEG) and polycaprolactone (PCL).

Different techniques are commonly used to prepare micro- and nanocapsules, including emulsion polymerisation, layer-by-layer assembly, solvent evaporation, and interfacial polymerisation [120-124].

For example, sodium alginate has been used to prepare micro- and nanocapsules to encapsulate different pesticides including, imidacloprid (IMI), azadiractin (Aza), and chlorpyrifos [125-127]. Pesticide stability was significantly improved after encapsulation. Wenbing Zhang *et al*. introduced a controlled release formulation of prochloraz pesticide. The stability of pesticide was detected, although the microcapsules were treated under different conditions including UV radiation and alkaline solution. Interestingly, the slow release profile of prochloraz also was observed for up to 60 days [128]. In addition, using chitosan to entrap pesticides, with a reasonable loading efficiency as well as pesticide stability, has also been reported [129]. Noteworthy, synthetic polymers can also play a major role in agrochemical encapsulations, for example PEG, PCL, poly (methyl methacrylate) (PMMA), poly (benzyl methacrylate) (PBnMA), polydopamine (PA), and poly(lactic-co-glycolic acid) (PLGA) [130-136]. As an illustration, Wenbo Sheng *et al.* prepared an avermectin (AV) microcapsule composed of poly(2-(dimethylamino) ethyl methacrylate) (PDMAEMA) and polydopamine (PDA). They indicated that the sustainable release of the pesticide was observed [137].

1.4 Spray drying and encapsulated applications

Spray-drying is a powerful microencapsulation technique (single-step assembly) for different ingredients in many applications, for example, food materials, cosmetics, and agrochemicals [138-143]. The technique is the transformation of liquid to a dried powder [144]; four consecutive steps occur including, atomization, droplet-hot gas contact, evaporation of water, and powder-humidity separation. In the beginning, atomization produces a small liquid droplet to maximise the heat transfer of particle and hot air in the spray drying chamber. The droplet contacts with hot gas resulting in water evaporation; the temperature of the liquid droplet increases to a stable value caused by the heat transfer from the hot gas to particle droplet which provides a vapour pressure difference. Once the water content in the droplet reaches a critical value, dried product is immediately formed. Finally, dried powder is directly separated from humidity through the cyclone chamber, where the product stays at the base. On the other hand, less dense product (humidity) is removed [145,146]. Different forms can be applied via this technique including emulsion, suspension, solution, and slurries [147-151]. Probably the most common example of this technique is dried milk manufacture [152-153].

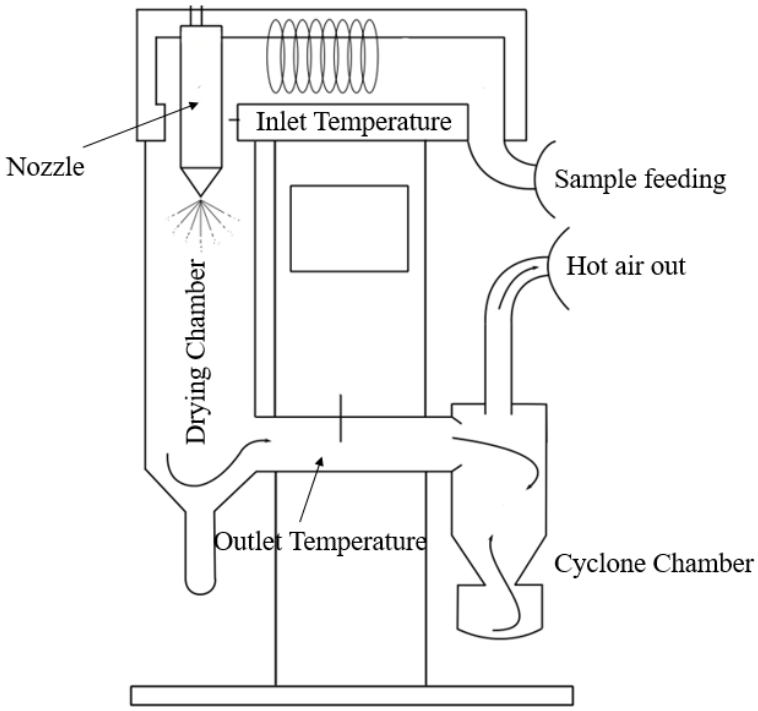

Figure 1.17: Schematic diagram of spray dryer operation.

The spray drying process is commonly used for the encapsulation of oils, in general, samples are prepared from micro/nanoemulsion. The surfactant which acts as the emulsion emulsifiers is carefully chosen to optimise the highest oil encapsulation efficiency. The selection of the wall material is crucial; the encapsulated material could determine the property of both emulsion droplet and dried powder particle. Both synthetic and natural materials, for example, ethyl cellulose, maltodextrin, gum, poly(lactic-co-glycolic acid) (PLGA), chitosan, and poly(ε-caprolactone) (PCL), are widely applied to encapsulate different AIs in various applications, particularly food, cosmetic, medical delivery and crop protection [154-159]. Interestingly, maltodextrin offers several advantages including high water solubility, low cost and less agglomeration after spray drying. In addition, Arabic gum (GA) is also mostly used both as emulsifier and shell

material. The stable emulsion from Arabic gum solution is considered as a convenient method to synthesise chemical encapsulation [160-163]. An example of using synthetic polymer materials to encapsulate an active ingredient via the spray drying technique was introduced by Fontana *et al.*; where they used ε-PCL to encapsulate dexamethasone. Spherical particles were observed by SEM characterisation where high encapsulated yield was also obtained [143].

Chapter 2

Synthesis of stable isocyanate containing copolymer via SET-LRP

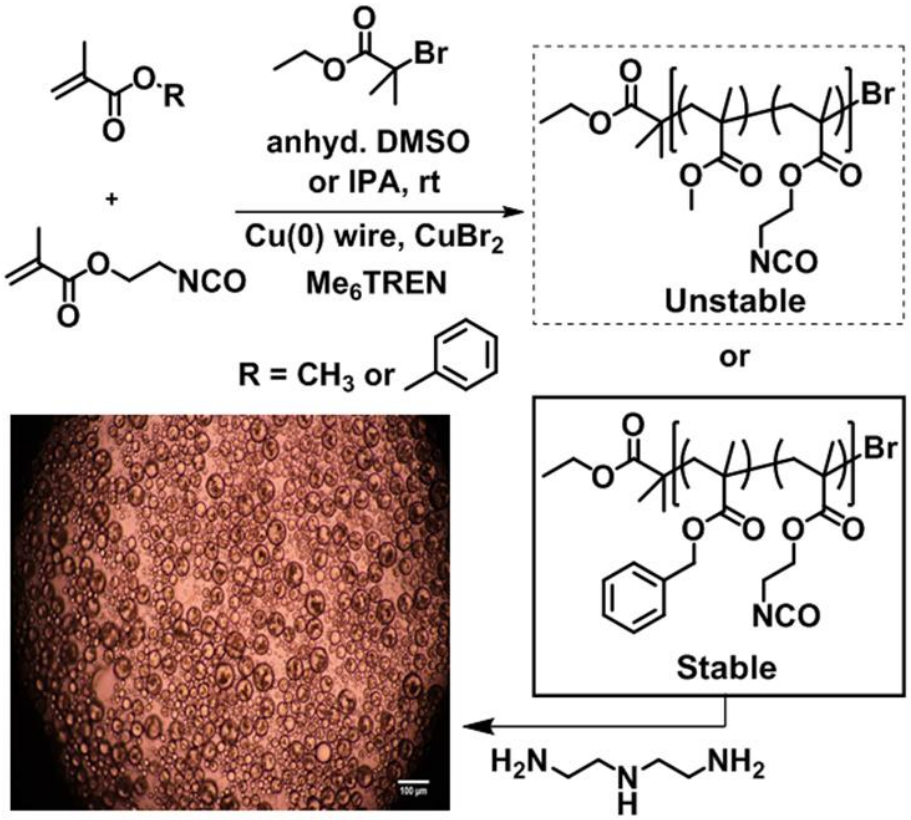

This chapter details the synthesis of two types of isocyanate side chain containing copolymers, poly(methyl methacrylate-*co*-isocyanatoethyl methacrylate) (P(MMA_m-*co*-IEM_n)) and poly(benzyl methacrylate-*co*-isocyanatoethyl methacrylate) (P($BnMA_m$-*co*-IEM_n)), which were synthesised via Cu(0)-mediated controlled radical polymerisation. Polymerisation proceeded to a reasonably high conversion giving polymers of relatively narrow molar mass distributions. The incorporation of the bulky aromatic groups in the latter copolymer rendered it sufficiently stable towards hydrolysis and enabled the isolation of the products. Both P(MMA_m-*co*-IEM_n) and P($BnMA_m$-*co*-IEM_n) were functionalised with dibutylamine, octylamine, and (R)-(+)-α-methylbenzylamine, which further proved the successful incorporation of the isocyanate groups. Furthermore, P($BnMA_m$-*co*-IEM_n) was used for the fabrication of liquid core microcapsules via oil-in-water interfacial polymerisation with diethylenetriamine (DETA) as a crosslinker. The particles were obtained in the size range of 10 to 90 µm in diameter.

2.1 Background

2.1.1 Isocyanate-containing copolymers

Searching for the term “Isocyanate copolymer” provides more than one thousand publication hits on “Web of knowledge”, indicating a large contribution of isocyanate chemistry to polymer research; the isocyanate functional group is represented as R-N=C=O [164]. The extraordinary reactivity of isocyanates towards nucleophiles, which is attributed to the high electronegativity of oxygen and nitrogen generating a very electrophilic carbon centre, is of great interest as a synthetic tool. As

a result, isocyanate functional groups are frequently employed as the reactive intermediates [165]. They are, however, highly sensitive to moisture. Dry reaction conditions, or the use of a glove box is frequently required to conduct successful reactions or for storage. Isocyanate-containing polymers are generally prepared through either modification of the initiator incorporating [166,167] an isocyanate containing monomer [168] or post-polymerisation modification [169]. Chemical protection can be used to preserve isocyanate functionality during a reaction, followed by deprotection and subsequent modification [170]. Alternatively, Endo and coworkers incorporated styrene monomers into polyisocyanates to improve the stability of the isocyanate functional group [171].

Use of isocyanatoethyl methacrylate (IEM), to provide isocyanate-containing copolymers, has been suggested with many polymerisation techniques. Eick and coworkers introduced polymerisation of IEM via conventional free radical polymerisation; they suggested a successful synthesis achieved as isocyanate absorbance was detected in FTIR [172]. However, controlled radical polymerisation offers several advantages over free radical polymerisation as it was previously mentioned in chapter 1, thus, in order to prepare a well-defined isocyanate containing copolymer, reversible deactivation radical polymerisation of IEM is required, for example, both Hawker and coworkers and Perrier and coworkers, reported the reversible deactivation radical polymerisation of IEM via RAFT polymerisation to prepare nanoparticles by intramolecular cross-linking and modification of isocyanate functional groups, respectively [168,173]. To the best of our knowledge, Cu(0)-mediated

polymerisation of this monomer has not been previously reported. Furthermore, with a lack of control over polymer composition, and high temperature requirements, there are still major barriers to the full exploitation of this monomer.

2.1.2 Polycondensation interfacial polymerisation

Polymeric capsules have been intensively studied and applied to encapsulate many active ingredients (AI) in different applications, including, household chemicals, food ingredients, agrochemicals, cosmetics, and pharmaceuticals [174-178]. To synthesise polymeric capsules, polycondensation interfacial polymerisation is generally used; this is the chemical encapsulation technique which occurs at the interface of two immiscible liquids [179]. An emulsion droplet is generated followed by the condensation reaction of functional monomers at a droplet interface, where polymeric capsules complete the wall formation [180].

Emulsion encapsulation is composed of three components, including water, oil, and surfactants. There are two main emulsion formulations used. The system that an oil phase disperses in an aqueous phase is named as an oil in water emulsion (O/W). Conversely, the term of water in oil emulsion (W/O) represents the opposite phase dispersion [181]. Encapsulation of hydrophobic AI is ordinarily performed via oil phase of O/W emulsion. The emulsion droplet size can be used to classify emulsion type: microemulsion and nanoemulsion. Both emulsion systems are formed by applying enough energy in order to generate liquid droplets. Notably, high input energy, for example, an ultrasound generator and high-pressure homogenizers are required to obtain a nanoemulsion, however, microemulsions can be easily produced with gentle

overhead stirring. More importantly, the droplet size can be altered by changing the ratio of oil and surfactant weights and also the ratio of oil to water.

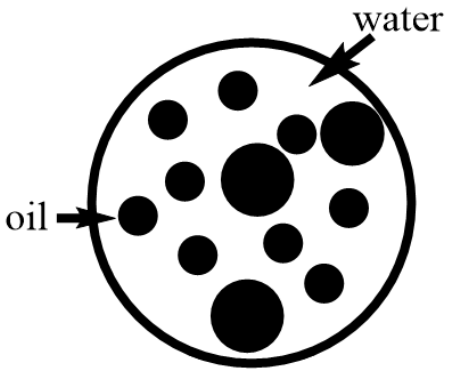

Figure 2.1: A model of oil in water emulsion (O/W).

Encapsulation via polycondensation interfacial polymerisation has been known for half a century. At the early stage of the investigation, polymeric capsule, for example, polynylon, was widely studied [182-184]. Later, polyurethanes were introduced, for example, K. Bouchemal and coworkers reported a nanocapsule from the interfacial polymerisation of isophorone diisocyanate (IPDI) and different diols, including 1,2-ethanediol (EG), 1,4-butanediol (BD), and different molecular weights of poly (ethylene glycol) diol. The successful interfacial polymerisation and acceptable encapsulation efficiency were informed [179]. Polyurethane and polyamide shell capsules have been broadly applied in many applications because their preparation requires simple chemistry, cost effective, and less time consuming [185, 186].

2.2 Results and Discussion

2.2.1 P(MMA$_m$-co-IEM$_n$) synthesis and modification

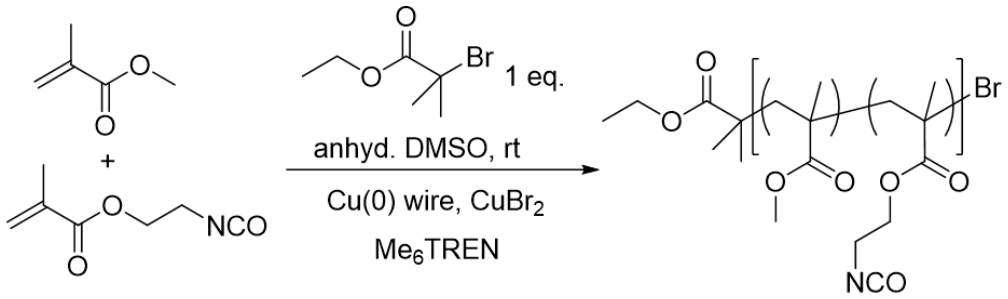

Figure 2.2: SET-LRP copolymerisation of MMA and IEM in an anhydrous solvent.

MMA and IEM (10 mol %) were copolymerised using a Cu(0)-mediated controlled radical polymerisation system with ethyl 2-bromoisobutyrate (EBiB) as initiator, anhydrous DMSO as solvent and a Cu(II)Br$_2$/Me$_6$Tren/EBiB ratio of 0.05:0.12:1 (Table 2.1). Within three hours no further monomer conversion occurred, at monomer conversions of 25 and 40 % (as determined by ^{1}H NMR) for MMA and IEM, respectively. This could be the result of a decrease in the reactivity of catalyst/ligand system over time. Subsequently, the concentration of Me$_6$Tren ligand was increased to 0.36 equivalents, resulting in a higher degree of polymerisation, with approximately 60 % conversion for both monomers (Table 2.1). In addition, different feed ratios of IEM were also studied to determine the effect on the monomer conversion and dispersity (Figure 2.3). Of note, the SEC trace of the copolymer that polymerised from 15 % of IEM monomer shows a bimodal and broad molecular distribution (entry 4 in table 2.1). A broad molecular weight distribution could occur from several causes, including the reaction between isocyanate and moisture in the solvent; DMSO is known as a

hygroscopic solvent. This is a result of the isocyanate reacting with water to generate carbamic acid which subsequently decomposes to carbon dioxide [187] and a primary amine, which can form a urea bond with another isocyanate. Also, the reaction between the primary amines in the copolymer and the isocyanate in another copolymer leads to the bimodal distribution. Thus, at high levels of isocyanate functionality in the copolymer, a lack of stability in the presence of moisture prevents this copolymer from being a suitable candidate to prepare microcapsules. In addition, a white precipitate of highly crosslinked polyurethane was observed within a few minutes of exposure of the polymer solution to moisture as represented in figure 2.4.

Entry	($CuBr_2$: Me_6Tren: EBiB)	% IEM	Conversion (%)*		$M_{n,\,SEC}$**	Đ
			MMA	IEM	(g mol^{-1})	
1	(0.05:0.12:1.00)	10	25	40	3630	1.44
2	(0.05:0.36:1.00)	5	60	67	6450	1.77
3	(0.05:0.36:1.00)	10	52	65	5800	1.58
4	(0.05:0.36:1.00)	15	50	64	9040	1.83

*monomer conversion was determined by using ^{1}H NMR **THF eluent

Table 2.1: Summary of the results of P(MMA_m-*co*-IEM_n) polymerisation by SET-LRP (targeted DP 50) for five hours at ambient temperature.

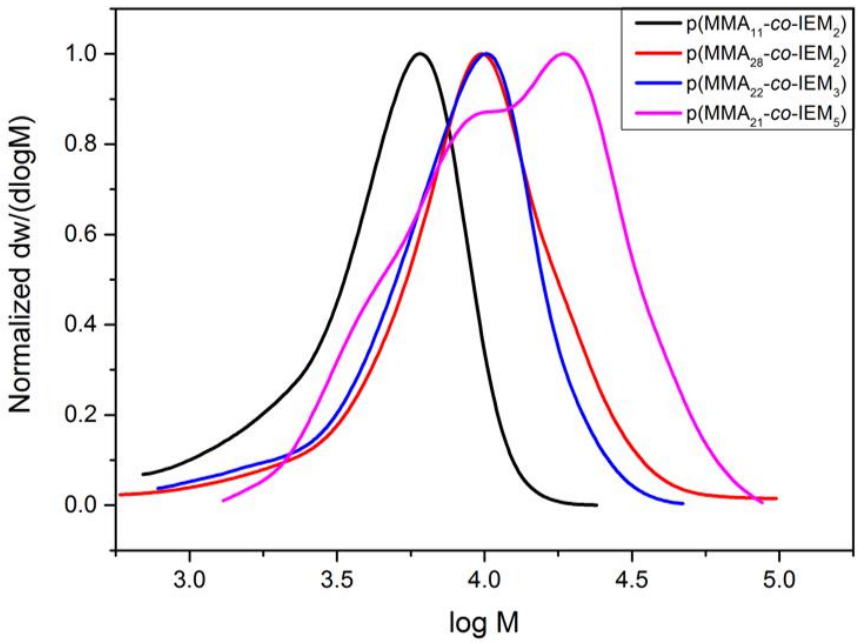

Figure 2.3: SEC traces of P(MMA_m-*co*-IEM_n) polymerisation at different conditions.

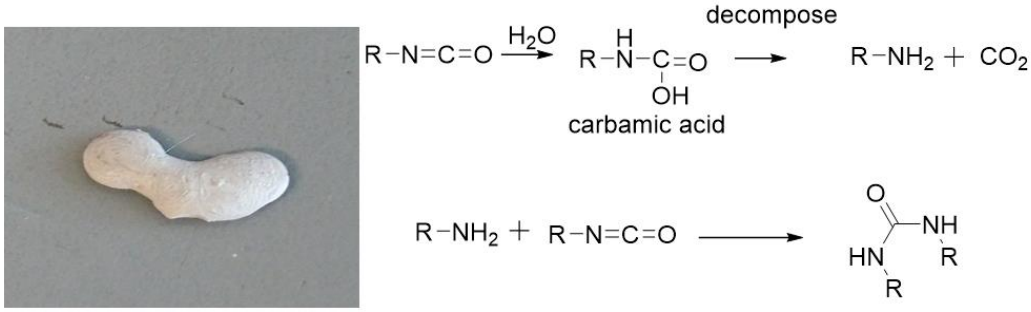

Figure 2.4: P(MMA_m-*co*-IEM_n) solution behaviour after exposing to atmosphere.

Modification of the isocyanate group in the copolymer, in this case *in-situ*, is a simple method to confirm if isocyanates are still present, and reactive, following polymerisation. Three different amines: dibutylamine, octylamine and (R)-(+)-α-methylbenzylamine were used to examine this. To this end, the P(MMA_{22}-*co*-IEM_3) copolymer (Entry 3 Table 2.1) solution was transferred directly after polymerisation to the amine solution using a cannula under N_2 and left to stir for three hours at ambient temperature. After purification, ^1H and ^{13}C NMR spectroscopy were used to indicate

successful modification by amines; Figure 2.5 shows the successful modification with dibutylamine and in the ^{13}C NMR (Figure 2.6) spectra a new signal at 159 ppm can be attributed to the newly formed urea bond. Furthermore, FTIR spectroscopy (Figure 2.7) confirmed the successful functionalisation, by disappearance of the characteristic $V_{N=C=O}$ vibration at 2250 cm^{-1} in the product IR spectrum. Pleasingly, functionalisation had little effect on dispersity (Figure 2.8).

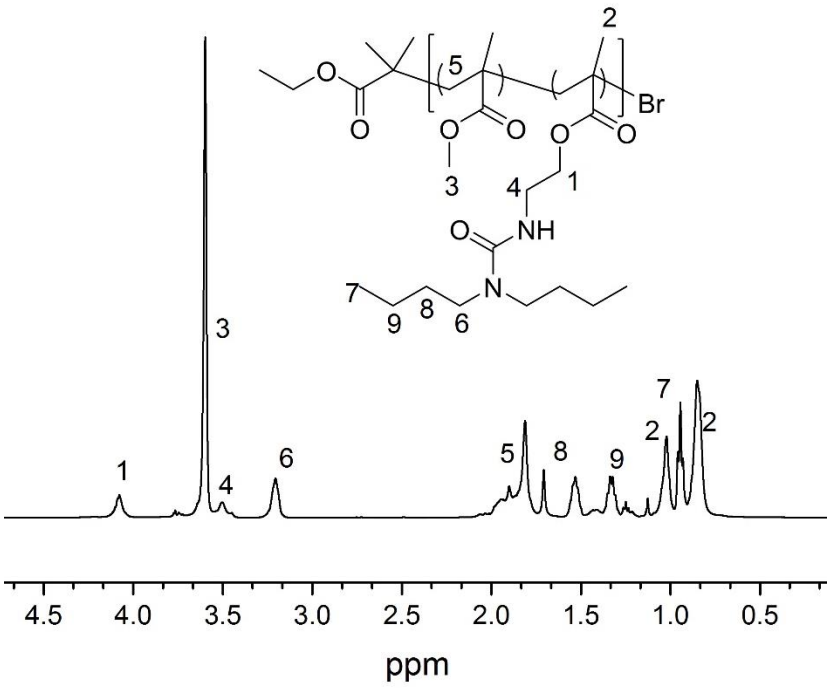

Figure 2.5: ^{1}H NMR of P(MMA_{22}-*co*-IEM_3) modified with dibutylamine ($CDCl_3$, 400 MHz).

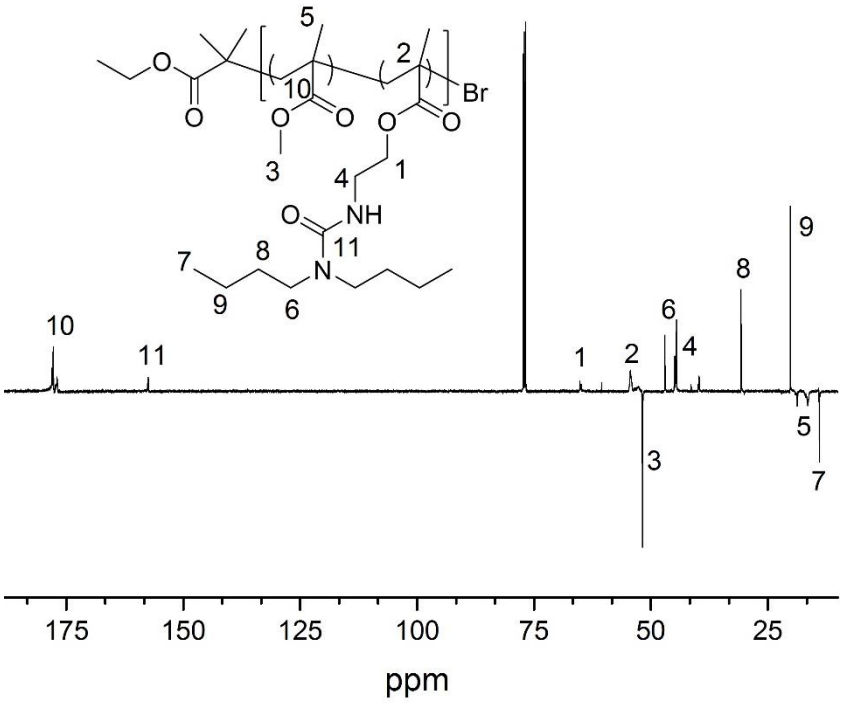

Figure 2.6: ^{13}C NMR (J-modulated) of P(MMA_{22}-*co*-IEM_3) modified with dibutylamine ($CDCl_3$, 400 MHz).

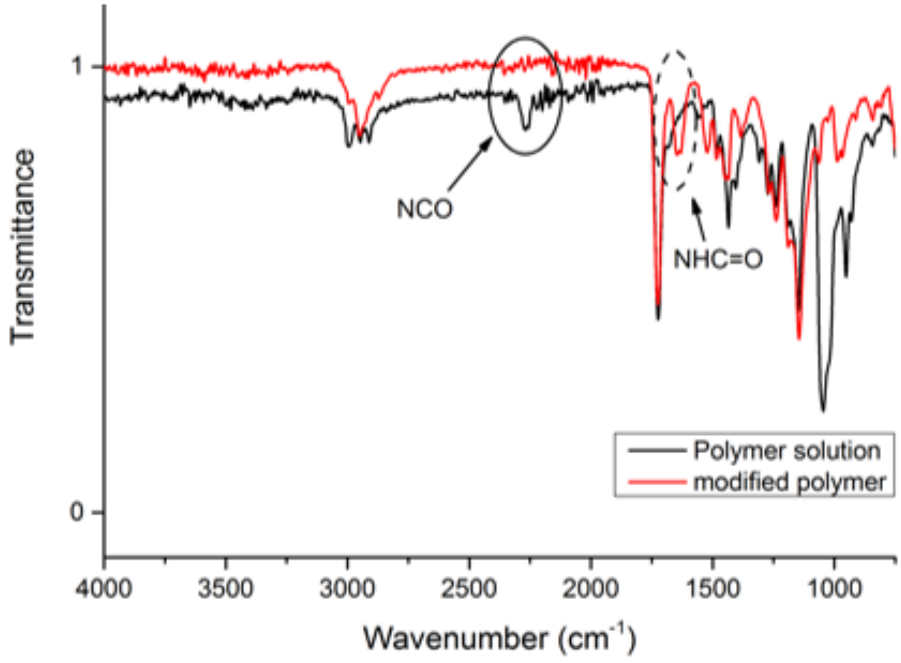

Figure 2.7: FTIR spectra of polymer solution of P(MMA_{22}-*co*-IEM_3) in DMSO and P(MMA_{22}-*co*-IEM_3) modified with dibutylamine.

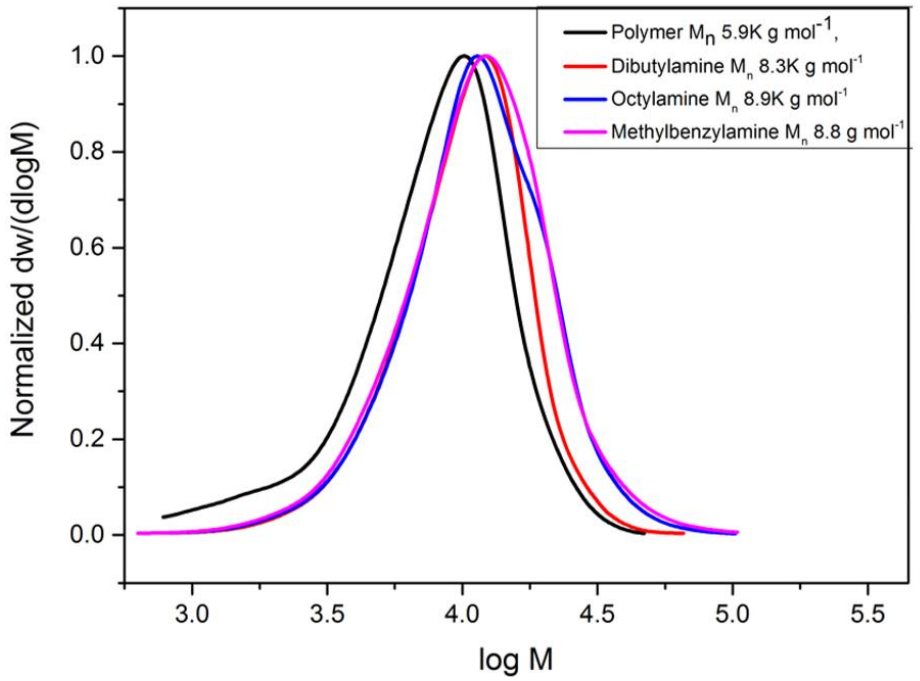

Figure 2.8: SEC traces of P(MMA_{22}-*co*-IEM_3) before and after modification by different amines.

2.2.2 *P($BnMA_m$-co-IEM_n) synthesis and modification*

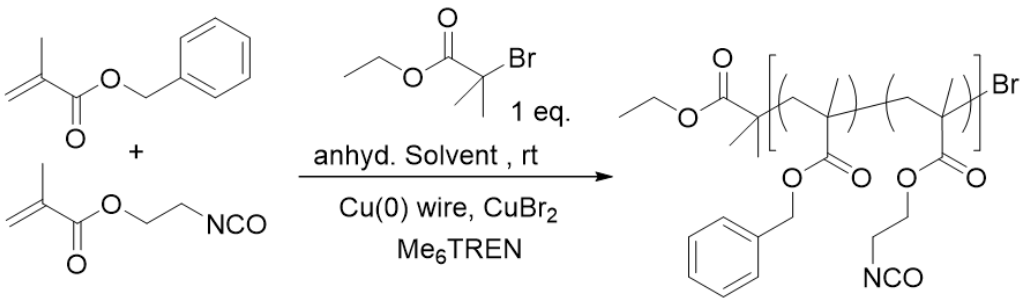

Figure 2.9: SET-LRP copolymerisation of BnMA and IEM in an anhydrous solvent.

In order to preserve the isocyanate functionality and allow isolation of the IEM copolymer, rapid monomer conversion and a straightforward purification protocol are

required. DMSO is the most common solvent for Cu(0)-mediated controlled radical polymerisation, although the difficulty of removing this solvent is still a major limitation. Alternatively, isopropanol (IPA) is easier to remove while not affecting the dispersity of the resultant well-defined polymer, as has been shown with various acrylate, methacrylate and acrylamide monomers [53, 188, 189]. In an attempt to prepare stable IEM copolymers, IEM was copolymerised with benzyl methacrylate (BnMA) in IPA using $CuBr_2$: Me_6Tren: EBiB = 0.05:0.12:1. The polymerisation ceased within five hours, in line with the P($BnMA_m$-*co*-IEM_n) polymerisation above, resulting in conversions of 10 % and 70 % of BnMA and IEM by ^{1}H NMR, respectively. No further increase in molecular weight, determined by SEC, was observed (Figure 2.10), however, monomer conversion was successfully increased in the presence of increased Me_6Tren concentration, thus a $CuBr_2$:Me_6Tren = 0.05:0.36 catalyst was employed. Notably, G. Raspoet reported the reactivity of IPA and PhNCO with an approximation of 1 x 10^{-4} $m^{-1}s^{-1}$ [190]. This reaction would also occur during the polymerisation process. Nevertheless, no bimodal distribution was detected by SEC which indicates that the reaction between isocyanate in the monomer/polymer and IPA does not significantly occur.

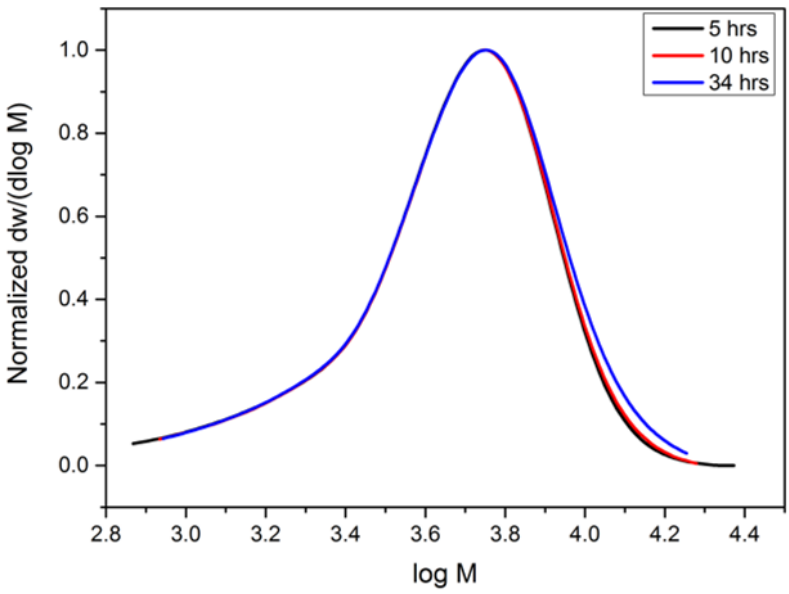

Figure 2.10: SEC traces of P(BnMA$_m$-*co*-IEM$_n$) shows no increasing of conversion after leaving polymerisation for 34 hours at ambient temperature.

Kinetic studies of P(BnMA-*co*-IEM) formation showed a linear increase in molar mass up to two hours with monomer conversion as monitored by ^{1}H NMR spectroscopy (Figure 2.11). P(BnMA-*co*-IEM) copolymer may consist of a random composition of PEIM and PBnMA, however, the conversion of IEM monomer is significantly higher than BnMA (Table 2.2). Therefore, to predict the microstructure of this copolymer, the possibility to form PIEM segment at the initiator end is more likely than PBnMA. Notably, the concentration of BnMA in the polymerisation solution is considerably high compared to IEM, thus the microstructure at the initiator end could randomly contain both PBnMA and PIEM. Nevertheless, PBnMA could only be polymerised at the chain end of the copolymer (Figure 2.12 left). A perceptible drop in polymerisation rate can be seen after two hours due to phase separation between polymer and monomer/solvent (Figure 2.12 right). Polymerisations were left for up to six hours and interestingly, similar BnMA monomer conversion was detected for two, four, and six hours, while an increasing

amount of IEM was consumed with time (90% at six hours) (Table 2.3). Unfortunately, increasing IEM monomer conversion significantly increased the dispersity of the copolymer to $Đ$ = 2.35. This is indicative of the loss of control in the system and an enhanced occurrence of side reactions with increasing reaction time. Thus, it was decided that [$CuBr_2$]: [Me_6Tren] = 0.05:0.36 catalyst and a reaction time of 3 hours were the best conditions to synthesise P(BnMA$_m$-*co*-IEM$_n$) with different monomer feed ratios.

Entry	Time (mins)	Conversion (NMR)		$M_{n,\ SEC}$ (g mol^{-1})	$M_{w,\ SEC}$ (g mol^{-1})	Đ
		BnMA	IEM			
1	30	5	27	2900	4100	1.38
2	45	10	30	3700	5300	1.42
3	60	20	34	4700	6900	1.44
4	90	29	38	6900	10000	1.49
5	120	34	41	7900	12000	1.57
6	150	37	43	8000	12300	1.52
7	180	42	48	8100	12400	1.54

Table 2.2: Summary of the results of P(BnMA$_m$-*co*-IEM$_n$) polymerisation by SET-LRP (targeted DP 50) for three hours at ambient temperature.

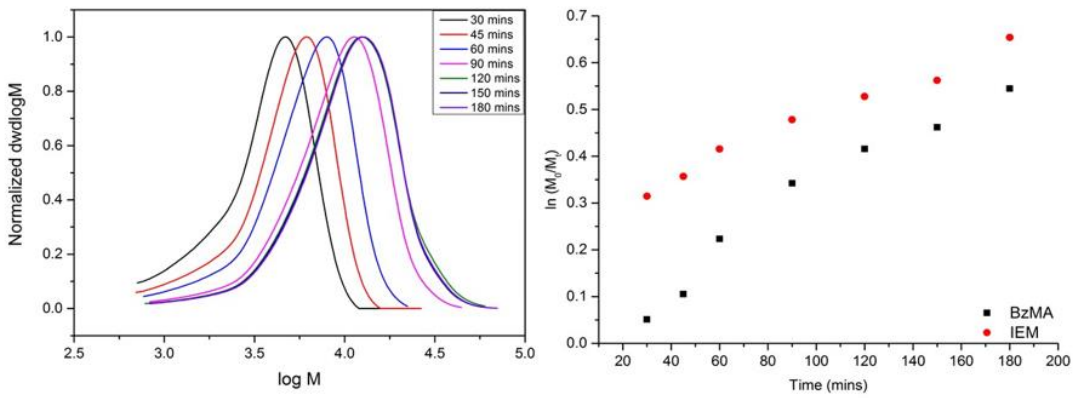

Figure 2.11: SEC traces (left) and kinetic plot of monomer conversion measured by ^{1}H NMR (right) for the synthesis of P(BnMA$_m$-*co*-IEM$_n$).

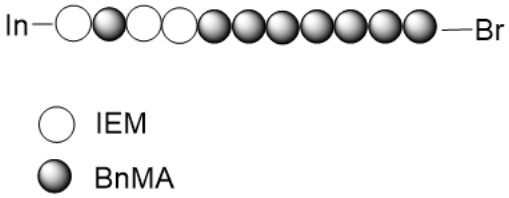

Figure 2.12: The proposed microstructure of the P(BnMA$_m$-*co*-IEM$_n$) (left) and polymerisation mixture after three hours shows phase separation between polymer and solvent (right).

Entry	Time	Conversion (%NMR)		$M_{n,\ Theory}$ (g mol^{-1})	$M_{n,\ SEC}$ (g mol^{-1})	$M_{w,\ SEC}$ (g mol^{1})	Đ
		BnMA	ICM				
1	2	48	46	4180	7900	12500	1.57
2	4	49	75	4450	8200	13700	1.67
3	6	50	99	4720	8500	20000	2.35

Table 2.3: SET-LRP polymerization result of P(BnMAm-co-IEMn) from two to six hours at ambient temperature (EBiB: $CuBr_2$: Me_6Tren = 1: 0.05: 0.12 catalyst system).

FTIR was used to determine the incorporation of the isocyanate functional group in to the copolymer. Strong transmittance of characteristic NCO stretches at 2250 cm^{-1} demonstrates that the isocyanate group is still intact (Figure 2.13). We observed an acceptable control over molecular weight and dispersity (Figure 2.14). No significant difference of the dispersity was observed for both the homopolymer and copolymer. The PBnMA homopolymer has a uniform SEC trace, whereas the copolymer traces have a molecular weight shoulder and higher dispersity, indicative of side reaction of isocyanate functionality. Although polymerisations were carried out under N_2 and using anhydrous solvents, reaction of the isocyanate group with a nucleophile such as water

could have occurred, despite every effort to exclude water. Notably, SEC of $PBnMA_{10}$-*co*-$PIEM_2$ (Figure 2.14 red) shows a small molecular shoulder which indicates that the composition of PBnMA and PIEM is also crucial; side reaction of the isocyanate during the polymerisation and purification is likely to happen unless enough bulky PBnMA segment is contained in the copolymer.

Entry	Target DP		Conv. (%)		Polymer	$M_{n,theo}$ ($g\ mol^{-1}$)	$M_{n,SEC}$ ($g\ mol^{-1}$)	Đ
	Overall	% IEM	BnMA	IEM				
1	50	0	45	0	$PBnMA_{22}$	4071	3400	1.48
2	25	10	43	60	P($BnMA_{10}$-*co*-IEM_2)	2267	4100	1.61
3	50	10	49	40	P($BnMA_{22}$-*co*-IEM_2)	4381	7700	1.41
4	100	10	54	45	P($BnMA_{48}$-*co*-IEM_4)	9273	12700	1.51

Table 2.4: Summary of SET-LRP result of BnMA/IEM copolymerisation at room temperature after three hours.

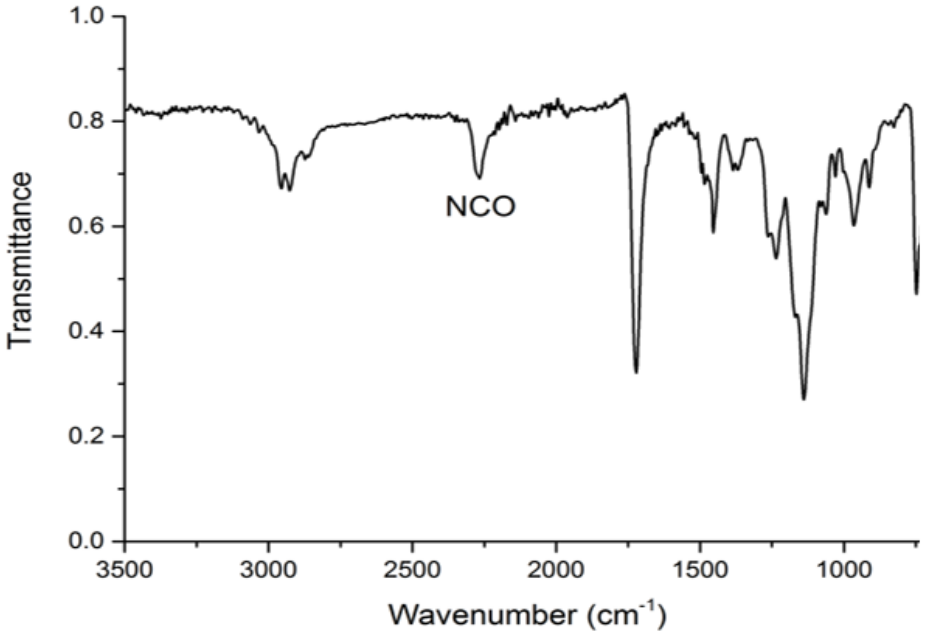

Figure 2.13: FTIR spectra of solid P($BnMA_{22}$-*co*-IEM_2) copolymer, strong transmittance of characteristic NCO stretches at 2250 cm^{-1} demonstrates that the isocyanate group is still intact.

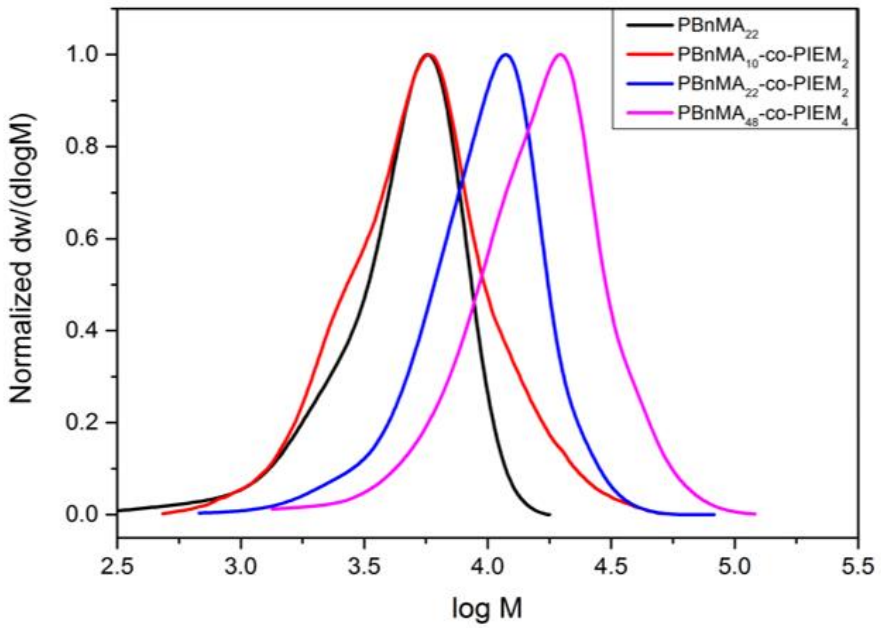

Figure 2.14: SEC traces of P(BnMA$_m$-*co*-IEM$_n$) which is polymerised via SET-LRP in anhydrous IPA, in $CHCl_3$ eluent with DRI detection.

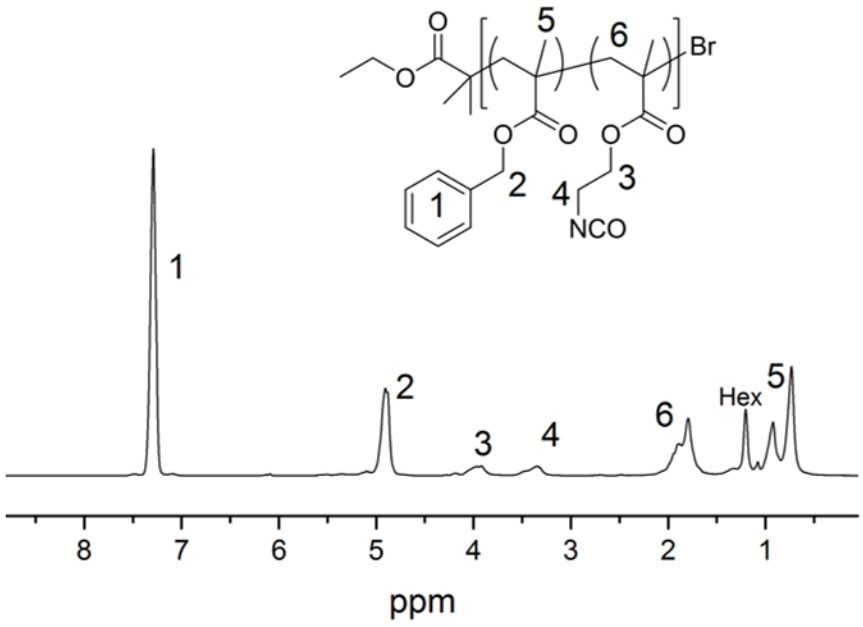

Figure 2.15: ^{1}H NMR P(BnMA$_{22}$-*co*-IEM$_2$) copolymer after purification, position 3 and 4 indicate the C*H*$_2$ group of PIEM segment. Position 1 and 2 represent aromatic C*H* and PhC*H*$_2$ of PBnMA segments, respectively.

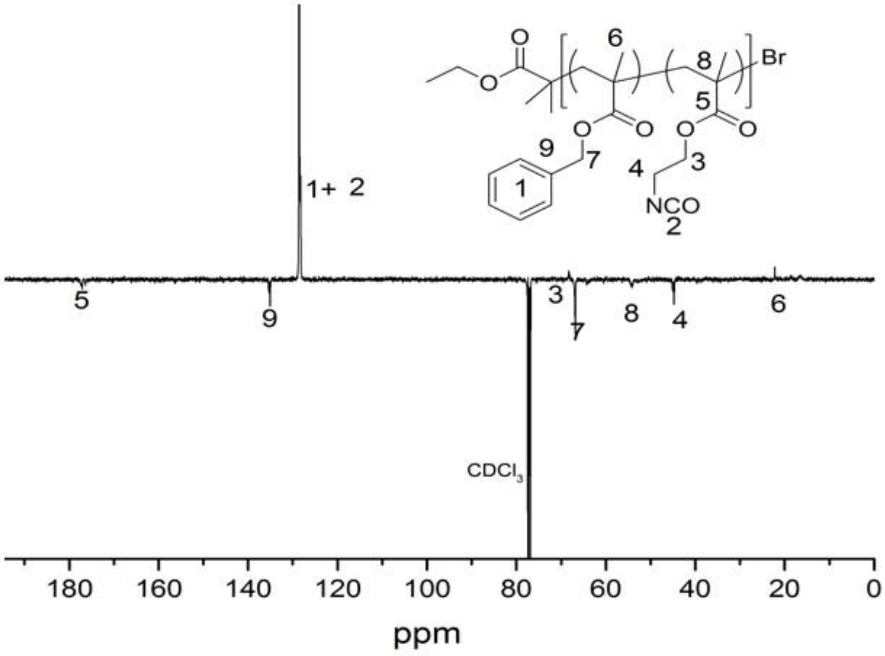

Figure 2.16: ^{13}C NMR of P(BnMA$_{22}$-*co*-IEM$_2$) copolymer after purification which indicates the successful polymerization and purification; position 5 and 6 represent *C*=O and CH_3, respectively.

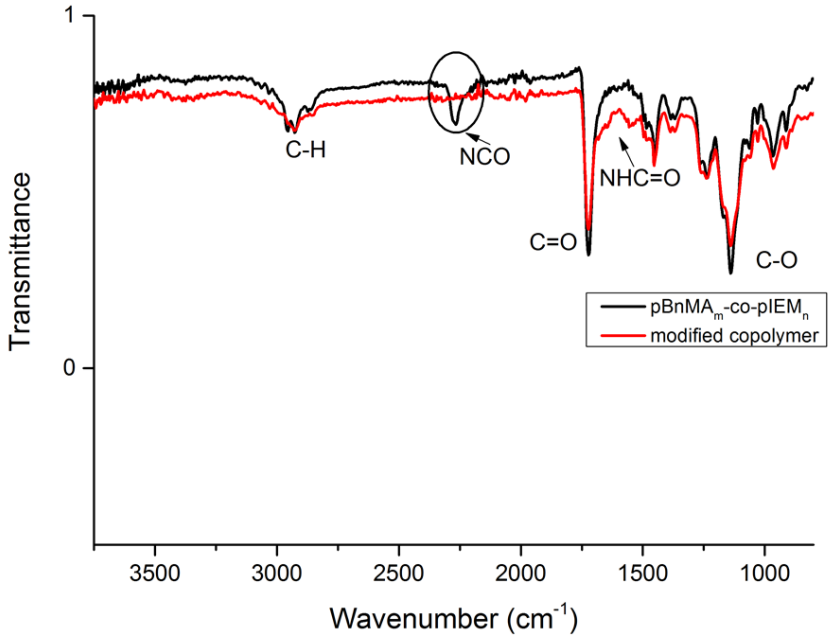

Figure 2.17: FTIR spectra of P(BnMA$_{22}$-*co*-IEM$_2$) and copolymer modified by dibutylamine.

The use of BnMA as a comonomer proves to have a beneficial effect on the stability of the copolymers, similar to the observation made by Endo [171]. Upon successful polymerisation, the copolymer was isolated by precipitation into cold *n*-hexane. Further analysis of the isocyanate functionality was carried out post-purification, to ensure that the polymer would be suitable for preparing microcapsules. Purified P($BnMA_{22}$-*co*-IEM_2) was functionalised with octylamine, dibutylamine and (R)-(+)-α-methylbenzylamine. The products were analysed by FTIR and NMR spectroscopy. An absence of a peak at 2250 cm^{-1}, indicative of isocyanate, and a detection of C=O urea stretch at 1647 cm^{-1} shows that isocyanate functional groups in P($BnMA_{22}$-*co*-IEM_2) were successfully modified by dibutylamine (Figure 2.17).

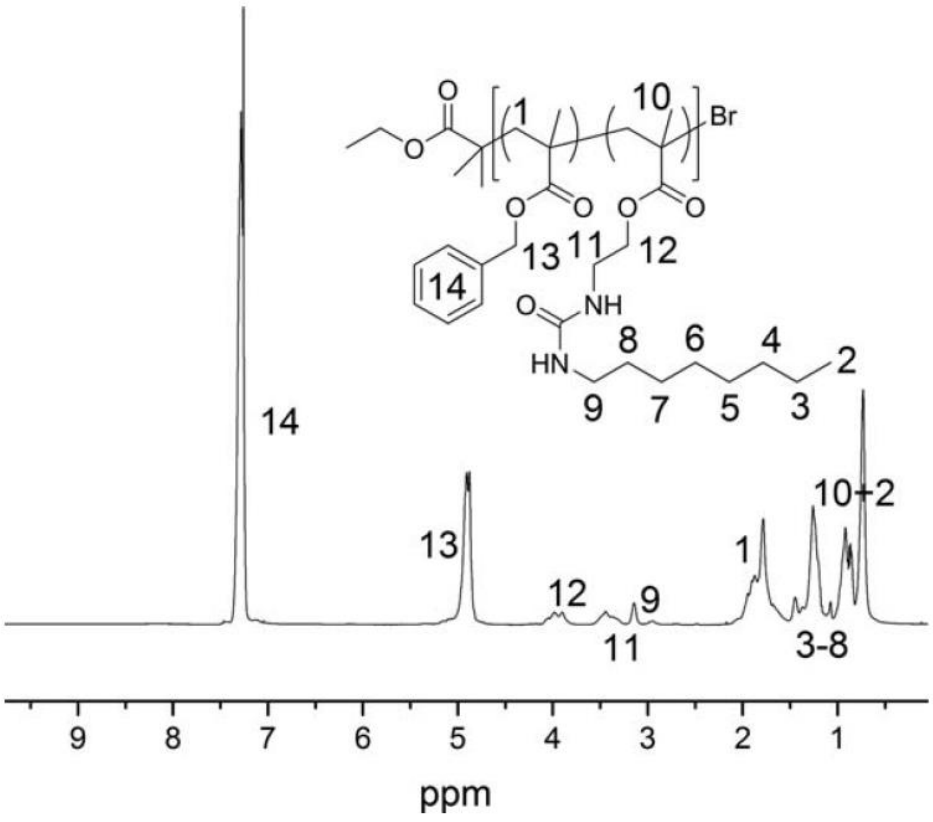

Figure 2.18: ^1H NMR of modified P($BnMA_{22}$-*co*-IEM_2) with octylamine.

^{13}C NMR shows the formation of a urea functional group (156.5 ppm) for all three modified samples, which was confirmed by ^{1}H NMR. The chemical shift of the methylene group in the copolymer modified by octylamine (Figure 2.18, position 11 and 12) indicates no variation of chemical shift when compared to non-functional P(BnMA$_{22}$-*co*-IEM$_2$). The molar mass of the amine-functionalised copolymer was slightly different from P(BnMA$_{22}$-*co*- IEM$_2$), however, the observation that there is no change in the dispersity values indicates that no inter/intramolecular cross-linking occurred during modification and purification (Figure 2.20).

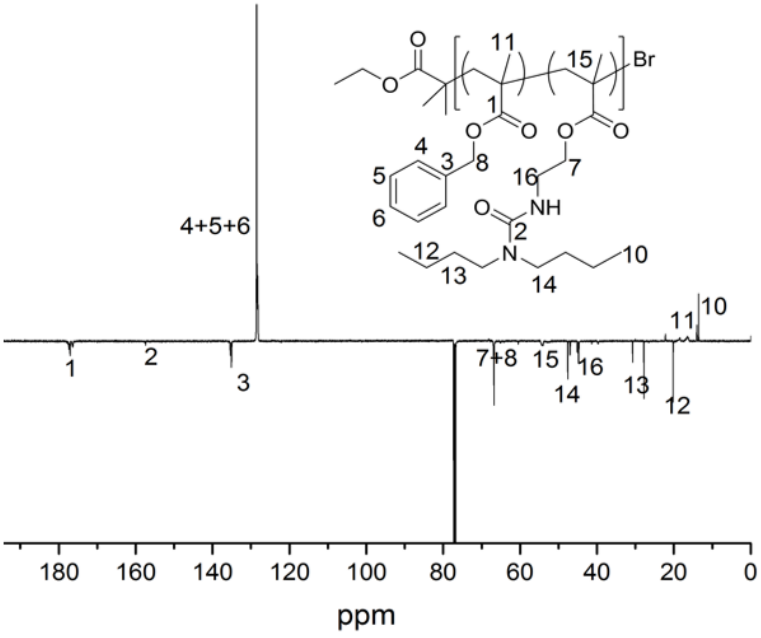

Figure 2.19: ^{13}C NMR of modified P(BnMA$_{22}$-*co*-IEM$_2$) with dibutylamine. J-modulated mode was applied to distinguish the signal between C, CH_2 (negative) and CH, CH_3 (positive). Also, a new signal at 159 ppm (position 2) after modification can be attributed to the newly formed urea bond.

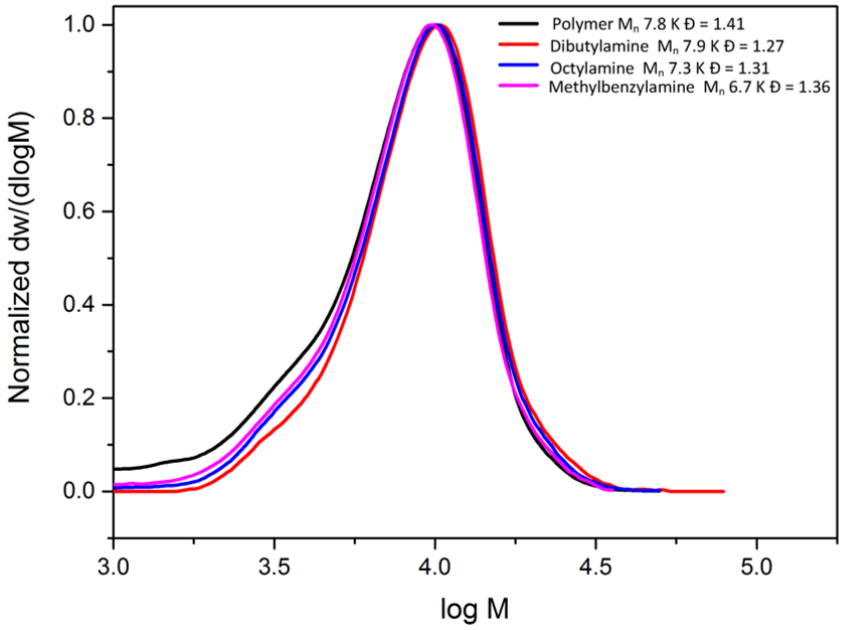

Figure 2.20: SEC traces of p(BnMA$_m$-*co*-IEM$_n$) copolymer before and after modification by different amines; no change in the dispersity values indicates that no inter/intramolecular cross-linking occurred during modification and purification.

2.2.3 Microcapsule Synthesis

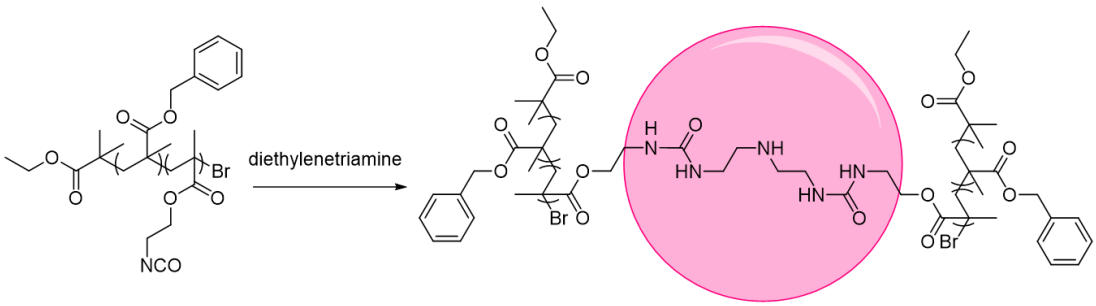

Figure 2.21: Microcapsule fabrication via oil-in-water interfacial polymerisation of P(BnMA$_m$-*co*-IEM$_n$).

With this robust protocol for preparing isocyanate containing copolymers in hand, these polymers were used to prepare polyurea microcapsules via oil-in water

interfacial polymerization [183]. To this end, the P(BnMA$_m$-*co*-IEM$_n$) was dissolved in anhydrous dichloromethane followed by the addition of carrier oil and stabiliser poly(vinyl alcohol) solution. Subsequently, the solution mixture was homogenised and cross-linked by addition of diethylenetriamine. The size of the resulting particles was determined by light optical microscope and dynamic light scattering. Variation of either the molecular weight of the copolymer, or percentage of isocyanate functionality, afforded no significant differences in particle size according to optical microscopy measurements. Exemplarily, figure 2.22 shows that a range of differently sized particles from 10 to 90 µm in diameter, were prepared. This analysis was confirmed by dynamic light scattering with a range of sizes of 20 to 100 µm.

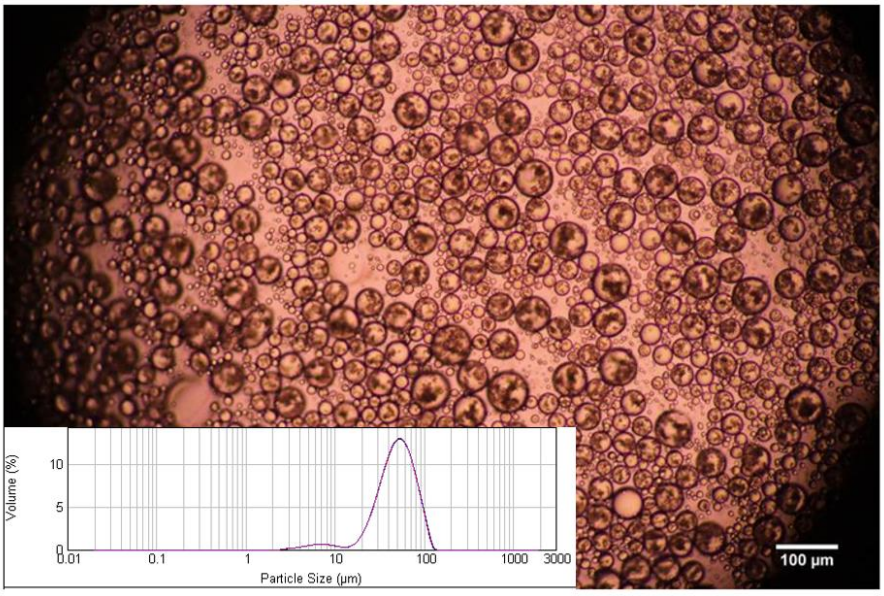

Figure 2.22: Optical microscope and dynamic light scattering result of microcapsule fabrication via oil in water interfacial polymerisation of P(BnMA$_{22}$-*co*-IEM$_2$).

2.3 Conclusion

Isocyanate functional copolymers were successfully synthesised via Cu(0)-mediated controlled radical polymerisation at ambient temperature. P(MMA_m-*co*-IEM_n) was prepared and modified with three different amines. In order to improve the stability of the isocyanate functional group, benzyl methacrylate was incorporated into the polymerisation protocol. This allowed the preparation of stable copolymers which can be isolated through a simple polymer purification strategy. The isocyanate-containing copolymers were used for the fabrication of polyurea microcapsules via oil-in-water interfacial polymerisation. Interestingly, particle sizes showed no significant differences when copolymers of different molecular weights and isocyanate compositions were used. In conclusion, we introduced a facile synthetic method to prepare moisture stable isocyanate containing copolymers, and demonstrate their use to fabricate functional polyurea microcapsules. This tool will be incorporated into the biodegradable polymer in the following chapter, to synthesise isocyanate containing biodegradable copolymers to obtain the microcapsules which are considered as the promising materials to use as the pesticide carriers.

2.4 Experimental

2.4.1 Materials

Acetone, ethyl α-bromoisobutyrate, dimethyl sulfoxide anhydrous, isocyanatoethyl methacrylate (IEM), methyl methacrylate (MMA), benzyl methacrylate (BnMA), deuterated chloroform ($CDCl_3$), deuterated chloroform anhydrous, 2

isopropanol (anhydrous) (IPA) , dimethyl sulfoxide anhydrous (DMSO), dichloromethane anhydrous (DCM), diethylenetriamine, poly(vinyl alcohol) (M_w 130,000 g mol^{-1}), copper(II) bromide, 35% aqueous hydrochloric acid, octylamine, dibutylamine and (R)-(+)-α-methylbenzylamine were purchased from Sigma-Aldrich UK. Carrier oil was purchased from Stephan Company. Me_6Tren was synthesised according to literature procedure [191].

2.4.2 Characterisation

Size exclusion chromatography measurements were performed on an Agilent 390 MDS Multi-Detector GPC system ($CHCl_3$ + 2 % TEA Mixed C column set, THF + 2 % TEA + 0.01 wt. % BHT with PLgel Mixed C column set, 30 °C flow rate 1 mL/min, narrow standards of PMMA were used as calibration polymers between 955000 and 1010 g mol^{-1} and fitted with a third order polynomial) by DRI detection. ^{1}H NMR (standard) and ^{13}C NMR (long acquisition long delay) were recorded on a Bruker Avance III HD 400 MHz and Bruker Avance III HD 300 MHz with $CDCl_3$ and anhydrous $CDCl_3$ as the solvent. IR spectra were recorded on a Bruker Vector 22 FTIR spectrometer with OPUS software used to analyse absorbance data. Particle size in aqueous solution was obtained by Malvern Instruments Mastersizer 2000 System and Olympus microscope (2x, *10x and 20x).*

2.4.3 P(MMA$_m$-co-IEM$_n$) polymerisation

5 cm of copper wire was entwined with a magnetic stirrer bar, and placed into 3 mL of 35 % HCl solution for 5 minutes, washed with deionized water then acetone. Once dried, the cleaned wire was placed in a Schlenk tube containing $CuBr_2$ (5.70 mg, 2.55 x

10^{-5} mol (0.05 eq. relative to initiator) and sealed with a rubber septum. Ethyl α-bromoisobutyrate (75 µL, 5.11 x 10^{-4} mol, 1 eq.), 2-isocyanatoethyl methacrylate (0.36 mL, 2.55 x 10^{-3} mol. 5 eq.) and methyl methacrylate (2.45 mL, 2.29 x 10^{-2} mol, 45 eq.) and anhydrous dimethyl sulfoxide (3 mL) were then added in to a Schlenk tube. The reaction mixture was degassed under a flow of N_2 for 15 minutes, then Me_6Tren (49.2 µL, 1.84 x 10^{-4} mol, 0.36 eq.) was added. The reaction was stirred for five hours, polymer solution was characterised by NMR, IR and SEC. ^{1}H NMR (300MHz, $CDCl_3$, δ): 1.02 (m, CH_2), 1.82 (m, CH_3), 1.97 (m, CH_3 (monomer)), 2.63 (s, CH_3 (DMSO)), 3.48 (m, CH_2N) 3.59 (s, CH_3O), 3.75 (s, CH_3O (monomer)) 4.00 (s, CH_2OCO), 4.11 (m, CH_2OCO), 5.57 (s, CH, (monomer)), 5.65, (s, CH, (monomer)), 6.10 (s, CH, (monomer)), 6.18 (s, CH, (monomer)); IR: *v* = 1750 (C=O), 2250 (NCO), 2950 (C-H); $SEC_{(THF)}$: Mn= 5900 g mol^{-1}, *Đ* = 1.58.

2.4.4 General modification of P(MMA$_m$-co-IEM$_n$) by amines

The polymerisation mixture (1 mL) was transferred by cannula into a 15 mL vial under positive N_2 pressure. Amine (0.5 mL, 3.86 x 10^{-3} mol) was directly injected into the reaction mixture. The reaction was left for three hours and then THF (10 mL) was added. The solution was dialysed by MWCO 1K dialysis tubing against THF for 24 hours. The product was then precipitated in cold *n*-hexane and filtered by Buchner filtration. Modified polymer (70 % yield) was characterised by NMR, IR and SEC.

2.4.5 P(MMA$_m$-co-IEM$_n$) modification by dibutylamine

^{1}H NMR (400 MHz, $CDCl_3$, δ): 0.85 (m, 14H, CH_3), 0.94 (m, 6H, CH_3), 1.02 (m, 6H, CH_3), 1.34-1.53 (m, 8H, CH_2), 1.81 (m, 13H, CH_2), 3.21 (s, 4H, CH_2N) 3.50 (s, 2H, CH_2N),

3.60 (s, 17H, CH_3OCO), 4.08 (s, 2H, CH_2OCO); ^{13}C NMR (100.61 MHz, $CDCl_3$, δ): 13.96 (s, CH_3), 16.49, 18.72 (s, C backbone), 20.21 (s, CH_2), 30.72 (s, CH_2), 39.85 (s, CH_2N), 44.55 (s, CH_2N), 51.83 (s, CH_3O), 54.39 (s, CH_3), 65.22 (s, CH_2OCO), 157.46 (s, NC=O), 177.81 (s, C=O); IR: v = 2951 (C-H), 1725 (C=O), 1647 (C=O amide), 1239 (C-O); SEC $_{(THF)}$: M_n = 8300 g mol^{-1}, $Đ$ = 1.37.

2.4.6 P(MMA$_m$-co-IEM$_n$) modification by octylamine

^1H NMR (400 MHz, $CDCl_3$, δ): 0.85-1.02 (m, 18H, CH_3), 1.27-1.48 (m, 9H, CH_2), 1.76-1.90 (m, 10H, CH_2), 3.18 (s, 2H, CH_2N) 3.53 (m, 2H, CH_2N), 3.60 (s, 14H, CH_3OCO), 4.03 (m, 2H CH_2OCO); ^{13}C NMR (100.61 MHz, $CDCl_3$, δ): 14.13 (s, CH_3), 16.49, 18.72 (s, C backbone), 22.66, 26.95, 29.28, 31.84 (s, CH_2), 40.33 (s, CH_2N), 44.55 (s, CH_2N), 51.83 (s, CH_3O), 54.48 (s, CH_3), 65.40 (s, CH_2OCO), 158.18 (s, NC=O), 178.11 (s, C=O); IR: v = 2951 (C-H), 1725 (C=O), 1647 (C=O amide), 1239 (C-O); $SEC_{(THF)}$: M_n =8900 g mol^{-1}, $Đ$ = 1.49.

2.4.7 P(MMA$_m$-co-IEM$_n$) modification by (R)-(+)-α methylbenzylamine

^1H NMR (400 MHz, $CDCl_3$, δ): 0.84-1.02 (m, 21H, CH_3), 1.46 (m, 3H, CH_3), 1.81-1.94 (m, 16H, CH_2), 3.55 (m, 2H, CH_2N) 3.60 (s, 18H, CH_3OCO), 4.03 (s, 2H, CH_2OCO), 7.24-7.33 (m, CH aromatic); ^{13}C NMR (100.61 MHz, $CDCl_3$, δ): 16.37, 18.71 (s, C backbone), 23.14 (s, CH_3), 38.70 (s, CH_2N), 44.54 (s, CH_3O), 51.83 (s, CH_3O), 54.20 (s, CH_3), 64.85 (s, CH_2OCO), 125.96 (s, CH aromatic), 128.52 (s, C aromatic) 157.78 (s, NC=O), 178.12 (s, C=O); IR: v = 2950 (C-H), 1725 (C=O), 1645 (C=O amide), 1553 (C-C aromatic), 1365 (C-O); $SEC_{(THF)}$: M_n =8800 g mol^{-1}, $Đ$ = 1.54.

2.4.8 P(BnMA$_m$-co-IEM$_n$) polymerisation

5 cm of copper wire was entwined with a magnetic stirrer bar and placed into 3 mL of 35 % HCl solution for 5 minutes, washed with deionized water then acetone. Once dried, the clean wire was placed in a Schlenk tube containing $CuBr_2$ (1.59 mg, 7.15x 10^{-6} mol) (0.05 eq. relative to initiator) and sealed with a rubber septum. Ethyl α-bromoisobutyrate (21 µL, 1.43 x 10^{-4}mol, 1 eq.), 2-isocyanatoethyl methacrylate (0.10 mL, 7.15 x 10^{-4} mol, 5 eq.), benzyl methacrylate (1.09 mL, 6.43 x 10^{-3} mol, 45 eq.) and anhydrous 2-isopropanol (1.2 mL) were then added. The reaction mixture was degassed under a flow of N_2 for 15 minutes, then Me_6Tren (14 µL, 5.15 x 10^{-5} mol, 0.36 eq.) was added. The reaction was stirred for three hours. Polymer was precipitated in cold *n*-hexane and isolated by filtering through a sintered glass funnel. The resultant white powder (75 % yield) was characterised by NMR, IR and SEC. ^{1}H NMR (400 MHz, $CDCl_3$, δ): 0.73-0.92 (m, 36H, CH_3), 1.79-1.89 (m, 24H, CH_2), 3.40 (m, 2H, CH_2NCO), 4.00 (m, 2H, CH_2OCO), 4.95 (s, 22H, $PhCH_2OCO$), 7.40 (m, 55H, CH aromatic); ^{13}C NMR (100.61 MHz, $CDCl_3$, δ): 16.71 (s, CH_2), 22.23 (s, CCH_3), 44.48 (s, CH_2N), 54.22 (s, CH_3), 66.82 (s, $PhCH_2O$), 68.29 (s, CH_2OCO), 128.26 (s, NCO), 128.57 (s, CH aromatic), 135.08 (s, C aromatic), 177.13 (s, C=O); IR: *v* = 1500 (CH aromatic), 1750 (C=O), 2250 (NCO), 2950 (C-H); $SEC_{(CHCl3)}$: M_n =7700 g mol^{-1}, $Đ$ = 1.41.

2.4.9 General modification of P(BnMA$_m$-co-IEM$_n$) by amines

P(BnMA$_m$-*co*-IEM$_n$) (1.14 x 10^{-5} mol) was added into a 15 mL vial which contained 1 mL anhydrous dichloromethane and magnetic follower. The desired amine (5.93 x 10^{-4} mol, excess) was added and the reaction mixture stirred for three hours. The modified

polymer (70 % yield) was precipitated in cool *n*-hexane, and characterised by NMR, IR and SEC.

2.4.10 P(BnMA$_m$-co-IEM$_n$) modification by dibutylamine

^{1}H NMR (400 MHz, $CDCl_3$,δ): 0.73-0.95 (m, 27H, CH_3), 1.20-1.49 (m, 10H, CH_2), 1.70-1.89 (m, 16H, CH_2), 3.15 (s, 2H, NCH_2), 3.42 (s, 2H, CH_2NCO), 3.97 (s, 2H, CH_2OCO), 4.95 (m, 10H, $PhCH_2OCO$), 7.40 (CH, 31H, aromatic); ^{13}C NMR (100.61 MHz, $CDCl_3$, δ): 13.56 (s, CH_3), 18.63, 16.18 (s, CH_2), 20.18 (s, CH_2), 27.81 (s, CH_2), 39.72 (s, CH_2N), 44.77 (s, CH_2N), 54.04 (s, CH_3), 66.78 (s, $PhCH_2O$), 67.80 (s, CH_2OCO), 128.55 (s, CH aromatic), 135.08 (s, C aromatic), 157.39 (s, NC=O) 177.13 (s, C=O); IR: *v* = 2958 (C-H), 1725 (C=O), 1650 (C=O amide), 1454 (C-C aromatic), 1368 (C-O); $SEC_{(CHCl3)}$: M_n = 7900 g mol^{-1}, $Đ$ = 1.27.

2.4.11 P(BnMA$_m$-co-IEM$_n$) modification by octylamine

^{1}H NMR (400 MHz, $CDCl_3$, δ): 0.73-0.92 (m, 26H, CH_3), 1.26-1.45 (m, 14H, CH_2), 1.78-1.90 (m, 16H, CH_2), 3.14 (s, 2H, CH_2NCO), 3.44 (s, 2H, CH_2NCO), 3.97 (s, 2H, CH_2OCO), 4.88 (m, 15H, $PhCH_2OCO$), 7.40 (m, 37H, CH_2 aromatic); ^{13}C NMR (100.61 MHz, $CDCl_3$, δ): 14.14 (s, CH_3), 16.65, 18.72 (s, CH_2), 22.66, 26.98, 29.31, 31.84 (s, CH_2), 40.39 (s, CH_2N), 44.78 (s, NCH_2), 54.46 (s, CH_3), 66.78 (s, $PhCH_2O$), 66.98 (s, CH_2OCO), 128.53 (s, CH aromatic), 135.09 (s, C aromatic), 158.07 (s, NC=O), 177.40 (s, C=O); IR: *v* = 2930 (C-H), 1723 (C=O), 1652 (C=O amide), 1454 (C-C aromatic); $SEC_{(CHCl3)}$: M_n = 7200 g mol^{-1}, $Đ$ = 1.31

2.4.12 P(BnMA$_m$-co-IEM$_n$) modification by (R)-(+)-α methylbenzylamine

^{1}H NMR (400 MHz, $CDCl_3$, δ): 0.72-0.92 (m, 24H, CH_3), 1.40 (d, 3H, CH_3), 1.78-1.88 (m, 16H, CH_3), 3.38 (m, 2H, CH_2N), 3.91 (m, 2H, CH_2OCO), 4.80 (m, 14H, $PhCH_2OCO$), 4.90 (m, 2H, PhCHN), 7.28 (m, 40H, CH_2 aromatic); ^{13}C NMR (100.61 MHz, $CDCl_3$, δ): 16.44, 18.58 (s, CH_2), 23.08 (s, CH_3), 39.59 (s, NCH_2), 44.77 (s, NCH_2), 54. 53 (m, CH_2), 66.79 (s, $PhCH_2O$), 67.07 (s, CH_2OCO), 126.01, 128.55 (m, CH aromatic), 135.11 (s, C aromatic), 157.37 (s, NC=O), 177.27 (m, C=O); IR: *v* = 2949 (C-H), 1724 (C=O), 1650 (C=O amide), 1448 (C-C aromatic), 1365 (C-O); $SEC_{(CHCl3)}$:M_n = 6700 g mol^{-1}, $Đ$ = 1.36.

2.4.13 Microcapsule synthesis

P(BnMA$_m$-*co*-IEM$_n$) copolymer (0.2 g) was added into a 50 mL vial containing 2 mL anhydrous DCM. Neobee carrier oil (5 g) was added, followed by 18.4 mL of 1.3 % polyvinyl alcohol (Mowiol 18-88) aqueous solution. The mixture was homogenised at 2000 rpm for 3 minutes using an overhead dissolver disc. The mixture was transferred to a 100 mL RBF and then stirred at 400 rpm using an overhead paddle mixer. To this, a 40 % aqueous solution of diethylenetriamine (0.1 mL) was added dropwise into the reaction; the mixture was then left to stir at room temperature. After 1 hr the temperature was increased to 50 °C, after another hour the temperature was increased to 90 °C. Microcapsule size was determined by dynamic light scattering and optical microscopy.

Chapter 3

Biodegradable Polyurea Microcapsules

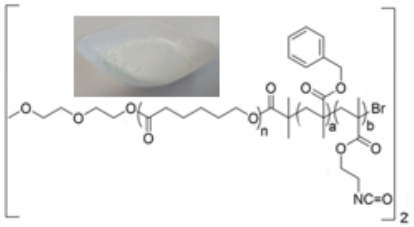

1. Polymer synthesis

2. O/W interfacial polymerization

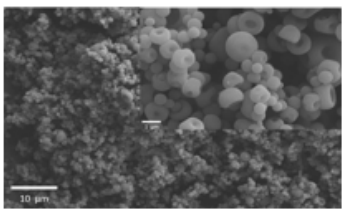

3. Spray dryer

The microcapsules have found use as carriers in personal care, agrochemical and drug delivery applications [174-178]. Microcapsules composed of polyureas have recently attracted significant interest due to their ability to efficiently encapsulate numerous active ingredients. These microcapsules are usually prepared via an interfacial polymerisation in an emulsion [179-181]. Recently, isocyanate has been employed to efficiently cross-link these microspheres, as well as nanoparticles, due to its high reactivity [168, 173]. In this chapter, ring-opening polymerisation, Cu(0)-mediated reversible deactivation radical polymerisation (RDRP), interfacial polymerisation, and a convenient drying process have been combined to prepare biodegradable microcapsules. First, α, ω-poly(ε-caprolactone) SET-LRP initiator was prepared by esterification to obtain a degradable halide initiator. Poly(benzyl methacrylate-*co*-isocyanatoethyl methacrylate) (P($BnMA_m$-*co*-IEM_n)) was prepared from the α, ω-PCL macroinitiator. Subsequently, isocyanate-containing copolymers were used to fabricate microcapsules via interfacial polymerisation in order to encapsulate imidacloprid (IMI), a neonicotinoid pesticide. Water removal via spray dryer followed. Characterisation of all products has been carried out with ^{1}H, ^{13}C NMR, FTIR spectroscopy, SEC, laser light scattering, matrix-assisted laser desorption/ionization mass spectrometry (MALDI-TOF MS), thermogravimetric analysis (TGA), UV-Vis spectroscopy (UV-Vis), and scanning electron microscopy (SEM).

3.1 Background

3.1.1 Biodegradable polymers and microcapsule synthesis

The use of biodegradable materials has increased significantly in the past few years, especially synthetic polymers such polyesters and polyurethanes. Natural materials, mostly polysaccharide derivatives, are also heavily used in different fields, particularly in food and therapeutic applications [192-195]. A key feature of these materials is an ability for self-degradation. The degradation process generally occurs through the scission of the polymer backbone by various mechanisms such as hydrolysis, photolysis and thermal degradation [196]. Polyester derivatives, including polyglycolide (PGA), polylactide (PLA) and polycaprolactone (PCL), (Figure 3.1) are increasingly applied as polymeric drug carriers in many applications, for example, biomedical and pharmacological materials, environmentally friendly packaging, carrier matrices for slow release and microelectronics [197-204]. PCL is classified as a semi-crystalline polymer, in other words, the degree of crystallinity influences the polymer property. Interestingly, facile synthesis, cost effectiveness, good drug permeability and slow degradation make PCL one of the promising candidates in long-term controlled release [197, 205-206]. Different tools are exploited in order to use PCL derivatives, including polymer films, micro- and nanocapsule, polymeric micelles, scaffolds and nanoparticle [207]. Notably, during the degradation process, the amorphous phase of PCL degrades, first through bulk erosion process, followed by a crystalline phase. This degradation leads to an unpredictable release profile, which makes PCL unsuitable for some applications. Microcapsules of PCL derivatives can be prepared via different techniques, including emulsion solvent evaporation, spray drying, solution enhanced dispersion, and hot melt

techniques, to encapsulate a number of active ingredients such as ketorolac trimethamine, insulin, antigens, ribozymes and doxycycline [206-212]. Consequently, most of the microcapsules show a significant improvement of active ingredients (AIs) stability, as well as a reduction of initial burst release period. In general, there are two major AI release mechanisms, which are surface erosion and diffusion through the media. The chemical property of AIs also influences the release profile, particularly the hydrophilic and hydrophobic characteristics.

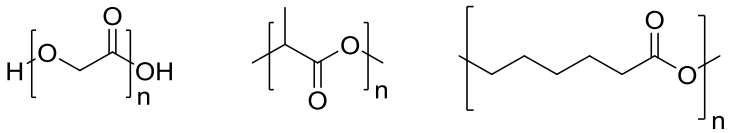

Figure 3.1 Examples of biodegradable polyesters.

Spray-drying is a powerful microencapsulation technique and has many advantages, including cost effectiveness, a facile process, and speed. Thus, this technique is highly attractive from an industrial point of view [213]. A common example of the spray drying technique is the manufacture of dried milk. There are a few reports of using the spray drying method as a synthetic tool to encapsulate AI by using PCL as the capsule wall. For example, Sastre *et al.* showed the microcapsule formulation of PCL to deliver 5-fluoro uracil (5-FU) [214]. One finding indicated the successful encapsulation with a reasonable controlled release profile. In addition, Blanco and co-workers recently proved the ability of PCL as a promising material in order to encapsulate AIs via a spray drying process. Furthermore, acceptable encapsulated efficiency and slow release of paclitaxel (PTX) indicated the benefit of microcapsules [215]. Polymerisation of PCL is

straightforward through ring-opening polymerisation (ROP) from an inexpensive ε-caprolactone monomer. The brief polymerisation process will be discussed in the next section.

3.1.2 Ring-opening polymerisation (ROP)

Ring-opening polymerisation (ROP) is classified as chain-growth polymerisation. The concept of ROP is demonstrated when an active centre reacts with monomers via opening an n-cyclic ring (n = 3-8); the ring strain can play a vital role as the driving force in the polymerisation process. Most of the linear aliphatic biodegradable polyesters, including PCL, PLLA, and PGA, are synthesised via ROP because of several benefits, particularly the facile synthetic process.

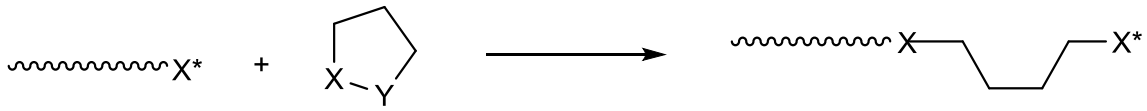

Figure 3.2: A simple schematic of ring-opening polymerisation (ROP).

PCL was selected for use as the biodegradable material in this thesis because of several reasons, including the inexpensive nature of the ε-CL monomer, its outstanding physical properties and the facile polymerisation procedure. In general, polymerisation of PCL can be achieved via two main routes: ring opening polymerisation of ε-CL and condensation polymerisation, for example, the reaction of 6-hydroxyhexanoic acid, however, the ring-opening process is a favoured technique, because the condensation reaction generates by-products such as water. Thus, some polycondensation

polymerisation features, such as low molecular weight and high polydispersity, are detected. There are different methods used to synthesise PCL via ROP, for example, via activated monomer, anionic, cationic and coordination insertion [216]. A commonly used catalyst for coordination insertion ring-opening polymerisation of cyclic esters is tin(II) ethyl hexanoate ($Sn(Oct)_2$), which is a low toxicity catalyst, easy to handle and soluble in most organic solvents. ($Sn(Oct)_2$) is approved by the US Food and Drug Administration (FDA), thus, it has been widely applied in different applications, including food additives [217]. The mechanism and kinetics of lactone polymerisation by using $Sn(Oct)_2$ as the catalyst has been intensively studied by Penczek *et al.* [218-220].

Initially, the reaction between an alcohol and ($Sn(Oct)_2$) catalyst provides an active species. Subsequently, the catalyst is reformed and a polycaprolactone dormant species is generated. The process of transforming the active species to a polymer dormant species occurs quickly, which leads to narrowed molecular weight distribution. Thus, ROP via this catalytic system is also acknowledged as controlled polymerisation [221].

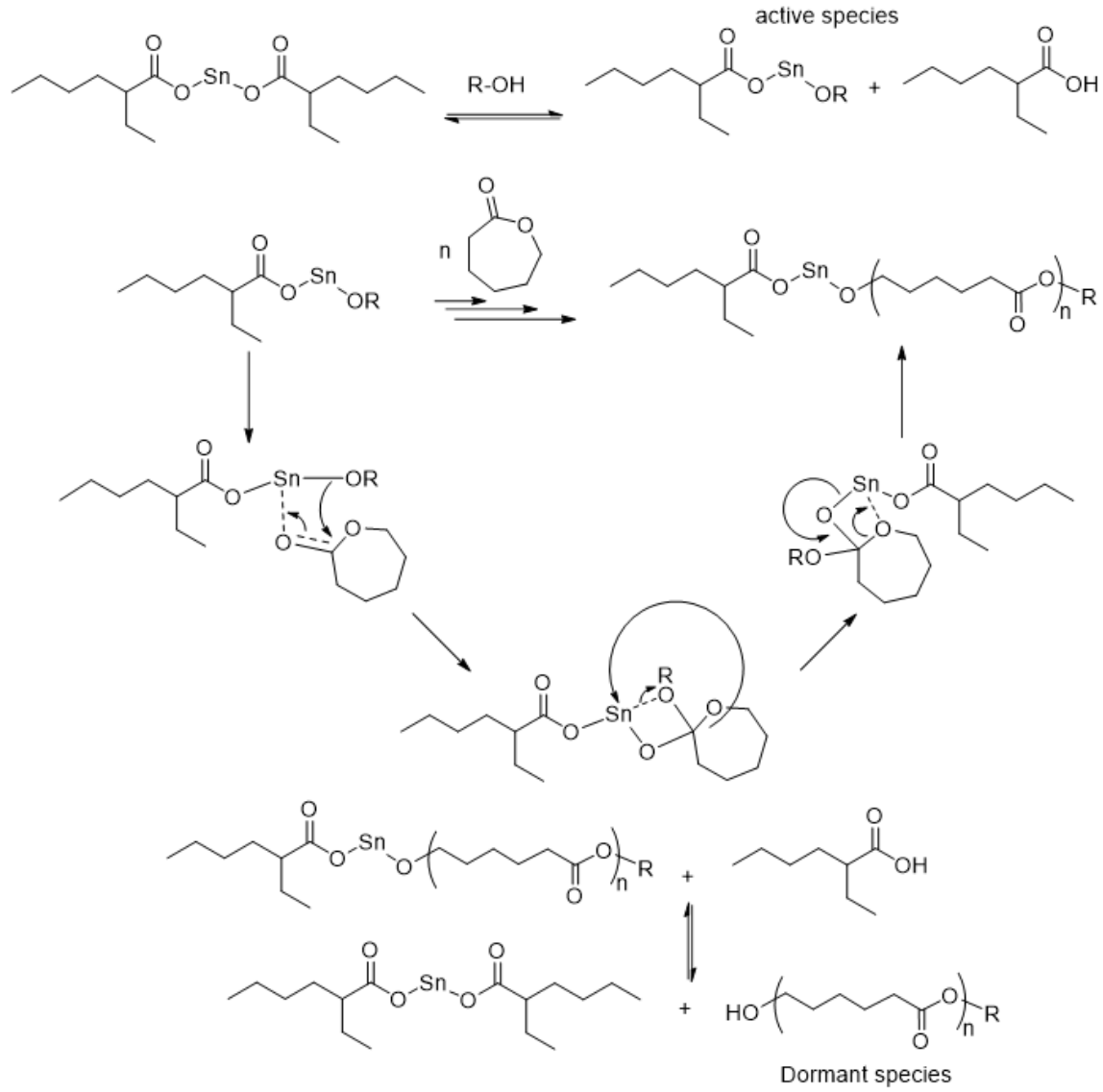

Figure 3.3: The proposed mechanism of ROP of ε-CL by using ($Sn(Oct)_2$) as the catalyst.

3.2 Results and Discussion

3.2.1 α, ω-Hydroxyl terminated PCL polymerisation

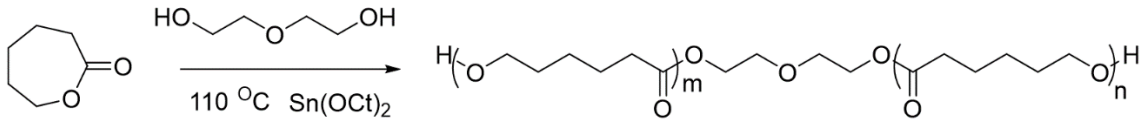

Figure 3.4: Ring-opening polymerisation of ε-caprolactone initiates by diethylene glycol.

α, ω-Hydroxyl terminated polycaprolactone (α, ω-PCL) was synthesised through conventional ring-opening polymerisation by using diethylene glycol as an initiator. Polymerisation was catalysed by tin(II) 2-ethylhexanoate ($Sn(Oct)_2$) and left at 110 ˚C under N_2 for 15 hours. After purification, the polymer was characterised using different techniques, including NMR, FTIR, SEC, and MALDI-TOF. SEC indicated a successful ring opening of caprolactone according to the increase of molecular weight (M_n = 3700 g mol^{-1}). Moreover, the dispersity was acceptable $Đ$ = 1.15. The molecular weight of synthetic α, ω -PCL was considered from both SEC and ^1H NMR spectroscopy; the ratio of integration of position 3 (from initiator) to 5 offers a degree of polymerisation (Figure 3.5), thus, a molecular weight of α, ω -PCL is derived. Interestingly, the molecular weight of polymers from both characterisation techniques was significantly different. This could be the result of hydrodynamic volume differences of the calibration standards used in SEC.

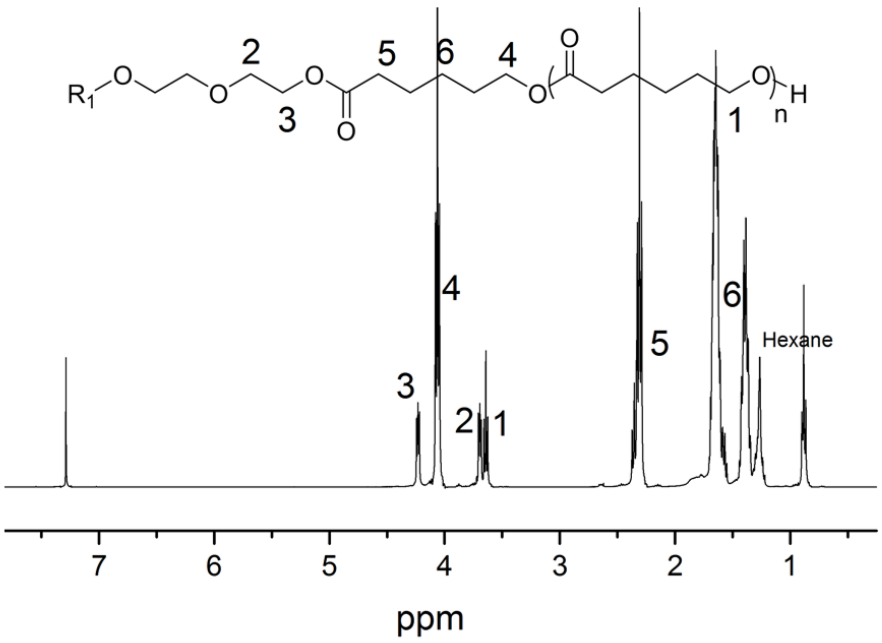

Figure 3.5: ^{1}H NMR of α, ω-poly(ε-caprolactone) synthesised via ROP by using $Sn(Oct)_2$ as the catalyst ($CDCl_3$, 400 MHz).

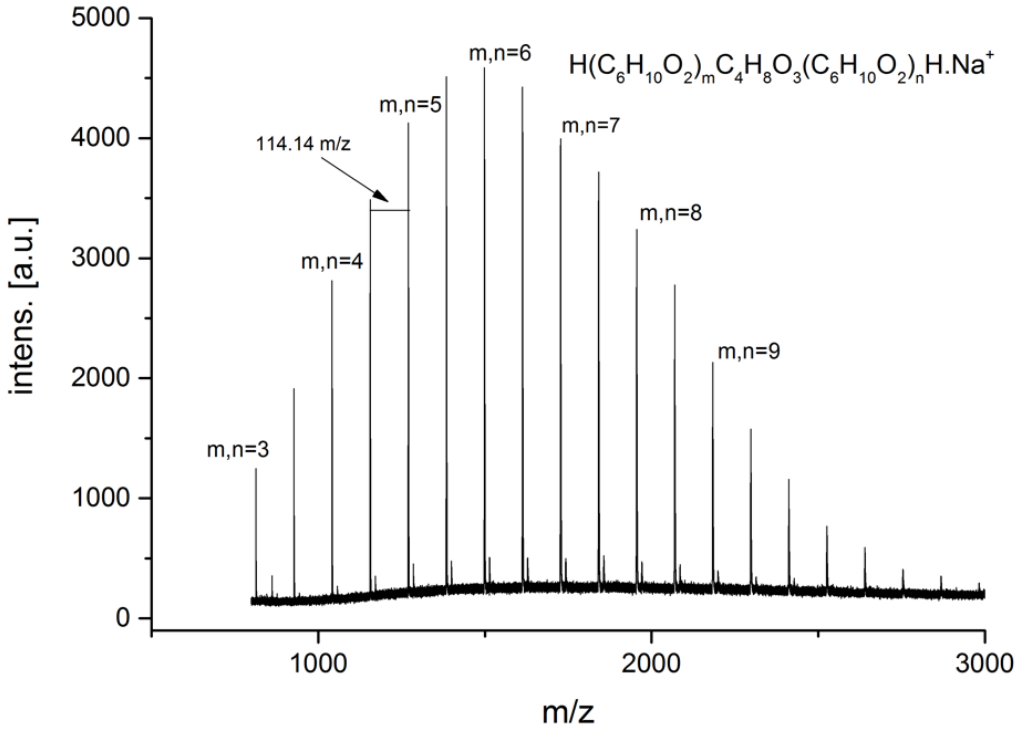

Figure 3.6: MALDI-TOF (MS) spectra of α, ω-poly(ε-caprolactone) synthesised via ROP by using $Sn(Oct)_2$ as the catalyst.

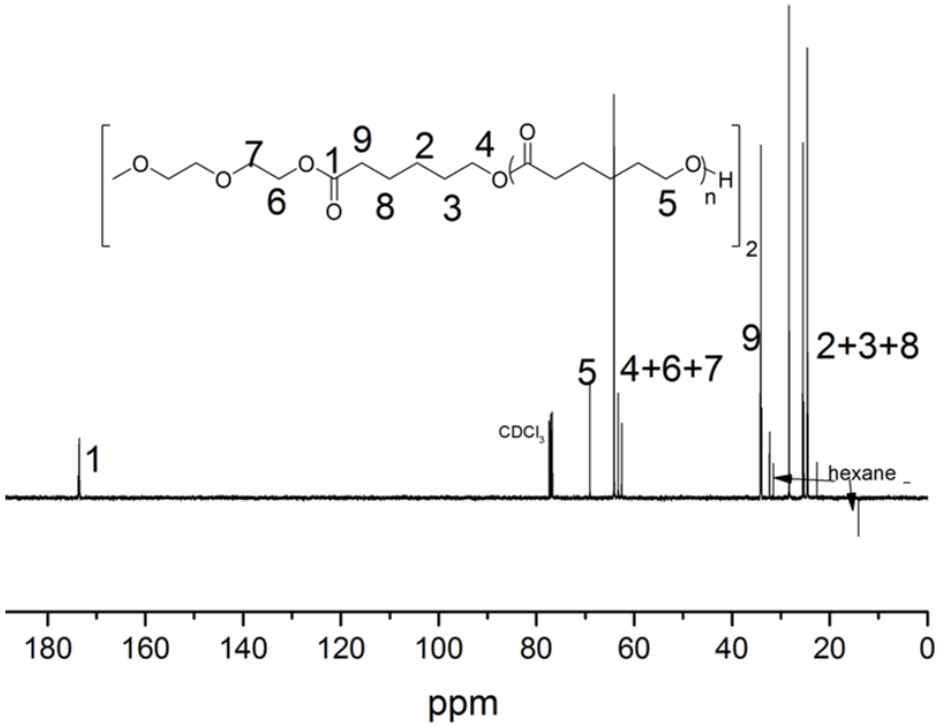

Figure 3.7: ^{13}C NMR of α, ω-poly(ε-caprolactone) synthesised via ROP by using $Sn(Oct)_2$ as the catalyst ($CDCl_3$, 400 MHz).

To resolve the differences between SEC and ^{1}H NMR on the measured molecular weight, MALDI-TOF MS was used. Degree of polymerisation (DP_n) of α, ω - PCL from MALDI-TOF MS measurement is 6 to 18 (Figure 3.6). Moreover, the m/z repeating unit = 114.14, indicating a ε-caprolactone. The narrow molar mass distribution of polycaprolactone from SEC data and degree of polymerisation of 12 from ^{1}H NMR coincides with the result from mass spectroscopy. As a result, the polymeric structure of $H(C_6H_{10}O_2)_6C_4H_8O_3(C_6H_{10}O_2)_6H.Na^+$ is used to determine a molecular weight of α, ω - hydroxyl terminated polycaprolactone in order to synthesise a macroinitiator in a further step.

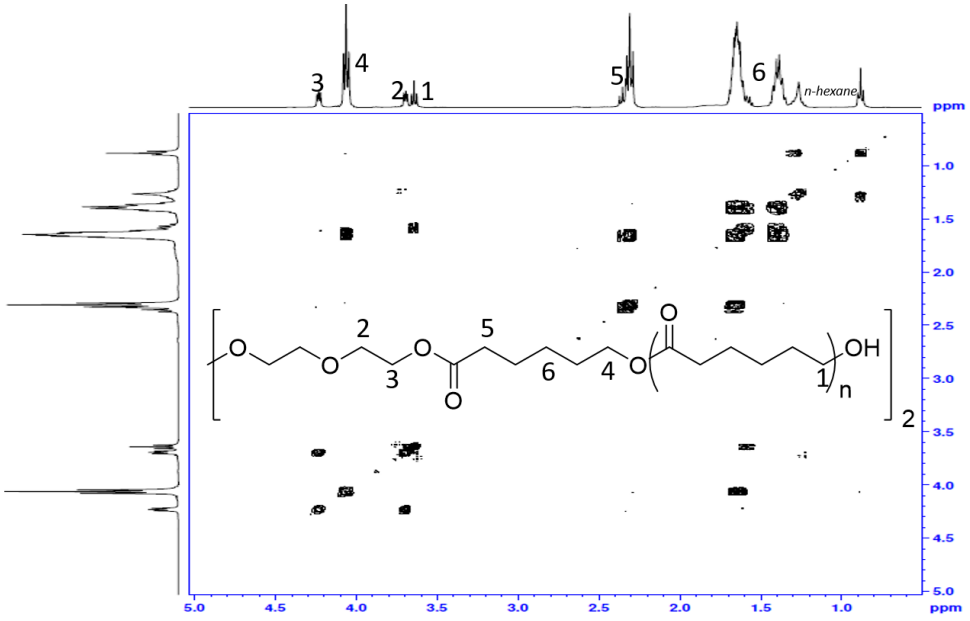

Figure 3.8: COSY NMR of α, ω-poly(ε-caprolactone) synthesised via ROP by using $Sn(Oct)_2$ as the catalyst ($CDCl_3$, 400 MHz).

3.2.2 α, ω-poly(ε-caprolactone) SET-LRP macroinitiator synthesis

α, ω-Poly(ε-caprolactone) SET-LRP macroinitiator is synthesised via the esterification reaction of an acid halide, α, ω-bromoisobutyryl bromide (BiBB), with two different molecular weight α, ω-hydroxyl terminated poly(ε-caprolactone)s: α, ω-PCL_{12} and α, ω-PCL_5. α, ω-PCL_{12} was polymerised via ring opening polymerisation (ROP) of ε-caprolactone initiated by diethylene glycol, while α, ω-PCL_5 was purchased from a commercial source. SEC analysis after modification of α, ω-PCL_{12} shows a slight increase of relative molecular weight after purification (M_n = 3700 g mol^{-1}). In addition, the molar mass distribution ($Đ$ = 1.11) demonstrates a similar distribution as for unmodified α, ω-poly(ε- caprolactone) (Figure 3.10).The ^1H NMR spectrum, figure 3.11, demonstrates a successful modification of both hydroxyl groups of α, ω-PCL due to a disappearance of CH_2OH peak at 3.64 ppm and an evolution of the peak at 4.14 ppm of CH_2COO. COSY

NMR of α, ω-hydroxyl terminated poly(ε-caprolactone) also indicates that the signal at 3.64 ppm represents C*H*$_2$ adjacent to the hydroxyl functionality (Figure 3.8). Thus, the chemical shift of new ester bond in the macroinitiator and the disappearance of C*H*$_2$ next to the hydroxyl group are also confirmed by COSY (Figure 3.12). The ^{1}H NMR signal of methyl groups (position 1 in Figure 3.11) adjacent to the bromine at 1.91 ppm is observed. The absence of a signal from BiBB at 1.85 ppm is also seen. Finally, integration of all peaks shows a successful modification and purification. Furthermore, ^{13}C NMR confirms the successful modification by the carbon at C(CH$_3$)$_2$Br at 28 ppm (Figure 3.13). FTIR spectra also proves the disappearance of O-H stretching (3450 cm^{-1}) after modification (Figure 3.14).

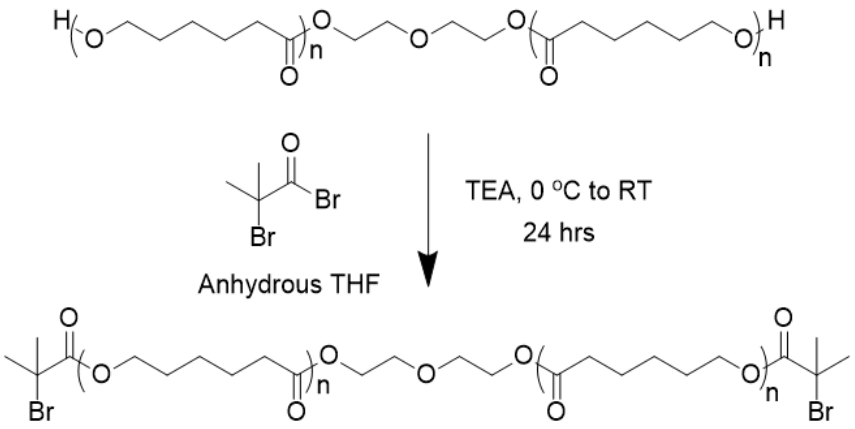

Figure 3.9: SET-LRP macroinitiator synthesised via esterification reaction of an acid halide and α, ω-hydroxyl terminated poly(ε-caprolactone).

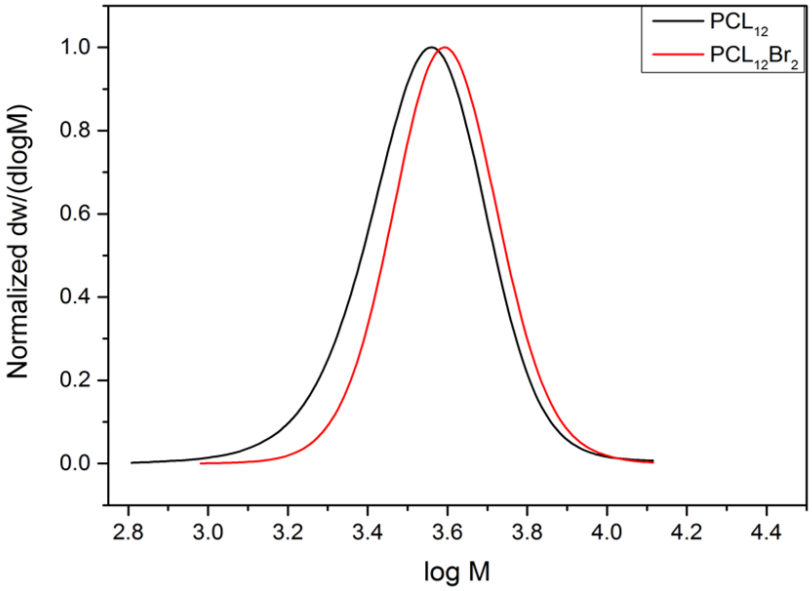

Figure 3.10: SEC showing successful modification of α, ω-poly(ε-caprolactone) (α, ω-PCL_{12}) with an acceptable narrow distribution.

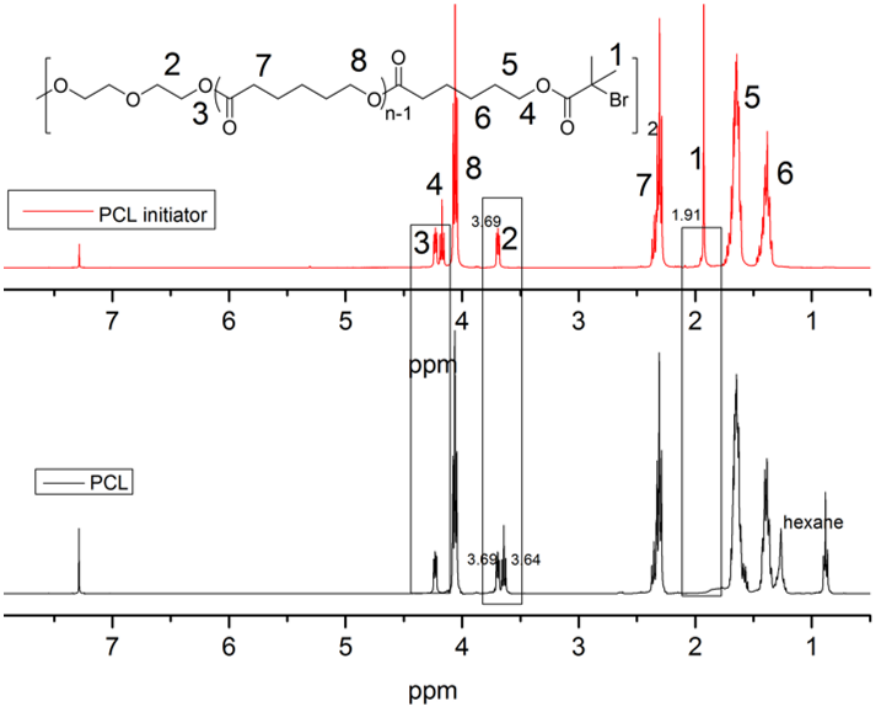

Figure 3.11: ^{1}H NMR of before and after modification of α, ω-PCL_{12} ($CDCl_3$, 400 MHz). The signal of methyl groups adjacent to the bromine and CH_2COO in the initiator are detected at 1.91 and 4.14 ppm, respectively. Notably, the chemical shift at 3.64 ppm indicates the CH_2 next to the hydroxyl group of α, ω-PCL_{12}.

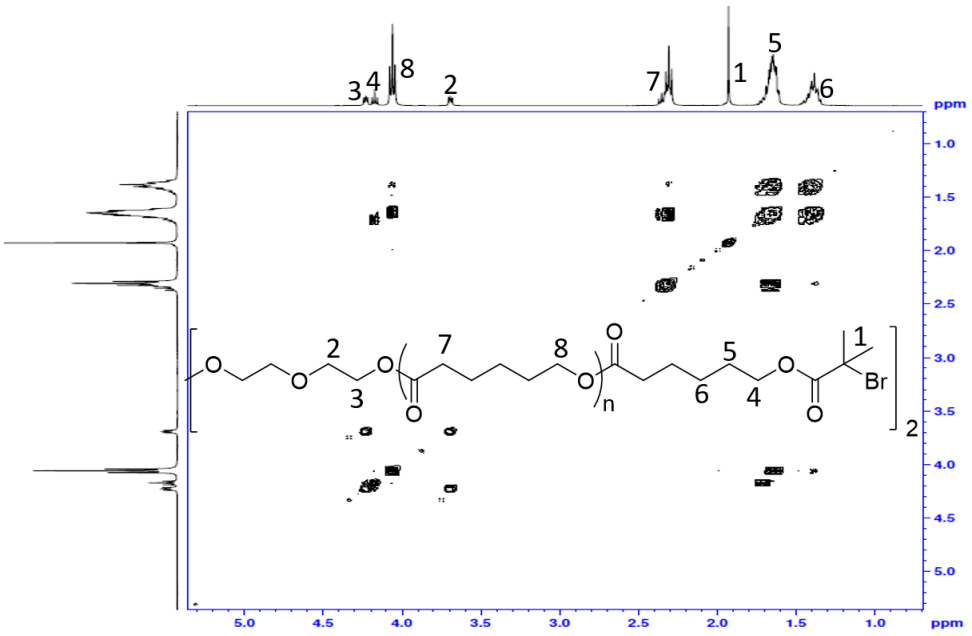

Figure 3.12: COSY NMR of modified α, ω-poly(ε- caprolactone) (α, ω-PCL_{12})($CDCl_3$, 400 MHz).

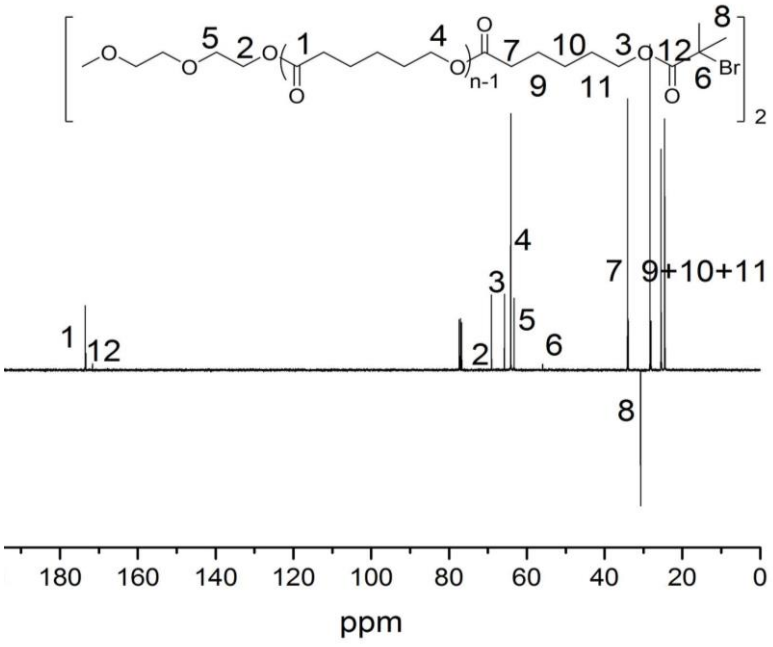

Figure 3.13: ^{13}C NMR spectra of modified α, ω-poly(ε- caprolactone) (α, ω-PCL_{12})($CDCl_3$, 400 MHz).

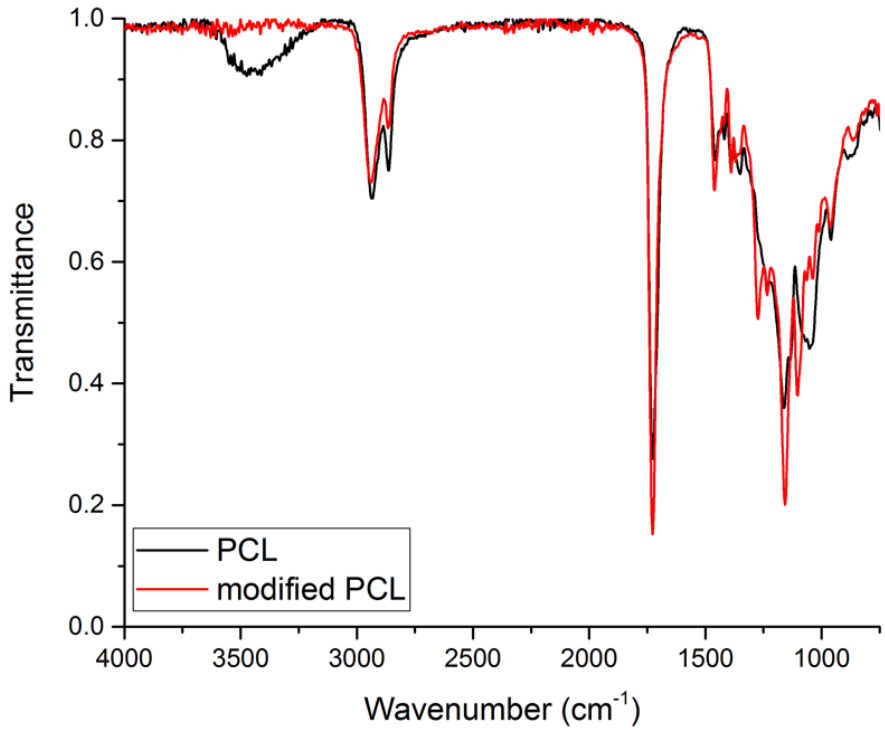

Figure 3.14: FTIR spectra of non-modified and modified α, ω-poly(ε- caprolactone) (α, ω-PCL_{12}); the disappearance of O-H stretching (3450 cm^{-1}) was observed after modification.

In addition, mass spectroscopy, MALDI-ToF MS, was applied to further characterise the modified α, ω-PCL_{12}. Figure 3.15 shows the MALDI-ToF MS analysis of the macroinitiator; the molecular formula is represented as $C_4H_6OBr(C_6H_{10}O_2)_mC_4H_8O_3(C_6H_{10}O_2)_nC_4H_6OBr.Na^+$, where m and n are detected from 4-10. The ε-caprolactone monomer repeating m/z is represented by the mass difference of 114.14. Additionally, the theoretical and measured m/z of $C_4H_6OBr(C_6H_{10}O_2)_6C_4H_8O_3(C_6H_{10}O_2)_6C_4H_6OBr.Na^+$ is also shown in figure 3.16. Thus, MALDI-ToF MS characterisation showed the successful modification of both hydroxyl groups as demonstrated by an overlaid spectrum of non-modified PCL and bifunctional PCL macroinitiator, with the m/z increasing by 298.052 (Figure 3.17). Characterisation details, MALDI-ToF MS, of modified α, ω-PCL_5 are also shown in Figure 3.18

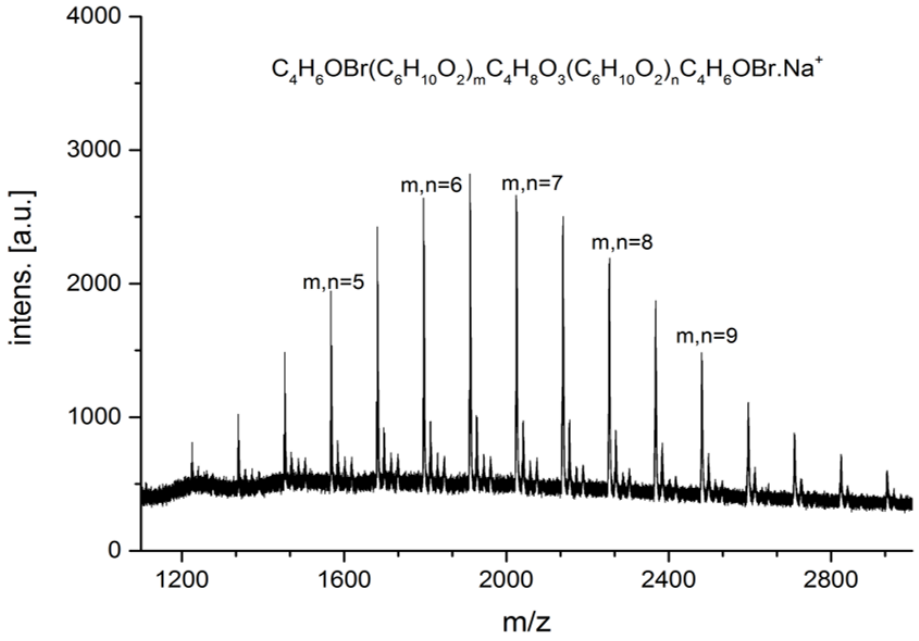

Figure 3.15: MALDI-ToF spectra of α, ω-poly(ε-caprolactone) (α, ω-PCL_{12}) SET-LRP macroinitiator.

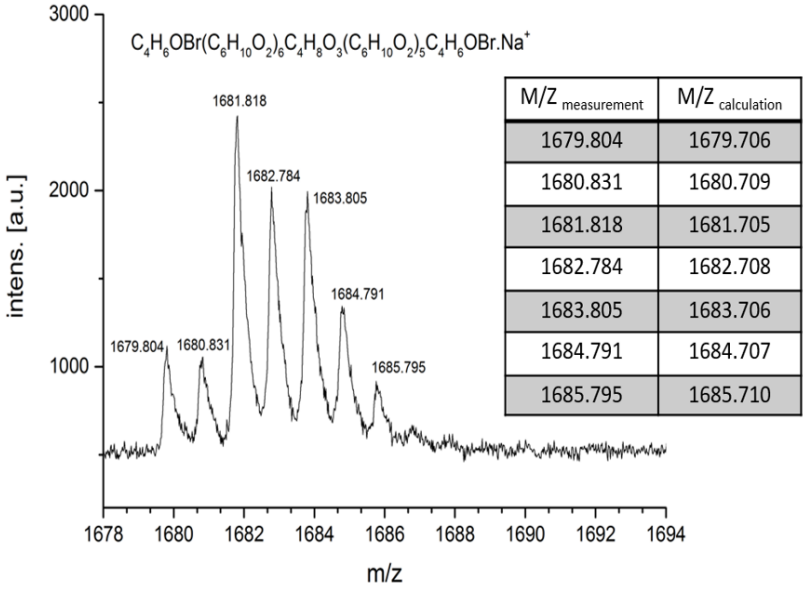

$M/Z_{measurement}$	$M/Z_{calculation}$
1679.804	1679.706
1680.831	1680.709
1681.818	1681.705
1682.784	1682.708
1683.805	1683.706
1684.791	1684.707
1685.795	1685.710

Figure 3.16: MALDI-ToF MS spectra represents the similar result of m/z measurement and m/z calculation of (α, ω-PCL_{12}) SET-LRP macroinitiator. The isotropic pattern indicates that the initiator contains two bromines. The abundance of ^{79}Br and ^{81}Br is 51 % and 49 %, respectively, thus 1: 1 intensity should be observed. However, other stable isotopes also consist in the initiator resulting in the difference of bromine intensity.

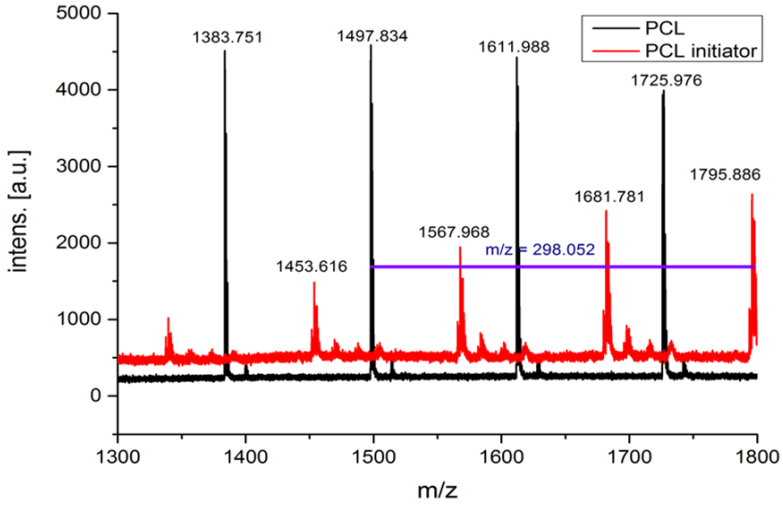

Figure 3.17: Overlaid MALDI-ToF spectra of α, ω-poly(ε-caprolactone) (α, ω PCL_{12}) SET-LRP macroinitiator and α, ω-poly(ε-caprolactone); the successful modification of both hydroxyl groups is approved by the increasing of m/z by 298.052 (m/z of 2 x $C{=}OC(CH_3)_2Br$).

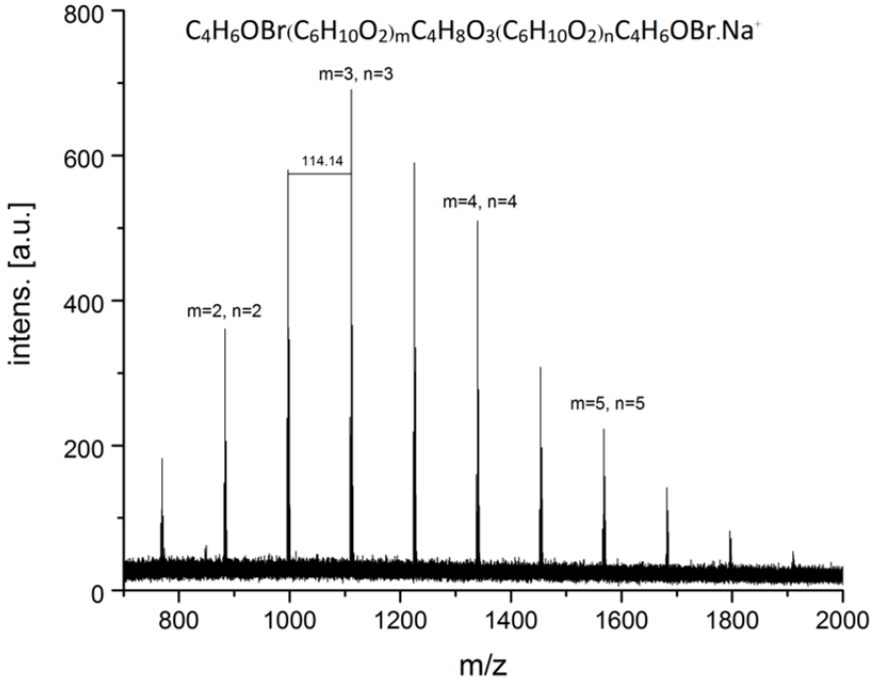

Figure 3.18: MALDI-ToF spectra of α, ω-poly(ε-caprolactone) (α, ω-PCL_5) SET-LRP macroinitiator.

3.2.3 Synthesis of P(BnMA-co-IEM) copolymers from an α, ω-poly(ε-caprolactone) SET-LRP macroinitiator

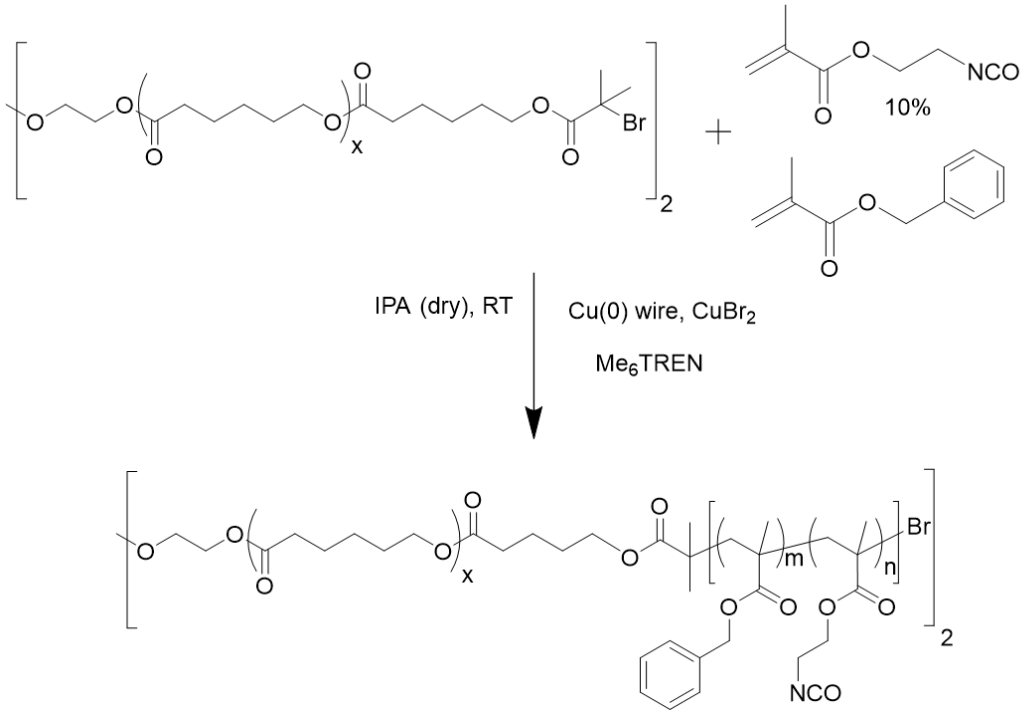

Figure 3.19: SET-LRP polymerisation of BnMA and IEM monomer by α, ω polycaprolactone SET-LRP macroinitiator.

Polymerisation conditions for poly (benzyl methacrylate-*co*-isocyanatoethyl methacrylate), P(BnMA$_m$-*co*-IEM$_n$) copolymers were investigated and presented in chapter 2 [49], thus these polymerisation conditions were duplicated to synthesise isocyanate-containing copolymers initiated by the α, ω-macroinitiator. The polymerisation (10 mol% IEM) was performed in anhydrous isopropanol at ambient temperature, and phase separation between polymer and monomer/solvent was detected after five hours. This straightforward purification process was used with the top layer removed, and the copolymer layer re-dissolved in anhydrous dichloromethane (DCM) and subsequently precipitated in cold hexane, followed by filtration through a

sintered glass funnel. The extraordinary reactivity of isocyanates towards nucleophiles leads to care concerning the stability of the isocyanate functionality in the copolymer being taken, thus the copolymer (white powder) was first characterised by FTIR to prove whether an isocyanate functional group (2250 cm^{-1}) is retained in the copolymer after polymerisation and purification (Figure 3.20).

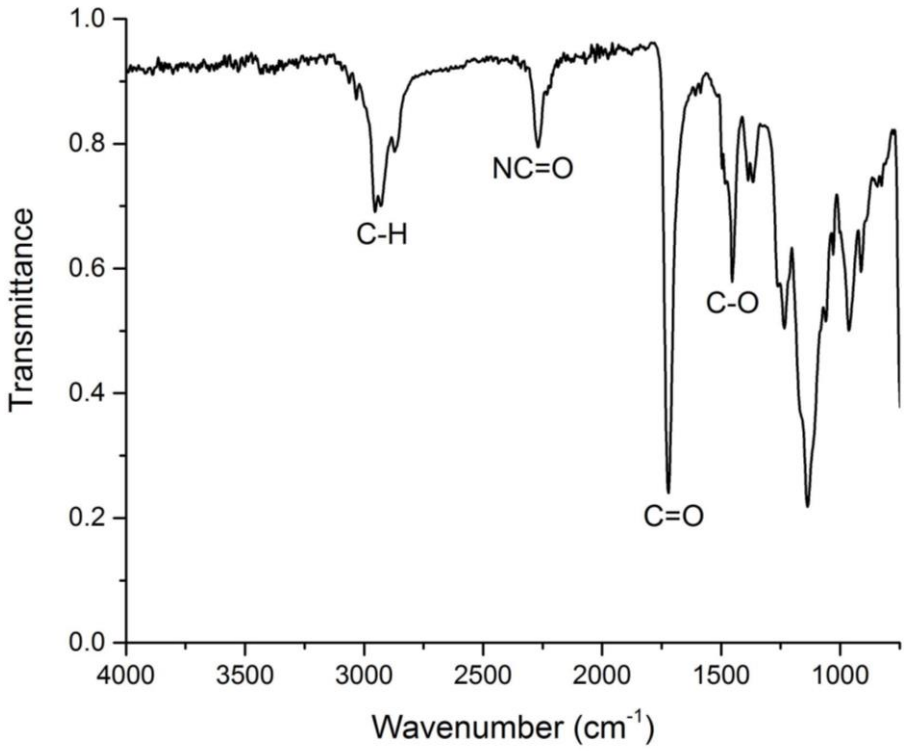

Figure 3.20: FTIR spectra of PCL_{12}-P($BnMA_{44}$-*co*-IEM_6) indicates that isocyanate function is preserved after purification.

Two molecular weights of the SET-LRP macroinitiator were used to polymerise P($BnMA_m$-*co*-IEM_n) with a feed ratio of initiator: BnMA: IEM = 1: 45: 5, 1: 90: 10, and 1: 180: 20. SEC measurement revealed that a molar mass distribution (*Đ*) of the copolymer is approximately 1.40 to 1.50 (Table 3.1). In addition, the symmetrical chromatogram, figure 3.21, indicates a reasonable controlled radical character. The absence of a shoulder peak indicates that no significant termination of living polymer chain occurs

during the polymerisation and purification processes. Monomer conversion was followed and calculated by ^{1}H NMR due to phase separation system, which was approximately 50 % to 60 % for both monomers, and, interestingly, no further BnMA or IEM was consumed when the polymerisation was left overnight.

No.	In	Composition (%)		copolymer	$M_{n,NMR}$ (g mol^{-1})	$M_{n,SEC}$ (g mol^{-1})	$Đ$
		BnMA	IEM				
In 1	-	-	-	-	990	1200	1.21
In2	-	-	-	-	1770	3700	1.15
1	1	91	9	PCL_5-P(BnMA$_{20}$-*co*-IEM$_3$)	4860	7900	1.52
2	1	91	9	PCL_5-P(BnMA$_{52}$-*co*-IEM$_8$)	11080	14000	1.49
3	1	87	13	PCL_5-P(BnMA$_{63}$-co-IEM$_{10}$)	13480	17200	1.45
4	2	86	14	PCL_{12}-P(BnMA$_{24}$-*co*-IEM$_6$)	6690	13400	1.48
5	2	92	8	PCL_{12}-P(BnMA$_{44}$-*co*-IEM$_6$)	10210	17800	1.42
6	2	88	12	PCL_{12}-P(BnMA$_{75}$-co-IEM$_6$)	17020	20200	1.48

Table 3.1: Summary of PCL_x-P(BnMA$_m$-*co*-IEM$_n$) copolymers synthesised via SET-LRP at ambient temperature.

^{1}H NMR indicates that α, ω-PCL macroinitiators contain 5 and 12 ε-CL repeating units. Thus, this result was used to calculate monomer repeating units of PBnMA and PIEM in the copolymer. The known integrated area of the C*H*$_2$ groups adjacent to the ester group in the macroinitiators (position 4 in Figure 3.22) was compared to position 8 and 2, which are assigned to C*H*$_2$-NC=O and Ph-C*H*$_2$, respectively. Consequently, ^{1}H NMR reveals a polymeric formula of PCL_5-P(BnMA$_{52}$-*co*-IEM$_8$) for the copolymer synthesised from α, ω-PCL_5 macroinitiator and PCL_{12}-P(BnMA$_{44}$-*co*-IEM$_6$) copolymer polymerised from α, ω-PCL_{12} macroinitiator. ^{13}C NMR (Figure 3.23) of the copolymers also showed a successful polymerisation of our system. Notably, all carbon positions are considered alongside the HSQC NMR experiment that represents the signal of a carbon

and proton correlation (Figure 3.24). A molecular weight difference between ^{1}H NMR and SEC analysis was observed as a result of the SEC calibration with PMMA.

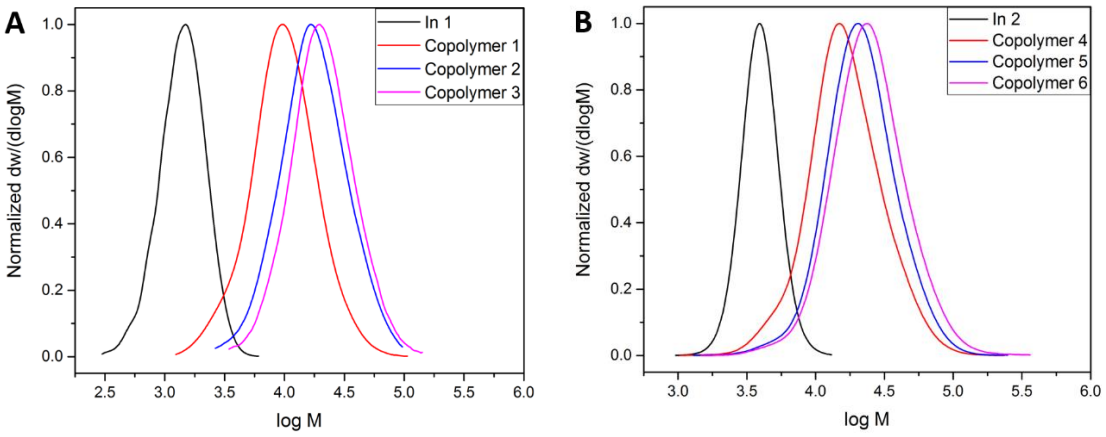

Figure 3.21: SEC traces of PCL_x-P($BnMA_m$-*co*-IEM_n) copolymers synthesised from α, ω-PCL_5 (A) and α, ω-PCL_{12} (B) macroinitiators. The absence of a shoulder peak indicates that no significant termination occurs during the polymerisation and purification processes.

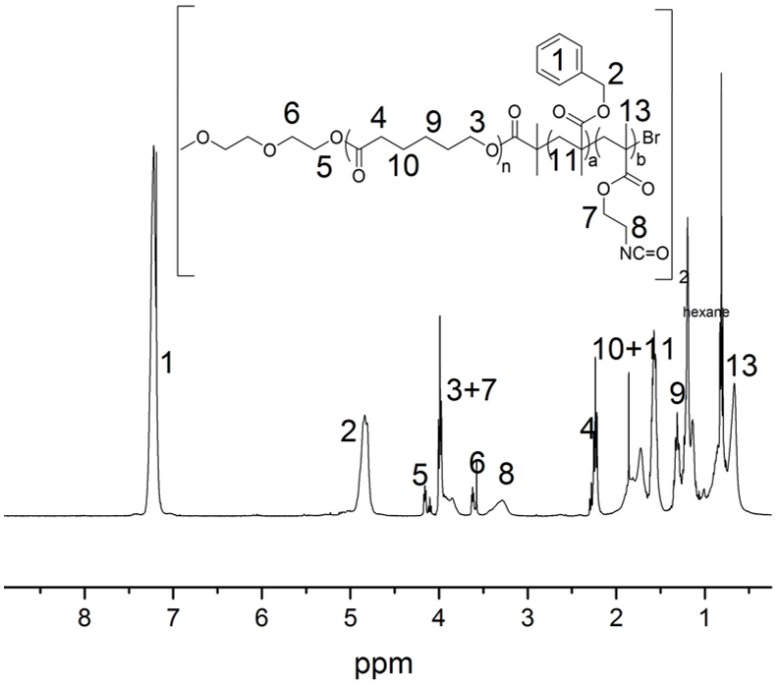

Figure 3.22: ^{1}H NMR spectra of PCL_{12}-P($BnMA_{24}$-*co*-IEM_6) copolymer synthesised from the α, ω-PCL_{12} macroinitiator ($CDCl_3$, 400 MHz). The copolymer composition and monomer repeating unit are calculated from the integrated area of the CH_2 groups

adjacent to the ester group in the macroinitiators, position 4, compared to position 8 and 2, which are assigned to C*H*$_2$-NC=O (IEM)and Ph-C*H*$_2$ (BnMA), respectively.

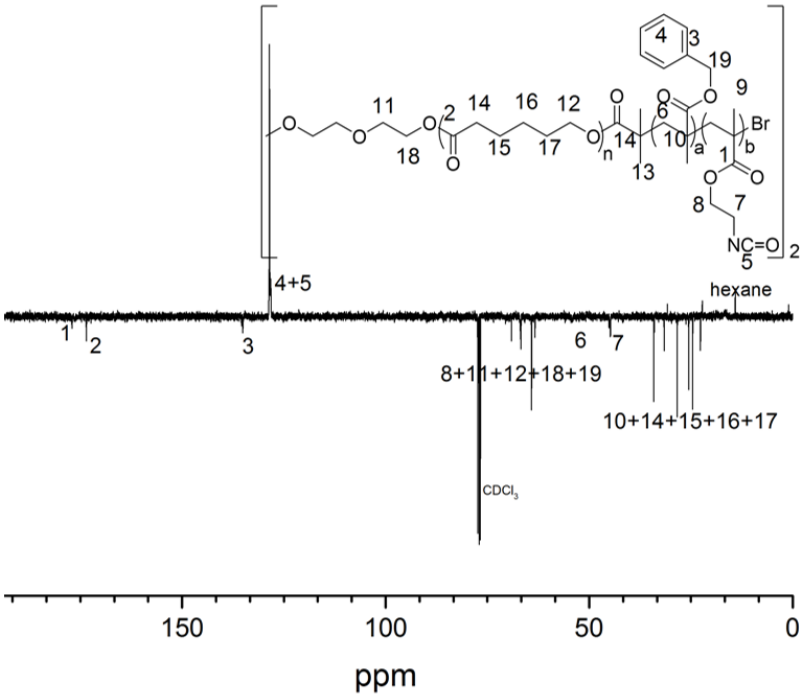

Figure 3.23: ^{13}C NMR spectra of PCL$_{12}$-P(BnMA$_{24}$-*co*-IEM$_6$) copolymer synthesised from the α, ω-PCL$_{12}$ macroinitiator ($CDCl_3$, 400 MHz).

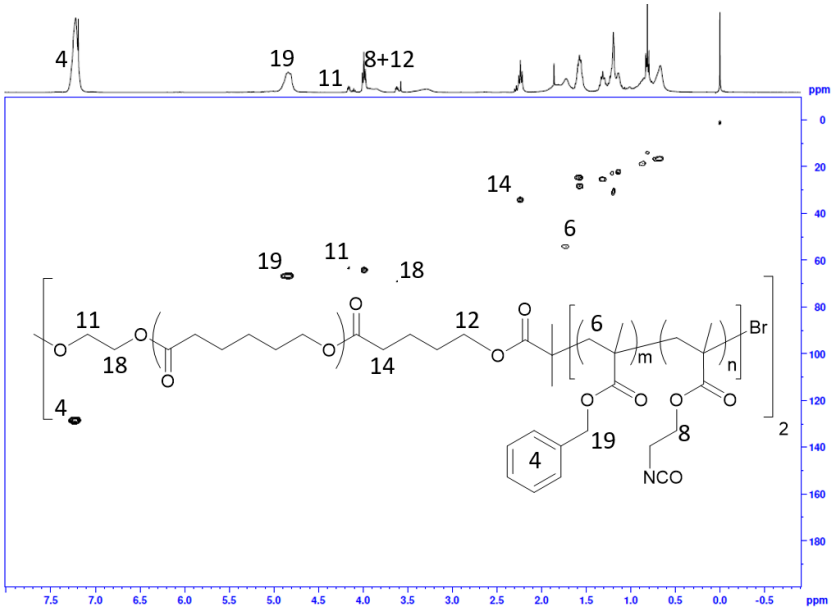

Figure 3.24: HSQC NMR spectra, NMR experiment that represents the signal of a carbon and proton correlation, of PCL$_{12}$-P(BnMA$_{24}$-*co*-IEM$_6$) copolymer synthesised from the α, ω-PCL$_{12}$ macroinitiator ($CDCl_3$, 400 MHz).

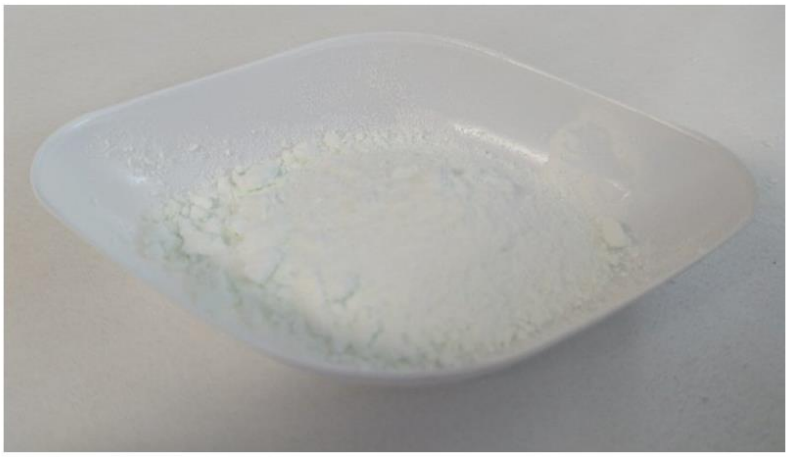

Figure 3.25: White powder of PCL_x-P($BnMA_m$-*co*-IEM_n) copolymer after purification.

3.2.4 Emulsion droplet size

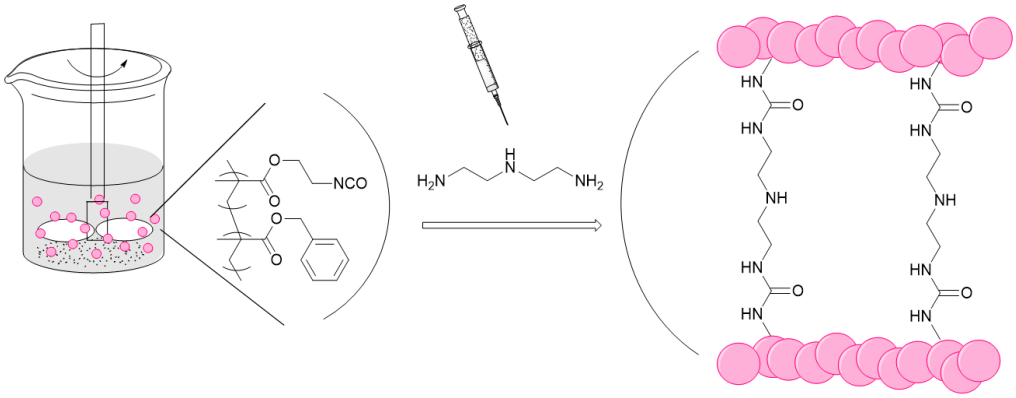

Figure 3.26: Microcapsule fabrication via an oil-in-water interfacial polymerisation of PCL_x-P($BnMA_m$-*co*-IEM_n).

A protocol for the synthesis of polyurea microcapsules from isocyanate containing copolymers was presented in chapter 2. PCL_x-P($BnMA_m$-*co*-IEM_n) copolymers were dissolved in anhydrous dichloromethane followed by the addition of carrier oil and stabiliser poly (vinyl alcohol) (PVA) solution. The solution was homogenised by overhead stirring and cross-linked by addition of diethylenetriamine (DETA). Some conditions were modified to observe an influence on the emulsion droplet size, including

copolymer molecular weight and copolymer composition, the percentage of carrier oil/ stabiliser (w/v) and copolymer solid content in an organic solvent. Consistent droplet size was observed by both laser scattering measurements and optical microscope, although the copolymer content, copolymer molecular weight and a different number of isocyanate functions were alternated (Figure 3.27). Interestingly, only a percentage of carrier oil/ stabiliser (w/v) influences particle size; 1.1 %, 2.2 % and 27 % of carrier oil were studied. Laser scattering measurements and optical microscope results both show that the emulsion droplet size is directly proportional to the percentage of the carrier oil. The droplet size of the emulsion samples that were prepared with 27 % (w/v) of carrier oil/stabiliser showed a similar result from these characterisation techniques, approximately 50 µm in diameter (Figure 3.28a). Conversely, the particle size significantly decreases when 1.1% and 2.2% (w/v) of carrier oil/stabiliser system was applied, roughly 23 and 18 µm, respectively. (Figure 3.28b)

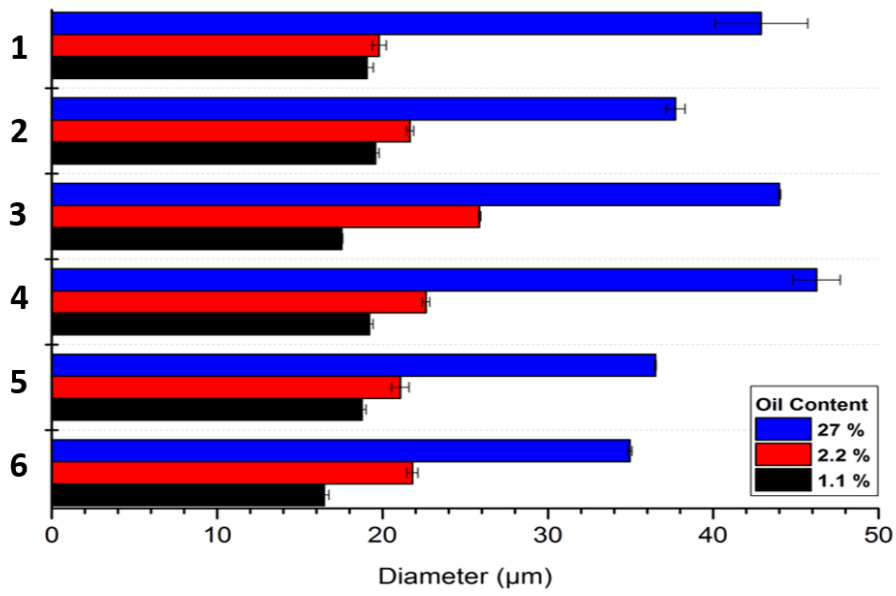

Figure 3.27: Laser scattering measurement of the emulsion droplets prepared from different copolymers (Table 3.1).

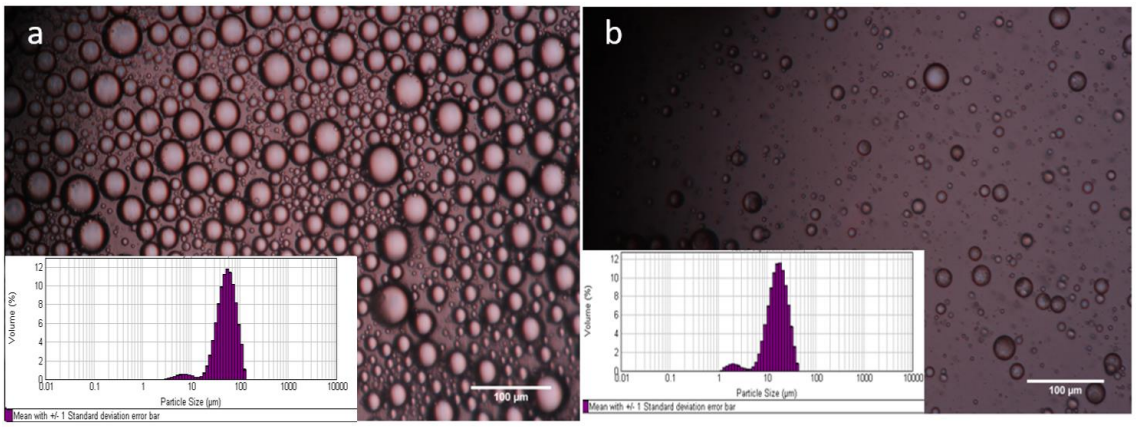

Figure 3.28: Optical microscope and mastersizer results of emulsion droplet when different ratios carrier oil/stabilizer (w/v) was applied, 27 % (a) and 2.2 % (b).

3.2.5 Drying process and microcapsule distribution

Figure 3.29: BUCHI mini Spray Dryer B-290

After the organic solvent (DCM) removal, the dispersed microcapsules were collected by evaporation by a lab scale spray dryer. The drying process conditions,

including inlet temperature, feeding rate and copolymer solid content, were optimised. An emulsion solution, prepared from 1.1 and 2.2 % (w/v %) of (PCL_5-P($BnMA_{52}$-*co*-IEM_8) copolymer to stabiliser, was sprayed with 10 % (3.3 mL/min) and 15 % (4.95 mL/min) feeding rate. The size of dried microcapsules was characterised by laser scattering measurements. However, the dried microcapsules had to be re-dispersed in 1 % (w/v) of aqueous Aerosol OT-100 surfactant, followed by sonication for 10 minutes before the measurement. Both copolymer solid content and feeding rate during the drying process showed a negligible influence on particle size (Table 3.2). Interestingly, the volume moment mean of the particle diameter ($D_{4,3}$) from light scattering measurements illustrate that particle size slightly depends on the inlet temperature; microcapsules that were dried at 110 °C inlet temperature showed a slightly larger size compared to samples when operated at 140 °C and 160 °C. Surprisingly, Figure 3.30 and 3.31 present laser scattering measurement alongside SEM microphotography. Different operation temperatures produce a similar particle size, with approximately 2 to 10 µm. However, a small distribution trace in the range of 10 to 50 µm was detected from the microcapsule powder in which dehydration occurs at 110 °C (Figure 3.31). The evidence from SEM microphotography indicates that agglomeration of microcapsules occurs when 110 °C operation temperature is applied. Clearly, this result indicates a slight difference in particle size when laser diffraction measurement is used to characterise powder microcapsules.

Inlet air Temperature (°C)	Solid content (%)	Feeding rate (%)	Diameter [4,3] (μm)*
110	1.1	10	3.10±0.10
		15	5.26±0.05
	2.2	10	6.89±0.08
		15	6.71±0.29
140	1.1	10	4.16±0.09
		15	3.18±0.24
	2.2	10	3.93±0.08
		15	4.97±0.07
160	1.1	10	3.71±0.11
		15	3.48±0.13
	2.2	10	4.51±0.02
		15	3.05±0.20

*Average±SD(n=3)

Table 3.2: Laser scattering measurement of dry microcapsules prepared from PCL_5-P($BnMA_{52}$-*co*-IEM_8).

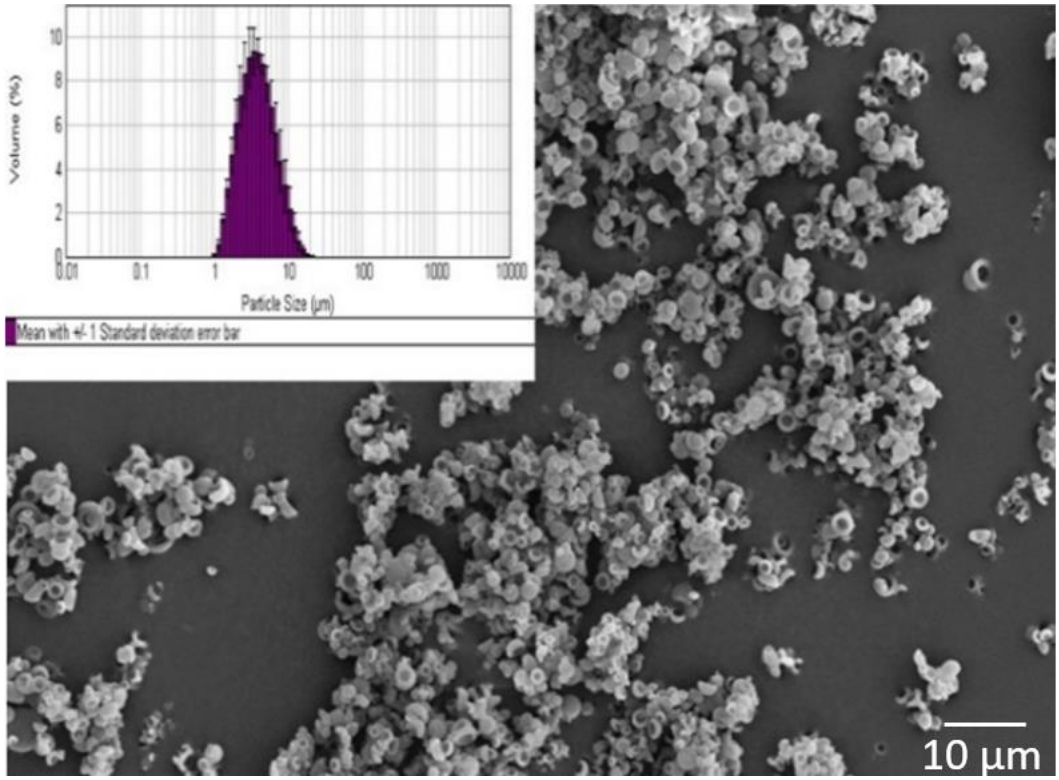

Figure 3.30: SEM image and laser scattering measurement of microcapsules prepared from PCL_5-P($BnMA_{52}$-*co*-IEM_8) after water removal by spray dryer at 160 °C inlet temperatures.

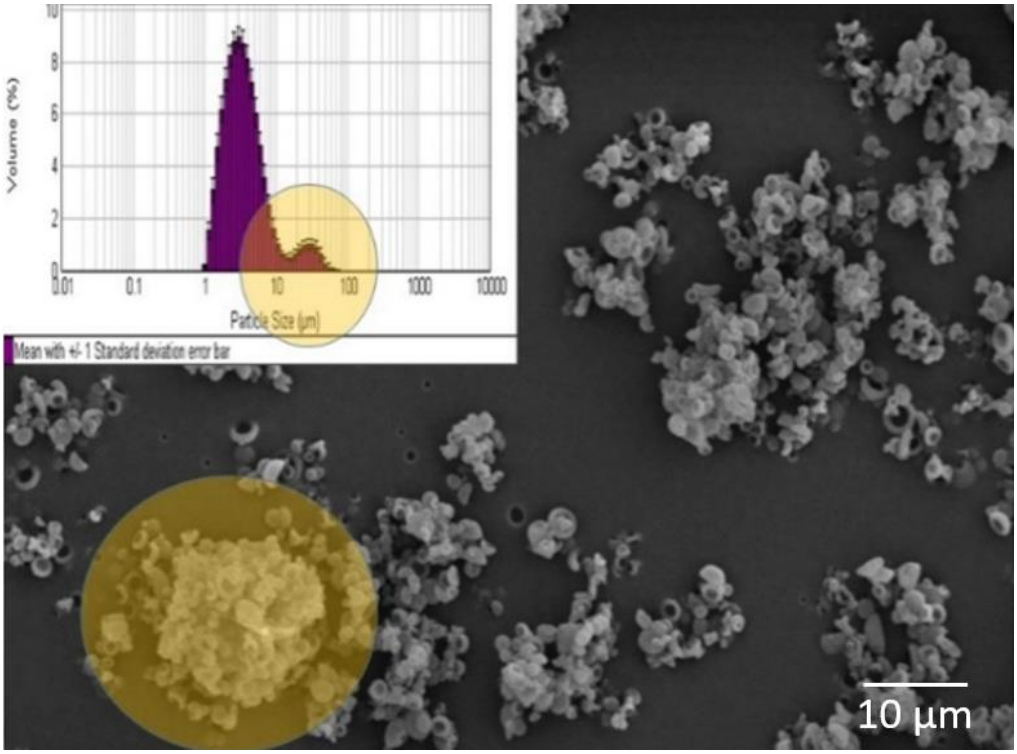

Figure 3.31: SEM image and laser scattering measurement of microcapsules prepared from PCL_5-P($BnMA_{52}$-*co*-IEM_8) after water removal by spray dryer at 110 °C inlet temperatures.

3.2.6 Microcapsule morphology

Herein, particle morphology is generally defined as particle size, shape and surface property. The spray drying process was investigated, 10 % (3.3 mL/min) feeding rate with 140 °C inlet temperature, and showed promise as conditions for other emulsion microcapsules. The previous section mentioned the independence of copolymer solid content of PCL_5-P($BnMA_{52}$-*co*-IEM_8) copolymers on microcapsule size after water removal. Unsurprisingly, a similar microcapsule size was observed, although copolymer solid content was increased up to 3.3 % (w/v). Moreover, Arabic gum (GA) was added to stabiliser solution to investigate its influence on the emulsion droplet size

and dried powder morphology after the drying process. Table 3.3 represents the summary of dried microcapsule size. Particles that were prepared from the PCL_5-P($BnMA_{52}$-*co*-IEM_8) copolymer show a smaller particle size than PCL_{12}-P($BnMA_{44}$-*co*-IEM_6) microcapsules. Further, adding GA in PVA stabiliser does not influence particles according to laser scattering measurement. Particle sizes ($D_{4,3}$) of 10 to 14 µm were detected for dried microcapsules prepared from PCL_{12}-P($BnMA_{44}$-*co*-IEM_6) copolymer. On the other hand, approximately 3 to 6 µm was measured from microcapsules produced from the PCL_5-P($BnMA_{52}$-*co*-IEM_8) copolymer. Interestingly, no significant tendency of microcapsule distribution was detected. Thus further particle size and morphology characterisations are required.

MC	Polymer	Interfacial Polymerization condition		Particle size ($D_{4,3}$, µm) *
		Copolymer content (%W/V)	GA in stabilizer	
1	A	1.1	No	14.269±0.294
2	A	2.2	No	11.034±0.923
3	A	3.3	No	12.082±0.080
4	A	1.1	Yes	14.763±0.020
5	A	2.2	Yes	13.664±0.905
6	A	3.3	Yes	10.299±0.006
7	B	1.1	No	3.194±0.134
8	B	2.2	No	3.000±0.156
9	B	3.3	No	6.031±0.116
10	B	1.1	Yes	4.466±0.041
11	B	2.2	Yes	5.268±0.020
12	B	3.3	Yes	13.939±0.161

*Average±SD (n=3)

Table 3.3: Summary of powder polyurea microcapsules synthesised from polymer A (PCL_{12}-P($BnMA_{44}$-*co*-IEM_6) and polymer B (PCL_5-P($BnMA_{52}$-*co*-IEM_8), determined via laser diffraction measurements (Mastersizer Malvern 2000, UK).

The scanning electron microscopy (SEM) characterisation shows that broad particle size distribution is the result of light scattering measurements. Approximately 1

to 15 µm of microcapsule size was observed. Figure 3.32 shows the SEM microphotography of powder particles which were synthesised from PCL_5- P($BnMA_{52}$-*co*-IEM_8) copolymer, with only aqueous PVA used as a stabiliser. The SEM analysis of the dried powder displayed a consistent wall without any ruptures or cracks, indicating a strong microcapsule wall with particles of a relatively rounded shape. This data reflects that this microcapsule holds potential for use as a carrier for active ingredients, especially applications that require reasonably strong particle walls in order to preserve active ingredients before reaching the target. However, the external structure of microparticles is described as concave or, during the initial driving process, as a shrinking sphere. This observation is a typical characteristic of microcapsules that are synthesised using the spray-drying method. Other research groups have made similar observations [163, 222, 223].

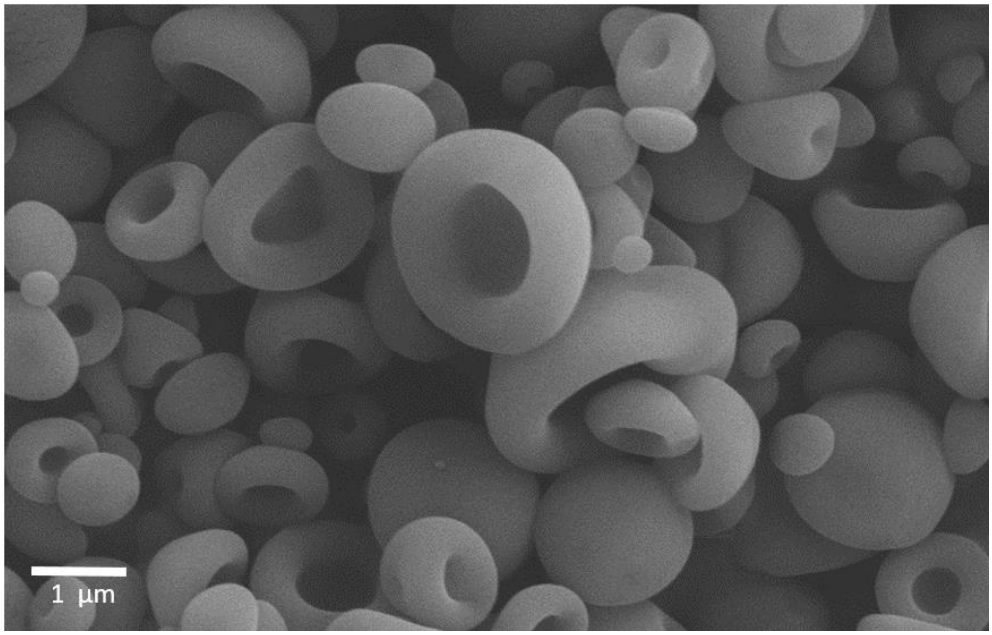

Figure 3.32: SEM image of powder microcapsules synthesised from PCL_5- P($BnMA_{52}$-*co*-IEM_8) copolymer. Only aqueous PVA was used as a stabilizer during the emulsion preparation.

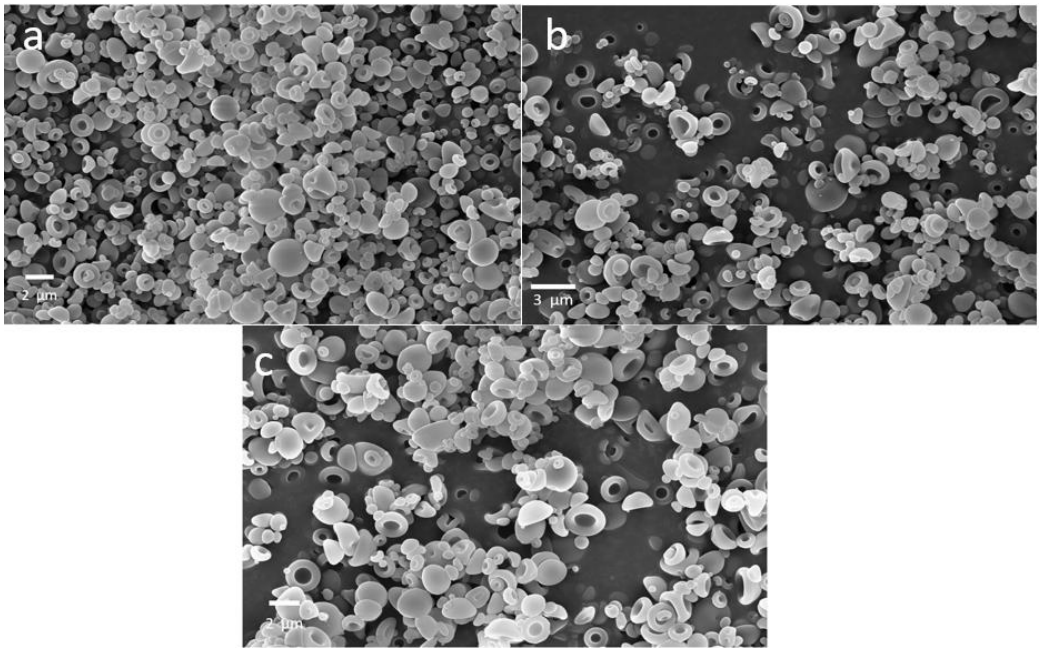

Figure 3.33: SEM images of powder microcapsules synthesised from different copolymer contents (1.1 % (a) 2.2 % (b) 3.3 % (c)).

Furthermore, no significant difference in particle morphology was observed when experimental conditions such as copolymer content were altered; (PCL_5-P($BnMA_{52}$-*co*-IEM_8)) copolymer in emulsion synthesis was increased from 1.1 % to 2.2 % and 3.3 %. (Figure 3.32) In addition, laser scattering measurements showed a broader and larger particle size of the microcapsule, which was synthesised from (PCL_{12}-P($BnMA_{44}$-*co*-IEM_6)) compared to (PCL_5-P($BnMA_{52}$-*co*-IEM_8)) copolymer. These observations are confirmed by the SEM microphotography; Figure 3.34 represents a larger and broader particle distribution of microcapsules. Interestingly, a different stabiliser, PVA + Arabic gum (GA) solution, provided an interesting microcapsule morphology after drying via spray drying. Figure 3.35 shows the SEM of powder microcapsules synthesised from 3.3 % copolymer content and stabilised by PVA + Arabic Gum (GA) solution. A smooth and round particle shape was observed. Moreover, less

shrinkage was also detected when compared to an aqueous PVA stabiliser. A similar particle morphology was still observed even though the copolymer content was varied. Figure 3.36 illustrates the SEM microphotography of microcapsules that were synthesised from 2.2 % of PCL_5-P($BnMA_{52}$-*co*-IEM_8) copolymer. Aqueous PVA + Arabic gum was used as a stabiliser during emulsion preparation. This result indicates that GA co-stabiliser plays an important role in providing a sphere and less shrinkage of microcapsule occurs when water is eliminated via the spray drying process.

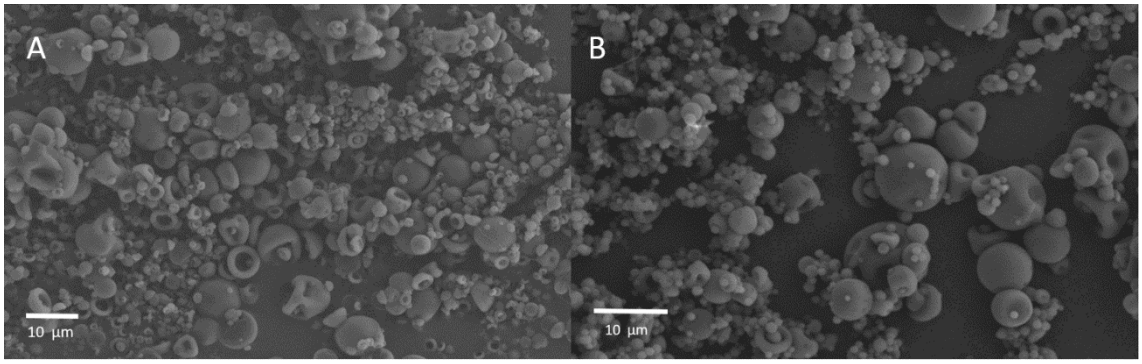

Figure 3.34: SEM image of microcapsules synthesised from the PCL_{12}-P($BnMA_{44}$-*co*-IEM_6) copolymer. An aqueous PVA (A) and PVA+ Arabic gum (B) were used as stabilisers.

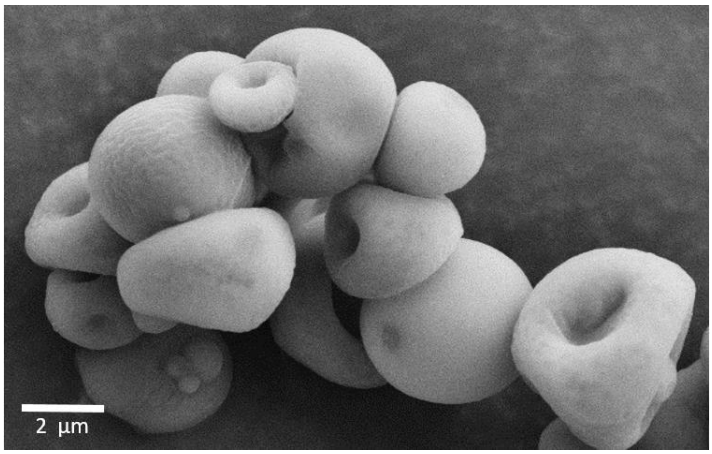

Figure 3.35: SEM of microcapsules synthesised from the PCL_5-P($BnMA_{52}$-*co*-IEM_8) copolymer. An aqueous PVA + Arabic gum was used as a stabiliser.

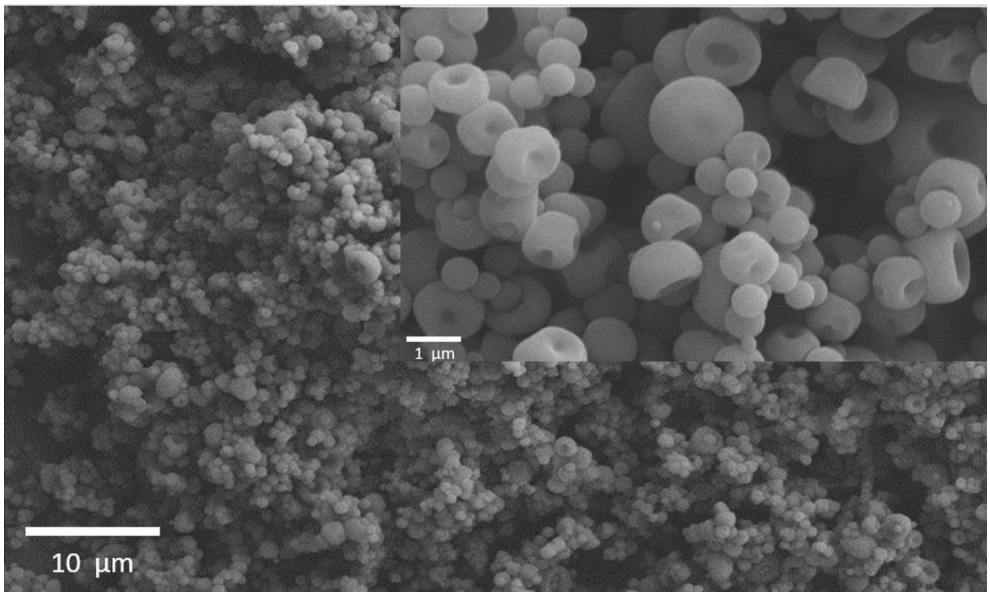

Figure 3.36: SEM image of microcapsules synthesised from 2.2 % of the PCL_5- P($BnMA_{52}$-*co*-IEM_8) copolymer. An aqueous PVA + Arabic Gum was used as a stabiliser.

3.2.7 Microcapsule thermal stability

The thermal stability of all microcapsules, including PCL_x-P($BnMn_m$-*co*-IEM_n) copolymer, has been determined by thermogravimetric analysis (TGA). Initial degradation of PBnMA was previously reported as 150 °C. Meanwhile, rapid weight loss occurs when the temperature reaches approximately 250 °C [224]. In addition, 50 % weight decomposition temperature ($T_{\%50}$) of PCL homopolymer is reported at approximately 420 °C, while the initial degradation occurs at about 300 °C [225]. The PCL_5-P($BnMA_{52}$-*co*-IEM_8) copolymer shows an intermediate thermal behaviour between PCL and PBnMA homopolymers; 50 % weight decomposition temperature occurs at 378 °C, while the copolymer decomposes by almost 65 % at 400 °C (Figure 3.37). This observation indicates the increased thermal stability of PBnMA homopolymer after

copolymerisation with PCL. Table 3.4 represents the summary of the thermal character of all spray dried microcapsules. A similar tendency of the weight loss curve of all microcapsules was observed (Figure 3.38), while a 50 % weight loss of all microcapsules appears just after the temperature reaches 310 °C. Approximately 10 % of weight loss was noticed at 200 °C. This result illustrates an estimated percentage of carried oil content; there was no significant weight loss of the copolymer in this temperature range (Figure 3.38). Moreover, a small weight loss at 40 °C and 100 °C was observed. This demonstrates that both DCM and water were not entirely removed during interfacial polymerisation and the spray drying process, respectively. It is worth noting that the TGA results indicate good thermal stability of this material, which could offer a potential use of these microcapsules in different applications.

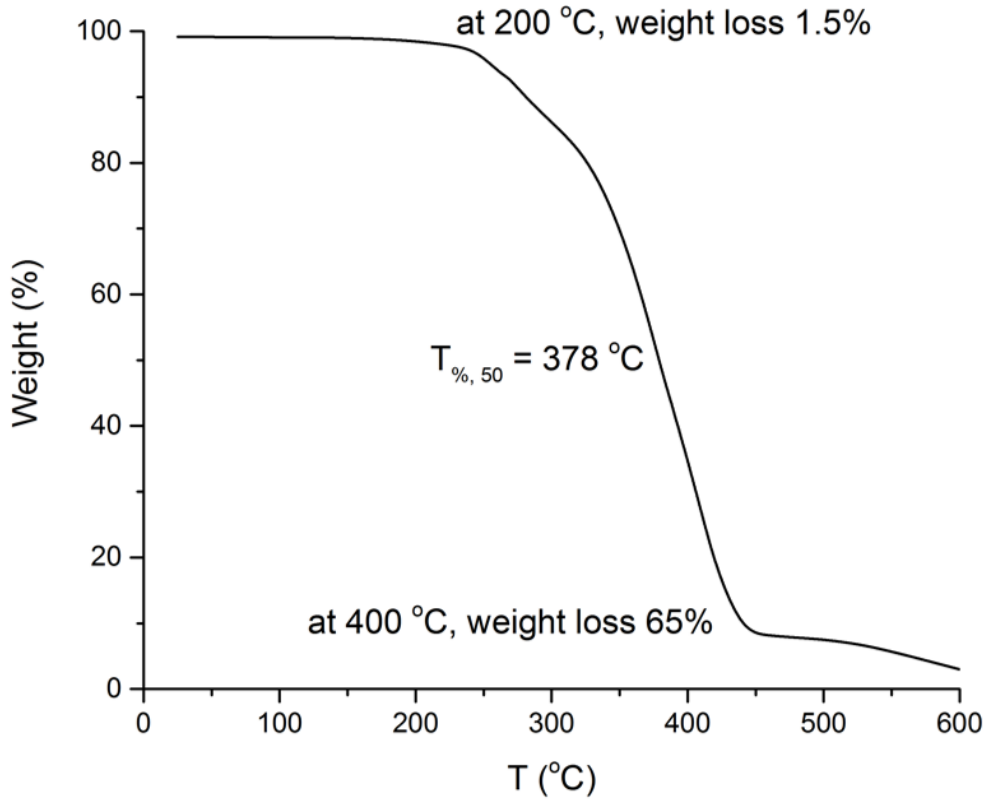

Figure 3.37: TGA curve of the PCL_5-P($BnMA_{52}$-*co*-IEM_8) copolymer.

MC	$T_{\%50}$ (°C)	% Weight Loss at 200 °C	% Weight Loss at 400 °C	% Residue at 500 °C
1	342	6	72	8
2	362	6	67	6
3	312	9	74	14
4	340	5	79	5
5	312	9	79	12
6	316	14	76	11
7	327	9	82	5
8	345	5	77	5
9	350	6	71	6
10	309	9	78	13
11	314	10	78	12
12	315	11	77	12

*Decomposition temperature at 50% weight loss

Table 3.4: Summary of the TGA result of all microcapsules; MC 1-6 and MC 7- 12 were synthesised from PCL_{12}-P($BnMA_{44}$-*co*-IEM_6) and PCL_5-P($BnMA_{52}$-*co*-IEM_8) copolymers, respectively.

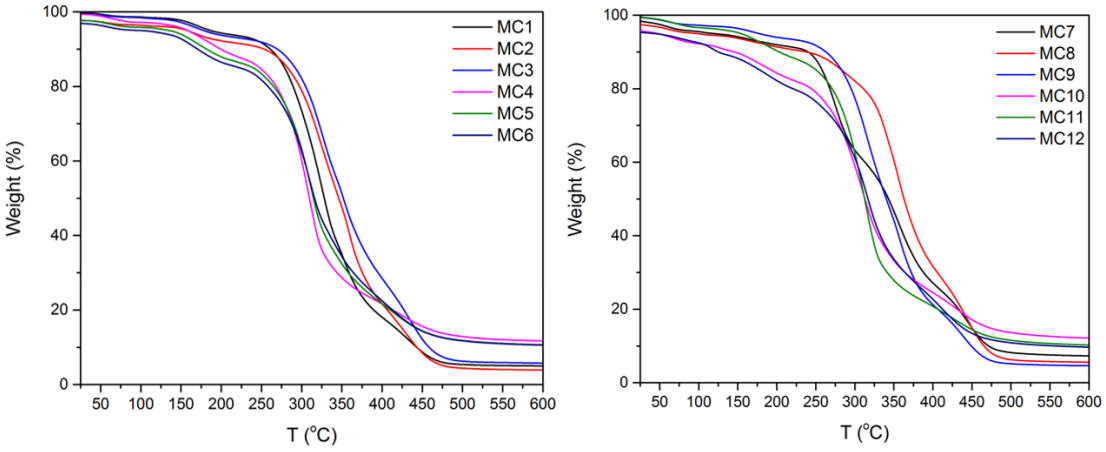

Figure 3.38: TGA curve of all microcapsules; MC 1-6 and MC 7-12 were synthesised from PCL_{12}-P($BnMA_{44}$-*co*-IEM_6) and PCL_5-P($BnMA_{52}$-*co*-IEM_8) copolymers, respectively

3.2.8 Encapsulation and release study of imidacloprid (IMI)

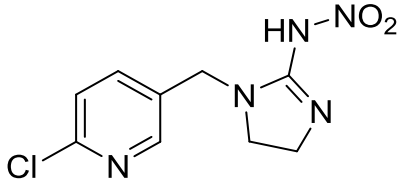

Figure 3.39: Structure of imidacloprid (IMI).

Varying conditions for microcapsule preparation have been evaluated in the previous section, but there is no significant difference in terms of the resulting particle surface. The particle shape depends on the initial stabiliser during emulsion formation. Microcapsules synthesised from 2.2 wt. % copolymer solid content with aqueous PVA and Arabic gum as the stabiliser (MC 11 in table 3.3) was used as the model microcapsule to encapsulate an imidacloprid (IMI) pesticide. IMI is classified as neonicotinoid systemic insecticide which interferes with the impulse transmission of the nervous system [226]. IMI has been widely used in order to control sucking insects in different crops, including potatoes, rice, sugar beets, sugarcane, and vegetables [101]. The literature reviewed indicates various polymers are considered for encapsulating IMI in order to prevent degradation, as well as increase its stability, for example, lignin/poly(ethylene glycol) matrices [226], chitosan (CHI) and sodium alginate (ALG) [120,126], chitosan-poly(lactide) copolymer[105], polyethylene glycol (PEG)[101], and poly(propylene carbonate) (PPC) [227]. In this study, IMI was dissolved in DCM with isocyanate pre-polymer during the emulsion preparation step. After the drying process, the amount of pesticide was followed by Soxhlet extraction in water. As a result, UV, absorption at 270 nm, showed that the weight percentage of pesticide loading in the microcapsules is

approximately 0.5 wt. %. In addition, the encapsulation efficiency, which considers the weight of feeding pesticide and copolymer composition, showed that approximately 75 % of pesticide was covalently reacted after the drying process. Notably, the temperature of spray drying process might influence the stability of the pesticide; the melting point of IMI is approximately 140-146 °C. The drying process condition, 140 °C inlet temperature, could lead to the loss of both pesticide stability and encapsulated efficiency. Nevertheless, IMI was used as a model chemical. Thus, further study is required before using microcapsules in the field, including either changing pesticide (higher stability) or decreasing the drying temperature. The release profile of IMI in microcapsules in aqueous solution at 25 °C was also followed by UV-Vis spectrophotometry; an initial burst release was detected up to approximately 70 % after 30 minutes (Figure 3.40 right). Interestingly, the release profile of IMI in NaOH and HCl solution was significantly higher. This observation was affirmed by the different morphology of the microcapsules. The aggregation of microcapsules were observed after treating with acidic conditions (Figure 3.41 A) and basic solution (Figure 3.41 B). Notably, a microcapsule in normal water also showed an accumulation; however, no significant cracks were detected. (Figure 3.42)

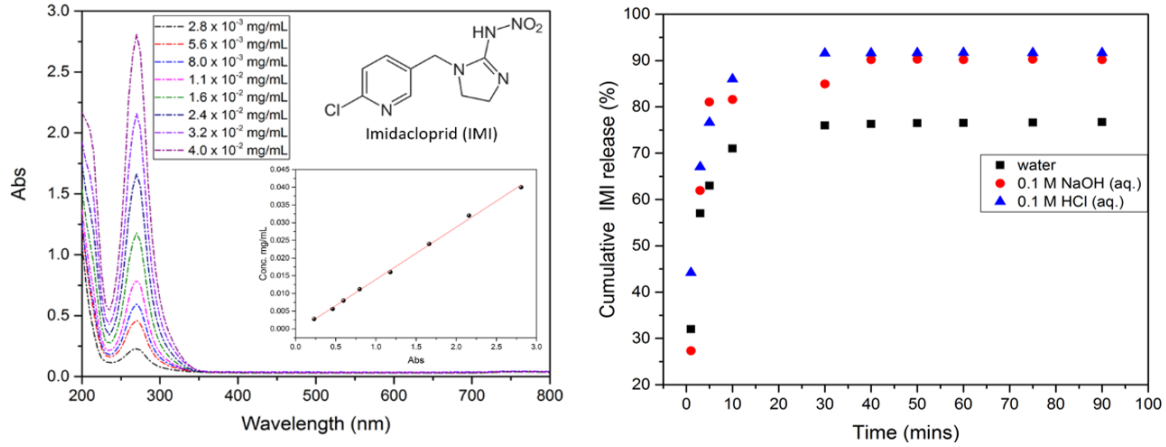

Figure 3.40: UV-spectrometry calibration of imidacloprid (IMI) in water at 25 °C (left) and the cumulative release profile of IMI in aqueous solutions (right).

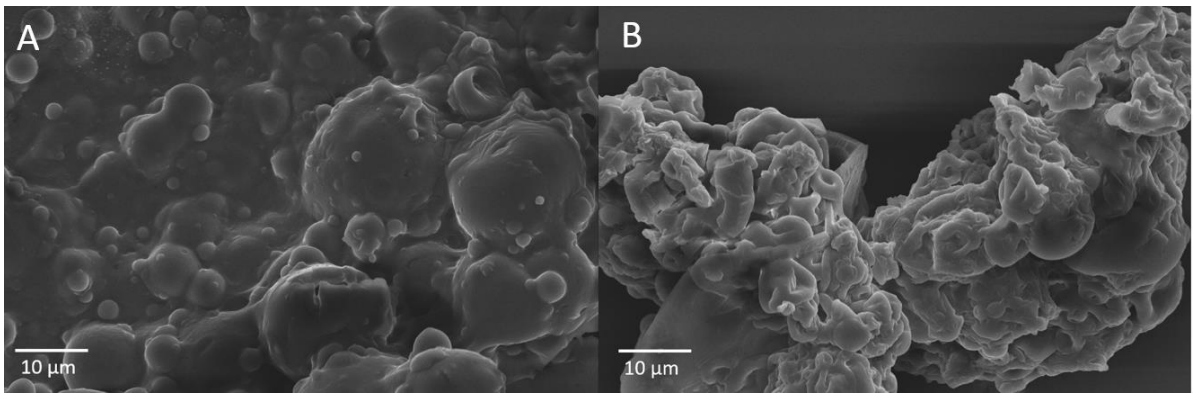

Figure 3.41: SEM of microcapsules synthesised from the PCL_5-P($BnMA_{52}$-*co*-IEM_8) copolymer after treating with 0.1 M HCl aq. (A) and 0.1 M NaOH aq.(B) overnight at 25 °C.

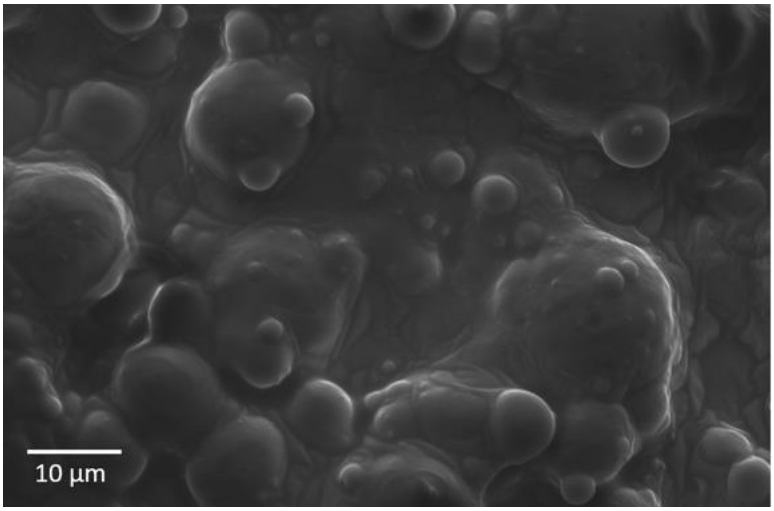

s

Figure 3.42: SEM of microcapsules synthesised from the PCL_5-P($BnMA_{52}$-*co*-IEM_8) copolymer after treating with HPLC water overnight at 25 °C.

3.3 Conclusion

Poly(ε-caprolactone) isocyanate functional copolymers were successfully synthesised *via* Cu(0)-mediated controlled radical polymerisation at ambient temperature. Two different molecular weights of macroinitiator were synthesised. α, ω-Poly(ε-caprolactone) was polymerised via ring-opening polymerisation, followed by esterification with an acid halide, α-bromoisobutyryl bromide (BiBB). Isocyanate functional copolymers were prepared and isolated using a simple method. Polyurea microcapsules were fabricated via oil-in-water interfacial polymerisation. Interestingly, the emulsion droplet size showed no significant difference, though different emulsion synthetic conditions were applied, including the different molecular weights of the copolymers, copolymer content and stabilisers. Microcapsule emulsions were dried by spray drying; a slight difference of dried microcapsules was observed by laser scattering measurement. SEM microphotography of the dried powder displayed a constant wall without any wall ruptures or cracks, indicating a strong microcapsule wall with a relatively rounded particle shape. In addition, the external structure of the microcapsule is described as concave or a shrinkage sphere, which results from the initial drying process. Interestingly, less shrinkage in the dried particles was detected after aqueous PVA + Arabic gum (GA) was used to prepare the microcapsule emulsion. In addition, TGA results of microcapsules showed a good thermal stability with a similar tendency of the weight loss curve. Further, approximately 10 % of carrier oil in microcapsule can also be estimated from the weight loss of shown by TGA at 200 °C. Notably, the temperature of spray drying process could influence the stability of the pesticide; the melting point of IMI is approximately 140-146 °C. Nevertheless, IMI was used as a model chemical. Thus,

further study is required before using microcapsules in the field, including either changing the pesticide (higher stability) or decreasing the drying temperature. Finally, a good thermal stability and the reasonable encapsulation efficiency make these microcapsules suitable candidates for a prolonged release encapsulation system.

3.4 Experimental

3.4.1 Materials

Acetone, anhydrous 2-propanol (IPA), ε-caprolactone, benzyl methacrylate (BnMA), poly(ε-caprolactone) diol average M_n = 530 g mol^{-1} (PCL_5), isocyanatoethyl methacrylate (IEM), deuterated chloroform ($CDCl_3$), anhydrous dichloromethane (DCM), diethylenetriamine (DETA), gum Arabic (GA), copper(II) bromide, 35 % aqueous hydrochloric acid, α-bromoisobutyl bromide, poly(vinyl alcohol) (M_w = 130,000 g mol^{-1}), triethylamine (TEA), trans-2-[3- (4-tert-Butylphenyl)-2-methyl-2-propenylidene] malononitrile (DCTB), sodium iodide (NaI), poly(ethylene glycol) (M_w = 1,500 g mol^{-1}), anhydrous tetrahydrofuran (THF) and imidacloprid (IMI) were purchased from Sigma-Aldrich UK. Carrier oil was purchased from Stephan Company. Tin(II) 2-ethylhexanoate was purchased from Alfa-Aesar. Me_6Tren was synthesised according to literature procedure. Caprolactone (ε-CL) was purified by vacuum distillation over CaH_2 prior to use

3.4.2 Characterisation

Size exclusion chromatography measurements were performed on an Agilent 390 MDS Multi-Detector GPC system ($CHCl_3$ + 2 % TEA Mixed C Column Set, THF + 2 % TEA and 0.01 wt. % BHT with PLgel Mixed C columns set, 30 °C flow rate 1 mL/min, narrow standards of PMMA were used as calibration polymers between 955000 and 1010 $gmol^{-1}$ and fitted with a third order polynomial) by DRI detection. ^{1}H NMR (standard) and ^{13}C NMR (long acquisition long delay) were recorded on a Bruker Avance III HD 400 MHz and Bruker Avance III HD 300 MHz with $CDCl_3$ as the solvent. FTIR spectra were recorded on a Bruker Vector 22 FTIR spectrometer and analysed with OPUS software. Particle sizes were obtained by a Malvern Instruments Mastersizer 2000 System. Emulsion droplet microcapsules were dried using a Buchi mini spray dryer B-290. Particle morphologies were characterised via scanning electron microscope (ZEISS SUPRA55VP). Thermogravimetric analysis was carried out on a Mettler Toledo TGA/DSC1. For the MALDI-ToF measurements an Autoflex ToF/ToF apparatus was used; *trans*-2-[3-(4-tert-butylphenyl)-2-methyl-2-propenylidene]malononitrile (DCTB), tethahydrofuran, sodium iodide (NaI) and poly(ethylene glycol) (M_w = 1,500 g mol^{-1}) were used as matrix, solvent, ionizing agent and calibrated polymer, respectively. Pesticide loading, encapsulation efficiency, and release profile was obtained via Synergy HTX Multi-Mode reader.

3.4.3 α, ω- Hydroxyl terminated Poly(ε-caprolactone) (ε-PCL_{12}) polymerisation

Diethylene glycol (0.17 mL, 1.79 mmol, 1 eq.) and $Sn(Oct)_2$ (10 mg, 0.025 mmol, 0.014 eq.) were added into a dried ampoule tube and purged with nitrogen. ε-CL (2.34 mL, 21.48 mmol, 12 eq.) was added into the reaction mixture, and polymerisation was carried out at 110 °C for 15 hours. The polymer solution was poured directly to cold n-hexane. Once the solvent was removed, the white solid product was characterised by NMR, IR and SEC and MALDI-ToF MS. ^{1}H NMR (400 MHz, CDCl3, δ): 1.34-1.40 (m, 24H, CH_2), 1.55-1.75 (m, 48H, CH_2), 2.25-2.40 (m, 24H, CH_2COO), 3.62 (t, 4H, $HOCH_2$, J = 6.50 Hz), 3.69 (t, 4H, $HOCH_2$, 5.90 Hz), 3.96 (t, 4H, OCH_2, J = 6.70 Hz), 4.04 (t, 22H, $COOCH_2$, J = 6.70 Hz), 4.21 (t, 4H, $COOCH_2$, J = 5.90 Hz), ^{13}C NMR (100.61 MHz, $CDCl_3$, δ): 24.50 (s, CH_2), 25.46 (s, CH_2) 28.27, (s, CH_2), 34.05 (s, CH_2), 69.01, (s, C-O), 64.08, (s, C-O), 63.22, (s, C-O(backbone)), 62.56 (s, C-O), 173.48 (s, C=O), IR: *v* = 3450 (O-H), 2937, 2863 (C-H), 1728 (C=O) , MALDI-TOF MS (m/z) $(C_6H_{11}O_2)_mC_4H_8O_3(C_6H_{11}O_2)n.Na^+$, 927.298 (m=3, n=4), 1041.439 (m=4, n=4), 1155.561 (m=4, n=5), 1269.666 (m=5, n=5), 1383.7758 (m=5, n=6), 1497.842 (m=6, n=6), 1611.918 (m=6, n=7), 1725.986 (m=7, n=7), 1842.053 (m=7, n=8), 1955.119 (m=8, n=8), 2096.183 (m=8, n=9), 2183.252 (m=9, n=9), 2297.325 (m=9, n=10), $SEC_{(CHCl3)}$: Mn = 3200 g mol^{-1}, $Đ$ = 1.15.

3.4.4 α, ω-PCL_{12} SET-LRP macroinitiator

Polycaprolactone (2.8 g, 1.87 mmol, 1 eq.) was added to 250 mL round bottom flask containing stirrer bar and sealed by a rubber septum. Anhydrous tetrahydrofuran (THF) (100 mL) was canulated into a round bottom flask and followed by triethylamine (1.4 mL, 10 mmol, 5.4 eq.) The reaction was degassed with N_2 for 20 minutes. The reaction mixture was cooled in an ice bath and α-bromoisobutyryl bromide (BiBB) (0.5

mL, 4 mmol, 2.1 eq.) was dropwise added. Once BiBB was completely added, the ice bath was removed and the reaction was carried out at ambient temperature overnight. THF was removed under reduced pressure and crude initiator product was re-dissolved by anhydrous DCM (100 mL). $NaHCO_3$ aqueous solution (2 x 150 mL) was used to wash the crude product. DCM was removed by rotary evaporator. Finally, the macroinitiator was re-dissolved in dichloromethane (15 mL) and precipitated in cold *n*-hexane. After solvent removal, the resultant white solid product (90 % yield) was characterised by NMR, IR, SEC and MALDI-ToF MS. ^{1}H NMR (400 MHz, $CDCl_3$, δ): 1.33-1.42 (m, 24H, CH_2), 1.59-1.79 (m, 48H, CH_2), 1.91 (s, 12H, 2x$COO(CH_3)_2Br$), 2.27-2.36 (m, 24H, CH_2COO), 3.69 (t, 4H, OCH_2, J = 4.90 Hz), 4.06 (t, 24H, $COOCH_2$, J = 6.70 Hz), 4.17 (t, 4H, $COOCH_2$, J = 6.50 Hz), 4.23 (t, 4H, $COOCH_2$, J = 4.90 Hz), ^{13}C NMR (100.61 MHz, $CDCl_3$, δ): 24.56, 25.52 (s, CH_2), 28.34 (s, CH_3), 28.75 (s, CH_3), 34.10 (s, CH_2), 55.86 (s, C-Br) 63.27 (s, C-O), 64.13 (s, C-O (backbone)), 65.76 (s, C-O), 69.08 (s, C-O), 173.53 (s, C=O), IR: *v* = 2950, 2866 (C-H), 1730 (C=O), MALDI-TOF MS (m/z): $C_4H_6OBr(C_6H_{10}O_2)_mC_4H_8O_3(C_6H_{10}O_2)_nC_4H_6OBr.Na^+$, 1339.552 (m=4, n=4), 1453.636 (m=4, n=5), 1567.725 (m=5, n=5), 1681.807 (m=5, n=6), 1795.888 (m=6, n=6), 1909.055 (m=6, n=7), 2024.024 (m=7, n=7), 2140.081(m=7, n=8), 2253.157(m=8, n=8), 2368.209(m=8, n=9), 2481.293 (m=9, n=9), $SEC_{(CHCl3)}$: M_n = 3700 g mol^{-1}, $Đ$ = 1.11

3.4.5 PCL_x-P($BnMA_m$-co-IEM_n) polymerisation

A magnetic stirrer bar was coiled with copper wire (8 cm) and placed into 3 mL of 35 % HCl solution for 5 minutes, washed with deionized water then acetone. Once dried, the cleaned wire was placed in a Schlenk tube containing α, ω-poly(ε-

caprolactone) initiator (0.2 g, 0.11 mmol, 1 eq.) and $CuBr_2$ (2.4 mg, 1.1 x 10^{-5} mol (0.1 eq. relative to initiator). Next, the Schlenk tube was sealed with a rubber septum, anhydrous 2-propanol (1 mL), 2-isocyanatoethyl methacrylate (78 µL, 0.55 mmol. 5 eq.) and benzyl methacrylate (0.85 mL, 5.01 mol, 45 eq.) were added. The reaction mixture was degassed under a flow of N_2 for 15 minutes, then Me_6Tren (20 µL, 8.02 x 10^{-5} mol, 0.72 eq.) was added. The reaction was stirred for 5 hours after which phase separation was observed. The upper layer was removed and anhydrous dichloromethane then was added to re-dissolved polymer layer. The polymer was precipitated in cold *n*-hexane and isolated by filtering through a sintered glass funnel. The resultant white polymer powder (71 % yield) was characterised by NMR, IR and SEC. ^{1}H NMR (400 MHz, $CDCl_3$, δ): 0.67-0.86 (m, 90H, CH_3), 1.15-1.35 (m, 80H, CH_2), 1.57-1.88 (m, 108H, CH_2), 2.22-2.30 (m, 24H, CH_2C=O), 3.29 (m, 12H, CH_2NCO), 3.61-3.63 (m, 4H, CH_2O), 3.84-4.01 (m, 36H, $COOCH_2$), 4.15-4.17 (m, 4H, $COOCH_2$), 4.81-4.84 (m, 48H, $PhCH_2OCO$), 7.14-7.22 (m, 120H, CH_2 aromatic), ^{13}C NMR (100.61 MHz, $CDCl_3$, δ): 22.18 (s, CCH_3), 24.59, 25.55, 28.37, 34.14 (s, CH_2), 30.78 (s, CCH_3), 44.81 (s, CH_2N), 54.95 (s, CH_3), 63.30, 64.15 (s, CH2O), 66.78 (s, $PhCH_2O$), 69.10 (s, CH_2OCO), 128.21 (s, CH aromatic), 128.54 (s, CH_2 aromatic), 173.54, 177.04 (s, C=O) IR: *v* = 1500 (CH aromatic), 1750 (C=O), 2250 (NCO), $SEC_{(CHCl3)}$: M_n = 13400 g mol^{-1}, *Đ* = 1.48

3.4.6 Spray drying emulsion preparation

PCL_x-P($BnMA_m$-*co*-IEM_n) copolymer (0.6 g) was added into a 50 mL vial containing 5 mL anhydrous DCM. Neobee Carrier Oil (0.4 g) was added, followed by 18.4 mL of 1.3 % polyvinyl alcohol (Mowiol 18-88) aqueous solution. The mixture was homogenised at

2000 rpm for 3 minutes using an overhead dissolver disc. The mixture was transferred to a 100 mL RBF and then stirred at 700 rpm using magnetic stirrer. A 40 % aqueous solution of diethylenetriamine (DETA) (0.6 mL, excess) was added dropwise into the reaction; the mixture was then left to stir at room temperature. After 1 hour the temperature was increased to 50 °C and, after another hour, the temperature was further increased to 90 °C. Microcapsule size was determined by dynamic light scattering and optical microscopy.

3.4.7 Spray drying process

The emulsion solution was dried by using a Buchi mini spray dryer B-290 with a nozzle atomization system of 0.5 mm. Drying experiments were carried out at 100 % of aspirator rate, 3.3 mL/min feeding rate, 140 °C inlet air temperature and 6.7 bar of atomising nitrogen pressure. Dried products (58 % yield) were removed and stored in vials for further analysis.

3.4.8 Particle morphology

Microcapsules were dotted onto a two-sided adhesive tab and sputter coated with gold for 30 seconds. Morphological characteristic of microcapsules were observed by scanning electron microscopy (SEM; ZEISS SUPRA55VP) with an accelerated voltage of 10 kV.

3.4.9 Particle size distribution

Particle mean diameter was measured by using a laser light diffraction instrument, Mastersizer S (Malvern Instrument Malvern, UK). Powder particles were re-dispersed into aqueous solution of Aerosol OT-100 (1 %) and sonicated for 10 minutes. The particle size was represented as $D_{(4,3)}$, the volume weight mean diameter.

3.4.10 Particle thermal stability

Thermogravimetric analysis (TGA) was recorded on a Mettler Toledo TGA/DSC1. Samples were measured from 25 to 600 C at 10 °C/min under nitrogen.

3.4.11 Determination of pesticide loading (PL), encapsulation efficiency (EE), and release profile

20 mg of microcapsule was placed in a Soxhlet thimble and extracted using HPLC water (25 mL) as a solvent at 160 °C for 5 hours. The concentration of IMI was measured by UV-Vis spectrometry. The pesticide loading (PL) is defined as the weight percentage of IMI in a certain amount of microcapsule. Encapsulation efficiency (EE) details the amount of pesticide considered from feeding composition [227]. For the release profile, 1.9 mg of microcapsule was placed in 96-well microplates, followed by 350 µL of HLPC grade water. The concentration of IMI over time was detected by UV-Vis spectrometry at λ = 270 nm.

PL = [(weight of pesticide)/(weight of microcapsule)] x 100

EE = [(weight of pesticide)/(weight of microcapsule x pesticide content from the feeding composition)] x 100

Chapter 4

Hydrosilylation: An efficient tool for polymer synthesis and modification

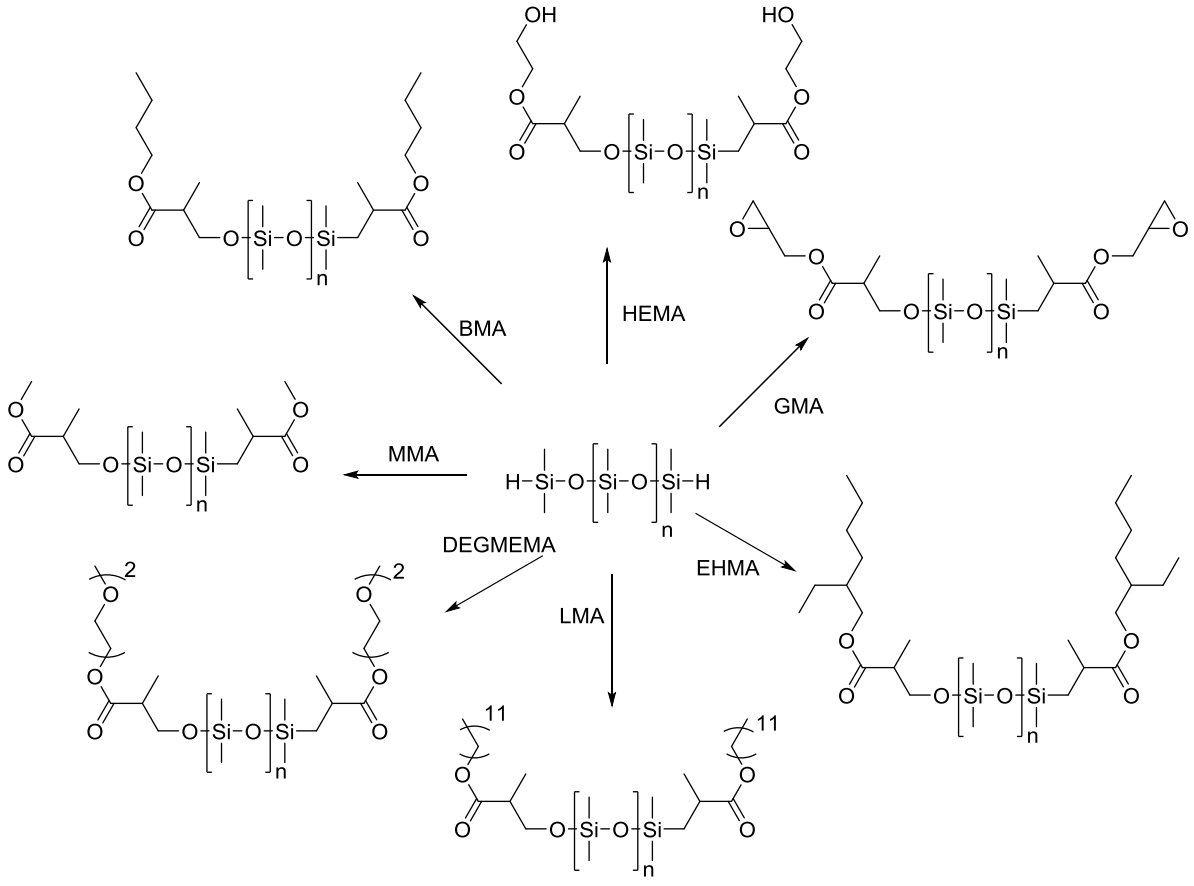

The use of amphiphilic block copolymers for active ingredient (AI) delivery has drawn the attention of researchers in recent decades [228-231]. In this chapter, commercially available telechelic PDMS hydrides (h_2PDMS) have been modified with a range of different methacrylates via hydrosilylation as the precursor of ABA amphiphilic copolymers as promising materials for the carrying of water-insoluble agrochemicals. Poly(dimethyl siloxanes) (PDMS) are an important class of polysilicone due to their excellent glass transition temperature (T_g) and non-toxicity. The hydrophobicity of PDMS is a feature of these materials, making them ideal for use as hydrophobic segments of amphiphilic block copolymers. Hydrosilylation is a well-established reaction for the preparation of organo-silicone compounds [258-260]. Hydrosilylation of functional methacrylates provides access to functional poly(dimethylsiloxane) (PDMS) from appropriate hydride terminated PDMS in very high yielding reactions without the formation of any side products, without odour, and without a need for labour-intensive purification. The versatility of hydrosilylation has been exploited for the preparation of ABA triblock copolymers using poly(ethylene glycol) methacrylate and more structurally demanding vinyl terminated methacrylic macromonomers. The latter are obtained by catalytic chain transfer polymerisation (CCTP). ^{1}H NMR revealed the formation of solely anti-Markovnikov products and the high tolerance of the reaction towards other functionalities.

4.1 Background

4.1.1. Poly(dimethylsiloxane) (PDMS)

Use of amphiphilic block copolymers for drug delivery, in order to increase drug solubility and stability, has drawn the attention of researchers in recent decades [228-231]. A number of polymers have been exploited to synthesise amphiphilic copolymers via different polymerisation methods, particularly reversible deactivated radical polymerisation (RDRP) [232-235]. A variety of water soluble polymers are employed as hydrophilic segments of copolymers. Interestingly, polyethylene glycol (PEG) seems to be a commonly used material for several reasons, including biocompatibility, FDA approval, commercial availability and cost effectiveness [236-238]. Conversely, the hydrophobic segment selection is significant in copolymer synthesis for active ingredient delivery, especially when it is further used to form micelles and exploited as the water-insoluble AI carrier, because hydrophobicity could influence the encapsulation efficiency resulting from intermolecular interactions [239, 240].

A further copolymer preparation method is the reaction between two polymers via organic reactions. Highly efficient organic reactions have been used for many years to modify and alter the properties of materials. The introduction of the click chemistry concept by Sharpless [241] and coworkers in 2001 has inspired researchers to seek new, and rediscover old, efficient reactions, which are, for instance, high yielding and stereospecific and which do not generate side products and, hopefully, do not require purification by chromatography. Numerous reactions have experienced a renaissance as

"click type" reactions and have been demonstrated to be applicable for the fabrication of diverse materials/ polymer architectures for applications in material science, biology and medicine [242-244]. Prominent recent examples include thiolene [245, 246] and Michael-addition and Diels-Alder reactions [247]. A highly efficient reaction that has not received as much attention in this context is catalytic hydrosilylation, i.e., the insertion of an unsaturated vinyl group into a Si-H bond [248]. The first hydrosilylation reaction of trichlorosilane and 1-octene in the presence of acetyl epoxide was reported by Sommer *et al.* in 1947 [249]. Since then, hydrosilylation has become a powerful reaction in silicone polymer and surface chemistry [250].

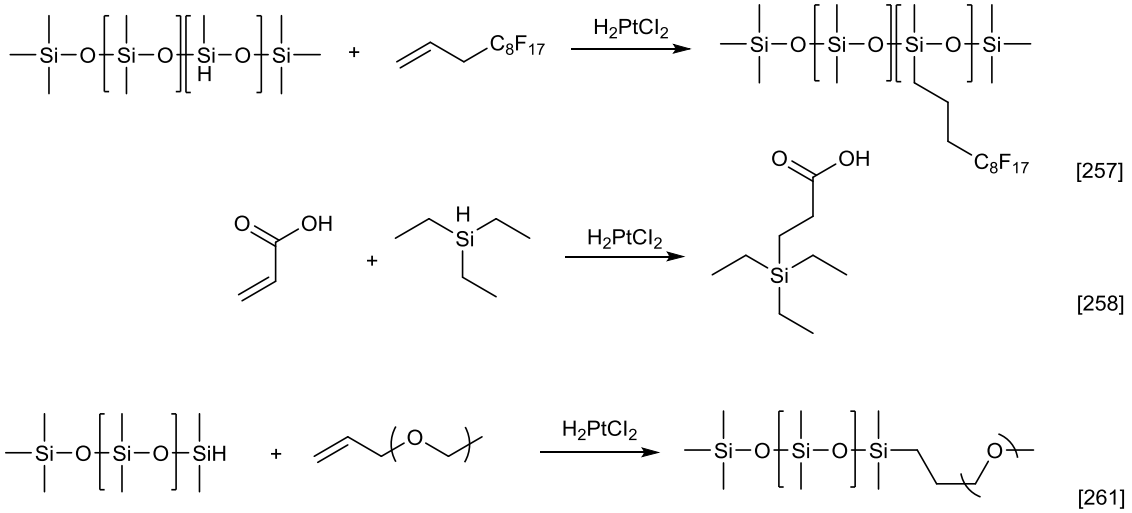

Figure 4.1: Examples of PDMS modification via hydrosilylation reaction.

Poly(organosiloxane)s (POS), also known as silicones, are exploited as building blocks in many industrial products. Poly(dimethylsiloxanes) (PDMS) are probably the most important member of the silicone class, exhibiting some excellent material properties, including high flexibility, excellent thermal oxidative stability, high moisture resistance, low glass transition temperature (T_g), and non-toxicity [251]. Due to these

unique properties, POS, in particular PDMS, are used in diverse applications, for example, in semiconductor devices, aerospace, decorative coatings, biomaterials, mould release agents, antifoam and foaming agents, personal care products, and additive materials. The non-toxicity and hydrophobicity of PDMS offer a unique aspect for use as a hydrophobic segment of the amphiphilic block copolymer. Amphiphilic PDMS-PEG copolymer synthesis has been successfully obtained via different techniques, particularly organic click reactions [252-254]. In addition, several studies on the modification of hydride terminated PDMS and copoly-(dimethyl)(methyl-hydrogen)siloxane have been reported [255]. The latter approach was used for the preparation of acrylate containing [256] and fluorinated PDMS, [257] respectively. Hydrosilylation of h_2PDMS systems was demonstrated as a technique for the introduction of (meth)acrylic acid, [258, 259] amine and epoxy terminal end groups [260]. The addition of Si-H can be favourably compared with thiolene chemistry (addition of S-H), which has been the focus of many publications in recent years. Hydrosilylation has the advantage of having starting materials with little or no odour and which are extremely stable other than reacting very selectively with vinyl groups in the presence of appropriate catalysts. PDMS-PEG copolymers, which are formed via a conventional addition reaction, have been used to utilise and modify PDMS derivative polymers for more than fifty years. Nevertheless, only diblock copolymers of PDMS-PEG have been reported with regard to this reaction. Moreover, long reaction times and high temperatures are noted as some of the disadvantages of hydrosilylation [261-265]. In this chapter, we investigate the utility of this reaction. Specifically, we sought a shortcut in amphiphilic PDMS synthesis by using different functional methacrylate in an effort to

modify hydride terminated PDMS (H_2PDMS). The high yielding and efficient hydrosilylation reactions were also shown by the successful modification of macromonomers prepared by catalytic chain transfer polymerisation (CCTP), as this sterically hindered the vinyl group. Based on these results, hydrosilylation of methacrylate-based materials is demonstrated as a tool for the synthesis of linear telechelic ABA amphiphilic block copolymers.

4.1.2 Hydrosilylation

Hydrosilylation is the insertion reaction of an unsaturated vinyl group into a Si-H bond. Since hydrosilylation was introduced, it has become one of the most powerful reactions in silicone polymer and surface chemistry. The mechanism for the late transition metal catalysed hydrosilylation (usually using d^8 and d^{10} metals) was proposed by Chalk and Harrod. Hydrosilylation occurs through four consecutive steps, Figure 4.2. Firstly, the oxidative addition of a silane to the metal complex occurs. Next, the M(II) complex is generated, followed by the ordination of catalytic complex with vinyl functional groups. Subsequently, the migratory insertion of the alkene into the MH bond occurs. Thereafter, the reductive elimination step takes place, leading to the formation of the Si-C bond and the initial catalytic complex [248].

A wide range of late transition metal catalysts have been employed in hydrosilylation reactions, however, the most commonly used in both industrial and research PDMS synthesis/modification is a platinum complex. In this thesis, Karstedt's catalyst (platinum-divinyltetramethyldisiloxane (Pt(dvs))), a platinum metal complexe

with the divinyl ligand, was exploited. In general, (Pt(dvs)) exists as the dimer structure, which is known as a pre-catalyst (Figure 4.3 left). It is worth noting that an equilibrium of organoplatinum compounds occurs during the reaction to generate an active catalyst.

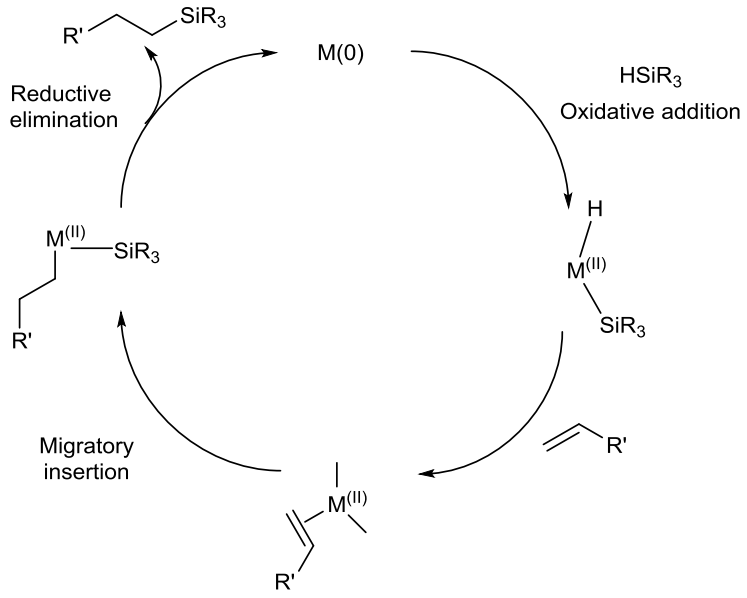

Figure 4.2: Chalk-Harrod hydrosilylation mechanism catalysed by a late transition-metal catalyst.

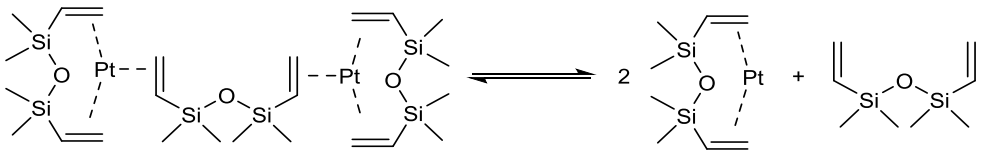

Figure 4.3: Structure of Karstedt's catalyst

4.2 Results and discussion

4.2.1 Modification of hydride terminated PDMS with methacrylates

Hydrosilylation was employed as a versatile and efficient method for the synthesis of functional telechelic PDMS. PDMS with hydride α, ω-end groups(h_2PDMS; average M_n 580 $gmol^{-1}$) was modified with different methacrylates (Figure 4.4), including methyl methacrylate (MMA), 2-hydroxylethyl methacrylate (HEMA), glycidyl methacrylate (GMA), lauryl methacrylate (LMA), 2-ethyl hexyl methacrylate (EHMA), butyl methacrylate (BMA) and diethylene glycol methyl ether methacrylate (DEGMEMA).

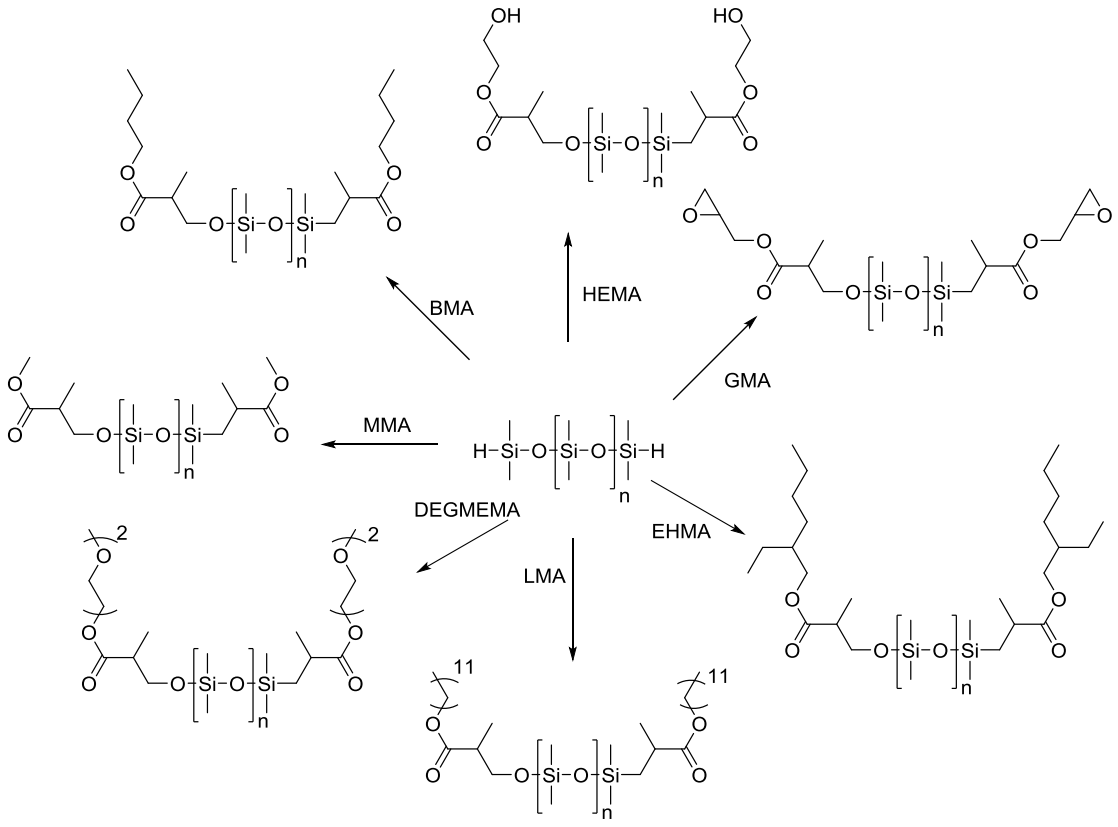

Figure 4.4: Hydrosilylation of methacrylate monomer and h_2PDMS hydride terminated.

Firstly, MMA was used in order to optimize the reaction conditions with regard to temperature and reaction time. Within 60 minutes at 37 °C the reaction was found to be complete, as determined by ^{1}H NMR. The characteristic Si-H signal at 4.80 ppm was used to follow the progress of the reaction (Figure 4.5). The insertion of the methacrylic alkene functionality into the Si-H bond results in the formation of a Si-C bond and loss of the Si-H group. After 60 minutes at 37 °C the Si-H signals disappeared whilst new signals between 0.5 and 1 ppm appeared, which can be assigned to the newly formed CH_2 group. A high-field shift of the methacrylate methyl group is observed, characteristic for the transition from an sp^2 to an sp^3 neighbouring group. Further evidence of the success of the reaction was obtained by IR spectroscopy (Figure 4.6) with the disappearance of the characteristic Si-H band at 2126 cm^{-1} and the appearance of the ester band at 1750 cm^{-1}.

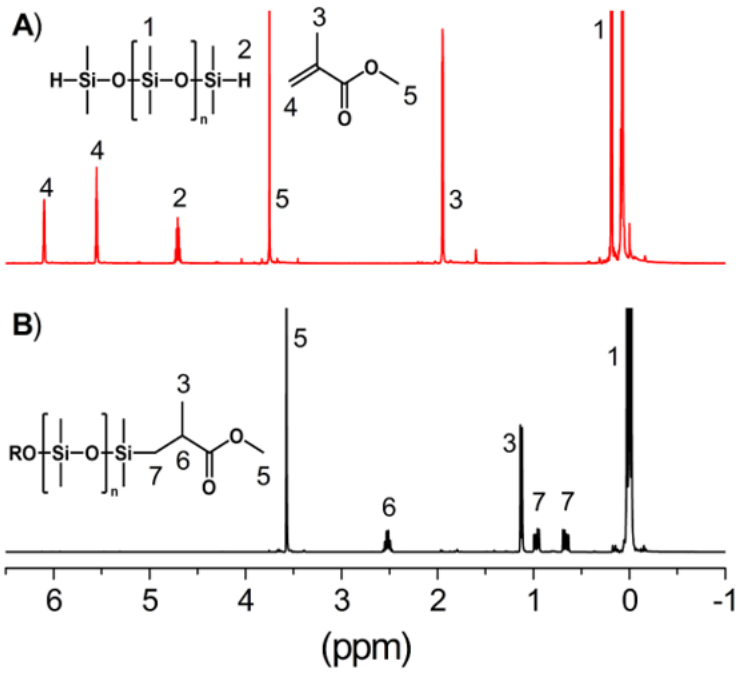

Figure 4.5: ^{1}H NMR spectra of the feed mixture of MMA and h_2PDMS (A) and the product MMA-PDMS$_n$-MMA (B) ($CDCl_3$, 250 MHz).

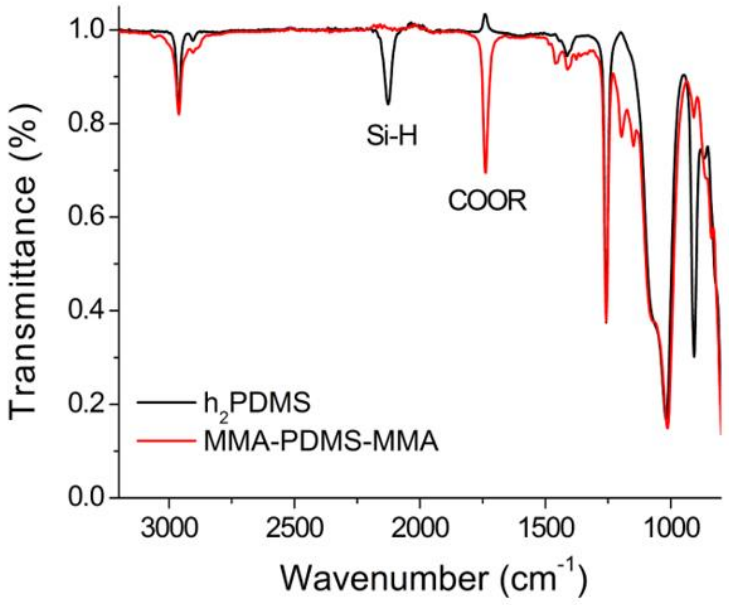

Figure 4.6: FTIR spectroscopy of h_2PDMS and MMA-PDMS$_n$-MMA.

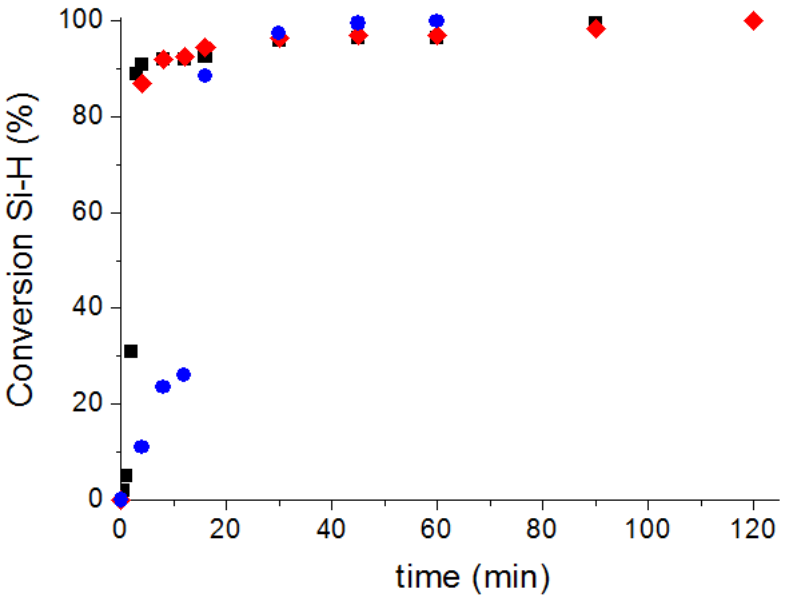

Figure 4.7: Conversion of Si-H groups with time at different temperatures; 100 °C (square), 70 °C (diamonds), and 37 °C (circles).

As a result, the temperature has a significant influence on the rate of hydrosilylation. Figure 4.7 indicates the kinetics of the reaction at different temperatures; faster reactions were observed at higher temperature, interestingly, the reaction was completed after 60 minutes at all studied temperatures. Hydrosilylation is a catalytic addition reaction and both the Markovnikov and the anti-Markovnikov products are possible. Previously, it has been reported that hydrosilylation catalysed by rhodium and rhenium complexes follow the anti-Markovnikov rule [266, 267]. Due to the asymmetric substitution of the methacrylates used in this study, valuable and conclusive information is obtained from the ^{1}H NMR spectrum of the final product (Figure 4.5B). A product according to the Markovnikov rule would result in the formation of a quaternary carbon substituted with two methyl groups, whereas an anti-Markovnikov product would contain CH_2 and CH_3 groups (Figure 4.8). ^{1}H NMR spectroscopy revealed the formation of the anti-Markovnikov product; the quartet of triplets at 2.5 ppm corresponds to a CH group neighbouring a CH_2 and CH_3 group, and the two signals between 0.5 and 1 ppm originate from the CH_2, which couples to the protons of the vicinal chiral carbon atom. In addition, ^{13}C NMR spectroscopy also indicates that the hydrosilylation product is anti-Markovnikov (Figure 4.9). Thus, the conditions applied in this study favour an anti-Markovnikov product, most likely due to the lower steric hindrance of the intermediate state. All modifications in this study were complete after 60 minutes at 37 °C with close to 100 % yields. The formation of anti-Markovnikov products was observed for all methacrylate additions as evidenced by the corresponding NMR spectra (Figure 4.10).

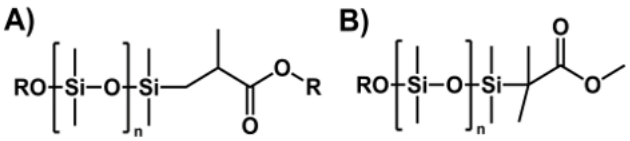

Figure 4.8: Structures of anti-Markovnikov (A) and Markovnikov (B) products, which can be obtained by hydrosilylation of methacrylates; R represents the same functional group as the right hand side.

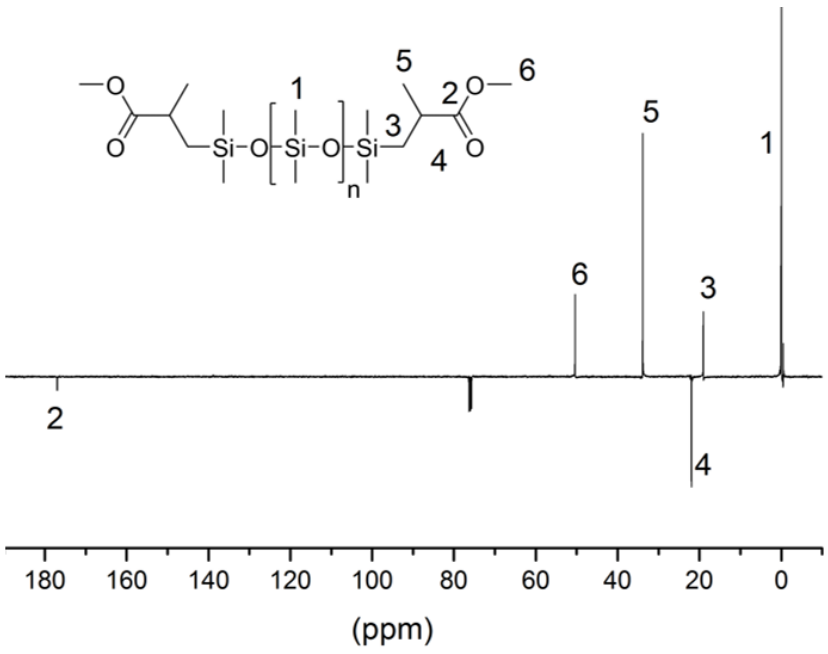

Figure 4.9: ^{13}C spectroscopy of h_2PDMS and MMA-PDMS$_n$-MMA.

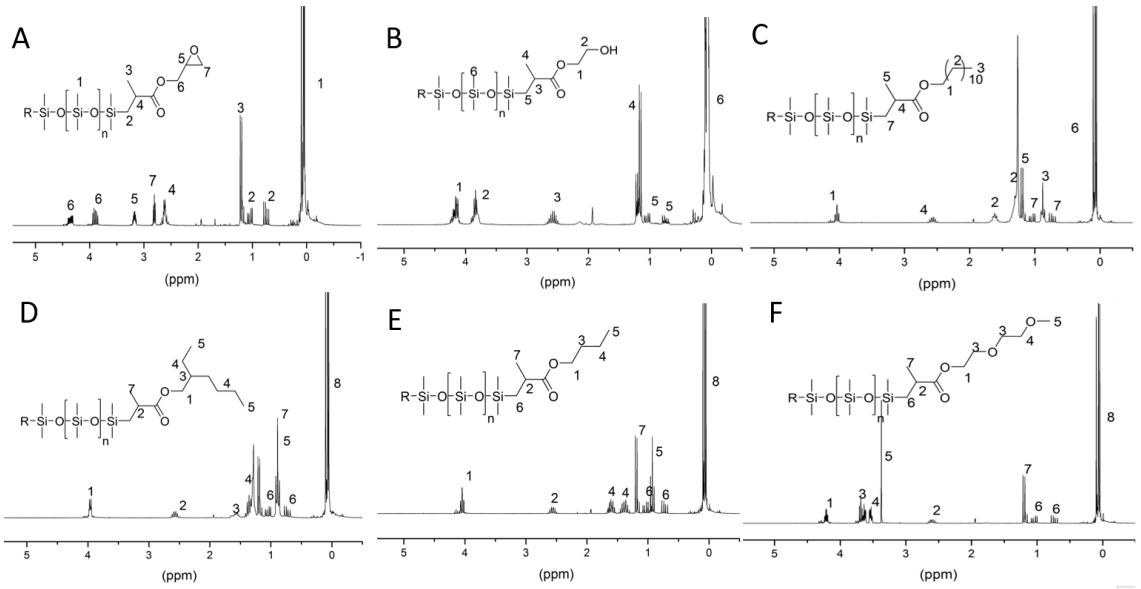

Figure 4.10: ^{1}H NMR spectrum of PDMS modification (A) GMA-PDMS$_n$-GMA, (B) HEMA-PDMS$_n$-HEMA, (C) LMA-PDMS$_n$-LMA, (D) EHMA-PDMS$_n$-EHMA, (E) BMA-PDMS$_n$-BMA, (F) DEGMEMA-PDMS$_n$- DEGMEMA.

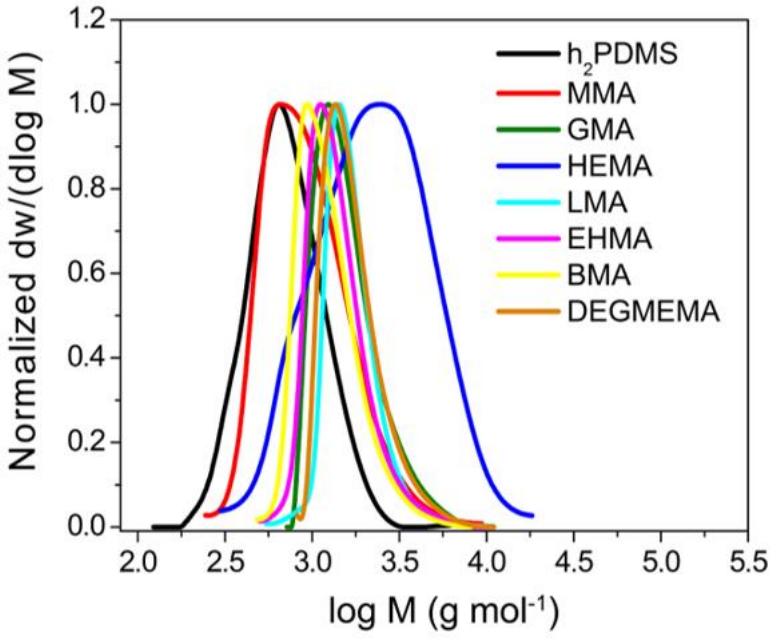

Figure 4.11: SEC traces of h_2PDMS and methacrylate (x) modified PDMS (x-PDMS$_n$-x).

Furthermore, the products were investigated by size exclusion chromatography (SEC) (Figure 4.11). Unmodified h_2PDMS showed a monomodal trace with a narrow dispersity ($Đ$ = 1.23). Notably, the retention time in SEC depends on the size of polymer in the solution; those with large hydrodynamic volume eluting first. Upon modification, a shift to higher molar mass was observed. For example, the molar mass of LMA-PDMS-LMA is greater than MMA-PDMS-MMA; LMA has a longer chain length than MMA which results in the larger hydrodynamic volume. The retaining narrow molar mass distributions for all hydrosilylation products was observed except HEMA-PDMS-HEMA. The reaction with HEMA resulted in a rather broad molar mass distribution ($Đ$ = 1.71). This could be the result of interactions with the column material and a non-suitable solvent system employed for the amphiphilic product obtained. However, ^{1}H NMR demonstrated quantitative conversion of the Si-H groups without the formation of any side products. To further elucidate the products formed, MALDI-ToF MS measurements were conducted.

Analysis of the MALDI-ToF MS spectra of the MMA and HEMA hydrosilylation products revealed the molecular composition of the two products with distributions which are in agreement with the expected composition (Figure 4.12). The products were analysed using dithranol as matrix and sodium iodide to improve the ionization. The molar mass increments (74.02 g mol^{-1}) were assigned to the DMS repeating units. End-group analysis proved the successful introduction of MMA and HEMA groups into the polymer, with chemical composition calculated according to $(C_2H_6SiO)_n$ $(C_7H_{15}SiO_2)_2O.Na^+$ and $(C_2H_6SiO)_n$ $(C_8H_{17}SiO_3)_2O.Na^+$, respectively. No further

distributions or side products were observed, indicative of the high yields and selectivity of this reaction. The same observations were made for modifications with the other methacrylates.

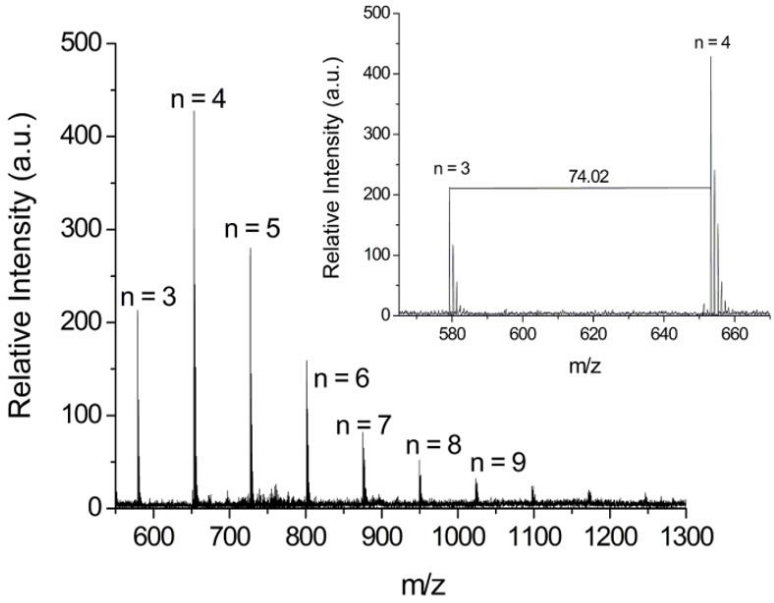

Figure 4.12: MALDI-ToF MS spectrum of MMA-PDMS-MMA with the molecular composition $(C_2H_6SiO)_n$ $(C_7H_{15}SiO_2)_2O.Na^+$, where n represents the repeating unit of PDMS.

4.2.2 Synthesis of ABA triblock copolymers

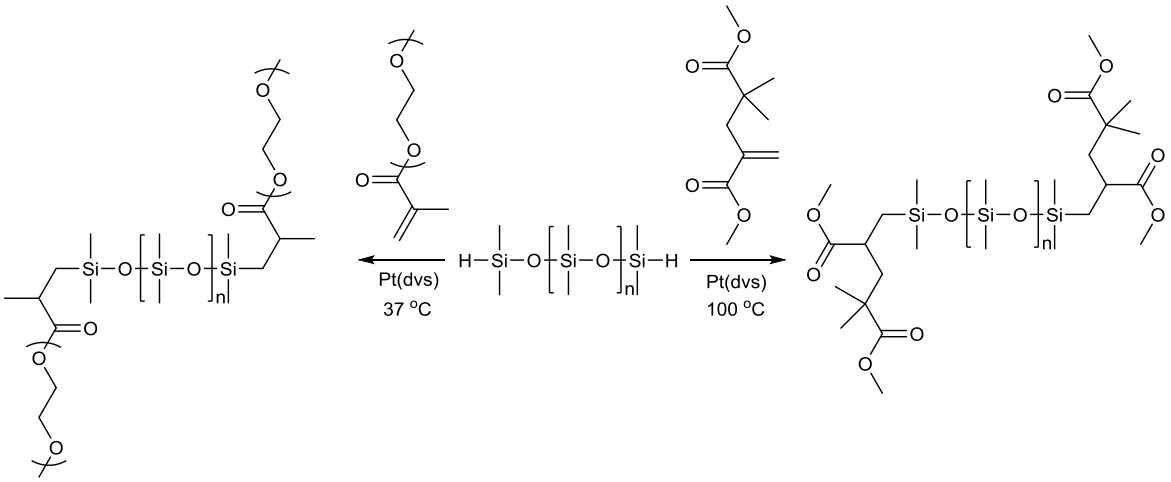

Figure 4.13: A schematic reaction of PEG_6-$PDMS_6$-PEG_6 and MMA_2-$PDMS_6$-MMA_2 formations.

Hydrosilylation was further employed for the synthesis of ABA triblock copolymers. Poly(ethylene glycol)methacrylate (PEGMA; average M_n 300 g mol^{-1}) was selected as a methacrylate terminated polyether. The reaction was conducted according to the protocol established for the small organic methacrylates. Full conversion of h_2PDMS was reached within 90 minutes, as indicated by the disappearance of the corresponding Si-H signal (4.80 ppm) in the ^{1}H NMR spectrum (Figure 4.14). In addition, even for the reaction with PEGMA, exclusively the anti-Markovnikov product was obtained. Further, SEC analysis further demonstrated the quantitative conversion of the starting materials (Figure 4.15). A complete shift of the SEC trace to higher molar mass was observed following the reaction. The absence of the PEGMA signal proved the high efficiency of the hydrosilylation modification. A well-defined ABA triblock copolymer

was obtained as suggested by the narrow molar mass distribution (M_n = 2200 g mol^{-1}, *Đ* = 1.19).

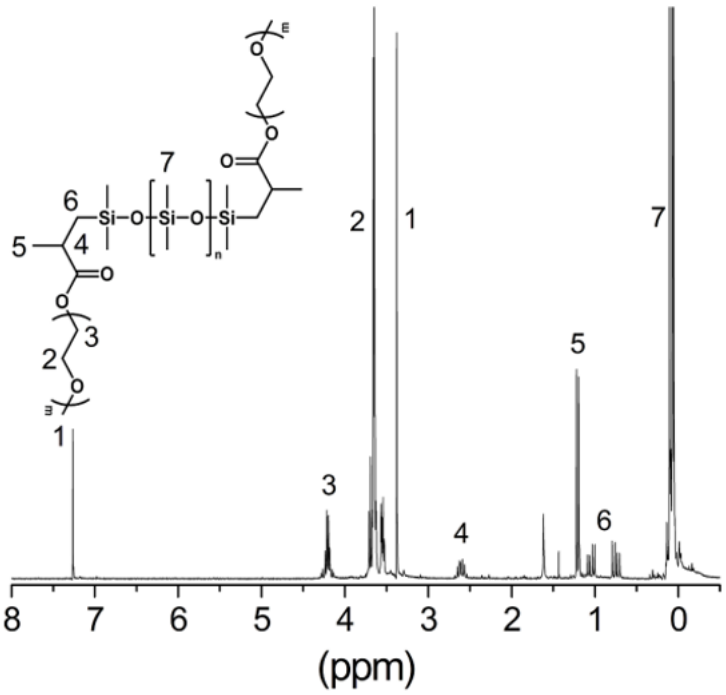

Figure 4.14: ^{1}H NMR spectrum of PEG_6-$PDMS_6$-PEG_6 triblock copolymer ($CDCl_3$, 250 MHz).

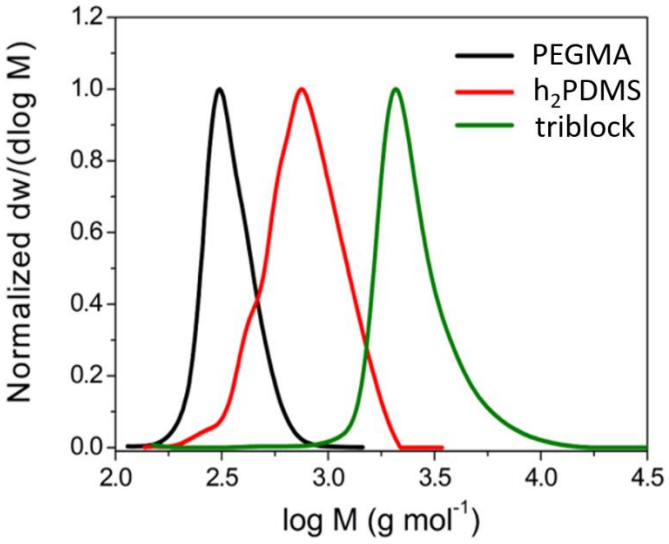

Figure 4.15: SEC elution traces of PEG_6-$PDMS_6$-PEG_6 triblock copolymer.

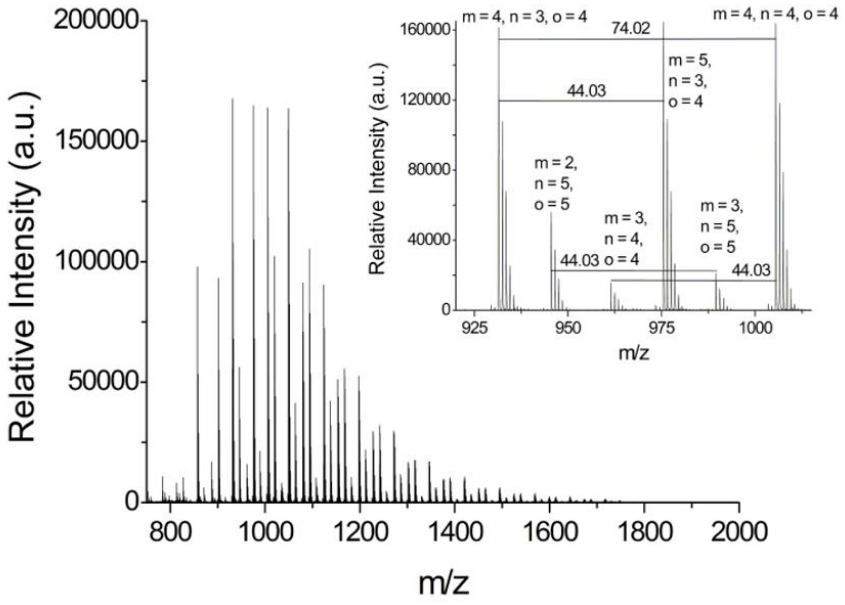

Figure 4.16: MALDI-ToF MS spectrum of PEG_6-$PDMS_6$-PEG_6.

The MALDI-ToF MS spectrum showed a peak pattern typical for (block) copolymers with molar mass increments corresponding to both the DMS (74.02 g mol^{-1}) and EG (44.03 g mol^{-1}) repeating units (Figure 4.16). The chemical composition was confirmed by the isotopic pattern. End group analysis revealed the formation of solely PEGMA modified PDMS with the chemical formula $C_7H_{15}SiO_3(C_2H_4O)_m(C_2H_6SiO)_n(C_2H_4O)_oC_7H_{15}SiO_2.Na^+$, where n, m and o represent the number of repeating units of DMS, EG and EG, respectively. For a detailed analysis, the peak at 931.48 m/z was selected corresponding to the formula $C_7H_{15}SiO_3(C_2H_4O)_4(C_2H_6SiO)_3(C_2H_4O)_4C_7H_{15}SiO_2.Na^+$. For a more comprehensive evaluation, the peaks in the inset in figure 4.16 are assigned with the corresponding number of repeating units. Thus, MALDI-ToF MS confirms that simple hydrosilylation can be used to synthesise amphiphilic copolymers containing silicone hydrophobic middle blocks.

To further demonstrate the versatility of the hydrosilylation reaction, structurally demanding vinyl end-functionalized CCT macromonomers were employed for the preparation of ABA triblock copolymers. In contrast to the hydrosilylation reactions described in this study, no reaction occurred at 37 °C, which is attributed to the steric hindrance of the substituents of the vinyl groups of CCT macromonomers. Thus, the reaction was conducted at elevated temperatures (100 °C) with a higher h_2PDMS-to-CCTP MMA dimer ratio. After 24 hours full conversion of the Si-H groups was observed by ^{1}H NMR (Figure 4.17) and IR spectroscopy (Figure 4.18), by the disappearance of the Si-H signal at 4.7 ppm and Si-H band at 2100 cm^{-1}, respectively.

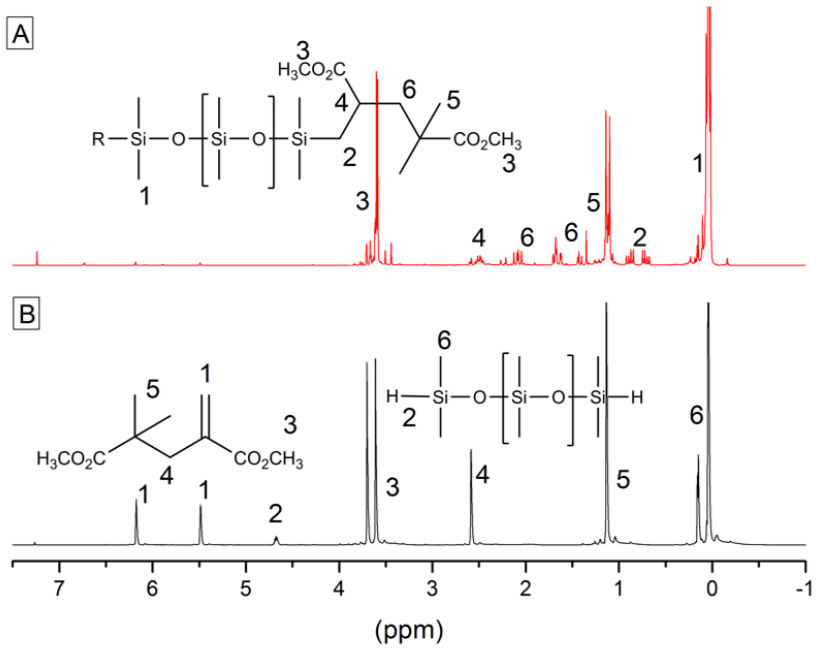

Figure 4.17: ^{1}H NMR spectra of (A) the ABA triblock $PMMA_2$-b-$PDMS_6$-b-$PMMA_2$ after 24 h reaction and (B) the feed reaction mixture.

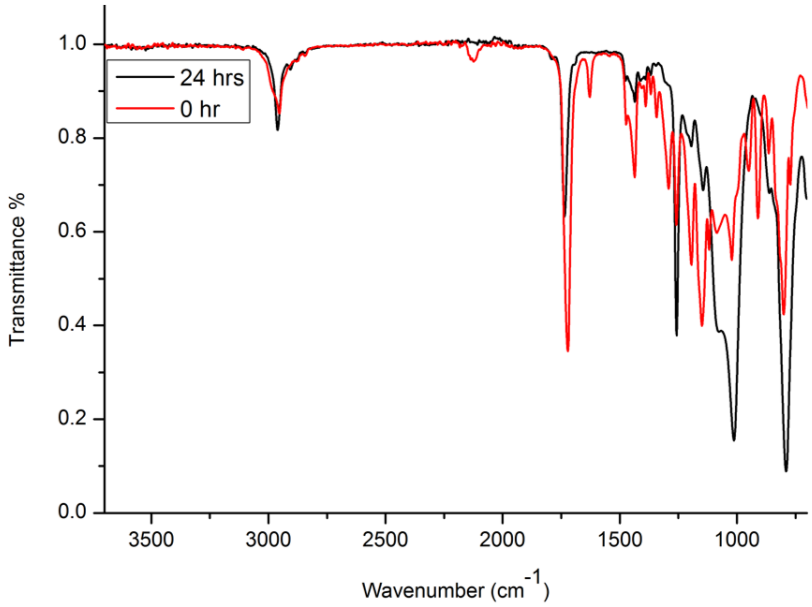

Figure 4.18: FTIR spectrum of $PMMA_2$-b-$PDMS_6$-b-$PMMA_2$ triblock copolymer.

4.3 Conclusion

Seven different small organic methacrylates have been used to modify terminal hydride substituted PDMS via hydrosilylation in the presence of a commercial platinum(II) catalyst (Pt(dvs)). It was demonstrated that the reactions proceed to very high conversions over 60 minutes under mild reaction conditions (37 °C). According to ^{1}H NMR spectroscopy and MALDI-ToF MS investigations, 100% conversions without the formation of side products were obtained for all methacrylates. ^{1}H NMR revealed the synthesis of anti-Markovnikov products. Moreover, hydrosilylation is described as an alternative approach for the synthesis of block copolymers. Well-defined block copolymers were obtained by modification with PEGMA, as proven by ^{1}H NMR spectroscopy, SEC and MALDI-ToF MS. Furthermore, adjustment of the reaction conditions enabled the synthesis of ABA triblock copolymers with sterically demanding

vinyl terminated CCT macromonomers. In summary, hydrosilylation represents a powerful tool for the fabrication of functional PDMS materials, including end-functional PDMS and block copolymers. The addition of Si-H can be compared to thiol-ene, S-H, chemistry which has found extensive use in polymer synthesis. The vast variety of commercially available hydride substituted PDMS and functional methacrylates in combination with the beneficial characteristics of the reaction, such as quantitative conversion at mild conditions, high selectivity and high tolerance towards various functionalities, makes hydrosilylation of methacrylates interesting for a broad range of applications. The examples of using polymeric micelles to improve the solubility and stability of hydrophobic pesticides are mentioned in chapter 1. This section demonstrates a facile synthetic route of an ABA amphiphilic triblock copolymer containing the hydrophobic PDMS. Thus, PEG_n-$PDMS_m$-PEG_n copolymers could be used to generate micelles which may be promising as carriers of water-insoluble agrochemicals like the microcapsules discussed in the previous chapter.

4.4 Experimental

4.4.1 Materials

Hydride terminated PDMS (h_2PDMS; average M_n 580 g mol^{-1}), toluene, methyl methacrylate (MMA), 2-ethyl hexyl methacrylate (EHMA) , glycidyl methacrylate (GMA), lauryl methacrylate (LMA), butyl methacrylate (BMA), diethylene glycol methyl ether methacrylate (DEGMEMA), poly(ethylene glycol methyl ether) methacrylate (PEGMA, average Mn 300 g mol^{-1}), dithranol, sodium iodide and THF were purchased from Sigma-

Aldrich and used as received. 2-hydroxylethyl methacrylate (HEMA) was obtained from Sigma-Aldrich and purified by deionized water/hexane extraction. Pt(dvs) was purchased from Gelest. The MMA macromonomer was synthesized according to literature procedure [267].

4.4.2 Characterisation

IR spectra were recorded on a Bruker Vector 22 FTIR spectrometer. OPUS software was used to analyse absorbance data. Size exclusion chromatography measurements were performed on an Agilent 390 MDS Multi-Detector GPC system ($CHCl_3$ + 2 % TEA Mixed C Column Set, THF + 2 % TEA and 0.01 wt.% BHT with PLgel Mixed C columns set, 30 °C flow rate 1 ml/min, narrow standards of PMMA were used as calibration polymers between 955000 and 1010 $gmol^{-1}$ and fitted with a third order polynomial) by DRI detection. ^{1}H NMR and ^{13}C NMR were recorded on a Bruker AC-250, with $CDCl_3$ as the solvent. The chemical shifts are given in ppm relative to the signal from residual non-deuterated solvent. For the MALDI measurements an Autoflex ToF/ToF apparatus (Bruker Daltonics, Bremen, Germany) was used.

4.4.3 Kinetic studies of hydrosilylation of methyl methacrylate

Hydrosilylation was performed at 100 °C, 70 °C and 37 °C. In all cases, up to 10 vials with each H_2PDMS (1 g, 1.72 mmol, 1 eq.), methyl methacrylate (0.36 g, 3.59 mmol, 2.1 eq.) and 11 µL of Pt(dvs) were prepared and stirred for a maximum of 120 min. At different time points samples were taken and the conversion of the Si-H bond was determined by ^{1}H NMR spectroscopy.

4.4.4 General procedure for the hydrosilylation of methacrylates

H_2PDMS (1 g, 1.72 mmol, 1 eq.), methacrylate (3.59 mmol, 2.1 eq.) and 11 µL of Pt(dvs) were added into a glass vial and stirred for 60 min at 37 °C. The product was isolated by removal of excess monomer under reduced pressure.

4.4.5 Synthesis of MMA-PDMS-MMA

^{1}H NMR (250 MHz, $CHCl_3$, δ): 0.00 (m, 36H, Si-CH_3), 0.65 (dd, 2H, Si-CH_2, J = 8.10, 14.85 Hz), 0.93 (dd, 2H, Si-CH_2, J = 6.60, 14.85 Hz), 1.20 (d, 6H, CH_3, J = 6.95 Hz), 2.5 (m, 2H, CH), 3.60 (s, 6H, O-CH_3), ^{13}C NMR (75.47 MHz, $CHCl_3$, δ): 0.00 (Si-C), 19 (Si-C), 22 (C-C), 30 (C-C), 50 (C-O), 175 (C=O), IR: *v* = 2961 (C-H), 1768 (C=O), 1257 (C-O). MALDI-ToF MS (m/z): $C_7H_{15}SiO_3$ $(C_2H_6SiO)_n$ $C_7H_{15}SiO_2.Na^+$, 579.30 (n=3), 653.34 (n=4), 727.38 (n=5), 801.42 (n=6), 875.46 (n=7), 949.50 (n=8), 1023.54 (n=9). SEC $_{(CHCl3)}$: Mn = 690 g mol^{-1}, *Đ* = 1.42.

4.4.6 Synthesis of HEMA-PDMS-HEMA

^{1}H NMR (250 MHz, $CHCl_3$, δ): 0.00 (m, 36H, Si-CH_3), 0.75 (dd, 2H, Si-CH_2, J = 8.00, 14.85 Hz), 1.10 (dd, 2H, Si-CH_2, J = 6.15, 14.85 Hz), 1.25 (m, 6H, CH_3), 2.58 (m, 2H, CH), 3.94 (m, 4H, CH_2-OH), 4.25 (m, 4H, O=C-O-CH_2), ^{13}C NMR (75.47 MHz, $CHCl_3$, δ): 0.00 (Si-C), 19 (Si-C), 23 (C-C), 30 (C-C), 55 (C-O), 64 (C-O), 175 (C=O), IR: *v* = 2962 (C-H), 1721 (C=O), 1258 (C-O), MALDI-ToF MS (m/z): $C_8H_{17}SiO_4$ $(C_2H_6SiO)_n$ $C_8H_{17}SiO_3.Na^+$, 639.24 (n=3), 713.26 (n=4), 787.28 (n=5), 861.30 (n=6), 935.32 (n=7), 1009.33 (n=8). SEC$_{(CHCl3)}$: M_n= 1,200 g mol^{-1}, *Đ* = 2.00.

4.4.7 Synthesis of GMA-PDMS-GMA

^{1}H NMR (250 MHz, $CHCl_3$, δ): 0.00 (m, 36H, Si-CH_3), 0.70 (dd, 2H, Si- CH_2, J = 8.50, 14.85 Hz), 1.10 (dd, 2H, Si-CH_2, J= 6.60, 14.85 Hz), 1.20 (d, 6H, CH_3, J = 6.95 Hz), 2.65 (m, 2H, CH), 2.80 (t, 2H, O-CH_2, J = 4.70 Hz), 3.20 (sex, 4H, O-CH, J = 3 Hz), 3.95 (m, 2H, O=C-O-CH2), 4.45 (m, 2H, O=C-O-CH_2), ^{13}C NMR (75.47 MHz, $CHCl_3$, δ): 0.00 (Si-C), 19 (Si-C), 22 (C-C), 35 (C-C), 44 (C-O), 49 (C-O), 63 (C-O) 178 (C=O), IR: *v* = 2961 (C-H), 1741 (C=O), 1258, (C-O), MALDI-ToF MS (m/z): $C_9H_{17}SiO_4(C_2H_6SiO)_n$ $C_9H_{17}SiO_3.Na^+$, 589.37 (n=2), 663.39 (n=3), 737.41 (n=4), 811.43 (n=5), 885.45 (n=6), 959.47 (n=7), 1033.49 (n=8), $SEC_{(CHCl3)}$: M_n= 1,400 g mol^{-1} , *Đ*= 1.18.

4.4.8 Synthesis of EHMA-PDMS-EHMA

^{1}H NMR (250 MHz, $CHCl_3$, δ): 0.00 (m, 36H, Si-CH_3), 0.75 (dd, 2H, Si-CH_2, J = 8.30, 14.85 Hz), 0.90 (t, 12H CH_3, 7.42 Hz) 1.00 (dd, 2H, Si-CH_2, J = 6.15, 14.85 Hz), 1.20 (d, 6H, CH_3, 6.95 Hz) 1.35 (m, 16H, CH_3), 1.55 (m, 2H, CH_2) 2.55 (m, 2H, CH), 4.00 (m, 4H, O=C-O-CH_2), ^{13}C NMR (75.47 MHz, $CHCl_3$, δ): 0.00 (Si-C), 9 (Si-C), 12,19,25,35 (C-C), 63 (C-O), 175 (C=O), IR: *v* = 2960 (C-H), 1735 (C=O), 1258 (C-O), MALDI-ToF MS (m/z): $C_{14}H_{29}SiO_3$ $(C_2H_6SiO)_n$ $C_{14}H_{29}SiO_2.Na^+$, 627.41 (n=1), 701.43 (n=2), 775.45 (n=3), 849.48 (n=4), 923.50 (n=5), 997.52 (n=6), 1071.54 (n=7), SEC $_{(CHCl3)}$: M_n = 1,300 (g mol^{-1}), *Đ* = 1.16.

4.4.9 Synthesis of BMA-PDMS-BMA

^{1}H NMR (250 MHz, $CHCl_3$, δ): 0.00 (m, 36H, Si-CH_3), 0.75 (dd, 2H, Si-CH_2, J = 8.20, 14.85 Hz), 0.90 (t, 6H, CH_3, J = 7.30 Hz) 1.00 (dd, 2H, Si-CH_2, J = 6.32, 14.69 Hz), 1.20 (d, 6H, CH_3, J = 6.95 Hz), 1.42 (m, 4H, CH_2), 1.55 (m, 4H, CH_2) 2.55 (m, 2H, CH), 4.00 (t, 4H

O=C-O-CH_2, J = 6.80 HZ), ^{13}C NMR (75.47 MHz, $CHCl_3$, δ): = 0.00 (Si-C), 11 (Si-C), 20, 23, 28, 30(C-C), 60 (C-O) , 175 (C=O), IR: *v* = 2961 (C-H), 1736 (C=O), 1257 (CO), MALDI-ToF MS (m/z): $C_{10}H_{21}SiO_3$ $(C_2H_6SiO)_n$ $C_{10}H_{21}SiO_2.Na^+$, 589.33 (n=2) 663.36 (n=3), 733.38 (n=4), 811.40 (n=5), 885.43 (n=6), 959.45 (n=7), 1033.48 (n=8), $SEC_{(CHCl3)}$: M_n= 1,100 g mol^{-1}, *Đ* = 1.17.

4.4.10 Synthesis of DEGMEMA-PDMS-DEGMEMA

^{1}H NMR (250 MHz, $CHCl_3$, δ): 0.00 (m, 36H, Si-CH_3), 0.75 (dd, 2H, Si-CH_2, J = 8.50, 14.85 Hz), 1.00 (dd, 2H, Si-CH_2, 6.32, 14.85 Hz), 1.18 (d, 6H, CH_3, 6.95 Hz), 2.55 (m, 2H, CH), 3.40 (s, 6H, O-CH_3), 3.5 (m, 4H, OCH_3), 3.60 (m, 8H, O-CH_3) 4.12 (m, 4H, O=C O-CH_2), ^{13}C NMR (75.47 MHz, CHCl3, δ): = 0.00 (Si-C), 19 (Si-C), 22, 30 (C-C), 58, 62, 78, 70, 72 (C-O), 175 (C=O), IR: *v* = 2961 (C-H), 1736 (C-H), 1258 (C-O). MALDI-ToF MS (m/z): $C_{11}H_{23}SiO_5$ $(C_2H_6SiO)_n$ $C_{11}H_{23}SiO_4.Na^+$, 681.33 (n=2), 755.31 (n=3), 829.31 (n=4) 903.33 (n=5), 977.35 (n=6), 1051.37 (n=7), SEC(CHCl3): M_n = 1,500 g mol^{-1}, *Đ* = 1.15

4.4.11 Synthesis of PEG_6-b-$PDMS_6$-b-PEG_6 copolymer

H_2PDMS (1 g, 1.72 mmol, 1 eq.) and PEGMA (1.04 g, 3.46 mmol, 2.01 eq.) were dissolved in 1.5 mL toluene and 11 µL of Pt(dvs) was added into a glass vial and stirred for 60 min at 37 °C. Subsequently, toluene was evaporated under reduced pressure and 45 mL water was added and the solution was centrifuged for 12 min (7,800 rpm). The supernatant was removed and the precipitate was dissolved in THF, the organic phase was dried over $MgSO_4$, filtered, and the volatiles were removed under reduced pressure to give the ABA triblock copolymer (85 % yield). ^{1}H NMR (250 MHz, $CHCl_3$, δ): 0.00 (m,

36H, Si-CH_3), 0.70 (dd, 2H, Si-CH_2, J = 8.40, 14.85 Hz), 1.05 (dd, 2H, Si-CH_2, J = 6.15, 14.85 Hz), 1.20 (d, 6H, CH_3, J = 6.95 Hz), 2.55 (m, 2H, CH), 3.46 (s, 6H, O-CH_3), 3.58 (m, 44H, O-CH_2), 4.25 (m, 4H, O=C-O-CH_2), ^{13}C NMR (75.47 MHz, $CHCl_3$, δ): = 0.00 (Si-C), 18 (Si-C), 22 (C-C), 30 (C-C), 55, 60, 65, 70 (C-O) 175 (C=O), IR: *v* = 2960 (C-H), 1734 (C=O), 1258 (C-O), MALDI-ToF MS (m/z) (g mol^{-1}): $C_7H_{15}SiO_3$ $(C_2H_4O)_m(C_2H_6SiO)_n(C_2H_4O)_o$ $C_7H_{15}SiO_2.Na^+$, 857.46 (m=4, n=2, o=4), 901.49 (m=5, n=2, o=4), 931.48 (m=4, n=3, o=4), 945.52 (m=5, n=2, o=5), 975.52 (m=4, n=3, o=5), 1005.51 (m=4, n=4, o=4), 1019.55 (m=5, n=3, o=5), 1049.54 (m=5, n=4, o=4), 1329.67(m=6, n=6, o=6), $SEC_{(THF)}$: M_n= 2,200 g mol^{-1}, *Đ* = 1.19.

4.4.12 Synthesis of $PMMA_2$-b-$PDMS_6$-b-$PMMA_2$ copolymer

H_2PDMS (5 g, 8.6 mmol, 1 eq.), MMA macromer (4.3 g, 21.5 mmol, 2.5 eq.) and 33 µL of Pt(dvs) were added into a glass vial and stirred for 24 h at 100 °C. The product (80 %) was isolated by removal of excess monomer under reduced pressure at 137 °C. ^{1}H NMR (250 MHz, $CHCl_3$, δ): 0.00 (m, 36H, Si-CH_3), 0.72 (dd, 2H, Si-CH_2, J = 7.16, 14.88 Hz), 0.85 (dd, 2H, Si-CH_2, J = 7.72, 14.88 Hz), 1.10, 1.44 (s, 12H, CH_3), 1.67 (m, 2H, CH_2), 2.08 (m, 2H, CH_2), 2.51 (m, 2H, CH), 3.60 (s, 12H, O-CH_3), ^{13}C NMR (75.47 MHz, $CHCl_3$, δ): 0.00 (Si-C), 21 (Si-C), 23 (C-C), 33 (C-C), 39 (C-C), 50 (C-O), 177 (C=O), IR: *v* = 2980 (C-H), 1700 (C=O), 1250(C-O). $SEC_{(THF)}$: M_n = 1400 g mol_{-1}, *Đ* = 2.10.

Chapter 5

Acid-labile containing polymers synthesised via SET-LRP and their subsequent degradation

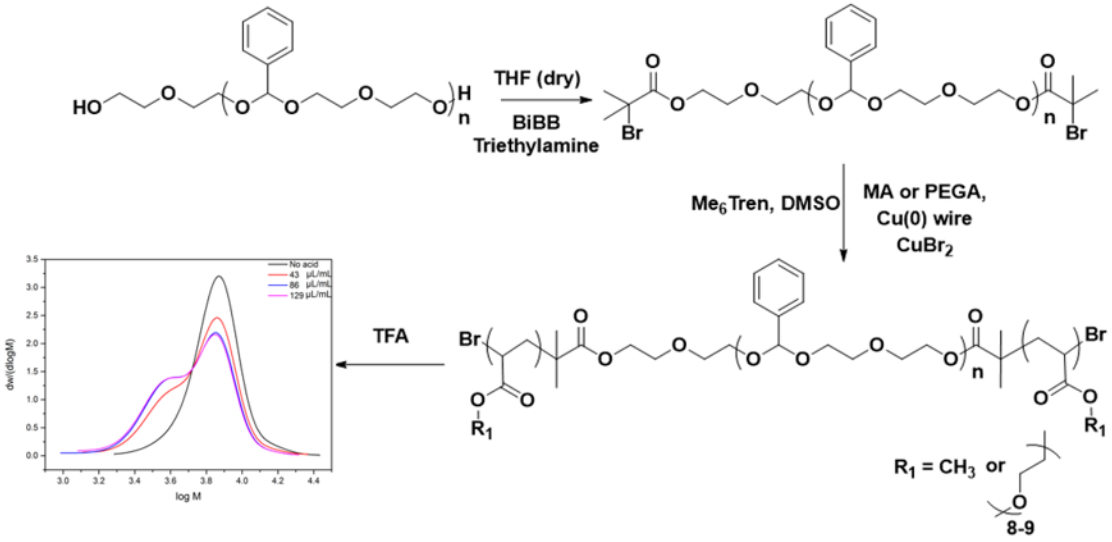

This chapter details the synthesis of acid-labile containing polymers via the Cu(0)-mediated polymerisation technique. Acid degradation is likely to be the potential focus of chemistry in literature reports on the pH-change in the rhizosphere, as this change is promising as a trigger condition for an agrochemical release. α, ω-Hydroxyl terminated poly(acetal) was synthesised from the condensation reaction of diethylene glycol and benzaldehyde. Subsequently, it was successfully converted to an α, ω -acetal functional SET-LRP initiator via esterification with an acid halide, α-bromoisobutyryl (BiBB). The initiator was exploited to polymerise methyl acrylate (MA) and poly(ethylene glycol) methyl ether acrylate (PEGA) (average M_n 480 g mol^{-1}) through SET-LRP at ambient temperature. A reasonably high monomer conversion (>90%) and narrow molecular weight distribution (*Đ*) (1.1-1.3) were obtained. After solvent removal, the acetal-containing polymer degradation under acidic conditions was investigated; the decrease in molecular weight, as well as the formation of benzaldehyde, were monitored by SEC and ^{1}H NMR, respectively.

5.1 Background

5.1.1 pH responsive polymers

Physical stimuli-responsive materials, such as pH, temperature, and redox responsive polymers, have drawn the attention of polymer chemists during the last decade [269, 270]. pH sentisive polymers refer to polymers whose properties, such as solubility, volume, and chain conformation, is tunable when a different pH environment is applied to a system, due to these polymers containing an ionizable group that can donate or accept protons [271]. There are three main pH responsive polymers that have

been extensively investigated: anionic polymers, cationic polymers and acid-labile polymers. The anionic polymers mainly consist of the carboxylic acid group (COOH), which can protonate at high pH, leading to an increase in the hydrophilic character of the polymer. Common anionic polymers, such as poly (methacrylic acid) (PMAA) and poly(acrylic acid) (PAA), have been widely exploited [272, 273]. Protonated groups containing a polymer backbone represent the cationic polymer, for example, poly (N, N-dimethyl aminoethyl methacrylate) (PDMAEMA) and poly (4-vinylpyridine) (PVP) [274, 275]. Furthermore, some acid-labile bonds, including ketal, acetal, and hydrazone, are stable at neutral pH, however, these linkages break down at low pH, resulting from a hydrolysis reaction [276, 277]. Literature indicates the intensive use of pH-responsive polymers as carrier materials in different applications, including pharmaceutical, biomedical, agriculture, and industrial coating [278-284].

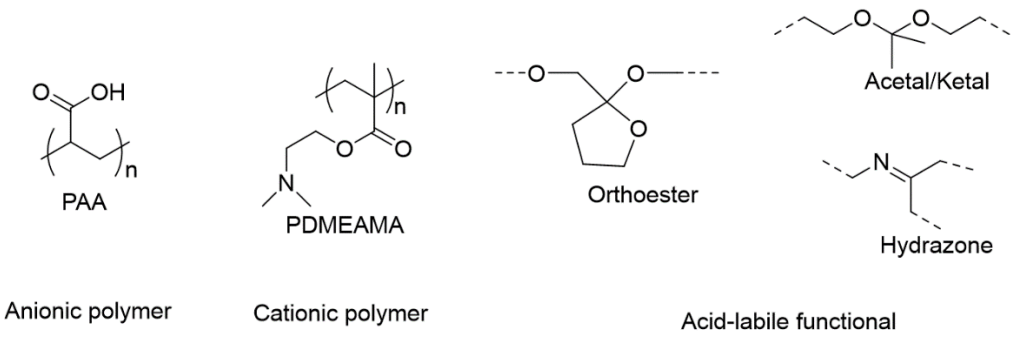

Figure 5.1: Examples of pH-responsive polymers.

In this chapter, the acid-labile acetal, which is a chemical group represented as $RCH(OR')_2$, is chosen as the building block due to several benefits including being

associated with a simple synthetic method and ease of degradation under mild acidic conditions. In general, acetal is prepared from the condensation reaction of a hydroxyl group and carbonyl compounds such as the reaction of alcohol and aldehyde under acidic conditions [285, 286]. It should be noted that acetal formation is a reversible process, thus, efficient water removal is important in obtaining a high reaction conversion. Dean-Stark apparatus has been widely utilised to remove condensation by-products [287-288]. Some acetal derivatives have been exploited in many applications, for example, acid degradation polymeric micelle/gels for drugs and protein delivery [289-295].

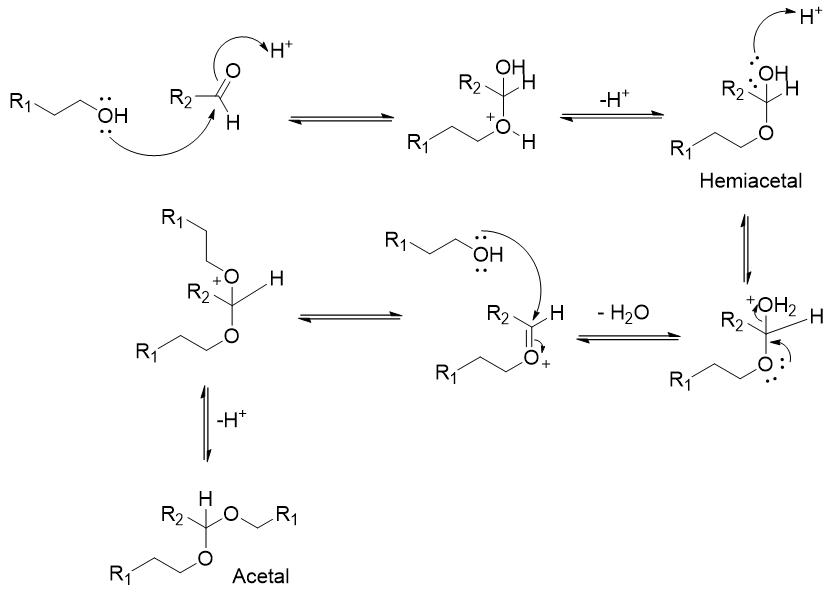

Figure 5.2: Proposed mechanism of acetal formation, the condensation reaction of alcohol and aldehyde, under acidic conditions.

5.1.2 pH change in soil root

pH-responsive polymers play a major role in material science, particularly in pharmacological and biomedical applications. The interest in polymers for agricultural

applications has increased significantly in the last few years [296, 297]. Acid degradation is likely to feature in literature reports on the pH-change in the rhizosphere, as this change is promising as trigger conditions for an active ingredient release. There are a few processes that alter the pH of the rhizosphere, primarily based on the variation of H^+ and OH^-, including cation-anion uptake, organic anion release, root respiration, and redox couple process. The uptake capacity of cations and anions influences the pH-change at the rhizosphere through preservation of the root-cell at a certain pH. The releasing of H^+ ions, when cations are more absorbed than anions [298]. Organic anion release, including citric, oxalic and malic acids, is considered as the major feature of pH change at root atmosphere (also known as rhizosphere acidification). Moreover, the redox couple process, which results from a change in the oxidation state of metals such as that between Fe(II) and Fe(III) in the soil, also influences the H^+ concentration [299]. Furthermore, microorganism activities also lead to the decrease of rhizosphere pH due to the production of carbonic acid (H_2CO_3), resulting from the respiration product (CO_2) of microorganisms [300, 301].

$$CO_2 \rightleftharpoons H_2CO_3 \rightleftharpoons HCO_3^- + H^+$$

$$2FeOOH + CHO_2^- + 5H_3O^+ \rightleftharpoons 2Fe^{2+} + CO_2 + 9H_2O$$

$$Fe^{2+} + O_2 + 14H_2O \rightleftharpoons 4FeOOH + 8H_3O^+$$

Figure 5.3: Some possible chemical reactions that influence soil pH.

5.2 Results and discussion

5.2.1 Synthesis of a α, ω-poly(acetal) SET-LRP initiator

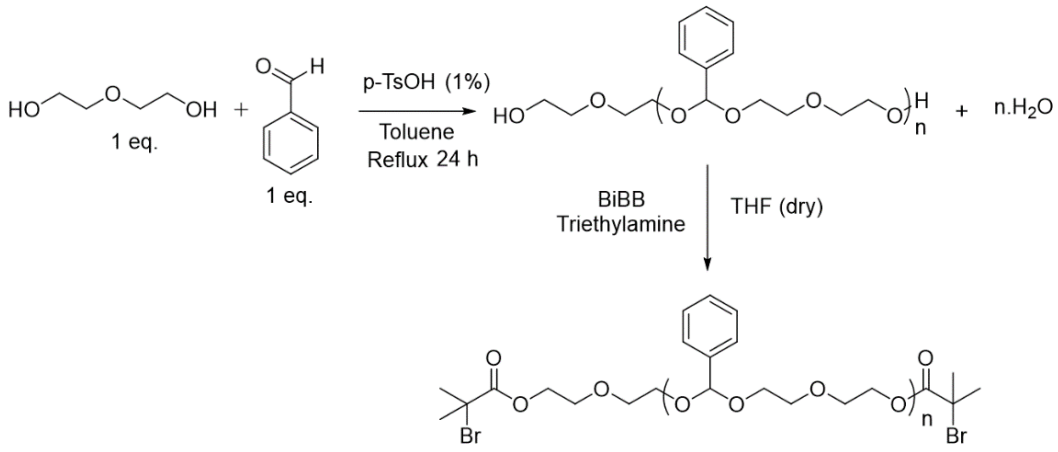

Figure 5.4: The schematic reaction of diethylene glycol and benzaldehyde.

Poly(acetal) was synthesised from diethylene glycol and benzaldehyde under reflux (Dean-Stark condensation). The reaction was successfully confirmed through different characterisation techniques, including, FTIR, ^{1}H, and ^{13}C NMR. IR spectroscopy indicates that the unreacted benzaldehyde was removed during the purification process from the absence of $\nu_{C=O}$ absorption at 1700 cm^{-1} (Figure 5.5). The broad absorption at approximately 3500 cm^{-1} signifies the OH absorption. Also, a successful acetal formation was proved by the strong detection of an acetal proton NMR signal at 5.65 ppm. Notably, a CH_2 signal of both environments (CH_2O and CH_2OH) shows an overlap signal at 3.40-3.60 ppm (Figure 5.6). It is noteworthy that the integration shows the repeating unit of polymer (DP) is approximately 1-2, which corresponds to SEC molecular weight (M_n = 400 g mol^{-1}, $Đ$ = 1.90). Finally, the peaks at 101.23 ppm and 126-128 ppm in the ^{13}C NMR

show the successful formation of acetal, representing acetal carbon and carbon of benzyl group, respectively (Figure 5.7).

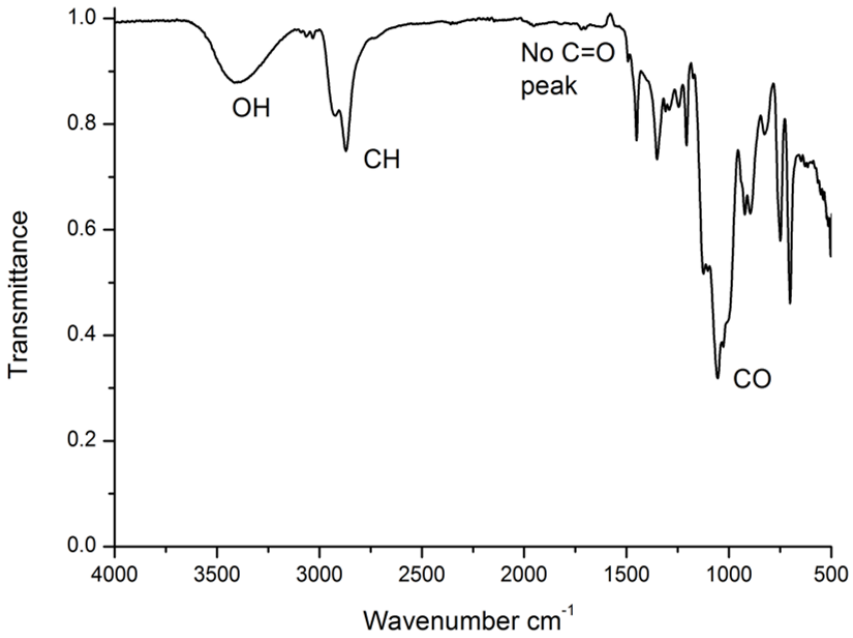

Figure 5.5: FTIR of α, ω-acetal synthesis from diethylene glycol and benzaldehyde.

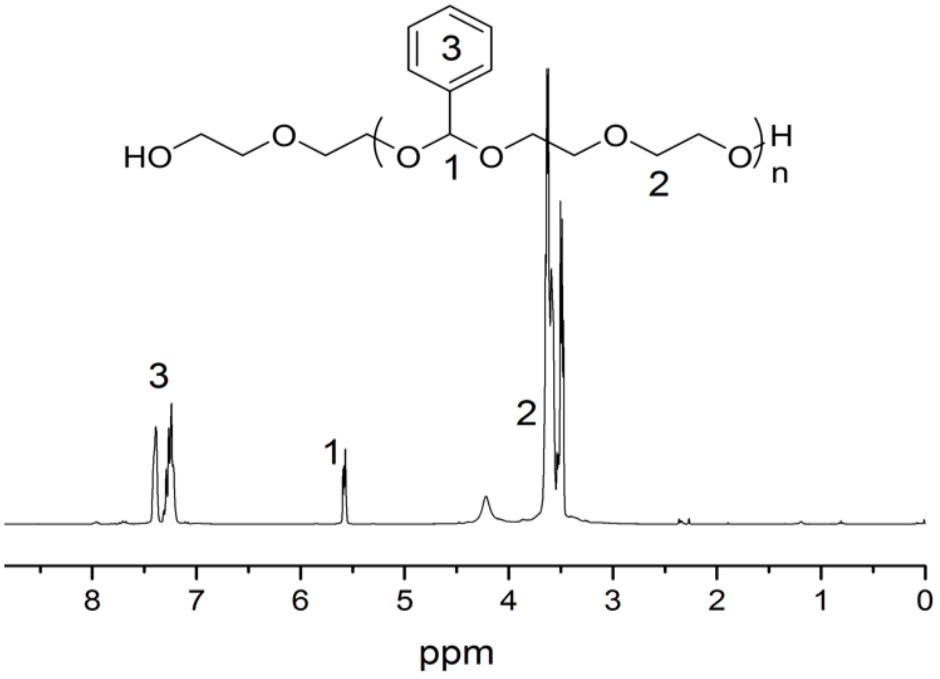

Figure 5.6: ^{1}H NMR of α, ω-acetal synthesis from diethylene glycol and benzaldehyde.

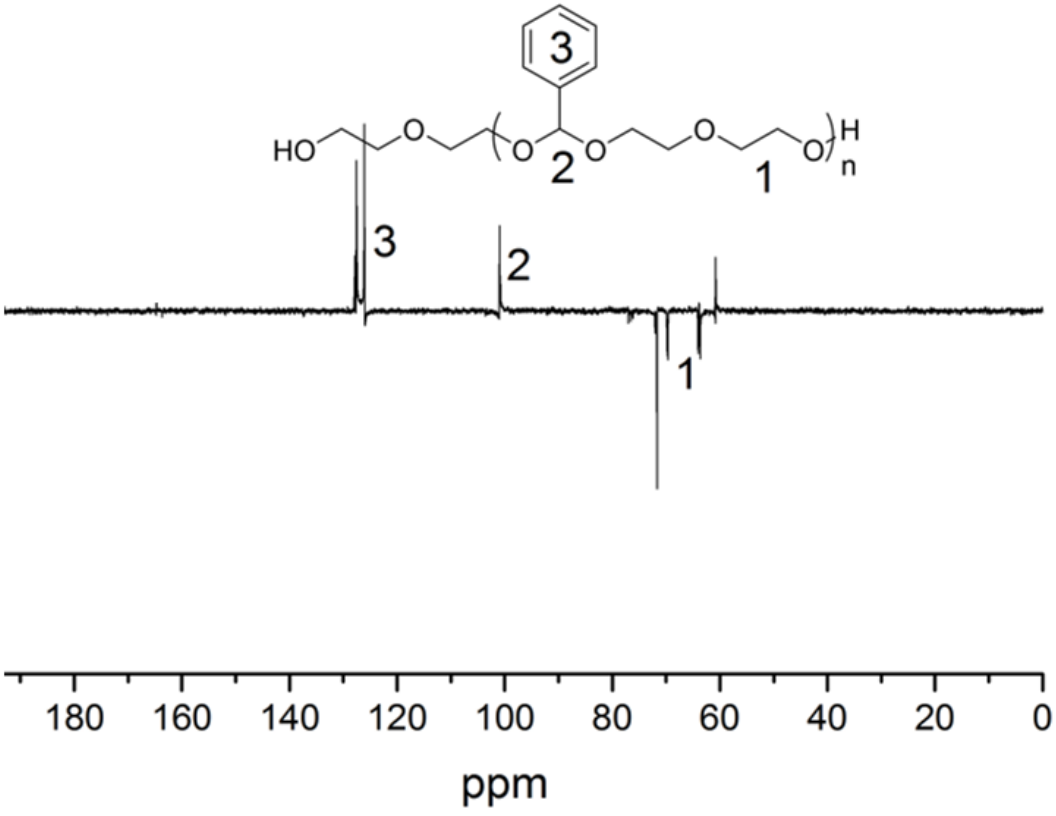

Figure 5.7: ^{13}C NMR of α, ω-acetal synthesis from diethylene glycol and benzaldehyde.

Subsequently, the α, ω-hydroxy terminated acetal was exploited to synthesise the SET-LRP initiator through esterification with bromoisobutyryl bromide (α-BiBB). FTIR reveals a peak at approximately 1700 cm^{-1} (C=O). Additionally, the disappearance of the absorption at about 3500 cm^{-1} indicates that the OH group was also present (Figure 5.8). The ^{13}C spectrum (Figure 5.9) supports the FTIR result, as two peaks at 164 and 30 ppm were detected, which correspond to C=O carbon and $C(CH_3)_2Br$, respectively. Furthermore, the ^{1}H NMR spectrum (Figure 5.10) demonstrates a successful modification of both hydroxyl groups of the polyacetal due to the formation of the peak at 4.30 ppm of CH_2COO (position 5), as well as CH_3 peaks at 1.90 ppm. Interestingly, two peaks at 1.90 and 1.96 ppm are detected; the sum of integration of these peaks (position 4 in Figure 5.10) equals 12H when the integration of position 5 is fixed to 4H. This shows that there are two types of hydroxyl terminal groups formed during the condensation reaction. Figure 5.2 represents the mechanism of acetal synthesis. Thus, the possibility of hydroxyl terminated poly(acetal) in our product possibly contains both hemiacetal and acetal.

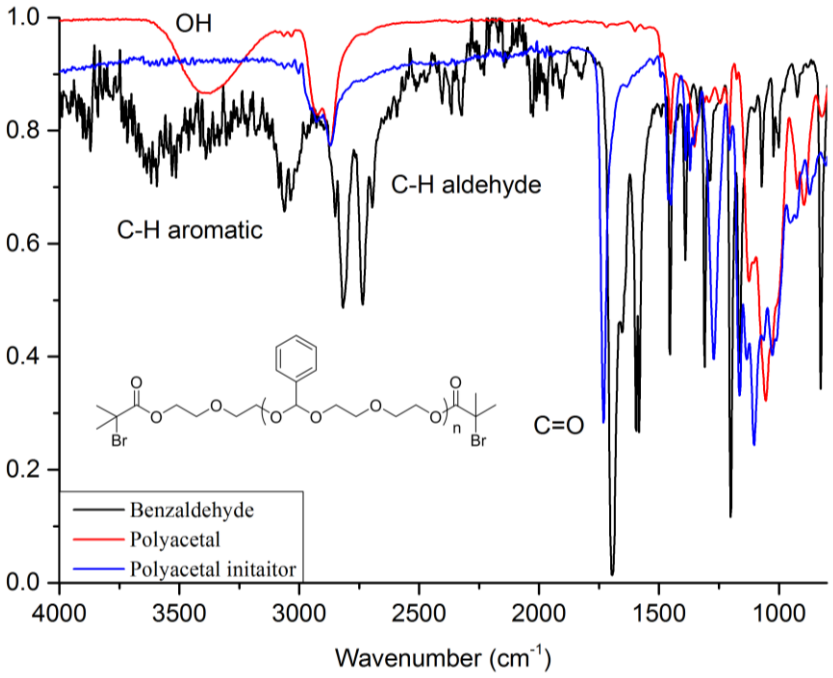

Figure 5.8: FTIR of α, ω-acetal SET-LRP initiator.

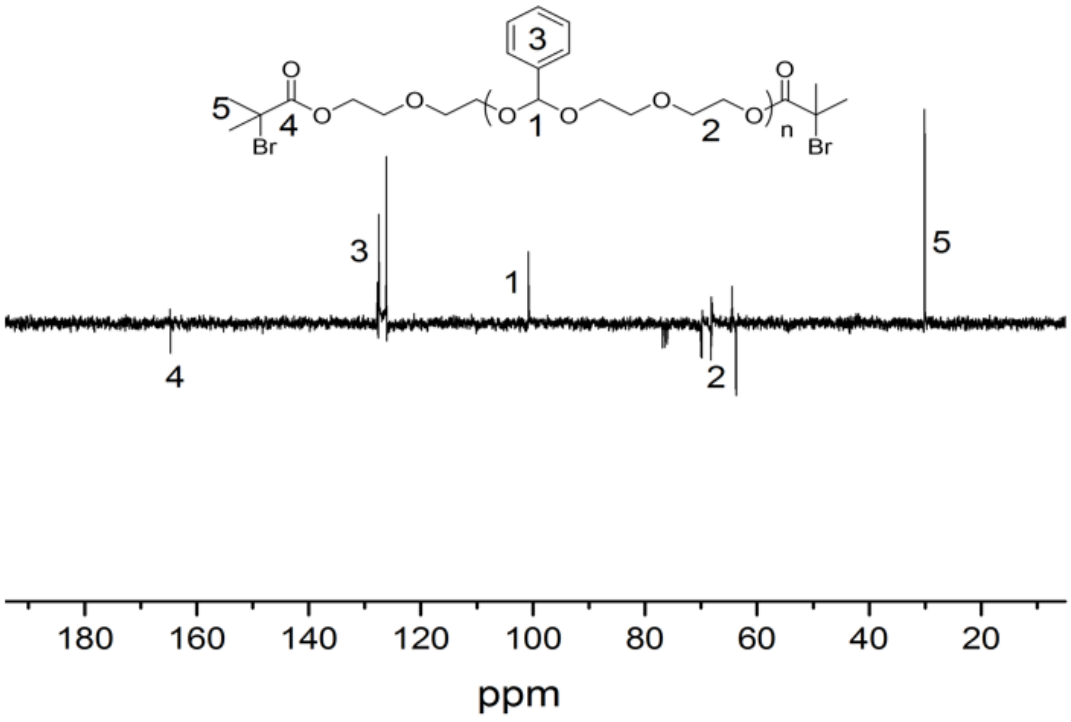

Figure 5.9: ^{13}C NMR of α, ω-acetal SET-LRP initiator.

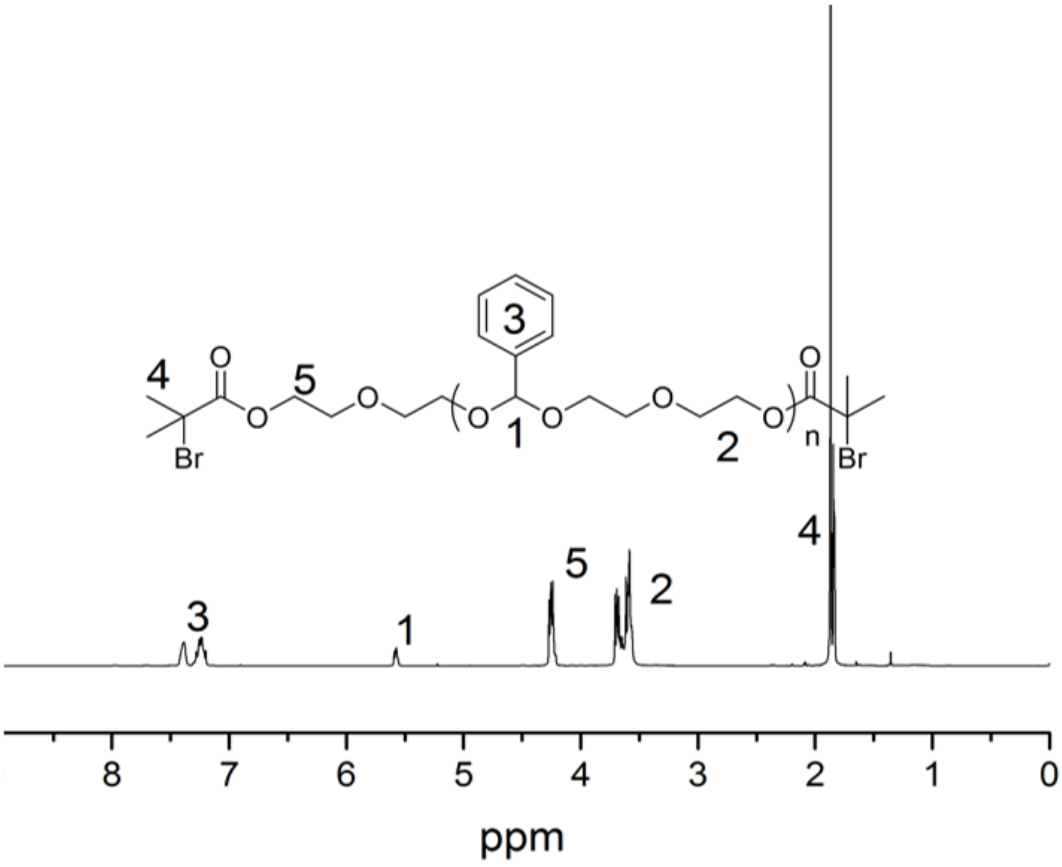

Figure 5.10: ^{1}H NMR of α, ω-acetal SET-LRP initiator.

5.2.2 Polymerisation

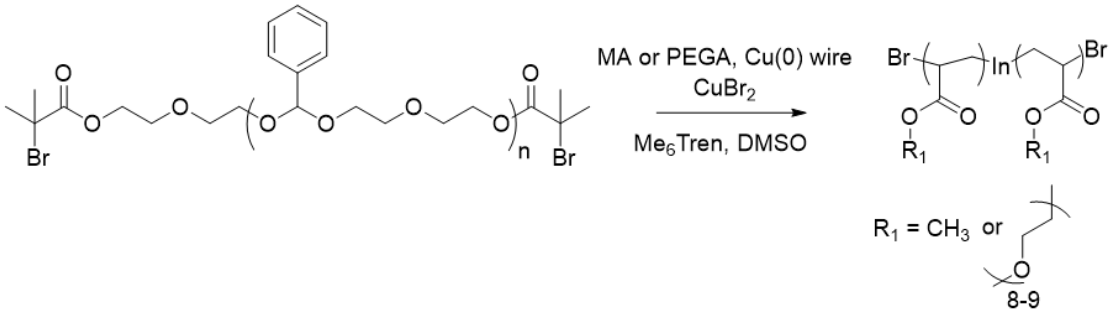

Figure 5.11: Schematic diagram of the polymerisation of methyl acrylate (MA) and poly(ethylene glycol) acrylate (PEGA) from α, ω-acetal SET-LRP initiator.

Methyl acrylate (MA) was polymerised by Cu(0)-mediated polymerisation in dimethyl sulfoxide (DMSO). 80 eq. of MA to the initiator was applied, and monomer conversion was followed by ^{1}H NMR. The decrease of the vinyl peaks of methyl acrylate monomer (5.70, 5.95 and 6.25 ppm) compared to the proton corresponding to a methyl group (C*H*$_3$) at 3.45 ppm is exploited to calculate the rate of monomer consumption (Figure 5.12). Interestingly, a considerably slowed polymerisation rate at the induction period is detected; about 30 % of the monomer is polymerised after one hour. This observation is affirmed by the SEC trace, in which a noticeably low molecular weight was observed after one hour. Also, a significantly broad molecular weight distribution (*Đ* > 2.0) of the polymer was also found after 15 and 30 minutes (Figure 5.13). The assumption of this observation could be because of the dissociation of acetal initiator; it was mentioned in the previous section that acetal formation is a reversible process, thus this reaction could influence the increase of polymer polydispersity. However, a significantly higher molecular weight with a narrowed molecular weight distribution was detected after three hours; monomer conversions of approximately 80 % and 90 % were obtained after two and three hours, respectively. In this chapter, three polymers, namely PMA$_{40}$, PMA$_{80}$, and PEGA$_{20}$, were successful synthesised. The ^{1}H NMR reveals the absence of vinyl peaks from the monomer. Additionally, the narrowed molecular weight of all polymers was detected by SEC as shown in Figure 5.14. Furthermore, no significant shoulder is observed in the SEC trace, thus, this result confirms that this acetal initiator can synthesise well-defined polymers.

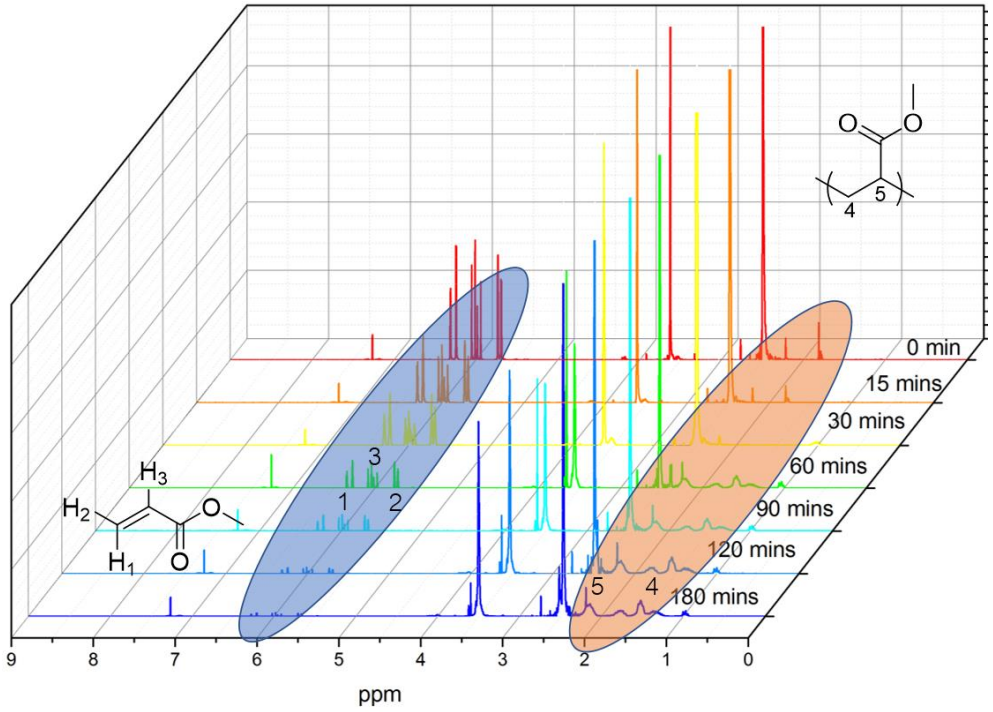

Figure 5.12: ^{1}H NMR of polymerisation at different times of PMA_{80} at ambient temperature, ($CDCl_3$, 250 MHz). The polymer formation was followed by the decrease of vinyl peaks of methyl acrylate monomer at 5.70, 5.95 and 6.25 ppm (blue) compared to the proton corresponding to a CH_2 group at 1.10-2.40 ppm (orange).

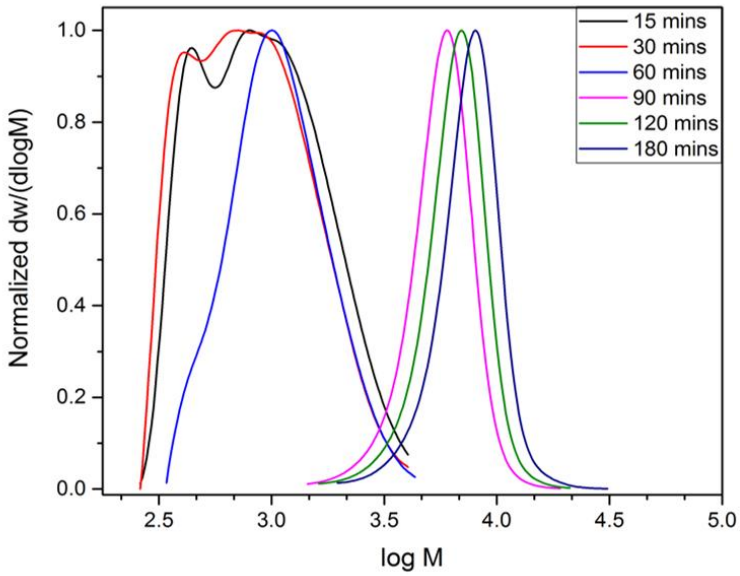

Figure 5.13: SEC trace of the polymerisation at different times of PMA_{80} at ambient temperature.

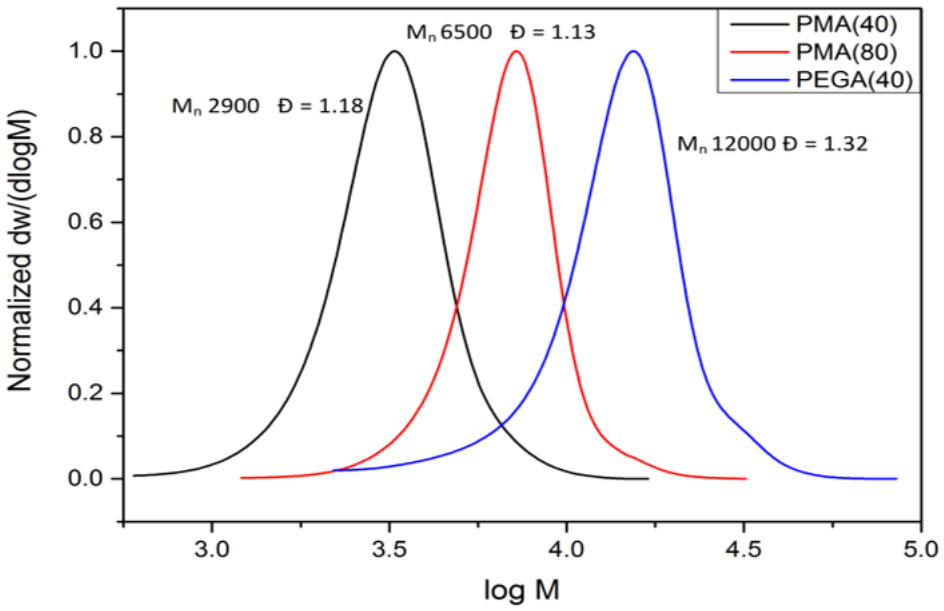

Figure 5.14: SEC trace of PMA_{40}, PMA_{80}, and $PEGA_{40}$ α, ω-acetal synthesis from SET-LRP initiator.

The polymer purification process was carried out through the precipitation of ($PMA_{40, 80}$) and dialysis method ($PEGA_{40}$), MWCO 1K dialysis tubing against water for 48 hours, followed by a freeze-drying process. Notably, ^{1}H spectra of purified pMA_{80} show correlated peaks with polymer structure (Figure 5.15). More importantly, the acetal signal at 5.65 ppm is still detected. This indicates the stability of acetal in the polymer. Purified $PEGA_{40}$ was also characterised by ^{1}H NMR. The acetal signal is also noticed, although it was placed in water for over two days (Figure 5.16). The strong singlet peak at 3.40 ppm also confirms the methyl group of PEGA in the polymer backbone, thus, Cu(0)-mediated controlled radical polymerisation of MA and PEGA by our SET-LRP initiator was successful.

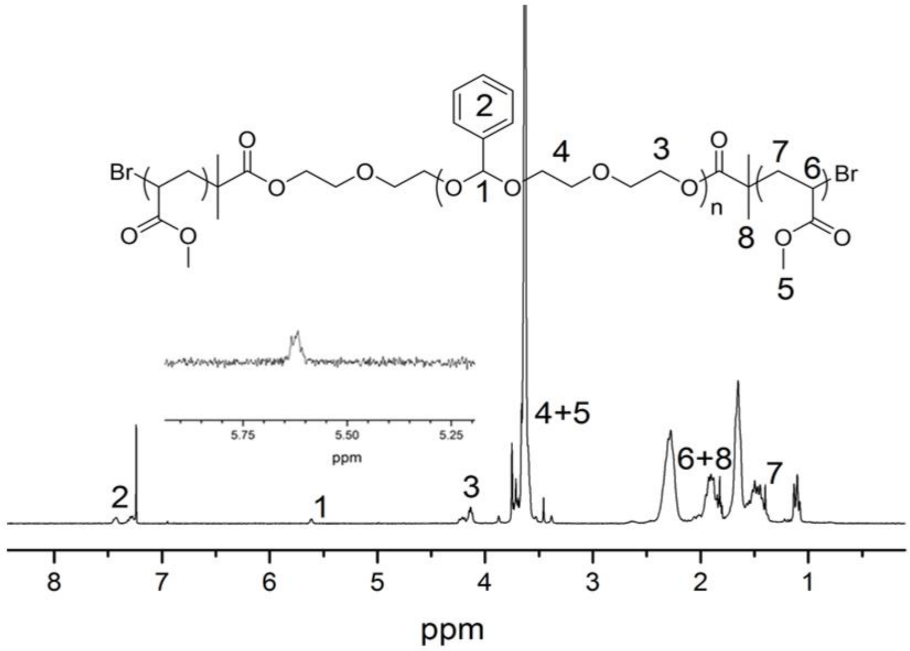

Figure 5.15: ^{1}H NMR of PMA_{80} after precipitation in methanol ($CDCl_3$, 300 MHz).

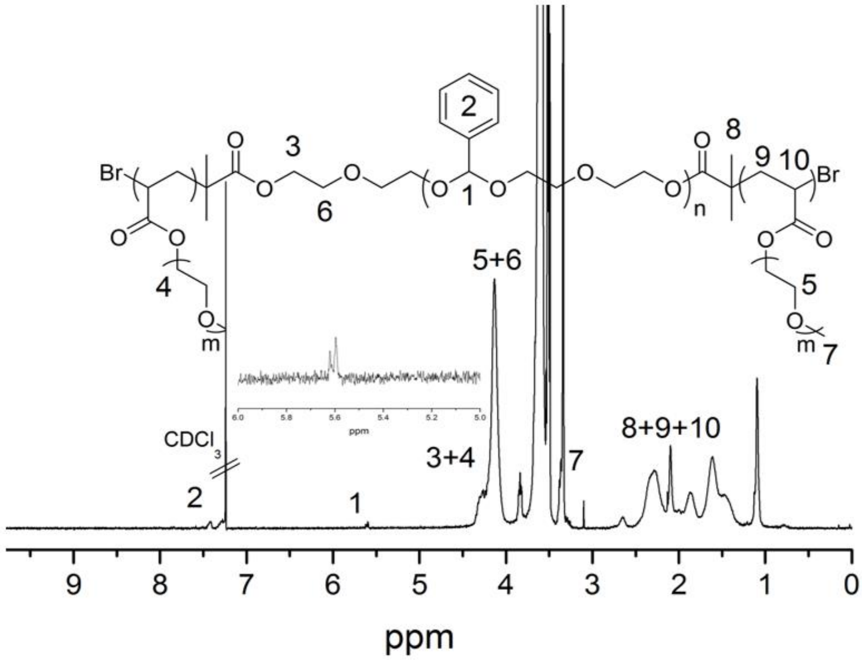

Figure 5.16: ^{1}H NMR of $PEGA_{40}$ after dialysis against water ($CDCl_3$, 300 MHz).

5.2.3 Degradation of PMA_{80}

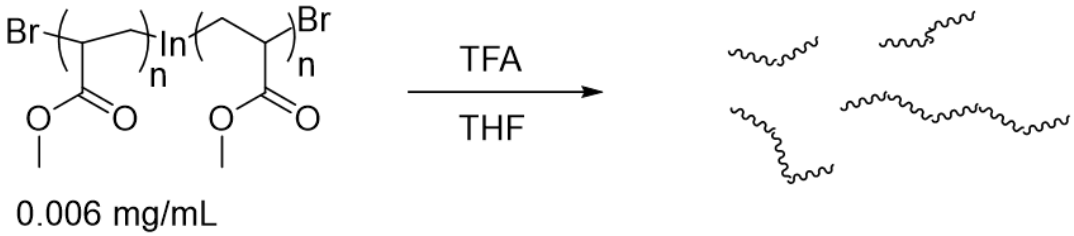

Figure 5.17: Schematic diagram of PMA_{80} degradation study in THF.

A purified polymer was dissolved in the THF GPC eluent to prepare a stock polymer solution. Subsequently, concentrated trifluoroacetic acid (TFA) was added to the solution. The influence of acid concentrations on the rate of degradation was first studied. Different TFA concentrations (43, 86 and 129 µL/mL) were added to the polymer solution (0.006 mg/mL). The degradation of the acetal in the polymer was followed by SEC after an hour. The result showed that the rate of degradation is proportional to the concentration of acid (Figure 5.18 left). Further, the degradation of PMA_{80} at a certain TFA concentration (43 µL/mL) at different time intervals, from 0 to 285 minutes, was investigated. The decrease of the polymer molecular weight indicates a breakdown of acetal after treating with acid. (Figure 5.18, right) Notably, SEC observed half of the polymer molecular weight (about 3.4 K $gmol^{-1}$) following the degradation of the polymer. Thus, this result supports the ^{1}H NMR spectra of the α, ω-acetal initiator in the previous section. Moreover, the SEC solvent was removed, and the dried sample was further characterised by ^{1}H NMR. No acetal signal was detected at 5.65 ppm. Furthermore, the signal of Ph-*H*C=O of benzaldehyde at 10.75 ppm was instead

monitored (Figure 5.19). The proposed mechanism of hydrolysis of acetal by acid is shown in Figure 5.20.

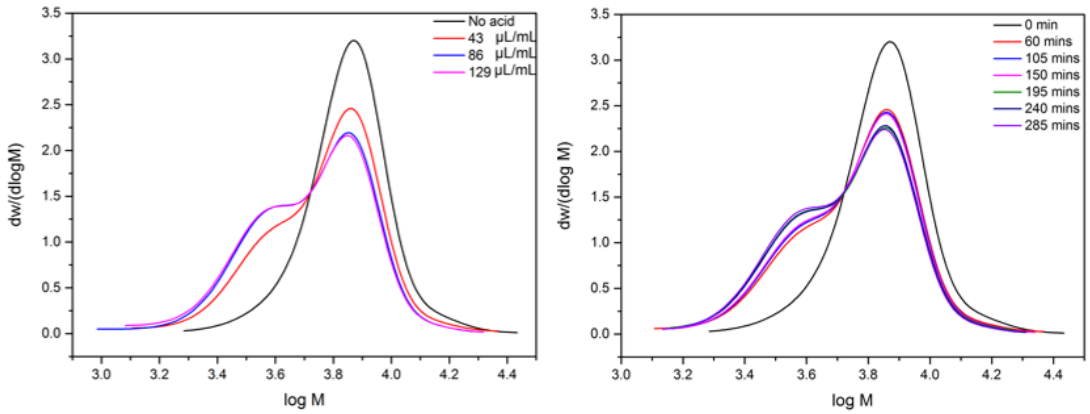

Figure 5.18: SEC traces (THF) of PMA_{80} after treating with an acid (TFA) at different concentration for an hour (left) and the degradation at different interval time (43 µL/mL).

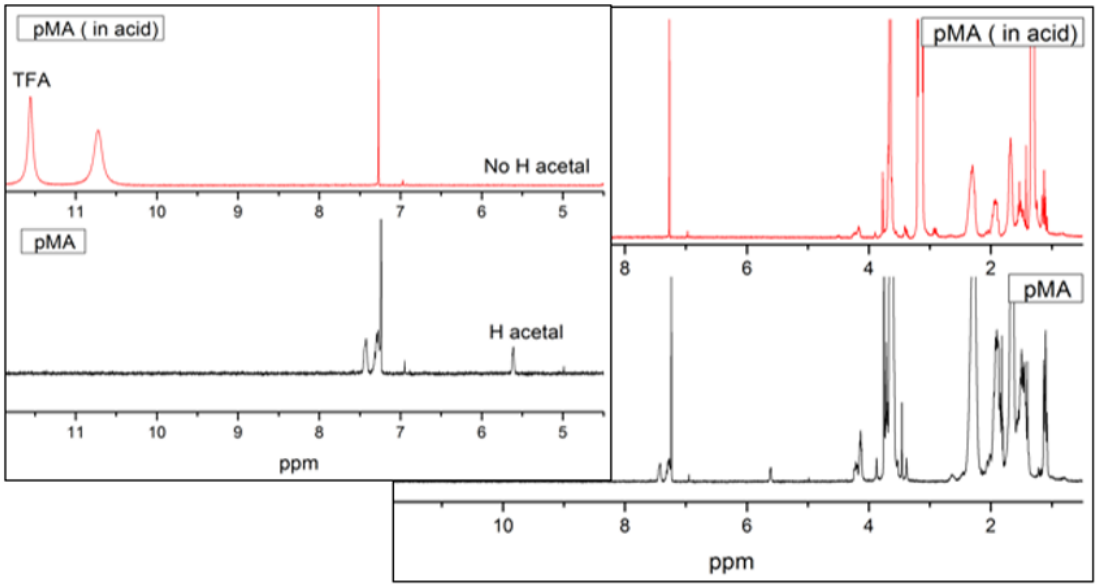

Figure 5.19: ^{1}H NMR spectra of PMA_{80} after treating with an acid (TFA) ($CDCl_3$, 300 MHz).

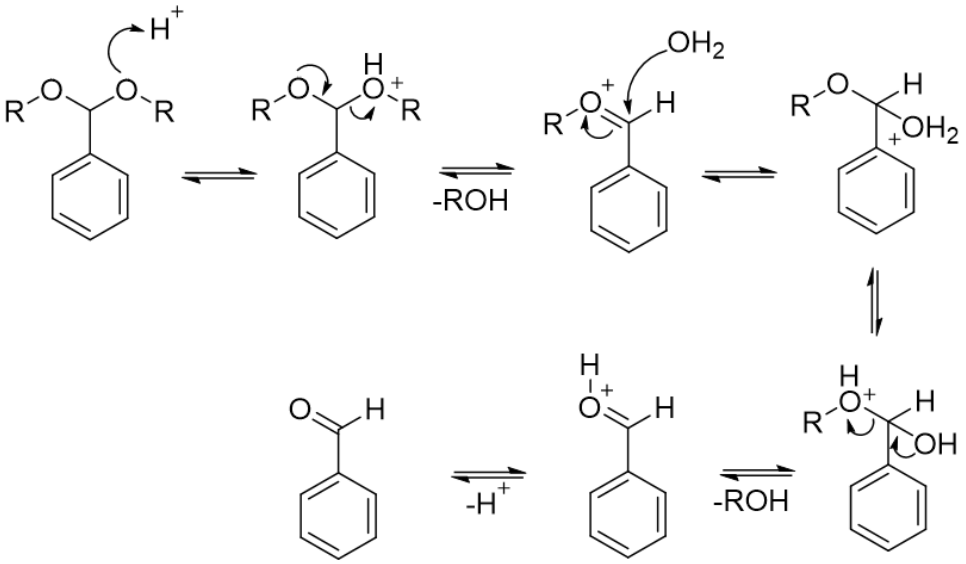

Figure 5.20: The proposed mechanism of acetal hydrolysis under acidic condition.

5.3 Conclusion

α, ω-Hydroxyl terminated poly(acetal)s were polymerised via the condensation reaction of diethylene glycol and benzaldehyde. Unfortunately, only 1-2 acetal bonds were formed. However, small α, ω-hydroxyl terminated acetal was successfully converted to SET-LRP initiator via esterification. Different characterisation techniques, including ^{1}H and ^{13}C NMR, FTIR and SEC were applied. Acetal formation was confirmed by the observation of the acetal peak at 5.65 ppm. Furthermore, 101.23 ppm was detected by ^{13}C NMR. The disappearance of OH absorption at about 3500 cm^{-1} was detected by FTIR. In addition, the ^{1}H and ^{13}C NMR signal of methyl groups adjacent to the bromine after modification were identified at 1.96 and 30.13 ppm. The initiator was exploited to polymerise methyl acrylate (MA) and poly (ethylene glycol) acrylate (PEGA) (average M_n = 480 g mol^{-1}). A reasonably high monomer conversion (>90%) and narrowed molecular weight distribution (*Đ*) (1.1-1.3) of polymers were obtained. After purification, polymer degradation under acidic conditions was investigated. The decrease of molecular weights and the formation of benzaldehyde were monitored by SEC and ^{1}H NMR, respectively. To sum up, this chapter offers a feasible technique to synthesise the acidic-labile polymers via controlled radical polymerisation, which is promising as trigger conditions for an agrochemical release at the rhizosphere. Also, polymerisation conditions of P($BnMA_m$-*co*-IEM_n) copolymers and fabrication of microcapsules via the spray drying technique were investigated and presented in chapter 2 and 3, respectively. Therefore, this chemistry could be potentially employed to synthesise acidic-responsive pesticide carriers.

5.4 Experimental

5.4.1 Materials

Acetone, dimethyl sulfoxide (DMSO), methyl acrylate (MA), poly (ethylene glycol) acrylate (PEGA) (average Mn = 480 g mol^{-1}), deuterated chloroform ($CDCl_3$), copper(II) bromide, 35 % aqueous hydrochloric acid, α-bromoisobutyl bromide, triethylamine (TEA), benzaldehyde, diethylene glycol, hexane, dichloromethane (DCM), toluene, sodium hydrogen carbonate ($NaHCO_3$), tetrahydrofuran (THF), sodium chloride (NaCl), *p*-toluenesulfonic acid monohydrate were purchased from Sigma-Aldrich UK.

5.4.2 Characterisation

Size exclusion chromatography measurements were performed on an Agilent 390 MDS Multi-Detector GPC system ($CHCl_3$ + 2 % TEA Mixed C Column Set, THF + 2 % TEA and 0.01 wt. % BHT with PLgel Mixed C columns set, 30 °C flow rate 1 mL/min, narrow standards of PMMA were used as calibration polymers between 955000 and 1010 g mol^{-1} and fitted with a third order polynomial) by DRI detection. ^{1}H NMR (standard) and ^{13}C NMR (long acquisition long delay) were recorded on a Bruker Avance III HD 300 MHz and Bruker Avance III HD 250 MHz with $CDCl_3$ as the solvent. FTIR spectra were recorded on a Bruker Vector 22 FTIR spectrometer and analysed with OPUS software.

5.4.3 Poly(acetal) synthesis

Diethylene glycol (5 g, 0.047 mole, 1 eq.) was added to a 250 mL round bottom flask containing *p*-toluenesulfonic acid monohydrate (89 mg, 4.67 x 10^{-4} mole, 0.01 eq.)

followed by benzaldehyde (5 g, 0.047 mole, 1 eq.) 150 mL of toluene and a magnetic stirrer bar were added. The reaction mixture was heated under reflux at 110 °C for 24 hours. Saturated $NaHCO_3$ aqueous solution (5 mL) was added to neutralize the reaction. The solvent was removed by rotary evaporator. The reaction was allowed to cool to ambient temperature. 3 X 50 mL of hexane was added to the crude product then the reaction mixture was centrifuged at 7000 rpm for 25 minutes. The polymer product (65% yield) was characterised by NMR, IR, and SEC. ^{1}H NMR (300 MHz, $CHCl_3$, δ): 3.55 (m, 12H, CH_2O), 4.20 (m, 4H, CH_2OH), 5.65 (s, H, OCHO), 7.50 (m, 5H, CH aromatic), ^{13}C NMR (75.47 MHz, $CHCl_3$, δ): 61.22, 64.05, 70.05, 72.45 (s, CH_2,), 101.23 (s, OCO), 126.48, 128.33 (s, C aromatic, CH_2), 137.83 (s, C aromatic, CH); IR: *v* = 3500 (OH), 2950 (C-H), 1500 (C-C aromatic) 1200 (C-O), $SEC_{(CHCl3)}$: M_n = 400 g mol^{-1}, *Đ* = 1.91.

5.4.4 α, ω-poly(acetal) SET-LRP initiator synthesis

α, ω-Hydroxyl terminated acetal (4.9 g, 0.0125 mol, 1 eq) was added into a 500 mL 3-necked round bottom flask containing a magnetic stirrer bar followed by cannulating anhydrous tetrahydrofuran (200 mL). Triethylamine (8.7 mL, 0.0625 mol, 5 eq) was added to the reaction mixture. The reaction was degassed with N_2 for 20 minutes after that α-bromoisobutyryl bromide (BiBB) (3.4 mL, 0.027 mol, 2.2 eq) was added dropwise to the reaction in an ice bath. Once BiBB was completely added, the ice bath was removed and the reaction was carried out at ambient temperature overnight. The volatiles were removed by rotary evaporator. DCM (50 mL) was added to the crude product to dissolve crude initiator. $NaHCO_2$ aqueous solution (2 x 150 mL) was used to wash the crude product, then the solvent was removed again by rotary evaporator. The

initiator (61 % yield) was characterised by IR, NMR, and SEC. ^{1}H NMR (300 MHz, $CHCl_3$, δ): 1.90, 1.96 (m, 12H, 2xCH_3), 3.5 (m, 12H, CH_2O), 4.30 (m, 4H, $COOCH_2$), 5.65 (s, 1H, OCHO), 7.50 (m, 5H, C aromatic) ppm. ^{13}C NMR (75.47 MHz, $CHCl_3$, δ): 30.13 (s, CH_3), 63.75, 64.50, 68.23, 69.85 (s, CH_2O), 100.80 (s, OCHO), 126.15-127.76 (m, C aromatic, CH_2), 136.83 (m, C aromatic, CH), 164.71 (s, C=O) ppm. IR: *v* = 2950 (C-H), 1500 (C-C aromatic) 1200 (C-O); SEC $_{(CHCl3)}$: Mn = 420 g mol^{-1}, *Đ* = 1.74

5.4.5 Polymerisation of poly(methyl acrylate) (PMA_{40})

5 cm of copper wire was entwined with a magnetic stirrer bar, then it was put into 3 mL of 35 % HCl solution and stirred for 5 minutes. Copper wire was washed with deionized water followed by acetone. Once dried, it was put into a Schlenk tube which contained 6.4 mg (2.9 x 10^{-5} mol, 0.10 eq.) of $CuBr_2$ and sealed with a rubber septum. Dimethyl sulfoxide (DMSO) (2.4 mL), acetal initiator (0.2 g, 2.90 x 10^{-4} mol, 1 eq.) and methyl acrylate (1.04 mL, 0.012 mol, 40 eq.). The reaction mixture was bubbled with N_2 for 15 minutes, then Me_6Tren (18.6 µL, 6.96 x 10−5 mol, 0.12 eq.) was added. The reaction was left overnight, the polymerization mixture crude product was characterized by ^{1}H NMR and SEC followed by precipitation in ice cool methanol then filtered and dried. Purified polymer (80 % yield) was characterised by NMR, IR, and SEC. ^{1}H NMR (300 MHz, $CHCl_3$, %): 1.1-1.70 (m, 80H, CH_2), 1.95-2.40 (m, 52H, CH and CH_3), 3.60-3.75 (m, 132H, CH_2O and OCH_3), 4.30 (m, 4H, $COOCH_2$), 5.65 (s, 1H, OCHO), 7.50 (m, 5H, C aromatic). IR: *v* = 2950 (C-H), 1720 (C=O), 1200 (C-O); SEC$_{(THF)}$: M_n = 2900 g mol^{-1}, *Đ* = 1.18

Poly(ethylene glycol acrylate) ($PEGA_{40}$)

The polymerization solution ($PEGA_{40}$) was purified by dialysis using MWCO 1K dialysis tubing against water for 48 hours followed by freeze-drying. Following purification, the polymer was characterised by NMR, IR, and SEC. ^{1}H NMR (300 MHz, $CHCl_3$, δ): 1.20-1.65 (m, 80H, CH_2), 1.90-2.45 (m, 52H, CH and CH_3), 3.40 (s, 120H, CH_3O), 3.55-3.80 (m, 720H, CH_3O), 4.05-4.35 (m, 84H, $CH_2OC{=}O$), 5.65 (s, 1H, OCHO), 7.50 (m, 5H, C aromatic); IR: *v* = 2950 (C-H), 1725 (C=O), 1200 (C-O); $SEC_{(THF)}$: M_n 12000 g mol^{-1}, *Đ* = 1.32

5.4.6 Degradation study

0.18 mg of purified PMA_{80} was dissolved in THF GPC eluent (26 mL). The polymer solution was separated into a small vial (1.4 mL). Trifluoroacetic acid (TFA) (60 µL) was added to the polymer solution, where the degredation was followed by SEC. The solvent was removed after GPC analysis and NMR was used to characterise the polymer after treating with TFA.

References

[1] M. Rinaudo, *Progress in Polymer Science (Oxford)*, 2006, **31**, 603–632.

[2] H. Otsuka, Y. Nagasaki and K. Kataoka, *Advanced Drug Delivery Reviews*, 2012, **64**, 246–255.

[3] S. Coyle, Y. Wu, K.-T. Lau, D. De Rossi, G. Wallace and D. Diamond, *MRS Bulletin*, 2007, **32**, 434–442.

[4] O. Breuer and U. Sundararaj, *Polymer Composites*, 2004, **25**, 630–645.

[5] T. M. Taylor, P. M. Davidson, B. D. Bruce and J. Weiss, *Critical reviews in food science and nutrition,* 2005, **45**, 587–605.

[6] S. Stankovich, D. A. Dikin, G. H. B. Dommett, K. M. Kohlhaas, E. J. Zimney, E. A. Stach, R. D. Piner, S. T. Nguyen, *Nature*, 2006, **442**, 282–286.

[7] S. Yang, M. Kertesz, *Journal of Physical Chemistry A*, 2007, **111**, 2434–2441.

[8] J. Dupont, G. S. Fonseca, A. P. Umpierre, P. F. P. Fichtner and S. R. Teixeira, *Journal of the American Chemical Society*, 2002, **124**, 4228–4229.

[9] A. Vigalok, *Chemistry-A European Journal*, 2008, **14**, 5102–5108.

[10] H. Matsumoto, T. Nakano and Y. Nagai, *Tetrahedron Letters*, 1973, **14**, 5147–5150.

[11] M. Kamigaito, T. Ando and M. Sawamoto, *Chemical Record*, 2004, **4**, 159–175.

[12] M. Kato, M. Kamigaito, M. Sawamoto and T. Higashimuras, *Macromolecules*, 1996, **28**, 1721–1723.

[13] K. Matyjaszewski, S. Coca, S. G. Gaynor, M. Wei and B. E. Woodworth, *Macromolecules*, 1997, **30**, 7348–7350.

[14] K. Matyjaszewski, *Chemistry A European Journal*, 1999, **5**, 3095–3102.

[15] D. M. Haddleton, D. R. Maloney and K. G. Suddaby, *Macromolecules*, 1996, **29**, 481-483.

[16] J. S. Wang and K. Matyjaszewski, *Journal of the American Chemical Society*, 1995, **117**, 5614–5615.

[17] J.-S.Wang and K. Matyjaszewski, *Macromolecules*, 1995, **28**, 7901–7910.

[18] F. di Lena and K. Matyjaszewski, *Progress in Polymer Science*, 2010, **35**, 959–1021.

[19] D. M. Haddleton, M. C. Crossman, B. H. Dana, D. J. Duncalf, A. M. Heming, D. Kukulj and A. J. Shooter, *Macromolecules*, 1999, **32**, 2110–2119.

[20] M. Ouchi, T. Terashima and M. Sawamoto, *Chemical Reviews*, 2009, **109**, 4963–5050

[21] K. Matyjaszewski, *Macromolecules*, 2012, **45**, 4015–4039.

[22] W. A. Braunecker and K. Matyjaszewski, *Progress in Polymer Science*, 2007, **32**, 93-146.

[23] M. Kamigaito, T. Ando and M. Sawamoto, *Chem. Rev.,* 2001, **101**, 3689-3745

[24] D. M. Haddleton, C. B. Jasieczek, M. J. Hannon and A. J. Shooter, *Macromolecules*, 1997, **30**, 2190–2193.

[25] A. Anastasaki, V. Nikolaou, G. Nurumbetov, P. Wilson, K. Kempe, J. F. Quinn, T. P. Davis, M. R. Whittaker and D. M. Haddleton, *Chemical Reviews*, 2016, **116**, 835–877.

[26] B. D. Hornby, A. G. West, J. C. Tom, C. Waterson, S. Harrisson and S. Perrier, *Macromolecular Rapid Communications*, 2010, **31**, 1276–1280.

[27] Q. Zhang, P. Wilson, Z. Li, R. McHale, J. Godfrey, A. Anastasaki, C. Waldron and D. M. Haddleton, *Journal of the American Chemical Society*, 2013, **135**, 7355–7363.

[28] S. R. Samanta, A. Anastasaki, C. Waldron, D. M. Haddleton and V. Percec, *Polymer Chemistry*, 2013, **4**, 5555–5562.

[29] T. G. McKenzie, E. H. H. Wong, Q. Fu, S. J. Lam, D. E. Dunstan and G. G. Qiao, *Macromolecules*, 2014, **47**, 7869–7877.

[30] Q. Zhang, P. Wilson, Z. Li, R. McHale, J. Godfrey, A. Anastasaki, C. Waldron and D. M. Haddleton, *Journal of the American Chemical Society*, 2013, **135**, 7355–7363.

[31] J. J. Li, Y. N. Zhou and Z. H. Luo, *Polymer*, 2014, **55**, 6552–6560.

[32] M. E. Levere, I. Willoughby, S. O'Donohue, A. de Cuendias, A. J. Grice, C. Fidge, C. Remzi Becer and D. M. Haddleton, *Polymer Chemistry*, 2010, **1**, 1086–1094.

[33] N. Nguyen, B. Rosen, G. Lligadas and V. Percec, *Macromolecules*, 2009, **42**, 2379–2386.

[34] N. H. Nguyen and V. Percec, *Journal of Polymer Science Part A: Polymer Chemistry*, 2010, **48**, 5109–5119.

[35] V. Percec, A. V. Popov, E. Ramirez-Castillo, M. Monteiro, B. Barboiu, O.Weichold, A. D. Asandei and C. M. Mitchell, *Journal of the American Chemical Society*, 2002, **124**, 4940-4941

[36] V. Percec, A. V. Popov, E. Ramirez-Castillo and O. Weichold, *Journal of Polymer Science Part A: Polymer Chemistry*, 2003, **41**, 3283–3299.

[37] B. Barboiu and V. Percec, *Macromolecules*, 2001, **34**, 8626–8636.

[38] N. H. Nguyen and V. Percec, *Journal of Polymer Science Part A: Polymer Chemistry*, 2011, **49**, 4241–4252.

[39] N. H. Nguyen, X. Leng, H. J. Sun and V. Percec, *Journal of Polymer Science, Part A: Polymer Chemistry*, 2013, **51**, 3110–3122.

[40] G. Lligadas, J. S. Ladislaw, T. Guliashvili and V. Percec, *Journal of Polymer Science Part A: Polymer Chemistry*, 2008, **46**, 278–288.

[41] W. Ren, L. Jiang, W. Wang and Y. Dan, *Journal of Polymer Science Part A: Polymer Chemistry*, 2010, **48**, 2793–2797.

[42] A. Ding, G. Lu, H. Guo, X. Zheng and X. Huang, *Journal of Polymer Science, Part A: Polymer Chemistry*, 2013, **51**, 1091–1098.

[43] D. Liu, H. Chen, P. Yin, N. Ji, G. Zong and R. Qu, *Journal of Polymer Science, Part A: Polymer Chemistry*, 2011, **49**, 2916–2923.

[44] R. Jing, G. Wang, Y. Zhang and J. Huang, *Macromolecules*, 2011, **44**, 805–810.

[45] F. Alsubaie, A. Anastasaki, P. Wilson and D. M. Haddleton, *Polymer Chemistry*, 2015, **6**, 406–417.

[46] A. Anastasaki, A. J. Haddleton, Q. Zhang, A. Simula, M. Droesbeke, P. Wilson and D. M. Haddleton, *Macromolecular Rapid Communications*, 2014, **35**, 965–970.

[47] V. Nikolaou, A. Simula, M. Droesbeke, N. Risangud, A. Anastasaki, K. Kempe, P. Wilson and D. Haddleton, *Polymer Chemistry*, 2016, **7**, 2452–2456.

[48] E. Nicol, T. Derouineau, F. Puaud and A. Zaitsev, *Journal of Polymer Science Part A: Polymer Chemistry*, 2012, **50**, 3885–3894.

[49] N. Risangud, T. R. Congdon, D. J. Keddie, P. Wilson, K. Kempe and D. M. Haddleton, *Journal of Polymer Science Part A: Polymer Chemistry*, 2016, **54**, 2698-2705

[50] W. Gu, Z. Jia, N. P. Truong, I. Prasadam, Y. Xiao and M. J. Monteiro, *Biomacromolecules*, 2013, **14**, 3386–3389.

[51] A. Anastasaki, C.Waldron, V. Nikolaou, P. Wilson, R.McHale, T. Smith and D. M. Haddleton, *Polymer Chemistry*, 2013, **4**, 4113–4119.

[52] N. H. Nguyen and V. Percec, *Journal of Polymer Science, Part A: Polymer Chemistry*, 2011, **49**, 4756–4765.

[53] G. Lligadas and V. Percec, *Journal of Polymer Science Part A: Polymer Chemistry*, 2008, **46**, 2745–2754.

[54] N. H. Nguyen, M. E. Levere, J. Kulis, M. J. Monteiro and V. Percec, *Macromolecules*, 2012, **45**, 4606–4622.

[55] N. H. Nguyen and V. Percec, *Journal of Polymer Science Part A: Polymer Chemistry*, 2011, **49**, 4227–4240.

[56] C. Boyer, A. Atme, C. Waldron, A. Anastasaki, P. Wilson, P. B. Zetterlund, D. M. Haddleton and M. R. Whittaker, *Polymer Chemistry*, 2013, **4**, 106–112.

[57] A. Anastasaki, C. Waldron, P. Wilson, R. McHale and D. M. Haddleton, *Polymer Chemistry*, 2013, **4**, 2672–2675.

[58] B. M. Rosen, X. Jiang, C. J. Wilson, N. H. Nguyen, M. J. Monteiro and V. Percec, *Journal of Polymer Science Part A: Polymer Chemistry*, 2009, **47**, 5606–5628.

[59] G. Lligadas and V. Percec, *Journal of Polymer Science Part A: Polymer Chemistry*, 2008, **46**, 4917–4926.

[60] T. Hatano, B. M. Rosen and V. Percec, *Journal of Polymer Science, Part A: Polymer Chemistry*, 2010, **48**, 164–172.

[61] L. Voorhaar, S. Wallyn, F. E. Du Prez and R. Hoogenboom, *Polymer Chemistry*, 2014, **5**, 4268–4276.

[62] A. Munoz-Bonilla, O. Leon, V. Bordege, M. Sanchez-Chaves and M. Fern´andez-Garc´ıa, *Journal of Polymer Science, Part A: Polymer Chemistry*, 2013, **51**, 1337–1347.

[63] W. Wang, Z. Zhang, J. Zhu, N. Zhou and X. Zhu, *Journal of Polymer Science Part A: Polymer Chemistry*, 2009, **47**, 6316–6327.

[64] J. Tom, B. Hornby, A. West, S. Harrisson and S. Perrier, *Polymer Chemistry*, 2010, **1**, 420–422.

[65] E. R. D. H. Solomon and P. Cacioli, *US4581429*, 1986.

[66] M. K. Georges, R. P. N. Veregin, P. M. Kazmaier and G. K. Hamer, *Macromolecules*, 1993, **26**, 2987–2988.

[67] C. J. Hawker, A. W. Bosman and E. Harth, *Chemical Reviews*, 2001, **101**, 3661–3688.

[68] J. Chiefari, Y. K. B. Chong, F. Ercole, and C. South, *Macromolecules*, 1998, **31**, 5559–5562.

[69] G. Moad, E. Rizzardo and S. H. Thang, *Australian Journal of Chemistry*, 2005, **58**, 379–410.

[70] G. Moad, E. Rizzardo and S. H. Thang, *Polymer*, 2008, **49**, 1079–1131.

[71] T. He, D. Li, X. Sheng and B. Zhao, *Macromolecules*, 2004, **37**, 3128–3135.

[72] C. Boyer, A. H. Soeriyadi, P. B. Zetterlund and M. R. Whittaker, *Macromolecules*, 2011, **44**, 8028–8033.

[73] N. Akeroyd and B. Klumperman, *European Polymer Journal*, 2011, **47**, 1207–1231.

[74] A. Anastasaki, V. Nikolaou, N. W. McCaul, A. Simula, J. Godfrey, C. Waldron, P. Wilson, K. Kempe and D. M. Haddleton, *Macromolecules*, 2015, **48**, 1404–1411.

[75] K. Ohno, Y. Tsujii, T. Miyamoto and T. Fukuda, *Macromolecules*, 1998, **31**, 1064–1069.

[76] D. Cohn and A. Hotovely Salomon, *Biomaterials*, 2005, **26**, 2297–2305.

[77] Y. Li, B. S. Lokitz and C. L. McCormick, *Macromolecules*, 2006, **39**, 81–89.

[78] M. Garcia, M. P. Beecham, K. Kempe, D. M. Haddleton, A. Khan and A. Marsh, *European Polymer Journal*, 2015, **66**, 444–451.

[79] L. Yuan, W. Chen, J. Li, J. Hu, J. Yan and D. Yang, J*ournal of Polymer Science, Part A: Polymer Chemistry*, 2012, **50**, 4579–4588.

[80] L. Y. Li, W. D. He, W. T. Li, K. R. Zhang, T. T. Pan, Z. L. Ding and B. Y. Zhang, *Journal of Polymer Science, Part A: Polymer Chemistry*, 2010, **48**, 5018–5029.

[81] A. Gogos, K. Knauer and T. D. Bucheli, *Journal of agricultural and food chemistry*, 2012, **60**, 9781–9792.

[82] M. Kah and T. Hofmann, *Environment International*, 2014, **63**, 224–235.

[83] M. Kah, S. Beulke, K. Tiede and T. Hofmann, *Critical Reviews in Environmental Science and Technology*, 2013, **43**, 1823–1867.

[84] W. J. Orts, R. E. Sojka and G. M. Glenn, *Industrial Crops and Products*, 2000, **11**, 19–29.

[85] M. Rai and A. Ingle, *Applied Microbiology and Biotechnology*, 2012, **94**, 287–293.

[86] D. Davidson and F. X. Gu, *Journal of Agricultural and Food Chemistry*, 2012, **60**, 870–876.

[87] Y. Yang, Z. Tong, Y. Geng, Y. Li and M. Zhang, *Journal of Agricultural and Food Chemistry*, 2013, **61**, 8166–8174.

[88] A. Roy, S. Singh, J. Bajpai and A. Bajpai, *Central European Journal of Chemistry*, 2014, **12**, 453–469.

[89] B. Symonds, N. R. Thomson, C. I. Lindsay and V. V. Khutoryanskiy, *ACS Applied Materials & Interfaces*, 2016, ***8*** **(22)**, 14220–14230.

[90] M. J. L. Castro, C. Ojeda and A. F. Cirelli, *Environmental Chemistry Letters*, 2014, **12**, 85–95.

[91] M. Nuruzzaman, M. M. Rahman, Y. Liu and R. Naidu, *Journal of Agricultural and Food Chemistry*, 2016, **64**, 1447–1483.

[92] N. Sarlak, A. Taherifar and F. Salehi, *Journal of Agricultural and Food Chemistry*, 2014, **62**, 4833–4838.

[93] F. A. Aouada, M. R. De Moura, W. J. Orts and L. H. C. Mattoso, *Journal of Materials Science*, 2010, **45**, 4977–4985.

[94] L. O. Ekebafe, D. E. Ogbeifun and F. E. Okieimen, *Biokemistri*, 2011, **23**, 81–89.

[95] N. Memarizadeh, M. Ghadamyari, M. Adeli and K. Talebi, *Environmental Sciences: Processes and Impacts*, 2014, **16**, 2380–2389.

[96] N. Memarizadeh, M. Ghadamyari, M. Adeli and K. Talebi, *Ecotoxicology and Environmental Safety*, 2014, **107**, 77-83.

[97] F. L. Yang, X. G. Li, F. Zhu and C. L. Lei, J*ournal of Agricultural and Food Chemistry*, 2009, **57**, 10156–10162.

[98] L. Schreiber, M. Riederer and K. Schorn, *Pesticide Science*, 1996, **48**, 117–124.

[99] N. A. Shakil, M. K. Singh, A. Pandey, J. Kumar, V. S. Parmar, M. K. Singh, R. P. Pandey and C. Arthur, *Pure and Applied Chemistry*, 2010, **1325**, 241–247.

[100] Pankaj, N. A. Shakil, J. Kumar, M. K. Singh and K. Singh, *J. Environ Sci Health B*, 2012, **47**, 520–528.

[101] T. Adak, J. Kumar, N. a. Shakil and S. Walia, *Journal of environmental science and health. Part. B, Pesticides, food contaminants, and agricultural wastes*, 2012, **47**, 217–225.

[102] K. M. Loha, N. a. Shakil, J. Kumar, M. K. Singh, T. Adak and S. Jain, *Journal of environmental science and health. Part. B, Pesticides, food contaminants, and agricultural wastes*, 2011, **46**, 201–206.

[103] D. J. Sarkar, J. Kumar, N. a. Shakil and S. Walia, *Journal of environmental science and health. Part A, Toxic/hazardous substances & environmental engineering*, 2012, **47**, 1701–1712.

[104] S. Song, X. Liu, J. Jiang, Y. Qian, N. Zhang and Q. Wu, *Colloids and Surfaces A: Physicochemical and Engineering Aspects*, 2009, **350**, 57–62.

[105] M. Li, Q. Huang and Y. Wu, *Pest Management Science*, 2011, **67**, 831–836.

[106] M. S. Kyriacou, S. C. Hadjiyannakou, M. Vamvakaki and C. S. Patrickios, *macromolecules,* 2004, **37 (19)**, 7181–7187.

[107] M. Gennari, C. Messina, C. Abbate, A. Baglieri and C. Boursier, *Journal of environmental science and health. Part. B, Pesticides, food contaminants, and agricultural wastes*, 2009, **44**, 235–240.

[108] N. a. Suciu and E. Capri, *Journal of environmental science and health. Part. B, Pesticides, food contaminants, and agricultural wastes*, 2009, **44**, 525–532.

[109] T. Adak, J. Kumar and S. Walia, *Journal of environmental science and health. Part. B, Pesticides, food contaminants, and agricultural wastes*, 2012, **47**, 217–225.

[110] V. Ramesh Babu, K. S. V. Krishna Rao, M. Sairam, B. Vijaya Kumar Naidu, K. M. Hosamani and T. M. Aminabhavi, *Journal of Applied Polymer Science*, 2006, **99**, 2671–2678.

[111] G. Liu and Z. An, *Polymer Chemistry*, 2014, **5**, 1559-1565

[112] K. Qian, Y. Ma, J. Wan, S. Geng, H. Li, Q. Fu, X. Peng, X. Kan, G. Zhou, W. Liu, B. Xiong, Y. Zhao, C. Zheng, X. Yang and H. Xu, *Journal of Controlled Release*, 2015, **212**, 41–49.

[113] D. M. Silva, C. Nunes, I. Pereira, A. S. P. Moreira, M. R. M. Domingues, M. A. Coimbra and F. M. Gama, *Carbohydrate Polymers*, 2014, **114**, 458–466.

[114] D. Wang, E. McLaughlin, and Y. S. Lin, *Separation and Purification Technology*, 2012, **99**, 28–35.

[115] B. Barkakaty, K. L. Browning, B. Sumpter, D. Uhrig, I. Karpisova, K. W. Harman, I. Ivanov, D. K. Hensley, J. M. Messman, S. M. Kilbey and B. S. Lokitz, *Macromolecules*, 2016, **49**, 1523–1531.

[116] D. Bhagat, S. K. Samanta and S. Bhattacharya, *Scientific reports*, 2013, **3**, 1294.

[117] M. Ziaee, S. Moharramipour and A. Mohsenifar, *Journal of Applied Entomology*, 2014, **138**, 763–771.

[118] Y. Xia, C. Cheng, R. Wang, C. Nie, J. Deng and C.-S. Zhao, *J. Mater. Chem. B*, 2015, **3**, 9295–9304.

[119] F. O. M. S. Abreu, E. F. Oliveira, H. C. B. Paula and R. C. M. De Paula, *Carbohydrate Polymers*, 2012, **89**, 1277–1282.

[120] H. Guan, D. Chi, J. Yu and X. Li, *Pesticide Biochemistry and Physiology*, 2008, **92**, 83–91.

[121] X. Wang and J. Zhao, *Journal of Agricultural and Food Chemistry*, 2013, **61**, 3789–3796.

[122] H. B. Scher, M. Rodson and K. S. Lee, *Pesticide Science*, 1998, **54**, 394–400.

[123] C. E. Mora-Huertas, H. Fessi and A. Elaissari, *International Journal of Pharmaceutics*, 2010, **385**, 113–142.

[124] H. Fessi, F. Puisieux, J. P. Devissaguet, N. Ammoury and S. Benita, *International Journal of Pharmaceutics,* 1989, **55**, 1–4.

[125] L. Chen, Y. Li, T. Wang, Y. Jiang, K. Li and Y. Yu, *Journal of Environmental Sciences,* 2014, **26**, 2322–2330.

[126] S. Kumar, G. Bhanjana, A. Sharma, M. C. Sidhu and N. Dilbaghi, *Carbohydrate Polymers*, 2014, **101**, 1061–1067.

[127] S. A. Riyajan and J. T. Sakdapipanich, *Polymer Bulletin*, 2009, **63**, 609–622.

[128] W. Zhang, S. He, Y. Liu, Q. Geng, G. Ding, M. Guo, Y. Deng, J. Zhu, J. Li and Y. Cao, *ACS Applied Materials and Interfaces*, 2014, **6**, 11783–11790.

[129] C. Sun, K. Shu, W. Wang, Z. Ye, T. Liu, Y. Gao, H. Zheng, G. He and Y. Yin, *International Journal of Pharmaceutics*, 2014, **463**, 108–114.

[130] A. E. S. Pereira, R. Grillo, N. F. S. Mello, A. H. Rosa and L. F. Fraceto, *Journal of Hazardous Materials*, 2014, **268**, 207–215.

[131] X. Jia, W. B. Sheng, W. Li, Y. B. Tong, Z. Y. Liu and F. Zhou, *ACS Applied Materials and Interfaces*, 2014, **6**, 19552–19558

[132] T. Takei, M. Yoshida, K. Yanagi, Y. Hatate, K. Shiomori and S. Kiyoyama, *Polymer Bulletin*, 2008, **61**, 119–127.

[133] S. V. Prudnikova, A. N. Boyandin, G. S. Kalacheva and A. J. Sinskey, *Journal of Polymers and the Environment*, 2013, **21**, 675–682.

[134] L. C. Greene, P. a. Meyers, J. T. Springer and P. a. Banks, *Journal of Agricultural and Food Chemistry*, 1992, **40**, 2274–2278.

[135] Z. Ao, Z. Yang, J. Wang, G. Zhang and T. Ngai, *Langmuir*, 2009, **25**, 2572–2574.

[136] J. Asrar, Y. Ding, R. E. La Monica and L. C. Ness, *Journal of Agricultural and Food Chemistry*, 2004, **52**, 4814–4820.

[137] W. Sheng, W. Li, B. Li, C. Li, Y. Xu and X. Guo, *Macromol. Rapid Commun*., 2015, **36**, 1640–1645.

[138] Y. J. Fu, S. S. Shyu, F. H. Su and P. C. Yu, *Colloids and Surfaces B: Biointerfaces*, 2002, **25**, 269–279.

[139] D. Sen, A. Khan, J. Bahadur, S. Mazumder and B. K. Sapra, *Journal of Colloid and Interface Science*, 2010, **347**, 25–30.

[140] P. Gong, L. Zhang, X. Han, N. Shigwedha, W. Song and H. Yi, *Drying technology*, 2014, **32**, 793-900

[141] A. M. Goula, K. G. Adamopoulos*, Drying technology*, 2012, **30**, 641-652

[142] M. C. Fontana, T. L. Durli, A. R. Pohlmann, S. S. Guterres and R. C. R. Beck, *Powder Technology*, 2014, **258**, 49–59.

[143] Cecilia Bustos-Garza, Jorge Yáñez-Fernández and Blanca E. Barragán-Huerta, *Food Research International*, 2013, **54**, 641–649

[144] R. F. Ribeiro, M. H. Motta, F. C. Flores, R. C. R. Beck, S. R. Schaffazick and C. De Bona Da Silva, *Materials Science and Engineering C*, 2016, **59**, 875–884.

[145] A. Sosnik and K. P. Seremeta, *Advances in Colloid and Interface Science*, 2015, **223**, 40–54.

[146] C. Freitas and R. H. Muller, *European Journal of Pharmaceutics and Biopharmaceutics*, 1998, **46**, 145–151.

[147] N. R. Rabbani and P. C. Seville, *Journal of controlled released*, 2005, **110**, 130–140.

[148] A. Abbaspourrad, S. S. Datta and D. A. Weitz, *Langmuir*, 2013, **29**, 12697–12702.

[149] X. Li, N. Anton, C. Arpagaus, F. Belleteix and T. F. Vandamme, Jo*urnal of Controlled Release*, 2010, **147**, 304–310.

[150] X. Liu, T. Atarashi, T. Furuta, H. Yoshii, M. Ohkawara and P. Linko, *Drying technology*, 207, **19**, 1361-1374

[151] C. G´omez-Gaete, E. Fattal, L. Silva, M. Besnard and N. Tsapis, *Journal of Controlled Release*, 2008, **128**, 41–49.

[152] L. Ozmen and T. A. G. Langrish, *Drying Technology*, 2003, **21**, 1253–1272.

[153] J. J. Nijdam and T. A. G. Langrish, *Drying technology*, 2005, **23**, 1043-1056

[154] H. Ho and J. Lee, *Macromolecular Research*, 2011, **19**, 815–821.

[155] S. Jafarinejad, K. Gilani, E. Moazeni, M. Ghazi-Khansari, A. R. Najafabadi and N. Mohajel, *Powder Technology*, 2012, **222**, 65–70.

[156] A. L. R. Rattes and W. P. Oliveira, *Powder Technology*, 2007, *171*, 7–14.

[157] N. Schafroth, C. Arpagaus, U. Y. Jadhav, S. Makne and D. Douroumis, *Colloids and Surfaces B: Biointerfaces*, 2012, **90**, 8–15.

[158] F. Ungaro, I. D'Angelo, C. Coletta, R. D'Emmanuele Di Villa Bianca, R. Sorrentino, B. Perfetto, M. A. Tufano, A. Miro, M. I. La Rotonda and F. Quaglia, *Journal of Controlled Release*, 2012, **157**, 149–159.

[159] E. Cevher, Z. Orhan, L. Mulazimolu, D. ensoy, M. Alper, A. Yildiz and Y. Ozsoy, *International Journal of Pharmaceutics*, 2006, **317**, 127–135.

[160] P. K. Binsi, N. Natasha, P. C. Sarkar, P. M. Ashraf, N. George and C. N. Ravishankar, *Food Chemistry*, 2017, **221**, 1698–1708.

[161] M. P. Fuchs, M., C. Turchiuli, M. Bohin, M. Cuvelier, C. Ordonnaud and E. Dumoulin, *Journal of food engineering*, 2006, **75**, 7-35

[162] M. D. R. Hernandez Sanchez, M. E. Cuvelier and C. Turchiuli, *Journal of Food Engineering*, 2015, **167**, 99–105.

[163] H. C. F. Carneiro, R. V. Tonon, C. R. F. Grosso and M. D. Hubinger, *Journal of Food Engineering*, 2013, **115**, 443–451.

[164] S. Ozaki, *Chemical Reviews*, 1972, **72**, 457–496.

[165] D. A. McIlroy, B. J. Blaiszik, M. M. Caruso, S. R. White, J. S. Moore and N. R. Sottos, *Macromolecules*, 2010, **43**, 1855–1859.

[166] G. Gody, C. Rossner, J. Moraes, P. Vana, T. Maschmeyer and S. Perrier, *Journal of the American Chemical Society*, 2012, **134**, 12596–12603.

[167] N. Greving, H. Keul, M. Millaruelo, R. Weberskirch and M. Moeller, *Macromolecular Chemistry and Physics*, 2012, **213**, 1465–1474.

[168] J. Moraes, T. Maschmeyer and S. Perrier, *Journal of Polymer Science Part A: Polymer Chemistry*, 2011, **49**, 2771–2782.

[169] D. Klinger, J. Y. Chang and P. Theato, *Macromolecular Rapid Communications*, 2007, **28**, 718–724.

[170] E. Delebecq, J.-P. Pascault, B. Boutevin and F. Ganachaud, *Chemical Reviews*, 2013, **113**, 80–118.

[171] R. Seto, K. Matsumoto and T. Endo, *Journal of Polymer Science Part A: Polymer Chemistry*, 2015, **53**, 1934–1940.

[172] M. D. Power, C. C. Chappelow, C. S. Pinzino and J. D. Eick, J*ournal of Applied Polymer Science*, 1999, **74**, 1577–1583.

[173] J. B. Beck, K. L. Killops, T. Kang, K. Sivanandan, A. Bayles, M. E. Mackay, K. L. Wooley and C. J. Hawker, *Macromolecules*, 2009, **42**, 5629–5635.

[174] O. Kreft, A. M. Javier, G. B. Sukhorukov and W. J. Parak, *Journal of Materials Chemistry*, 2007, **17**, 4471–4476.

[175] S. P. Friedman and Y. Mualem, *Fertilizer Research*, 1994, **39**, 19–30.

[176] L. Kromidas, E. Perrier, J. Flanagan, R. Rivero and I. Bonnet, *International Journal of Cosmetic Science*, 2006, **28**, 103–108.

[177] P. Scarfato, E. Avallone, P. Iannelli, V. De Feo and D. Acierno, *Journal of Applied Polymer Science*, 2007, **105**, 3568–3577.

[178] B. G. De Geest, S. De Koker, G. B. Sukhorukov, O. Kreft, W. J. Parak, A. G. Skirtach, J. Demeester, S. C. De Smedt and W. E. Hennink, *Soft Matter*, 2009, **5**, 282–291.

[179] K. Bouchemal, S. Brian¸con, E. Perrier, H. Fessi, I. Bonnet and N. Zydowicz, *International Journal of Pharmaceutics*, 2004, **269**, 89–100.

[180] H. N. Yow and A. F. Routh, *Soft Matter*, 2006, **2**, 940–949.

[181] M. J. Lawrence and G. D. Rees, *Advanced drug delivery reviews*, 2000, **45**, 89–121.

[182] E. L. Wittbecker and P. W. Morgan, *Journal of Polymer Science Part A: Polymer Chemistry,* 1996, **34**, 521–529.

[183] E. Mathiowitz and M. D. Cohen, *Journal of Membrane Science*, 1989, **40**, 27–41.

[184] Y. Okahata, H. jin Lim, S. Hachiya and G. Nakamura, *Journal of Membrane Science*, 1984, **19**, 237–247.

[185] R. K. Hedaoo, P. D. Tatiya, P. P. Mahulikar and V. V. Gite, *Designed Monomers and Polymers*, 2014, **17**, 111–125.

[186] T. Dobashi, T. Furukawa, T. Narita, S. Shimofure, K. Ichikawa and B. Chu, *Langmuir*, 2001, **17**, 4525–4528.

[187] J. Yoon and P. A. Lovell, *Macromolecular Chemistry and Physics*, 2008, **209**, 279–289.

[188] M. E. Levere, N. H. Nguyen, X. Leng and V. Percec, *Polymer Chemistry*, 2013, **4**, 1635–1647.

[189] W. Ding, C. Lv, Y. Sun, X. Liu, T. Yu, G. Qu and H. Luan, *Journal of Polymer Science Part A: Polymer Chemistry*, 2011, **49**, 432–440.

[190] G. Raspoet and M. Nguyen, *The journal of organic chemistry*, 1998, **63**, 6878-6885.

[191] M. Ciampolini and N. Nardi, Inorganic Chemistry, 1966, **5**, 41–44.

[192] L. Fertier, H. Koleilat, M. Stemmelen, O. Giani, C. Joly-Duhamel, V. Lapinte and J. Robin, *Progress in Polymer Science*, 2013, **38**, 932–962.

[193] J. Panyam and V. Labhasetwar, *Advanced Drug Delivery Reviews*, 2003, **55**, 329–347.

[194] R. A. Jain, *Biomaterials*, 2000, **21**, 2475–2490.

[195] Y. Ikada and H. Tsuji, *Macromolecular Rapid Communications*, 2000, **21**, 117–132.

[196] L. S. Nair and C. T. Laurencin, *Progress in Polymer Science,* 2007, **32**, 762–798.

[197] C. X. Lam, S. H. Teoh and D. W. Hutmacher, *Polymer International*, 2007, **56**, 718–728.

[198] M. J. Jenkins, K. L. Harrison, M. M. C. G. Silva, M. J. Whitaker,K. M. Shakesheff and S. M. Howdle, *European Polymer Journal*, 2006, **42**, 3145–3151.

[199] J. L. Hedrick, T. Magbitang, E. F. Connor, T. Glauser, W. Volksen, C. J. Hawker, V. Y. Lee and R. D. Miller, *Chemistry A European Journal*, 2002, **8**, 3308–3319.

[200] O. Aydin, B. Aydin, A. Tezcaner and D. Keskin, *Journal of Applied Polymer Science*, 2015, **132**, 1–13.

[201] Y. Du, H. Liu, J. Shuang, J. Wang, J. Ma and S. Zhang, *Colloids and Surfaces B: Biointerfaces*, 2015, **135**, 81–89.

[202] K. Khoshroo, T. S. Jafarzadeh Kashi, F. Moztarzadeh, M. Tahriri, H. E. Jazayeri and L. Tayebi, *Materials Science and Engineering C*, 2017, **70**, 586–598.

[203] V. Delplace and J. Nicolas, *Nature Chemistry*, 2015, **7**, 771–784.

[204] M. Kim, J.S. Kim, H. Lee and J. h. Jang, *Macromol. Biosci*., 2016, **16**, 738–747.

[205] D. R. Chen, J. Z. Bei and S. G. Wang, *Polymer Degradation and Stability*, 2000, **67**, 455–459.

[206] V. R. Sinha, K. Bansal, R. Kaushik, R. Kumria and A. Trehan, *International Journal of Pharmaceutics*, 2004, **278**, 1–23.

[207] T. K. Dash and V. B. Konkimalla, *Journal of Controlled Release*, 2012, **158**, 15–33.

[208] K. Vivek, L. H. Reddy and R. S. R. Murthy, *Pharmaceutical Development and Technology*, 2007, **12**, 79–88.

[209] M. Petitti, A. A. Barresi and M. Vanni, *Chemical Engineering Research and Design*, 2009, **87**, 859–866.

[210] H. F. Florindo, S. Pandit, L. M. D. Gon¸calves, H. O. Alpar and A. J. Almeida, *Vaccine*, 2008, **26**, 4168–4177.

[211] J. K. Jackson, L. S. Liang, W. L. Hunter, M. Reynolds, J. A. Sandberg, C. Springate and H. M. Burt, *International Journal of Pharmaceutics*, 2002, **243**, 43–55.

[212] R. C. Mundargi, S. Srirangarajan, S. A. Agnihotri, S. A. Patil, S. Ravindra, S. B. Setty and T. M. Aminabhavi, *Journal of Controlled Release*, 2007, **119**, 59–68.

[213] A. Gharsallaoui, G. Roudaut, O. Chambin, A. Voilley and R. Saurel, *Food Research International*, 2007, **40**, 1107–1121.

[214] R. L. Sastre and M. D. Blanco, *Drug Development Research*, 2004, **63**, 41–53.

[215] P. Lopez-Gasco, I. Iglesias, R. Lozano, and M. D. Blanco, Journal of *Microencapsulation*, 2011, **28**, 417–429.

[216] M. Labet and W. Thielemans, *Chemical Society Reviews*, 2009, **38**, 3484–3504.

[217] D. Bratton, M. Brown and S. M. Howdle, *Macromolecules*, 2005, **38**, 1190–1195.

[218] A. Kowalski, A. Duda and S. Penczek, *Macromolecules*, 2000, **33**, 689–695.

[219] A. Kowalski, A. Duda, Stanis and S. Penczek, Macromolecular Rapid *Communications*, 1998, **19**, 567–572.

[220] A. Kowalski, J. Libiszowski, T. Biela, M. Cypryk, A. Duda and S. Penczek, *Macromolecules*, 2005, **38**, 8170–8176.

[221] Odile Dechy-Cabaret, Blanca Martin-Vaca and D. Bourissou, *American Chemical Society*, 2004, **104 (12)**, 6147–6176.

[222] R. V. Tonon, C. R. F. Grosso and M. D. Hubinger, *Food Research International*, 2011, **44**, 282–289.

[223] R. Vehring, *Pharmaceutical Research*, 2008, **25**, 999–1022.

[224] K. Demirelli, M. Coskun and E. Kaya, *Journal of Polymer Science, Part A: Polymer Chemistry*, 2004, **42**, 5964–5973.

[225] L. Rueda-Larraz, B. F. DArlas, A. Tercjak, A. Ribes, I. Mondragon and A. Eceiza, *European Polymer Journal*, 2009, **45**, 2096–2109.

[226] F. Flores-Cespedes, C. I. Figueredo-Flores, and M. Fernandez-Perez, *Journal of Agricultural and Food Chemistry*, 2012, **60**, 1042–1051.

[227] Q. Zheng, Y. Niu and H. Li, *Reactive and Functional Polymers*, 2016, **106**, 99–104.

[228] N. Kumar, M. N. V. Ravikumar and A. J. Domb, *Advance drug delivery reviews*, 2001, **53**, 23–44.

[229] G. He, L. L. Ma, J. Pan and S. Venkatraman, *International Journal of Pharmaceutics,* 2007, **334**, 48–55.

[230] D. Han, X. Tong and Y. Zhao, *Langmuir*, 2012, **28**, 2327–2331.

[231] A. Schulz, S. Jaksch, R. Schubel, E. Wegener, Z. Di, Y. Han, A. Meister, A. V. Kabanov, R. Luxenhofer, X. C. M. Papadakis and R. Jordan, *ACS Nano*, 2014, **8**, 2686–2696.

[232] M. H. Stenzel, *Chemical communications*, 2008, **0**, 3486–3503.

[233] X. S. Wang and S. P. Armes, *Macromolecules*, 2000, **33**, 6640–6647.

[234] J. Nicolas, Y. Guillaneuf, C. Lefay, D. Bertin, D. Gigmes and B. Charleux, *Progress in Polymer Science*, 2013, **38**, 63–235.

[235] J. F. Lutz, *Journal of Polymer Science, Part A: Polymer Chemistry*, 2008, 46, 3459–3470.

[236] V. P. Torchilin*, Journal of Controlled Release*, 2001, **73**, 137–172.

[237] V. P. Torchilin, *Pharmaceutical Research*, 2007, **24**, 1–16.

[238] A. B. Kutikov and J. Song, *ACS Biomaterials Science & Engineering*, 2015, **1**, 463–480.

[239] K. Jelonek, S. Li, B. Kaczmarczyk, A. Marcinkowski, A. Orchel, M. Musia l-Kulik and J. Kasperczyk, *International Journal of Pharmaceutics*, 2016, **510**, 365–374.

[240] Y. Li and L. Yang, *Journal of Microencapsulation*, 2015, **32**, 255–272.

[241] H. C. Kolb, M. G. Finn and K. B. Sharpless, *Angewandte Chemie International Edition*, 2001, 40, 2004–2021.

[242] R. K. Iha, K. L. Wooley, A. M. Nystrom, D. J. Burke, M. J. Kade and C. J. Hawker, *Chemical Reviews*, 2009, **109**, 5620–5686.

[243] C. Barner-Kowollik, F. E. Du Prez, P. Espeel, C. J. Hawker, T. Junkers, H. Schlaad and W. Van Camp, *Angewandte Chemie International Edition*, 2011, **50**, 60–62.

[244] A. S. Goldmann, M. Glassner, A. J. Inglis and C. Barner-Kowollik, *Macromolecular Rapid Communications*, 2013, **34**, 810–849.

[245] A. B. Lowe, C. E. Hoyle and C. N. Bowman, *Journal of Materials Chemistry*, 2010, **20**, 4745-4750

[246] A. B. Lowe, *Polymer Chemistry*, 2009, **1**, 17–36.

[247] G. Hizal, U. Tunca and A. Sanyal, *Journal of Polymer Science Part A: Polymer Chemistry*, 2011, **49**, 4103–4120.

[248] B. Marciniec, *Hydrosilylation of Unsaturated Carbon Heteroatom Bonds*, 2009, **1**, 289–339.

[249] L. H. Sommer, E. W. Pietrusza and F. C. Whitmore, *Journal of the American chemical society*, 1947, **69**, 2108-2110

[250] J. M. Buriak, *Chemistry of Materials*, 2014, **26**, 763–772.

[251] E. Yilgor and I. Yilgor, *Progress in Polymer Science*, 2014, **39**, 1165–1195.

[252] Z. Kong, W. Wu, J. Yan, B. Wu, Y. Zhou, W. Du and Z. Qi, *Journal of Polymer Research*, 2016, **23**, 245-452

[253] Y. Xia, H. Yao, Z. Miao, Y. Ma, M. Cui, L. Yan, H. Ling and Z. Qi, *RSC Advances*, 2015, **5**, 50955–50961.

[254] T. Rambarran, F. Gonzaga, M. A. Brook, F. Lasowski and H. Sheardown, *Journal of Polymer Science, Part A: Polymer Chemistry*, 2015, **53**, 1082–1093.

[255] S. Putzien, O. Nuyken and F. E. Kuhn, *Progress in Polymer Science*, 2010, **35**, 687–713.

[256] B. J. Kokko, *Journal of Applied Polymer Science*, 1993, **47**, 1309–1314.

[257] B. Boutevin, F. Guida-Pietrasanta and A. Ratsimihety, *Journal of Polymer Science Part A-Polymer Chemistry*, 2000, **38**, 3722–3728.

[258] O. Mukbaniani, G. Zaikov, N. Pirckheliani, T. Tatrishvili, S. Meladze, Z. Pachulia and M. Labartkava, *Journal of Applied Polymer Science*, 2007, **103**, 3243–3252.

[259] L. Cheng, Q. Liu, A. Zhang, L. Yang and Y. Lin, *Journal of Macromolecular Science, Part A*, 2014, **51**, 16–26.

[260] R. Chakraborty and M. D. Soucek, *Macromolecular Chemistry and Physics*, 2008, **209**, 604–614.

[261] M. Galin and A. Mathis, *Macromolecules*, 1981, **14**, 677–683.

[262] D. W. Grainger, S. W. Kim and J. Feijen, *Journal of Biomedical Materials Research*, 1988, **22**, 231–249.

[263] G. Kickelbick, J. Bauer, N. H¨using, M. Anderssorn and A. Palmqvist, *Langmuir*, 2003, **19**, 3198–3201.

[264] D. Li, C. Li, G. Wan and W. Hou, *Colloids and Surfaces A Physicochemical and Engineering Aspects*, 2010**, 372**, 1–8.

[265] J. Stein, L. N. Lewis, Y. Gao and R. a. Scott, *Journal of the American Chemical Society*, 1999, **121**, 3693–3703.

[266] X. Y. Guo, R. Farwaha and G. L. Rempel, *Macromolecules*, 1990, **23**, 5047–5054.

[267] W.G. Zhao and R. Huan, *European Journal of Organic Chemistry*, 2006, **24**, 5495–5498.

[268] D. M. Haddleton, D. R. Maloney, K. A. Clarke and S. N. Richards, *Polymer*, 1997, **38**, 6207–6217.

[269] D. Roy, J. N. Cambre and B. S. Sumerlin, *Progress in Polymer Science*, 2010, **35**, 278–301.

[270] Y. Shen, H. Tang, Y. Zhan, E. A. V. Kirk and W. J. Murdoch, *Nanomedicine: Nanotechnology, Biology and Medicine*, 2009, **5**, 192–201.

[271] G. H. Gao, Y. Li and D. S. Lee, *Journal of Controlled Release*, 2013, **169**, 180–184.

[272] B. R. Saunders, N. Laajam, E. Daly, S. Teow, X. Hu and R. Stepto, *Advances in Colloid and Interface Science*, 2009, **147**, 251–262.

[273] C. S. Brazel and N. A. Peppas, *Macromolecules*, 1995, **28**, 8016–8020.

[274] D. Li, Q. He, Y. Cui and J. Li, *Chemistry of Materials*, 2007, **19**, 412–417.

[275] F. J. Xu, E. T. Kang and K.-G. Neoh, *Biomaterials*, 2006, **27**, 2787–2797.

[276] Q. Yuan, R. Venkatasubramanian, S. Hein and R. D. K. Misra, *Acta Biomaterialia*, 2008, **4**, 1024–1037.

[277] M. Li, M. Gao, Y. Fu, C. Chen, X. Meng, A. Fan, D. Kong, Z. Wang and Y. Zhao, *Colloids and Surfaces B: Biointerfaces*, 2016, **140**, 11–18.

[278] H. L. Lim, Y. Hwang, M. Kar and S. Varghese, *Biomater. Sci.*, 2014, **2**, 603–618.

[279] M.-A. Yessine and J.-C. Leroux, *Advanced Drug Delivery Reviews*, 2004, **56**, 999–1021.

[280] N. Rapoport, *Progress in Polymer Science*, 2007, **32**, 962–990.

[281] J. Hu, J. He, M. Zhang and P. Ni, *Polymer Chemistry*, 2015, **6**, 1553–1566.

[282] S. Dai, P. Ravi and K. C. Tam, *Soft Matter*, 2008, **4**, 435-449

[283] M. J. Heffernan and N. Murthy, *Bioconjugate Chemistry*, 2005, **16**, 1340–1342.

[284] S. Matsumura, A. R. Hlil, C. Lepiller, J. Gaudet, D. Guay, Z. Shi, S. Holdcroft and A. S. Hay, *American Chemical Society, Polymer Preprints, Division of Polymer Chemistry*, 2008, **49**, 511–512.

[285] R. R. De Clercq, G. G. Trossaert, P. J. Hartmann, S. Walraedt and E. J. Goethals, *Macromolecular Symposia*, 1994, **77**, 395–403.

[286] Y. Wang, H. Morinaga, A. Sudo and T. Endo, *Journal of Polymer Science Part A: Polymer Chemistry*, 2011, **49**, 596–602.

[287] A. S. Amarasekara and M. A. Animashaun, *Catalysis Letters,* 2016, **146**, 1819–1824.

[288] H. P. Hsieh, Y. T. Wu, S. T. Chen and K. T.Wang, *Bioorganic & Medicinal Chemistry*, 1999, **7**, 1797–1803.

[289] N. Murthy, M. Xu, S. Schuck, J. Kunisawa, N. Shastri and J. M. J. Frechet, *Proceedings of the National Academy of Sciences*, 2003, **100**, 4995–5000.

[290] E. R. Gillies and J. M. J. Frechet, *Chemical Communications*, 2003, 1640–1641.

[291] S. D. Khaja, S. Lee and N. Murthy, *Biomacromolecules*, 2007, **8**, 1391–1395.

[292] S. E. Paramonov, E. M. Bachelder, T. T. Beaudette, S. M. Standley, C. C. Lee, J. Dashe and J. M. J. Frechet, *Bioconjugate Chemistry*, 2008, **19**, 911–919.

[293] a. P. Griset, J. Walpole, R. Liu, a. Ga↵ey, Y. L. Colson and M. W. Grinstaff, *J Am Chem Soc*, 2009, **131**, 2469–2471.

[294] J. K. Kim, V. K. Garripelli, U. H. Jeong, J. S. Park, M. A. Repka and S. Jo, *International Journal of Pharmaceutics*, 2010, **401**, 79–86.

[295] S. Binauld and M. H. Stenzel, *Chemical communications*, 2013, **49**, 2082–102.

[296] S. F. Peteu, F. Oancea, O. A. Sicuia, F. Constantinescu and F. Dinu, *Polymers,* 2010, **2**, 229–251.

[297] J. M. Green and G. B. Beestman, *Crop Protection*, 2007, **26**, 320–327.

[298] P. Hinsinger, C. Plassard, C. Tang and B. Jaillard, *Plant and Soil*, 2003, **248**, 43–59.

[299] S. R. Pezeshki and R. D. DeLaune, *Biology*, 2012, **1**, 196–221.

[300] a. Andrews and W. H. Schlesinger, *Global Biogeochemical Cycles*, 2001, **15**, 149-162.

[301] M. C. Rillig, K. M. Scow, J. N. Klironomos and M. F. Allen, *Soil Biology and Biochemistry*, 1997, **29**, 1387–1394.